PHYLOGENOMICS AND THE METABOLISM OF SULFUR COMPOUNDS IN THE ROSEOBACTER GROUP

by

JOSEPH S. WIRTH

(Under the Direction of William B. Whitman)

ABSTRACT

The roseobacter group comprise up to 25 % of the total bacterial community in the surface waters of the ocean, and its members possess a great deal of physiological and genetic diversity. Taxonomic assignments within the roseobacter group have been primarily based on 16S rRNA gene sequences. However, recent studies have demonstrated that this gene lacks the resolution for accurately assigning organisms within the roseobacter group. To address this problem, whole-genome sequence data was used to construct a taxonomy that accurately depicts evolutionary relationships. The result of these analyses was the taxonomic reassignment of 34 species and the proposal of six novel genera.

Dimethylsulfoniopropionate (DMSP) is abundant in marine surface waters and can reach micromolar concentrations, and *Ruegeria pomeroyi*, a member of the roseobacter group, is capable of metabolizing it. Previous studies have shown that the methyl carbon and sulfur of DMSP are incorporated into methionine, and this led to the hypothesis that the direct capture of methanethiol was the major pathway for methionine biosynthesis from DMSP. To test this hypothesis, a highly efficient method for synthesizing di(methyl-^{13}C)sulfonio-^{34}S-propionate ([^{13}C][^{34}S]DMSP) was developed. The [^{13}C][^{34}S]DMSP was subsequently fed to *R. pomeroyi* in chemostat and the resulting isotopic labeling of methionine was examined. These experiments

indicated that only one-third of methionine was synthesized via the direct capture of methanethiol while the remainder was synthesized by the random reassembly of the sulfur and methyl atoms. The findings also indicated that DMSP was the major source of sulfur even when present at concentrations <1 μM.

S-methylmethionine (SMM) is an abundant organosulfur compound that is synthesized exclusively by plants. Its catabolism has been studied in plants, animals, and bacteria, where it is either converted to DMS and homoserine or demethylated to methionine. Recent experiments have indicated that *R. pomeroyi* is capable of producing significant amounts of DMS from SMM, but the gene(s) and mechanism(s) responsible remain unknown. It is likely that SMM is converted to DMS via promiscuous activity of one or more of the DMSP lyases present in *R. pomeroyi*, but this hypothesis has not yet been confirmed.

INDEX WORDS: Roseobacter group, *Ruegeria pomeroyi*, *Ruegeria lacuscaerulensis*, *Rhodobacteraceae*, *Alphaproteobacteria*, Phylogenomics, Dimethylsulfoniopropionate, DMSP, Methionine, Cysteine, *S*-methylmethionine, SMM, Dimethylsulfide, DMS

PHYLOGENOMICS AND THE METABOLISM OF SULFUR COMPOUNDS IN THE ROSEOBACTER GROUP

by

JOSEPH S. WIRTH

B.S., University of Illinois at Urbana-Champaign, 2012

A Dissertation Submitted to the Graduate Faculty of The University of Georgia in Partial Fulfillment of the Requirements for the Degree

DOCTOR OF PHILOSOPHY

ATHENS, GEORGIA

2019

PHYLOGENOMICS AND THE METABOLISM OF SULFUR COMPOUNDS IN THE ROSEOBACTER GROUP

by

JOSEPH S. WIRTH

Major Professor:	William B. Whitman
Committee:	Zachary Lewis
	Mary Ann Moran
	Janet Westpheling

Electronic Version Approved:

Suzanne Barbour
Dean of the Graduate School
The University of Georgia
May 2019

ACKNOWLEDGEMENTS

There are many people to thank, but I will start with my parents, Joe and BethAnn Wirth, for always supporting me throughout my life, and my sister, Lauren Wirth, for being an awesome person and always making my life better. I would like to thank my grandparents, Dorothy Wirth and Steve and Jeannie Karabin, for being great role models and always being there for me. I would also like thank the rest my extended family, who are too numerous to list, for being great people and even better family members, in particular, Jeff, Mary, Chris, Corey, and Casey Geissen, for providing me with a home away from home whenever I needed one.

I would like to thank my some of my closest friends in Athens: Justin Bishop, Bays Anderson, Stefan Wolf, Kyle DeAngelis, Katelyn Moynihan, Andrew Dallas, and Sebastian Keller for helping me relax and making sure I didn't spend too much time in lab. I would also like to thank Nick Brown, Sean Klein, Devan McMenamin, and Megan Scibona for being great friends for most of my life.

I would like to thank The Lounge: Alan Rohde, Andrew "Brain" Nelson, Chris Hatten, Mike Halfmann, Robrown, that Scott Manley kid, Matt Castro, and Tim Lowder, as well as Ryan Hook and Rachel Fusello, for being pretty weird and not enforcing capacity. I would also like to thank Alyssa Cook for being a great friend when I needed it the most.

I would like to thank my advisor, Dr. William "Barny" Whitman, for helping me become a better scientist, and accepting me into his lab during a particularly tumultuous time in my life. I would like to thank Dr. Janet Westpheling for providing me with great advice and helping me through some difficult moments in my scientific career. I would also like to thank the two other members of my doctoral committee, Dr. Zachary Lewis and Dr. Mary Ann Moran, for their

extremely useful advice and guidance. I would like to thank the staff of the Department of Microbiology during my tenure here, Andrea Barnett, Kim Brown, Christie Haynes, Nancy Perkins, Janice Stuart, and Sophia Fleming, for helping me clear numerous hurdles that allowed me to be here today.

I would like to thank the past and present members of my class, Andrew Borchert, Rachel Burckhardt. Emily Carpinone, Alyssa Cook, Ashley Hagen, Kawanda Foster, Julie Grainy, Victoria Jeter, Bowen Meng, Alan Schmalstig, AJ Stasic, Mogan Teachey, and Walter Woodside. In particular, I would like to thank Alyssa, Kawanda, Alan, and Walter for being truly helpful and supportive. I would like to thank past and present members of the lab including Feng Long, Tao Wang, Zhe Lyu, Qiuyuan Huang, Taiwo Akinyemi, Suet Yee Chong, Nana Shao, Amala Malladi, and Courtney Grant for all of their help and encouragement during my time in the lab. I also would like to thank the undergraduates that I mentored, Alvin Soto-Soto for help isolating transposon mutants, and Temiloluwa Onafuye for help with enzyme assays.

TABLE OF CONTENTS

Page

CHAPTER 1

INTRODUCTION AND LITERATURE REVIEW

1. The roseobacter group

The roseobacter group are alphaproteobacteria within the *Rhodobacteraceae* family, and its members comprise up to 25 % of the total bacterial community in the surface of the ocean (1-3). Most members are marine in origin, but some genera of terrestrial origin exist (4). They have been isolated from diverse environments including seawater, marine sediments, and biofilms and are often associated with phytoplankton, macroalgae, and marine animals. Some species are highly abundant and have been observed with global distributions in marine environments in both bacterial isolates and metagenomic samples (5).

The first members of the roseobacter group, *Roseobacter denitfrificans* and *Roseobacter litoralis*, were originally described in 1991 (6). *R. denitrificans* was heavily studied after being isolated from seaweed in 1979 because it possessed bacteriochlorophyll *a* despite being an aerobe (7). In the decade following the description of the genus *Roseobacter*, analyses of 16S rRNA gene sequences identified a cluster of species that eventually became known as the "*Roseobacter* clade" (8-10). The *Roseobacter* clade was originally defined as genera sharing >89 % 16S rRNA gene sequence similarity, and this was the primary basis for taxonomic assignment (4, 11). The designation as a clade was based on the fact that its members formed a monophyletic clade in phylogenetic trees based on 16S rRNA gene sequences (2), and this topology was supported by trees based on 70 universal single-copy genes (12), 348 concatenated orthologous protein sequences (13), and 50 single-copy conserved protein sequences (11). However, these trees were based on a single inference method, used a single amino-acid substitution model, and

were not constructed in the context of the entire *Rhodobacteraceae* family. A recent study addressed these issues, and found that the monophyletic topology was not unambiguously supported, and that the topology was most likely polyphyletic (3). Because of this, the term "roseobacter group" was proposed to replace the term "*Roseobacter* clade" (3). Currently, the roseobacter group is comprised of 84 genera containing (2-4, 11, 14) containing 319 species (according to NCBI taxonomy).

The species within the roseobacter group possess a great deal of physiological diversity, which is reflected in the large variation of the genome size and gene content (11). Collectively, the roseobacter group is capable of metabolizing a large number of carbon sources, synthesizing B vitamins to facilitate eukaryotic interactions, assimilatory and dissimilatory nitrate reduction, and phototrophic growth (11). The earliest roseobacter has been estimated to exist approximately 260 million years ago, and the expansion of its genome and subsequent diversification around 250 million years ago coincided with the emergence of the dinoflagellates and coccolithophores (11). In addition to the chromosome, roseobacters with complete, whole-genome sequences possess replicons that vary in size (15).

Although 16S rRNA gene sequence similarity is useful for classifying an organism as a roseobacter group member, this gene lacks the resolution for accurately assigning organisms within the roseobacter group (3, 14, 16). To address this problem, whole-genome sequence data can be used to construct more robust phylogenetic trees and these trees can be evaluated using tree-independent genomic analyses (see Chapter 2 for more information).

2. Dimethylsulfoniopropionate

2.1 Importance of dimethylsulfoniopropionate

Dimethylsulfoniopropionate (DMSP) is a highly abundant compound in marine surface waters. In the North Sea, the concentration of DMSP cycles seasonally from micromolar levels

in the summer to picomolar levels in the spring and fall (17, 18). The majority of marine DMSP comes from halophytic plants and algae, where it is believed to regulate osmotic pressure, but it may also provide antioxidant, predator deterrent, and/or cryoprotectant functions (18). There is also evidence that bacteria produce significant amounts of DMSP in marine environments, and it has been estimated that at least 0.5 % of marine bacteria are capable of producing DMSP (19). Concurrent with its role as an osmoregulatory molecule, plants that produce the most DMSP are generally halotolerant and of marine origin, with sugarcane being the only non-marine exception. During ^{35}S-labeling studies with the protist, *Oxyrrhis marina*, approximately 15 % of added DMSP accumulated intracellularly but was not metabolized (20). Molar levels of intracellular DMSP have been observed in some organisms, and it is estimated that up to 10 % of the total fixed carbon is in the form of DMSP (21). Furthermore, DMSP released from phytoplankton blooms can satisfy up to 15 % of the microbial carbon demand and 100 % of the microbial sulfur demand (21).

DMSP is the precursor for the majority of atmospheric dimethylsulfide (DMS), which is a climatically-active gas and connects the marine and terrestrial sulfur cycles (22). It was previously believed that H_2S was responsible for the transfer of sulfur between marine and terrestrial environments, but the necessary atmospheric concentrations were never detected and the surface layers of the ocean are too oxidizing to sustain equilibrium with the atmosphere (22). However, the concentration of DMS in marine surface layers is sufficiently high, and DMS is resistant to oxidation in the lower atmosphere (22). Its photooxidation in the upper atmosphere produces sulfur species that can be transferred to terrestrial environments via rain and promote the formation of “cloud-condensation nuclei”, resulting in an increased albedo effect and global cooling (18, 21, 23, 24).

Bacterial catabolism of DMSP proceeds through one of two known pathways (Fig. 1-1). It can either undergo demethylation to form methylmercaptopropionic acid, which can be broken down into methanethiol, carbon dioxide, and acetaldehyde, or it can undergo cleavage to form DMS and acrylic acid (18, 25). In both cases, the resulting DMS and methanethiol can be metabolized further and assimilated into biomass. Because very few studies have performed isotope-labeling experiments with DMSP, the fate of DMSP in microbial biomass is not well understood (20, 26-28).

2.2 Biosynthesis of methionine from DMSP

A previous study examined the fate of isotopically labeled atoms from either di(methyl-^{13}C)sulfoniopropionate ([methyl-^{13}C]DMSP) (Fig. 1-2A) or dimethylsulfoniopropionate-1-^{13}C ([1-^{13}C]DMSP) (Fig. 1-2B) in *R. pomeroyi* (26). This study found that the methyl carbon of L-methionine and the C-3 position of L-serine were enriched by 99 % and 30 %, respectively, when grown on [methyl-^{13}C]DMSP (26). However, when *R. pomeroyi* was grown on [1-^{13}C]DMSP, L-methionine was not enriched with ^{13}C (26). Taken together, this demonstrated that the methyl carbon of L-methionine was coming directly from the methyl carbons of DMSP, but ruled out the hypothesis that methylmercaptopropionic acid (MMPA) (Fig. 1-1) was being directly converted to L-methionine via reductive carboxylation and transamination. The labeling observed at the C-3 position of L-serine when grown on [methyl-^{13}C]DMSP was most likely a result of its synthesis via L-glycine, water, and 5,10-methylenetetrahydrofolate (Fig. 1-3).

These results indicated that L-methionine was being synthesized from either one or both of the following pathways (Fig. 1-3): methanethiol was converted to L-methionine directly via a γ-substitution with *O*-acetyl-L-homoserine ("methanethiol" pathway) (Fig. 1-3: blue lines), or methanethiol was first reduced to sulfide, which was converted to L-homocysteine via a γ-

substitution with *O*-succinyl-L-homoserine, and subsequently converted to L-methionine through methylation via the THF pool ("reassembly" pathway) (Fig. 1-3: green lines).

In order to investigate which pathways are being used to synthesize L-methionine, *R. pomeroyi* DSS-3 must be grown in the presence of di(methyl-^{13}C)sulfonio-^{34}S-propionate ([^{13}C][^{34}S]DMSP). By feeding the cells a 1:1 mixture of DMSP and [^{13}C][^{34}S]DMSP, the resulting L-methionine isotopomers can be analyzed to determine which pathways are being utilized (Fig. 1-4). For example, if all L-methionine is synthesized via the "methanethiol" pathway (Fig. 1-3: blue lines), then the resulting L-methionine will be either unlabeled (mass shift = 0) or possess both ^{13}C and ^{34}S (mass shift = 3) (Fig. 1-4). However, if all the L-methionine is synthesized via the "reassembly" pathway (Fig. 1-3: green lines) then there should be a relatively even distribution of unlabeled L-methionine (mass shift = 0), L-methionine labeled with ^{13}C only (mass shift = 1), L-methionine labeled with ^{34}S only (mass shift = 2), and L-methionine labeled with both ^{13}C and ^{34}S (mass shift = 3) (Fig. 1-4). It is likely that both pathways are being used by *R. pomeroyi*, but examining the relative abundance of each isotopomer of L-methionine should provide insight into the fraction of L-methionine synthesized from each of the pathways. It is also necessary to examine the amount of ^{34}S-labeled L-cysteine as this will provide important information about the relative amount of unlabeled sulfide present in the cells. Because some of the L-cysteine is synthesized from the THF pool, it may also provide information about the relative amount ^{13}C present in the THF pool.

In order to perform these experiments, it is necessary to synthesize [^{13}C][^{34}S]DMSP. DMSP hydrochloride can be easily synthesized via a Michael addition of DMS to acrylic acid under acidic conditions in methylene chloride (29). Unfortunately, DMS enriched with a sulfur isotope is not commercially available, and the only commercially available form of isotopically-labeled sulfur suitable for conversion to DMS is elemental sulfur (S_8). Thus, incorporation of a

specific sulfur isotope requires a synthetic pathway to convert S_8 to DMSP. A method for converting $^{34}S_8$ to dimethylsulfonio-^{34}*S*-propionate ([^{34}S]DMSP) has been published, but it requires expensive reagents, multiple purifications, cannot be used to label both methyl carbons, and only has an overall yield of 26 % (30). This presents a problem, especially because $^{34}S_8$ costs several thousand dollars per gram. In order to circumvent these issues, an improved method is required to synthesize [^{34}S]DMSP from $^{34}S_8$ (see Chapter 5 for more information).

3. *S*-methylmethionine

S-methylmethionine (SMM) is an abundant organosulfur compound that is synthesized exclusively by plants via a methyl transfer from *S*-adenosylmethionine to methionine (31). In cells, SMM is converted back to methionine by transferring a methyl group to homocysteine using a different enzyme (31). SMM has been called "vitamin U" due to its ability to heal and prevent peptic ulcers, and it has also been shown to possess anti-inflammatory, analgesic, hypolipidemic, and radioprotective properties and to have a therapeutic effect on gastritis, diaphragmatic hernias, gastric duodenal, liver injuries, gastric ulcers, and renal damage (32-34). In plants, it is present in the free state, and its role is still not clear (31, 35). Because plants lack two negative feedback loops present in other eukaryotes that serve to regulate the synthesis of *S*-adenosylmethionine, it has been hypothesized that SMM is used as a source of free-methionine in the event that the too much *S*-adenosylmethionine has been synthesized (31).

The catabolism of SMM has been studied in plants, animals, and bacteria (33, 35-37). In plants and animals, it is converted to DMS and homoserine or demethylated as described above (31, 38). SMM is converted to methionine in *Escherichia coli* by the *S*-methylmethionine:homocysteine methyltransferase, MmuM (37). A soil bacterium has also been isolated that can grow on SMM as the sole carbon source, and it possesses an enzyme capable of producing DMS from SMM (36). However, this enzyme has never been characterized and its

composition and sequence are not known. Because SMM can be degraded to DMS, it is imperative to understand its metabolism in order to better understand DMS production on a global scale.

References

1. Brinkhoff T, Giebel HA, Simon M. 2008. Diversity, ecology, and genomics of the *Roseobacter* clade: a short overview. Archives of Microbiology 189:531-539.
2. Buchan A, González JM, Moran MA. 2005. Overview of the marine *Roseobacter* lineage. Applied and Environmental Microbiology 71:5665-77.
3. Simon M, Scheuner C, Meier-Kolthoff JP, Brinkhoff T, Wagner-Dobler I, Ulbrich M, Klenk HP, Schomburg D, Petersen J, Goker M. 2017. Phylogenomics of *Rhodobacteraceae* reveals evolutionary adaptation to marine and non-marine habitats. ISME Journal 11:1483-1499.
4. Pujalte MJ, Lucena T, Ruvira MA, Arahal DR, Macián MC. 2014. The family Rhodobacteraceae, p 439-512. *In* Rosenberg E, DeLong EF, Lory S, Stackebrandt E, Thompson F (ed), The Prokaryotes: *Alphaproteobacteria* and *Betaproteobacteria* doi:10.1007/978-3-642-30197-1_377. Springer Berlin Heidelberg, Berlin, Heidelberg.
5. Sonnenschein EC, Nielsen KF, D'Alvise P, Porsby CH, Melchiorsen J, Heilmann J, Kalatzis PG, Lopez-Perez M, Bunk B, Sproer C, Middelboe M, Gram L. 2017. Global occurrence and heterogeneity of the *Roseobacter*-clade species *Ruegeria mobilis*. ISME Journal 11:569-583.
6. Shiba T. 1991. *Roseobacter litoralis* gen. nov., sp. nov., and *Roseobacter denitrificans* sp. nov., aerobic pink-pigmented bacteria which contain bacteriochlorophyll *a*. Systematic and Applied Microbiology 14:140-145.

7. Shiba T, Simidu U, Taga N. 1979. Another aerobic bacterium which contains bacteriochlorophyll *a*. Bulletin of the Japanese Society of Scientific Fisheries 45:801-801.

8. Giovannoni SJ, Britschgi TB, Moyer CL, Field KG. 1990. Genetic diversity in Sargasso Sea bacterioplankton. Nature 345:60-63.

9. Rappe MS, Vergin K, Giovannoni SJ. 2000. Phylogenetic comparisons of a coastal bacterioplankton community with its counterparts in open ocean and freshwater systems. Fems Microbiology Ecology 33:219-232.

10. Suzuki MT, Beja O, Taylor LT, DeLong EF. 2001. Phylogenetic analysis of ribosomal RNA operons from uncultivated coastal marine bacterioplankton. Environmental Microbiology 3:323-331.

11. Luo H, Moran MA. 2014. Evolutionary ecology of the marine *Roseobacter* clade. Microbiology and Molecular Biology Reviews 78:573-587.

12. Newton RJ, Griffin LE, Bowles KM, Meile C, Gifford S, Givens CE, Howard EC, King E, Oakley CA, Reisch CR, Rinta-Kanto JM, Sharma S, Sun S, Varaljay V, Vila-Costa M, Westrich JR, Moran MA. 2010. Genome characteristics of a generalist marine bacterial lineage. ISME Journal 4:784-98.

13. Luo HW, Loytynoja A, Moran MA. 2012. Genome content of uncultivated marine *Roseobacters* in the surface ocean. Environmental Microbiology 14:41-51.

14. Wirth JS, Whitman WB. 2018. Phylogenomic analyses of a clade within the roseobacter group suggest taxonomic reassignments of species of the genera *Aestuariivita*, *Citreicella*, *Loktanella*, *Nautella*, *Pelagibaca*, *Ruegeria*, *Thalassobius*, *Thiobacimonas* and *Tropicibacter*, and the proposal of six novel genera. Internationl Journal of Systematic and Evolutionary Microbiology doi:10.1099/ijsem.0.002833.

15. Moran MA, Belas R, Schell MA, Gonzalez JM, Sun F, Sun S, Binder BJ, Edmonds J, Ye W, Orcutt B, Howard EC, Meile C, Palefsky W, Goesmann A, Ren Q, Paulsen I, Ulrich LE, Thompson LS, Saunders E, Buchan A. 2007. Ecological genomics of marine *Roseobacters*. Appl Environ Microbiol 73:4559-69.

16. Breider S, Scheuner C, Schumann P, Fiebig A, Petersen J, Pradella S, Klenk HP, Brinkhoff T, Goker M. 2014. Genome-scale data suggest reclassifications in the *Leisingera-Phaeobacter* cluster including proposals for *Sedimentitalea* gen. nov. and *Pseudophaeobacter* gen. nov. Frontiers in Microbiology 5:416.

17. van Duyl FC, Gieskes WWC, Kop AJ, Lewis WE. 1998. Biological control of short-term variations in the concentration of DMSP and DMS during a *Phaeocystis* spring bloom. Journal of Sea Research 40:221-231.

18. Reisch CR, Moran MA, Whitman WB. 2011. Bacterial catabolism of dimethylsulfoniopropionate (DMSP). Frontiers in Microbiology 2:172.

19. Curson ARJ, Liu J, Martinez AB, Green RT, Chan YH, Carrion O, Williams BT, Zhang SH, Yang GP, Page PCB, Zhang XH, Todd JD. 2017. Dimethylsulfoniopropionate biosynthesis in marine bacteria and identification of the key gene in this process. Nature Microbiology 2:9.

20. Saló V, Simó R, Vila-Costa M, Calbet A. 2009. Sulfur assimilation by *Oxyrrhis marina* feeding on a ^{35}S-DMSP-labelled prey. Environmental Microbiology 11:3063-3072.

21. Yoch DC. 2002. Dimethylsulfoniopropionate: its sources, role in the marine food web, and biological degradation to dimethylsulfide. Applied and Environmental Microbiology 68:5804-5815.

22. Lovelock JE, Maggs RJ, Rasmussen RA. 1972. Atmospheric dimethyl sulphide and the natural sulphur cycle. Nature 237:452.

23. Hatakeyama S, Okuda M, Akimoto H. 1982. Formation of sulfur dioxide and methanesulfonic acid in the photooxidation of dimethyl sulfide in the air. Geophysical Research Letters 9:583-586.

24. Charlson RJ, Lovelock JE, Andreae MO, Warren SG. 1987. Oceanic phytoplankton, atmospheric sulphur, cloud albedo and climate. Nature 326:655.

25. Reisch CR, Stoudemayer MJ, Varaljay VA, Amster IJ, Moran MA, Whitman WB. 2011. Novel pathway for assimilation of dimethylsulphoniopropionate widespread in marine bacteria. Nature 473:208-11.

26. Reisch CR, Crabb WM, Gifford SM, Teng Q, Stoudemayer MJ, Moran MA, Whitman WB. 2013. Metabolism of dimethylsulphoniopropionate by *Ruegeria pomeroyi* DSS-3. Molecular Microbiology 89:774-91.

27. Todd JD, Curson ARJ, Nikolaidou-Katsaraidou N, Brearley CA, Watmough NJ, Chan YH, Page PCB, Sun L, Johnston AWB. 2010. Molecular dissection of bacterial acrylate catabolism - unexpected links with dimethylsulfoniopropionate catabolism and dimethyl sulfide production. Environmental Microbiology 12:327-343.

28. Ruiz-González C, Galí M, Sintes E, Herndl GJ, Gasol JM, Simó R. 2012. Sunlight effects on the osmotrophic uptake of DMSP-sulfur and leucine by polar phytoplankton. Plos One 7:14.

29. Chambers ST, Kunin CM, Miller D, Hamada A. 1987. Dimethylthetin can substitute for glycine betaine as an osmoprotectant molecule for *Escherichia coli*. Journal of Bacteriology 169:4845-7.

30. Brock NL, Menke M, Klapschinski TA, Dickschat JS. 2014. Marine bacteria from the *Roseobacter* clade produce sulfur volatiles via amino acid and dimethylsulfoniopropionate catabolism. Organic & Biomolecular Chemistry 12:4318-23.

31. Ranocha P, McNeil SD, Ziemak MJ, Li C, Tarczynski MC, Hanson AD. 2001. The *S*-methylmethionine cycle in angiosperms: ubiquity, antiquity and activity. The Plant Journal 25:575-584.

32. Meinders A. 1955. Vitamin-U. Journal of the American Medical Association 157:1458-1458.

33. Gessler NN, Bezzubov AA, Podlepa EM, Bykhovskii VY. 1991. Metabolism of *S*-methylmethionine (vitamin U) in animals. Applied Biochemistry and Microbiology 27:275-280.

34. Oktay S, Bayrak G, Alev B, Ipekci H, Ustundag UV, Turkyilmaz IB, Pisiriciler R, Emekli-Alturfan E, Tunali-Akbay T, Yanardag R, Yarat A. 2018. The effect of vitamin U on the lung tissue of pentyleneterazole-induced seizures in rats. Naunyn-Schmiedebergs Archives of Pharmacology 391:177-184.

35. Gessler NN, Bezzubov AA, Podlepa EM, Bykhovskii VY. 1991. *S*-methylmethionine (vitamin U) metabolism in plants. Applied Biochemistry and Microbiology:192-199.

36. Mazelis M, Levin B, Mallinson N. 1965. Decomposition of methyl methionine sulfonium salts by a bacterial enzyme. Biochimica et Biophysica Acta 105:106-14.

37. Thanbichler M, Neuhierl B, Bock A. 1999. *S*-methylmethionine metabolism in Escherichia coli. Journal of Bacteriology 181:662-5.

38. Gessler NN, Bezzubov AA. 1988. *S*-methylmethionine sulfonium hydrolase activity in plant and animal tissues. Applied Biochemistry and Microbiology 24:200-205.

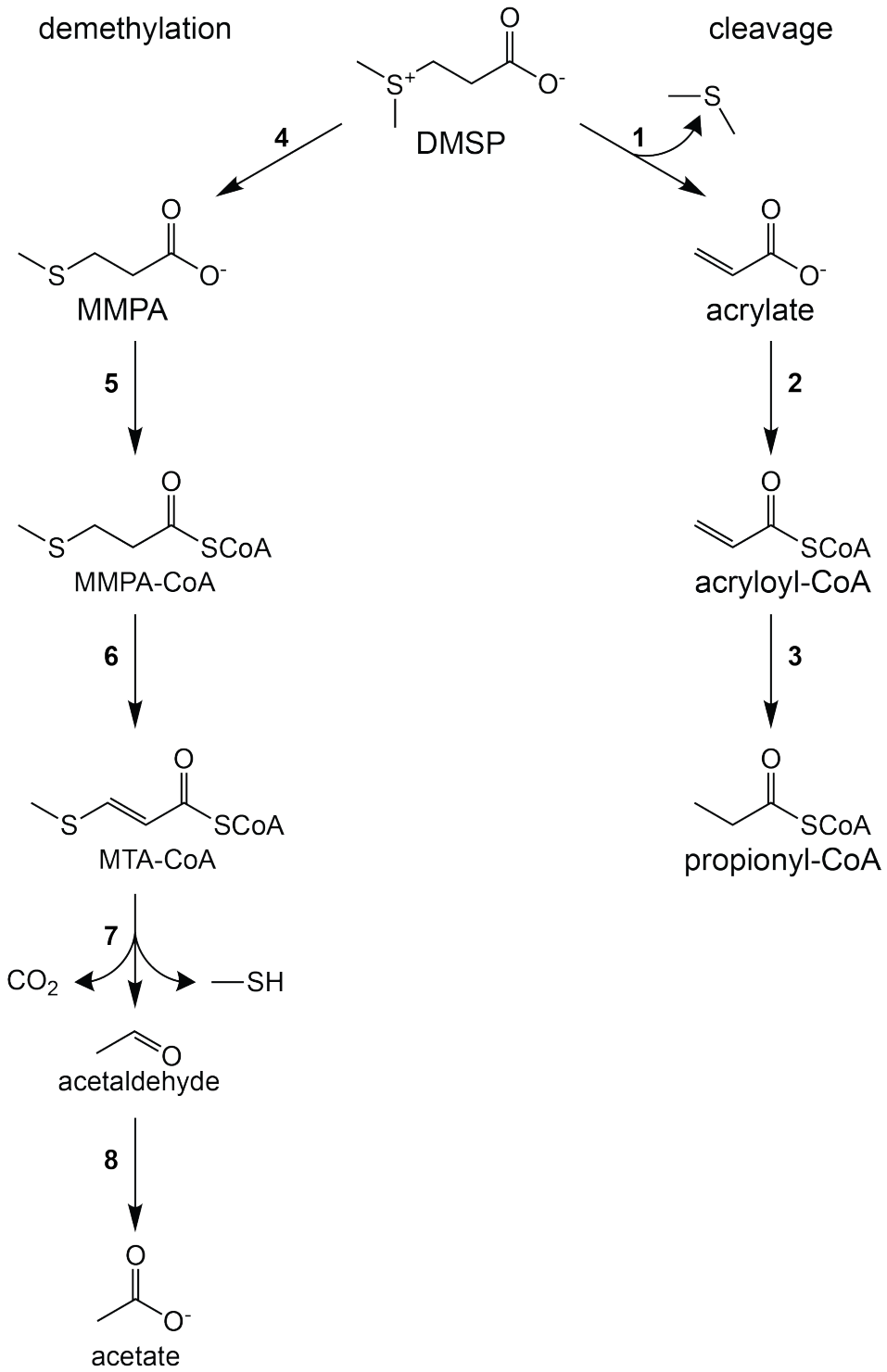

Figure 1-1. Metabolism of DMSP in *Ruegeria pomeroyi* DSS-3. The two possible pathways for DMSP degradation are shown with the cleavage pathway on the right and the demethylation/demethiolation pathway on the left. Abbreviations: MMPA, methylmercaptopropionic acid; MTA-CoA, methylthioacryloyl-CoA. Genes: 1, *dddD* (SPO1703), *dddP* (SPO2299), *dddQ* (SPO1596), and/or *dddW* (SPO0453); 2, *prpE* (SPO2934); 3, *acuI* (SPO1914); 4, *dmdA* (SPO1913); 5, *dmdB* (SPO2045/SPO0677); 6, *dmdC* (SPO3804/SPO0298/SPO2915); 7, *dmdD* (SPO3805); 8, aldehyde dehydrogenase (SPO0097).

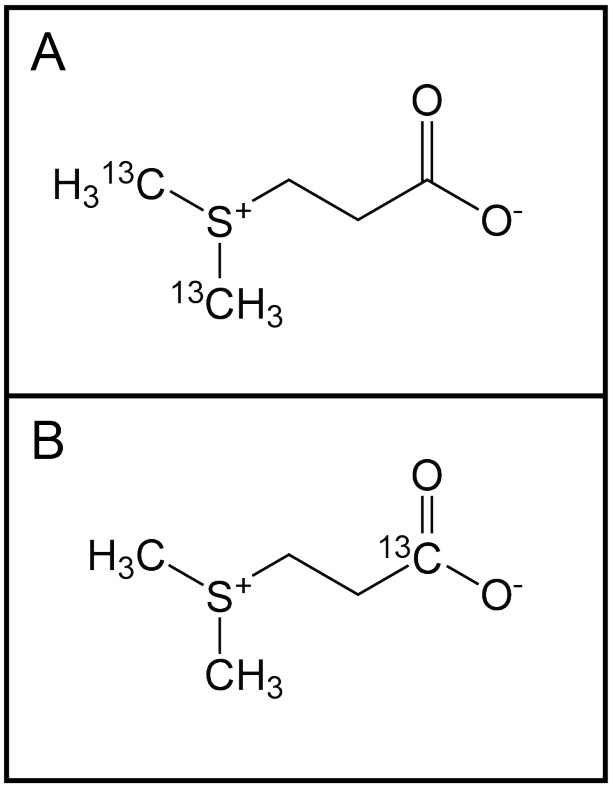

Figure 1-2. DMSP isotopomers employed in previous studies. (A) di(methyl-^{13}C)sulfoniopropionate. (B) dimethylsulfoniopropionate-1-^{13}C.

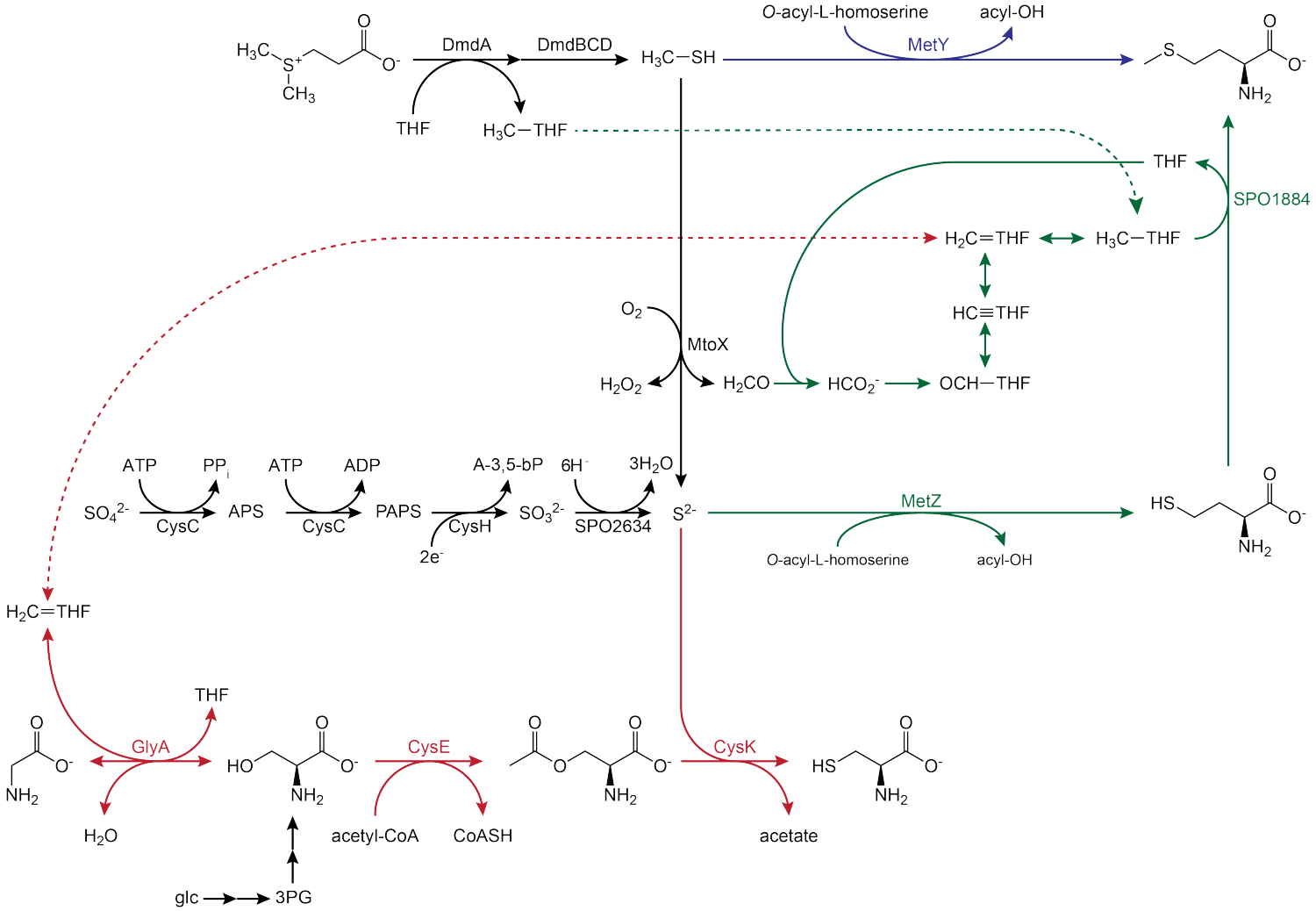

Figure 1-3. Putative pathways for the biosynthesis of L-methionine and L-cysteine from DMSP. Both possible routes for synthesizing L-methionine are shown with the "methanethiol" pathway highlighted in blue and the "reassembly" pathway highlighted in green. The pathway for L-cysteine biosynthesis is highlighted in red. Black arrows indicate reactions that are used in multiple pathways. Dashed lines connect common intermediates found in the THF pool. "glc" indicates glucose, "3PG" indicates 3-phosphoglycerate, "APS" indicates adenosine-5'-phosphosulfate, "PAPS" indicates 3'-phosphoadenosine-5'-phosphosulfate, and "A-3,5-bP" indicates adenosine-3',5'-bisphosphate.

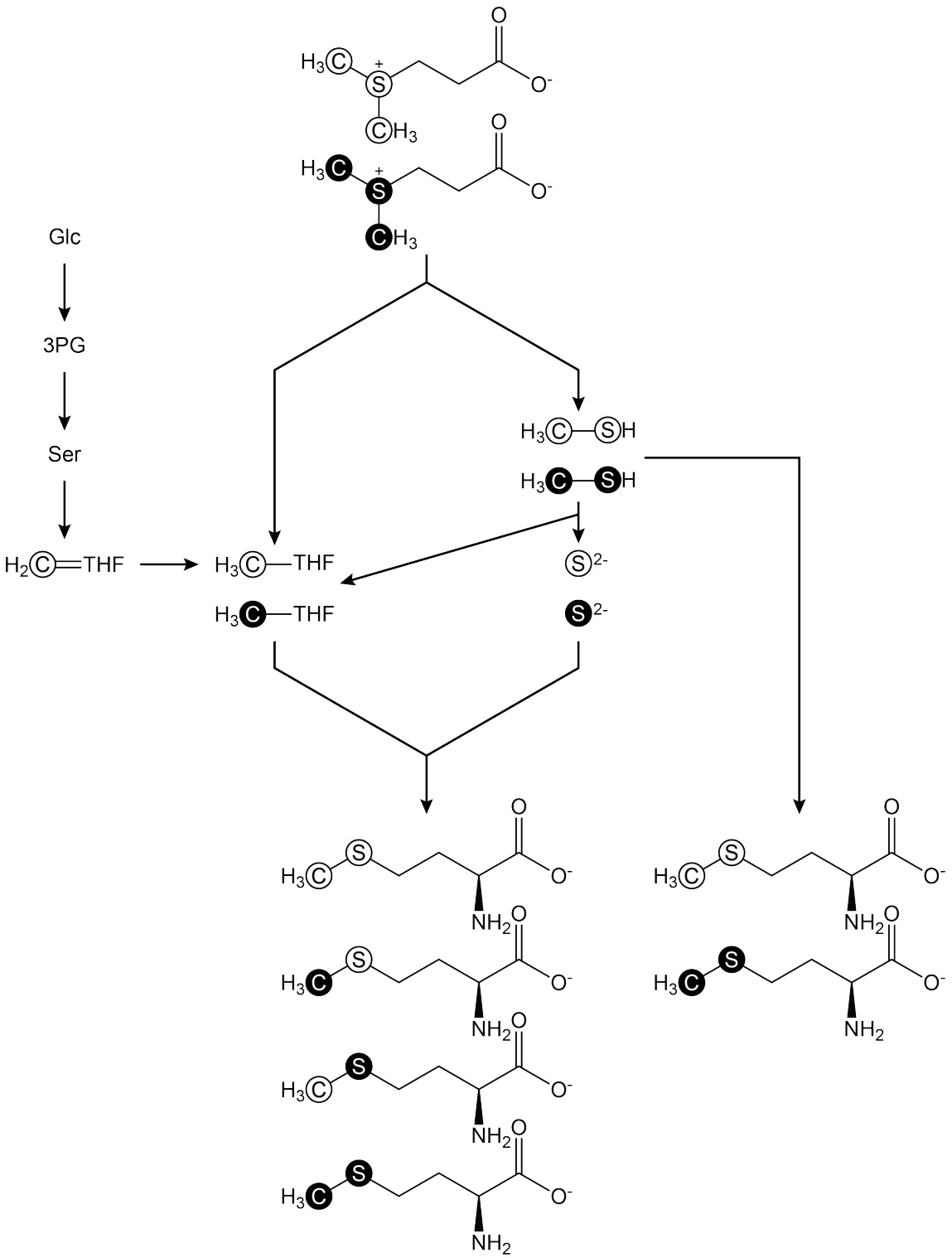

Figure 1-4. Using [^{13}C][^{34}S]DMSP to determine the methionine biosynthetic pathway flux. Pathway represents a simplified version of the pathways depicted in figure 1-3. Atoms with filled circles and white text indicate ^{13}C or ^{34}S. Atoms with hollow circles and black text indicate the natural abundance of isotopes. If the reassembly pathway is used (Fig. 1-3: green lines), then four isotopomers will be formed. If the methanethiol pathway is used (Fig. 1-3: blue lines), then only two isotopomers will be formed.

CHAPTER 2

PHYLOGENOMIC ANALYSES OF A CLADE WITHIN THE ROSEOBACTER GROUP SUGGEST TAXONOMIC REASSIGNMENTS OF SPECIES OF THE GENERA *AESTUARIIVITA*, *CITREICELLA*, *LOKTANELLA*, *NAUTELLA*, *PELAGIBACA*, *RUEGERIA*, *THALASSOBIUS*, *THIOBACIMONAS* AND *TROPICIBACTER*, AND THE PROPOSAL OF SIX NOVEL GENERA[1]

---

[1] Wirth, J.S. and W.B. Whitman. 2018. *International Journal of Systematic and Evolutionary Microbiology*. 68:2393-2411.

Abstract

Roseobacters are a diverse and globally abundant group of *Alphaproteobacteria* within the *Rhodobacteraceae* family. Recent studies and the cophenetic correlations suggest that the 16S rRNA genes are poor phylogenetic markers within this group. In contrast, the cophenetic correlation coefficients of the core-gene average amino acid identity (cAAI) and RpoC protein sequences are high and likely more predictive of relationships. A maximum likelihood phylogenetic tree calculated from 53 core genes demonstrated that some of the current genera were either polyphyletic or paraphyletic. The boundaries of bacterial genera were redefined based upon the cAAI, the percent of conserved proteins (POCP), and phenotypic characteristics and resulted in the following taxonomic proposals. *Loktanella vestfoldensis*, *Loktanella litorea*, *Loktanella maricola*, *Loktanella maritima*, *Loktanella rosea*, *Loktanella sediminilitoris*, *Loktanella tamlensis*, and *Roseobacter sp.* CCS2 should be reclassified into the novel genus *Yoonia*. *Loktanella hongkongensis*, *Loktanella aestuariicola*, *Loktanella cinnabarina*, *Loktanella pyoseonensis*, *Loktanella soesokkakensis*, and *Loktanella variabilis* should be reclassified in the novel genus *Limimaricola*. *Loktanella koreensis* and *Loktanella sediminum* should be reclassified in the novel genus *Cognatiyoonia*. *Loktanella marina* should be reclassified in the novel genus *Flavimaricola*. *Aestuariivita atlantica* should be reclassified in the novel genus *Pseudaestuariivita*. *Thalassobius maritima* should be reclassified in the novel genus *Cognatishimia*. Similarly, *Ruegeria mobilis*, *Ruegeria scottomollicae*, *Ruegeria sp.* TM1040, and *Tropicibacter multivorans* should be reclassified in the genus *Epibacterium*. *Tropicibacter litoreus* and *Tropicibacter mediterraneus* should be reclassified in the genus *Ruegeria*. *Thalassobius abyssi* and *Thalassobius aestuarii* should be reclassified in the genus *Shimia*. *Citreicella aestuarii*, *Citreicella manganoxidans*, *Citreicella marina*, *Citreicella thiooxidans*, *Pelagibaca bermudensis*, and *Thiobacimonas profunda* should be reclassified in the genus

Salipiger. *Nautella italica* should be reclassified in the genus *Phaeobacter*. Because these proposals to reclassify the type and all others species of *Citreicella*, *Nautella*, *Pelagibaca*, and *Thiobacimonas*, these genera are not used in this taxonomy.

Introduction

The roseobacter group form a clade within the *Rhodobacteraceae* family that comprises up to 25 % of the total bacterial community in the surface of the ocean (1-3). The majority of these species are marine in origin, but some genera of terrestrial origin exist (4). They have been isolated from seawater, marine sediments, and biofilms, and are often associated with phytoplankton, macroalgae, and marine animals. The members of this group also possess a great deal of physiological diversity, which is reflected in the large variation in the genome size and gene content (5). Collectively, the roseobacter group is capable of metabolizing a large number of carbon sources, synthesizing B vitamins to facilitate eukaryotic interactions, assimilatory and dissimilatory nitrate reduction, and phototrophic growth (5). The earliest roseobacter has been estimated to exist approximately 260 million years ago, and expansion of its genome around 250 million years ago and subsequent diversification coincided with the emergence of the dinoflagellates and coccolithophores (5).

Genera within the roseobacter group share >89% 16S rRNA sequence similarity, which was the primary basis for assignment to this group (4, 5). However, phylogenetic analyses of recently available genome sequences suggest that 16S rRNA gene sequences lack the resolution for proper phylogenetic reconstruction in this group (1-3, 5, 6). Thus, while the 16S rRNA sequence correctly assigns members to the group, their taxonomic position within the group is uncertain. Thus, there is a need to review the taxonomy and systematics of the roseobacter group.

Methods

Selection of organisms for analysis. A clade from the ARB-Silva 16S rRNA tree (Fig. S2-1) containing 72 strains was selected for analysis (7). Several genera in this clade possessed species that were outside of the clade. These species were added to the analysis so that all species for any genus within the clade were included. This resulted in the selection of 96 species

representing 29 genera, which will be referred to as the "original" data set of roseobacters. Whole-genome sequences were available for 70 of these species on September 13, 2017. All analyses (see below) were first performed with the original data set organisms.

When it became clear that the 16S rRNA gene sequence was a poor predictor of phylogeny within this group, other methods to identify closely related roseobacters were examined. Ultimately, BLASTp to RpoC was used to identify genome sequences of organisms closely related to members of the original roseobacters. Any hits whose bit scores were greater than or equal to that of the intra-genus comparisons for the query organism were then added to the analysis. This resulted in the addition of 12 species representing 5 genera to the data set, 11 of which possessed whole genome sequences. All analyses (see below) were then repeated with this "expanded" data set.

Phylogenetic analyses of 16S rRNA genes. 16S rRNA sequences were downloaded from NCBI on September 13, 2017 (Table S2-1). Sequences were aligned with the RDP Aligner tool (https://rdp.cme.msu.edu) using the RDPX-Bacteria-2 model (8). Alignments were downloaded and manually curated with Mesquite v3.2 to remove alignment errors (9). After curation, the multiple sequence alignment was used to calculate a similarity matrix with the following equation on each pairwise comparison:

$$M / L$$

where M is the number of identical characters excluding gaps, and L is the length of the alignment including gaps but excluding any gaps shared in both alignments. The curated multiple sequence alignment was then used as input for the PhyML 3.0 server (http://www.atgc-montpellier.fr/phyml/) with smart model selection (10, 11). AIC (Akaike information criterion) was used for smart model selection, BIONJ was used to generate the starting tree, NNI (nearest-neighbor interchange) was used for tree improvement, and 1000 bootstrap replicates were

performed to test for branch support. The tree was rooted on the genus "*Ketogulonicigenium"*, which was then pruned from the figures.

Genome sequence selection and analyses. If available, whole genome sequences of the type strains were downloaded from NCBI on September 13, 2017 for the species listed in **Table S1**. For those strains not publicly available on NCBI, whole genomes were downloaded from IMG (https://img.jgi.doe.gov). The core genome, average nucleotide identity (ANI), and core-gene average amino acid identity (cAAI) were calculated using the EDGAR 2.0 server (https://edgar.computational.bio.uni-giessen.de) (12). ANI was calculated as described by Goris *et al.* (13). Briefly, the query genome was cut into 1,020 b fragments, and these were used to search against the reference genome using BLASTN with a 30 % identity cut-off and an aligned sequence length ≥70 % of the query sequence length. The mean percent identity of the best hits for each fragment were then used to calculate the ANI for the pair of organisms (13). For draft genomes, the concatenated genome sequences were used to calculate ANI. The cAAI for any pair of organisms was determined by calculating the mean protein sequence similarity of each of the orthologous genes found in the core genomes, which was 448 genes in the original data set and 417 genes in the expanded data set. Because AAI is typically calculated from all genes shared between a pair of organisms, we have termed this value core-gene AAI (cAAI).

The amino acid sequences of the core genes, *i.e.* the orthologous genes shared in all genomes, identified by EDGAR 2.0 were downloaded. For each core gene, a multiple alignment was produced with MUSCLE v3.8.31 using the default settings (14). The aligned core genes were curated by discarding any core genes whose alignments contained more than 5 % missing data (gaps) for one or more taxa (15). The remaining genes were designated the curated core genes.

For calculation of the core genome maximum likelihood tree, two independent methods were employed. For both methods, the aligned amino acid sequences of the curated core genes were trimmed with trimAl v1.2rev59 using the 'automated1' option and the trimmed alignments were concatenated (16). For the first method, the concatenated alignment was used as input for the PhyML 3.0 server (http://www.atgc-montpellier.fr/phyml/) with smart model selection (10, 11). AIC (Akaike information criterion) was used for smart model selection, BIONJ was used to generate the starting tree, NNI (nearest-neighbor interchange) was used for tree improvement, and 100 bootstrap replicates were performed to test for branch support. For the second method, the concatenated alignment was used as input for IQ-TREE v1.6.3 with the TESTONLY model, which determined the L+F+I+G4 as the best model. The concatenated alignment was then used as input for IQ-TREE v.1.6.3 using L+F+I+G4 as the model and 100 bootstrap replicates as the statistical test (17, 18). Both trees were rooted on the genus "*Ketogulonicigenium*", which was later pruned from the figures.

Calculation of POCP. The percentage of conserved proteins (POCP) was calculated as described by Qin *et al*. 2014 (19). The amino acid sequences of all coding sequences (CDS) in each genome were downloaded from the EDGAR 2.0 server. For each species, makeblastdb v2.6.0 was used to generate a protein database from a fasta file containing the amino acid sequences of all the CDS in the genome. Using a custom PERL script, an all versus all BLASTp (v2.6.0) was performed for all pairwise combinations of species using an evalue cutoff 10^{-5}, 50 % query coverage per high-scoring segment pair (HSP), and ≥40 % identity (19). To calculate the POCP for each pair of species, the following equation was employed:

$$(C_1 + C_2)/(T_1 + T_2)$$

where C_1 is the number of conserved CDS in species 1, C_2 is the number of conserved CDS in species 2, T_1 is total number of CDS in species 1, and T_2 is the total number of CDS in species 2

(19). A POCP similarity matrix was generated by calculating the POCP for all pairwise combinations of all species.

Cophenetic correlation coefficients. Similarity matrices were converted into dissimilarity matrices by subtracting the fractional similarity from 1. For each metric, the observed dissimilarity matrix was used to produce a UPGMA tree using the 'upgma' function from the R package phangorn (20). The resulting tree was then the input for the function 'cophenetic' in R, which calculated a dissimilarity matrix composed of the cophenetic distances between taxa. The Pearson correlation coefficient between the observed dissimilarity distance matrix and the cophenetic dissimilarity matrix was calculated in R with the function 'cor'.

For each of the 65 curated, core genes conserved in the genomes of the original data set, a similarity matrix was calculated using the following equation on each pairwise comparison:

$$M / L$$

where M is the number of identical characters excluding gaps, and L is the length of the alignment including gaps but excluding any gaps present in both alignments. The resulting similarity matrices were used to determine the cophenetic correlation coefficient for each gene as described above.

Phylogenetic analysis of RpoC sequences. The RpoC sequences downloaded from the EDGAR 2.0 server were aligned with MUSCLE v3.8.31 using the default settings (14). The multiple sequence alignment was then used as input for the PhyML 3.0 server (http://www.atgc-montpellier.fr/phyml/) with smart model selection (10, 11). AIC (Akaike information criterion) was used for smart model selection, BIONJ was used to generate the starting tree, NNI (nearest-neighbor interchange) was used for tree improvement, and 1000 bootstrap replicates were performed to test for branch support. The tree was rooted on the genus "*Ketogulonicigenium"*, which was then pruned from the figures.

Selection of phenotypes for delimiting genera. For each organism, the original isolation paper was used to retrieve phenotypic data. If data were missing for specific characters, then other sources were used. Several characters were collected for all organisms including Gram type, morphology, motility, flagellation, growth conditions, reduction of nitrate, catalase activity, oxidase activity, DNA G+C content, isolation habitat, and results from the API-ZYM system. Individual characters were identified that appeared to vary with the core-genome phylogeny and were then used to inform taxonomic assignments.

Results and Discussion

Cophenetic correlation coefficients. Previous studies suggested that trees based on 16S rRNA gene sequences did not accurately reflect the phylogeny of the members of the roseobacter group (1, 3). Consistent with this observation, a maximum-likelihood tree based on 16S rRNA sequences exhibited low bootstrap support for many of the branches and was polyphyletic for several genera (Fig. 2-1). In order to further test if 16S rRNA gene sequences were a suitable indicator of phylogeny, the cophenetic correlation coefficient was calculated from a 16S rRNA gene sequence similarity matrix. Briefly, this coefficient describes the correlation between the observed evolutionary distances and the distances implied by a UPGMA tree (21, 22). If a certain character is ultrametric and likely to vary in a clock-like fashion, then the cophenetic correlation coefficient is expected to be close to 1. In guidelines on numerical taxonomy, Sneath and Sokal (21) recommend a cophenetic correlation coefficient of at least 0.8 for construction of a tree. However, Keswani and Whitman (22) suggest a more conservative value of 0.9 for the 16S rRNA gene sequences based upon correlations with DNA-DNA hybridization values. For the roseobacter group, the cophenetic correlation coefficient for the 16S rRNA gene sequence similarities was 0.72, suggesting that it was nonultrametric and a poor indicator of phylogenetic relationships (Table 2-1). Because of its low cophenetic correlation coefficient, 16S rRNA gene

sequence identity was not further considered when evaluating the taxonomic placement of the organisms in this study except when assigning organisms whose whole genome sequences were unavailable (Table S2-1).

In contrast, the cophenetic correlation coefficient was higher for the core-gene Average Amino acid Identity (cAAI), with a value of 0.98. The Percentage Of Conserved Proteins (POCP) and Average Nucleotide Identity (ANI) similarity matrices also yielded cophenetic correlation coefficients of 0.89 and 0.92, respectively (Table 2-1). Despite the high cophenetic correlation coefficient of ANI, it was not considered because it is unreliable when its values are below 80 %, and almost all of the ANI comparisons in this study were below this value (Fig. S2-2) (13). In part because of its high cophenetic correlation coefficient, cAAI was expected to accurately reflect the phylogenetic relationships between members of the roseobacter group and was used to delineate taxa (see below).

Core genome phylogeny. The EDGAR 2.0 server (edgar.computational.bio.uni-giessen.de) identified 417 genes conserved in the 81 taxa in this study with whole genome sequences available, but only 53 of the 417 genes had fewer than 5 % gaps in their alignments (12). A maximum likelihood tree was constructed using PhyML server 3.0 from the orthologues of these 53 genes, and the topology of the core gene tree was quite different from that of the 16S rRNA gene tree (Fig. 2-2). In addition, the clades within the core tree were also observed in a neighbor-joining tree based on the aligned sequences of all 417 core genes, although the deeper branches were not always congruent (data not shown). This tree was also largely congruent with a maximum likelihood tree constructed using IQ-TREE with only one minor change to the deep branches (data not shown). The topology also agreed with that of Simon *et al.* (3), which included 106 sequenced *Rhodobacteraceae* genomes, 73 of which were in the roseobacter group. Thus, the core gene tree appeared to present an accurate phylogeny for this group.

The core gene tree resolved the paraphyly of the genera *Leisingera* and *Phaeobacter* observed in the 16S rRNA gene tree but did not resolve the inconsistencies between the phylogeny and the taxonomy in many of the other genera. *Aestuariivita*, *Roseobacter*, *Ruegeria*, *Thalassobius*, and *Tropicibacter* all appeared to be polyphyletic. In addition, four major clades were present within the *Loktanella* genus. Lastly, a number of species currently classified in different genera were closely related in clades with high bootstrap support (Fig. 2-2). Thus, the classifications of species within this group were not consistent with the phylogeny.

Identification of RpoC as a phylogenetic marker. Because the 16S rRNA gene sequences proved to be an unreliable phylogenetic marker within this group, it was unclear if the original data set contained all closely related organisms. In order to ensure that close relatives of the roseobacters had not been omitted, a more robust phylogenetic marker was identified. The ultrametric properties of the 65 curated, core genes identified in the original data set were screened for genes that could be used to identify close relatives of this group. For that reason, their cophenetic correlation coefficients were calculated from similarity matrices, and 41 of these genes had cophenetic correlation coefficients greater than 0.9. In addition, three proteins, RpoC, an uncharacterized acyl-CoA synthetase, and SucA also had high correlations of 0.94, 0.91, and 0.90, respectively, with the cophenetic distances of the curated core-gene tree. In fact, RpoC protein sequence similarity was more highly correlated with the maximum likelihood tree than 16S rRNA sequence percent identity, ANI, or POCP (Table S2-2). RpoC sequence percent identity also had the highest correlation to cAAI of all other metrics in this study ($r = 0.93$) (Fig. S2-4, Table S2-3). Furthermore, other studies have proposed that the related RpoB protein be used in addition to 16S rRNA gene sequences when determining phylogenetic placement in the absence of whole genome data (23-25). Therefore, RpoC was used to search the data bases for additional genome sequences of related organisms.

Analyses of the original roseobacter data set identified eight clades of potentially novel genera that lacked the type species of a described genus. The RpoC sequences of these organisms were used to search for genome sequences from related organisms. Included were the RpoC protein sequences from all the *Loktanella* species except *Loktanella salsilacus*, *Loktanella atrilutea*, and *Loktanella fryxellensis*, which identified *Pseudooctadecabacter jejudonensis*, *Roseobacter* sp. CCS2, and the two *Wenxinia* species. RpoC sequences from *Thalassobius abyssi*, *Thalassobius aestuarii*, and *Thalassobius maritimus* identified several members of the genus *Shimia*. RpoC sequences from *Ruegeria mobilis*, *Ruegeria scottomollicae*, and *Ruegeria* sp. TM1040 identified *Epibacterium ulvae*. The RpoC sequence from *Aestuariivita atlantica* did not identify closely related genera that were not already present in the data set. From each of the five newly identified genera, all validly published species were added to data set, resulting in the addition of 12 species, and whole genome sequences were available for 11 of these (Table S2-1). These organisms were termed the "expanded" data set of roseobacters. Unless specified differently, all analyses shown here were performed with this expanded data set.

Delimiting genera within the roseobacter group. While the core genome phylogeny provided a good measure of the phylogenetic relationships within this group, reorganization of the taxonomy also required setting criteria for the amount of diversity allowed within genera. A genus boundary of 50 % POCP has been proposed (19). However, over 80 % of the POCP values for the inter-generic comparisons were greater than 50 % **(**Fig. 2-3a, Fig. S2-2), and this boundary would collapse nearly the entire roseobacter group into a single genus. Thus, this universal cut-off for prokaryotic genera of 50 % POCP cannot be applied to the roseobacter group. Similar studies have also concluded that the 50 % POCP boundary was too conservative for genus-level circumscription in the *Bacillaceae*, *Burkholderiaceae*, and *Neisseriaceae* (26-28).

This implies that a universal cut-off of 50 % POCP is inappropriate for delimiting many bacterial genera.

In order to understand these discrepancies with Qin *et al.* (19), their data set was examined more closely. When determining the genus boundary, they only included genera whose 16S rRNA gene sequences produced a monophyletic clade within a neighbor-joining tree (19). Because of this restriction, only 17 genera were used to evaluate the POCP boundary. Importantly, the data set was biased towards the *Lactobacillales*, which made up the majority of the comparisons examined. In fact, 11 of the 12 orders/families investigated by Qin *et al.* had inter-genus comparisons above 50 % POCP, the only exception being the *Thermoanaerobacteraceae* (19). Thus, while POCP likely provides useful information about taxonomic relationships, a cut-off defined by a single value is unlikely to be a universal threshold for delimiting prokaryotic genera.

Previous studies have shown that, although AAI is a powerful tool for delimiting taxonomic ranks, prokaryotic taxa exhibit a continuum of AAI values, and discrete boundaries are difficult to define (29). Instead, a gradient has been proposed to delimit genera (30). This gradient is defined by two values: a minimum value below which species should be separated into different genera and a maximum value above which species should be combined into the same genus. Luo *et al.* (30) showed that AAI values between members of related but different genera typically vary between 60-80 % and do not exceed 85 %. While, the current study used cAAI instead of AAI, the values did not differ greatly. There was no difference in the cophenetic correlation coefficients for cAAI or AAI, and the values had a Pearson correlation coefficient of 0.98 to one another. Furthermore, the criteria proposed by Luo *et al*. (30) were consistent with the cAAI values of the recent taxonomic rearrangements proposed by Breider *et al.* (6) for the

roseobacter genera *Leisingera* and *Phaeobacter* (Fig. 2-3a). Thus, these recommendations were adopted for this study.

In support of this approach, a UPGMA trees based on cAAI were congruent in terms of both distance and topology with the maximum likelihood tree based on whole genome sequences (data not shown). Not only did cAAI have a high cophenetic correlation coefficient (r_{ccc} = 0.98) indicating that it was ultrametric, but it also was strongly correlated with the cophenetic distances calculated from the maximum likelihood tree of the core genome (r = 0.95, Table S2-2), supporting the conclusion that the cAAI tree was topologically similar to the maximum likelihood tree. In contrast, the 16S rRNA gene sequence percent identity, ANI, and POCP were not well correlated with the cophenetic distances calculated from the maximum likelihood tree of the core genome and were not suitable as the primary indicators of generic thresholds (Table S2-2).

Thus, the delineation of genera considered the following factors. All proposed changes to the taxonomy had to remain congruent with the phylogeny determined from the core-gene tree. The POCP was correlated with the cAAI (r = 0.82) and was considered an important measure of relatedness (Fig. 2-3, Fig. S2-4c). However, the POCP varied by ~0.15 at cAAI values near 0.80. Thus, for species with cAAI values between 0.80 and 0.85, low POCP values were considered as evidence for classification in different genera. Furthermore, the phenotypic and chemotaxonomic characters of clades whose cAAI values were near the boundaries were examined in closer detail. In this regard, the fatty acid compositions and G+C content for the members of the roseobacter group were very similar, and the polar lipid profiles were often ambiguous due to differences in reporting and conflicting results reported by different authors. Because of this, these characters were not used in evaluating the taxonomy (data not shown). Finally, if a satisfactory answer was

not clear after examining the cAAI, POCP, and the phenotypic data, then priority was placed on preserving the current taxonomy.

Inter-genera comparison with cAAI greater than 85 %. Of the 2,982 inter-genus comparisons in the current taxonomy, only 18 comparisons had cAAI values greater than 85 %, and only 8 of those 18 comparisons had cAAI values greater than 86 % (Fig. 2-3a, Fig. S2-2). All 8 of these comparisons were confined to three clades on the tree: the *Nautella*/*Phaeobacter* clade, the *Citreicella/Pelagibaca/Thiobacimonas* clade, and the clade containing *Roseobacter* sp. CCS2 and several *Loktanella* species (Fig. 2-3a). All three of these clades formed monophyletic units with high bootstrap support and had minimum POCP values greater than 0.68 (Fig. 2-2). Based on this, we propose that *Nautella italica* be moved into the genus *Phaeobacter* and be renamed as *Phaeobacter italicus*. We also propose that *Roseobacter* sp. CCS2 be moved into the same genus as *Loktanella litorea*, *Loktanella maricola*, and *Loktanella rosea*. Although the phylogenetic tree and cAAI indicated that *Citreiclla thiooxidans*, *Pelagibaca bermudensis*, and *Thiobacimonas profunda* should be joined into a single genus, it was unclear whether or not this genus should also include *Citreicella marina* and *Salipiger mucosus* (Fig. 2-2, Fig. 2-4d). The minimum POCP value for the clade dropped from 0.68 to 0.57 when *Salipiger mucosus* was included but remained unchanged upon addition of *Citreicella marina*. However, none of these species are flagellated, and most can grow on >10 % NaCl, utilize sugars, and exhibit chemoorganoheterotrophic and chemolithoheterotrophic growth (Fig. 2-4d). Therefore, we propose that *Citreicella marina*, *Citreicella thiooxidans*, *Pelagibaca bermudensis*, and *Thiobacimonas profunda* be moved into the genus *Salipiger* as *Salipiger marinus*, *Salipiger thiooxidans*, *Salipiger bermudensis*, and *Salipiger profundus*, respectively. Because this classification removes the type and only species from the genera *Pelagibaca,* and *Thiobacimonas,* these genera are not used in this taxonomy. Similarly, while the type species of

Citreicella is also reclassified, genome sequences are not available for all species. Reclassification of the remaining species is discussed below.

Intra-genus comparisons with cAAI less than 80 %. Although 136 of the 258 intra-genus comparisons had cAAI values below 80 %, all of these comparisons belonged to six genera: *Aestuariivita*, *Loktanella*, *Roseobacter*, *Ruegeria*, *Thalassobius*, and *Tropicibacter* (Fig. 2-3b). With the exception of *Loktanella*, these genera were polyphyletic (Fig. 2-2). For the genus *Aestuariivita*, on the basis of the low cAAI and POCP, we propose that *Aestuariivita atlantica* be reassigned to the novel genus *Pseudaestuariivita* with the type species *Pseudaestuariivita atlantica*.

In the case of *Loktanella*, there were two possible solutions (Fig. 2-4a). In both solutions, the cAAI and phenotypic data supported moving all members out of *Loktanella* except for the clade containing the type species, *Loktanella salsilacus* (Fig. 2-4a). In both solutions, *Loktanella hongkongensis*, *Loktanella cinnabarina*, *Loktanella pyoseonensis*, and *Loktanella soesokkakensis* comprised a distinct phylogenetic clade, and we propose that these species be reclassified in the novel genus *Limimaricola* with *Limimaricola hongkongensis* as the type species. Similarly, we propose placing *Loktanella marina* in the novel genus *Flavimaricola*. For the remaining *Loktanella* species, they could either be grouped into a single novel genus or split into two novel genera. The minimum cAAI values for the individual clades were 0.80 and 0.82 but dropped to 0.78 when combined. Similarly, the minimum POCP values for these two clades were 0.69 and 0.60, but when combined dropped to 0.59. Moreover, nitrate reduction and gelatinase activity were present in one clade but absent in the other (Fig. 2-4a). After examining the core-gene phylogeny, cAAI, POCP, and phenotypic data, we propose that *Loktanella vestfoldensis*, *Loktanella litorea*, *Loktanella maricola*, *Loktanella maritima*, *Loktanella rosea*, *Loktanella sediminilitoris*, *Loktanella tamlensis*, and *Roseobacter* sp. CCS2 be moved into the novel genus

Yoonia with *Yoonia vestfoldensis* as the type species (Fig. 2-4a: solution 1). In addition, we propose that *Loktanella koreensis* and *Loktanella sediminum* be moved into the novel genus *Cognatiyoonia* with the former as the type species.

The cAAI was ambiguous about moving *Ruegeria pomeroyi* and *Ruegeria marina* into a novel genus. When excluded, the minimum cAAI and POCP values of the *Ruegeria* clade were 0.88 and 0.69, respectively. However, these values only dropped to 0.83 and 0.63, respectively, when *Ruegeria pomeroyi* and *Ruegeria marina* were included (Fig. 2-4b: solution 2). Furthermore, these organisms do not exhibit enough phenotypic diversity to justify removing them from the clade (Fig. 2-4b). In order to remain conservative to the current taxonomic classification, *Ruegeria pomeroyi* and *Ruegeria marina* were not reclassified at this time.

In contrast, the core-gene phylogeny (Fig. 2-2) indicated that *Ruegeria mobilis*, *Ruegeria scottomollicae*, and *Ruegeria* sp. TM1040 should be reclassified. The minimum cAAI and POCP values for the genus were 0.79 and 0.57, respectively, when these organisms were included in *Ruegeria*. The phenotypic data also supported this reclassification. Specifically, the presence of polar flagella was conserved in this group but was absent in all *Ruegeria* except for *Ruegeria pomeroyi* (Fig. 2-4b). However, the cAAI and POCP were ambiguous as to whether these organisms should form a novel genus or join the existing genus *Epibacterium* (Fig. 2-4b). Because all four species possessed polar flagellation and were isolated from similar environments, we propose that *Ruegeria mobilis*, *Ruegeria scottomollicae*, and *Ruegeria* sp. TM1040 should be moved into the genus *Epibacterium* (31-35).

The core-gene phylogeny, cAAI, and POCP indicated that *Tropicibacter litoreus* and *Tropicibacter multivorans* should be moved out of the genus *Tropicibacter*, but their placement was ambiguous. When *Tropicibacter litoreus* was included within the *Ruegeria*, the minimum cAAI and POCP of the genus remained unchanged (Fig. 2-4b: solution 3). Phenotypically, in

particular its lack of flagellation, it was similar to the other members of the *Ruegeria* genus (Fig. 2-4b). Likewise, the core-gene phylogeny (Fig. 2-2), cAAI, and POCP indicated that *Tropicibacter multivorans* was more closely related to *Ruegeria mobilis*, *Ruegeria scottomollicae*, *Ruegeria* sp. TM1040, and *Epibacterium ulvae* than other *Ruegeria*. The presence of polar flagella in *Tropicibacter multivorans* further supported this relationship (Fig. 2-4b). Thus, we propose that *Tropicibacter litoreus* be moved into the genus *Ruegeria* as *Ruegeria litorea*, and *Tropicibacter multivorans* be moved into the genus *Epibacterium* as *Epibacterium multivorans*.

Currently, two clades that were well supported by high bootstrap values are classified within the genus *Thalassobius* (Fig. 2-2). The low cAAI and POCP values between these two clades indicated that *Thalassobius aestuarii*, *Thalassobius abyssi*, and *Thalassobius maritimus* should be removed from the genus. However, it was not clear if these organisms should be moved into a novel genus or into the existing genus *Shimia*. The core-gene phylogeny (Fig. 2-2), cAAI, and POCP indicated that *Thalassobius abyssi* and *Thalassobius aestuarii* were closely related to *Shimia*. Phenotypically, these organisms were also very similar, especially in their inability to grow in >7% NaCl and ability to reduce nitrate to nitrite (Fig. 2-4c). Although *Thalassobius maritimus* was phenotypically similar to *Thalassobius abyssi*, *Thalassobius aestuarii*, and the *Shimia* species (Fig. 2-4c), its cAAI was below 0.80 when compared to these species (Fig. 2-4c). Thus, we propose that *Thalassobius abyssi* and *Thalassobius aestuarii* be moved into the genus *Shimia* and that *Thalassobius maritimus* be placed into the novel genus *Cognatishimia* with *Cognatishimia maritima* as the type species.

Placement of organisms without whole-genome sequences. For the genera that were included in this study, a number of species were omitted from the analyses due to the lack of publicly available genome sequences (Table S2-1). Species within genera whose taxonomic

assignments remained unchanged were not investigated further. However, several species were within genera where the taxonomy was changed, including two species from *Citreicella*, four species from *Loktanella*, one species from *Shimia*, two species from *Thalassobius*, and one species from *Tropicibacter*. In order to determine the placement of these species, the maximum likelihood tree of 16S rRNA gene sequences was compared to the phenotypic data (Fig. 2-1, Fig. S2-3). While the 16S rRNA gene sequence similarity was a poor phylogenetic marker for this group (Table 2-1, Fig. S2-4a), very high 16S rRNA gene sequence similarity was a strong predictor of a cAAI >0.80. For instance, the cAAI was ≥0.80 for 11 out of 12 comparisons with 16S rRNA sequence similarities ≥97 %. However, if the 16S rRNA sequence similarity was 95-97 %, only 55 out of 108 cAAI values were ≥0.80.

Because *Citreicella thiooxidans* and *Citreicella marina* were moved into *Salipiger*, the placement of the remaining two species, *Citreicella aestuarii* and *Citreicella manganoxidans*, was unclear. The 16S rRNA tree placed both of these species into the same clade as *C. thiooxidans* and *C. marina* (Fig. 2-1), and their phenotypes were similar to that of the other *Citreicella* and *Salipiger* species (Fig. S2-3d). Although whole genome analyses were not performed on *C. aestuarii*, its RpoC protein sequence was available (Table S2-1). A maximum likelihood tree based on the RpoC protein sequences clustered *C. aestuarii* with the other proposed members of *Salipiger* and provided strong evidence that it should be placed in this genus (Fig. S2-5). The 16S rRNA sequence similarity of *C. manganoxidans* with other proposed members of *Salipiger* was <97 % and did not provide strong support for either the inclusion or exclusion from this genus. To maintain the relationship within these species when other evidence was ambiguous or lacking, we propose that *C. aestuarii* and *C. manganoxidans* be moved into the genus *Salipiger*. Because *Citreicella thiooxidans* is the type species of the genus, the genus *Citreicella* is not used in the proposed taxonomy.

The genus *Loktanella* was divided into five different genera, and the placement of the four species without whole genome sequences was unclear. The 16S rRNA tree indicated that *Loktanella aestuariicola* and *Loktanella variabilis* were closely related to the members of the proposed genus *Limimaricola* (Fig. 2-1), and they each possessed >97 % sequence similarity to at least one member of that genus. Moreover, their phenotypes were significantly different from that of the remaining members of the genus *Loktanella* (Fig. S2-3a). Thus, we propose that *L. aestuariicola* and *L. variabilis* be moved into the genus *Limimaricola*. The 16S rRNA tree indicated that *Loktanella agnita* might be related to either the proposed genera *Yoonia* (*L. vestfoldensis*) or *Flavimaricola* (*L. marina*), although the sequence similarities were <97 % to any member of those groups. Although the phenotype of *L. agnita* was similar to that of *L. marina* (Fig. S2-3a), the reclassification of *L. agnita* into *Flavimaricola* is not proposed because of the ambiguity the 16S rRNA gene tree. Similarly, *Loktanella ponticola* 16S rRNA gene sequence was similar to that of the proposed genus *Cognatiyoonia* (*L. koreensis*) but the phenotype did not justify its reclassification. Thus, in order to remain conservative with the current taxonomy, we do not propose any taxonomic reassignments for *L. agnita* or *L. ponticola* at this time. When the genome sequences for these organisms become available, reclassification may be justified.

The genus *Thalassobius* was divided into three genera, and the placement of *Thalassobius aquaeponti* and *Thalassobius litorarius* was unclear. The 16S rRNA gene tree indicated that *T. aquaeponti* was closely related to *Thalassobius aestuarii*, with which it shared >97 % sequence similarity (Fig. 2-1). The phenotypic data, especially the inability to grow on >7% NaCl and the ability to reduce nitrate to nitrite, supported this conclusion (Fig. S2-3c). Thus, we propose that *T. aquaeponti* be moved into the genus *Shimia* along with *T. aestuarii*. The 16S rRNA gene tree did not place *Thalassobius litorarius* near any of the *Thalassobius* or

Shimia species (Fig. 2-1), and its phenotypic data did not provide compelling evidence to remove it from *Thalassobius* (Fig. S2-3c). Thus, in order to remain conservative with the current taxonomy, we do not propose reclassification of *T. litorarius* at this time. However, reclassification may be justified when whole genome sequences become available.

We proposed the reclassification of two species of the genus *Tropicibacter* into the genera *Ruegeria* and *Epibacterium*, but a whole genome sequence was not available for *Tropicibacter mediterraneus*. However, this species possessed >97 % 16S rRNA sequence similarity to *Tropicibacter litoreus*, which we proposed to be reclassified with *Ruegeria*. The phenotypic data, in particular the presence of peritrichous flagellation (Fig. S2-3b), further supports this reclassification. Thus, we propose that *T. mediterraneus* be moved into the genus *Ruegeria* as *Ruegeria mediterranea*.

Applying this method to other prokaryotic genera. The methods used to delimit genera in the roseobacter group were relatively simple, mostly automated, and easy to reproduce without extensive experience in bioinformatics. Because 16S rRNA gene sequences have been used to assign many prokaryotes to their respective genus, many existing genera may need to be reevaluated. In an effort to assist other researchers attempting to employ the workflow used in this paper, we have added a flow chart detailing the algorithm (Fig. S2-6).

Proposed taxonomic changes

Description of *Cognatishimia* gen. nov. *Cognatishimia* (Cog.na.ti.shi'mi.a. L. masc. adj. *cognatus* relative, related, kindred; N.L. fem. n. *Shimia* a bacteria generic name; N.L. fem. n. *Cognatishimia* related to *Shimia*.

Cells are Gram-negative, strictly aerobic rods. Motile by means of polar flagella. Catalase- and oxidase-positive. Reduces nitrate to nitrite. Moderately halophilic but NaCl is not required for growth. The predominant ubiquinone is Q-10. The major fatty acid (>10% of the

total fatty acids) is $C_{18:1}\omega 7c$. The major polar lipids are phosphatidylcholine, phosphatidylethanolamine, and phosphatidylglycerol. The DNA G+C content is 57 mol%. A member of the family *Rhodobacteraceae*, class *Alphaproteobacteria* according to 16S rRNA gene sequence analysis and phylogenomics. The type species (and sole species) for the genus is *Cognatishimia maritima*.

Description of *Cognatishimia maritima* comb. nov. *C. maritima* (ma.ri'ti.ma. L. fem. adj. *maritima* of the sea, referring to the marine environment). Basonym: *Thalassobius maritimus* Park *et al.* 2012.

The description is the same as for *T. maritimus* (36). Phylogenetic analysis of the core genome provided strong evidence for placement of this species in the novel genus *Cognatishimia*. The type strain is GSW-M6^T (DSM 28223^T, KCTC 23347^T, CCUG 60021^T).

Description of *Cognatiyoonia* gen. nov. *Cognatiyoonia* (Cog.na.ti.yoo'ni.a. L. masc. adj. *cognatus* relative, related, kindred; N.L. fem. n. *Yoonia*, a bacteria generic name; N.L. fem. n. *Cognatiyoonia* relative of *Yoonia*).

Cells are Gram-negative, aerobic, rod- to oval-shaped, and non-motile. Moderately halophilic. Nitrate reduction is positive. The predominant ubiquinone is Q-10. The major fatty acid (>10% of total fatty acids) is $C_{18:1}\omega 7c$. The DNA G+C content is 57.6-60.0 mol%. A member of the family *Rhodobacteraceae*, class *Alphaproteobacteria* according to 16S rRNA gene sequence analysis and phylogeomics. The type species for the genus is *Cognatiyoonia koreensis*.

Description of *Cognatiyoonia koreensis* comb. nov. *C. koreensis* (ko.re.en'sis. N.L. fem. adj. *koreensis* pertaining to Korea, from where the type strain was isolated). Basonym: *Loktanella koreensis* Weon *et al.* 2006.

The description is the same as for *L. koreensis* (37). Phylogenetic analysis of the core genome provided strong evidence for placement of this species in the novel genus *Cognatiyoonia*. The type strain is GA2-M3^T (DSM 17925^T, CIP 109899^T, KACC 11519^T).

Description of *Cognatiyoonia sediminum* comb. nov. *C. sediminum* (se.di'mi.num. L. gen. pl. n. *sediminum* of sediments, pertaining to source of isolation). Basonym: *Loktanella sediminum* Liang *et al.* 2015.

The description is the same as for *L. sediminum* (38). Phylogenetic analysis of the core genome provided strong evidence for the placement of this species in the novel genus *Cognatiyoonia*. The type strain is S3B03^T (DSM 28715^T, JCM 30120^T, MCCC 1K00257^T).

Emended description of the genus *Epibacterium* Penesyan *et al.* 2013. The description is the same as given by Penesyan *et al.* (2013) (31) with the following amendments. Most species are strict aerobes, but some species are capable of facultative anaerobic growth. Most species require sodium ions for growth, but some species can grow in the absence of sodium ions. The major fatty acids (>1%) are $C_{16:0}$, $C_{18:1}\omega7c$, $C_{10:0}$3-OH, and $C_{16:0}$2-OH. The DNA G+C content is 52.6-61 mol%. The type species for the genus is *Epibacterium ulvae*.

Description of *Epibacterium mobile* comb. nov. *E. mobile* (mo'bi.le. L. neut. adj. *mobilis* mobile). Basonym: *Ruegeria mobilis* Marumatsu *et al.* 2007.

The description is the same as for *R. mobilis* (34) emend. (35). Phylogenetic analysis of the core genome provided strong evidence for the placement of this species in the genus *Epibacterium*. The type strain is MBIC01146^T (DSM 23403^T, NBRC 101030^T, CIP 109181^T).

Description of *Epibacterium multivorans* comb. nov. *E. multivorans* (mul.ti.vo'rans. L. adj. *multus* many, numerous; L. v. *vorare* to devour, swallow; N.L. part. adj. *multivorans* devouring many, referring to the utilization of numerous different substrates for growth). Basonym: *Tropicibacter multivorans* Lucena *et al.* 2014.

The description is the same as for *T. multivorans* (39). Phylogenetic analysis of the core genome provided strong evidence for the placement of this species in the genus *Epibacterium*. The type strain is MD5^T (DSM 26470^T, CECT 7557^T, KCTC 23350^T).

Description of *Epibacterium scottomollicae* comb. nov. *E. scottomollicae* (scot.to.mol.li'cae. N.L. gen. n. *scottomollicae* in honor of Dr. Victoria Scotto-Mollica and Dr. Alfonso Mollica, both of whom were pioneers in the field of microbe-induced corrosion of steels and the generation of electroactive seawater biofilms). Basonym: *Ruegeria scottomollicae* Vandecandelaere *et al.* 2008.

The description is the same as for *R. scottomollicae* (35). Phylogenetic analysis of the core genome provided strong evidence for the placement of this species in the genus *Epibacterium*. The type strain is LMG 24367^T (DSM 25328^T, CCUG 55858^T).

Description of *Flavimaricola* gen. nov. *Flavomaricola* (Fla.vi.ma.ri'co.la. L. masc. adj. *flavus* yellow, golden, blonde, flaxen; L. neut. n. *mare, maris* the sea; L. suff –*cola* (from L. n. *incola*) dweller, inhabitant; N.L. masc. n. *Flavimaricola* inhabitant of the Yellow Sea, referring to the isolation environment of the type species).

Cells are Gram-negative, aerobic, non-motile, and rod- to coccoid-shaped. Catalase- and oxidase-positive. Nitrate reduction is positive. Moderately halophilic; requires NaCl to grow. The predominant ubiquinone is Q-10. The major fatty acid (>10% of the total fatty acids) is $C_{18:1}\omega 7c$. The major polar lipids are diphosphatidylglycerol, phosphatidylcholine, phosphatidylglycerol, and an unidentified aminolipid. The DNA G+C content is 62.6 mol%. A member of the family *Rhodobacteraceae*, class *Alphaproteobacteria* according to 16S rRNA gene analysis and phylogenomics. The type species (and sole species) for the genus is *Flavimaricola marinus*.

Description of *Flavimaricola marinus* comb. nov. *F. marinus* (ma.ri'nus. L. masc. adj. *marinus* of or belonging to the sea, marine). Basonym: *Loktanella marina* Jung *et al.* 2016.

The description is the same as for *L. marina* (40). Phylogenetic analysis of the core genome provided strong evidence for the placement of this species in the novel genus *Flavimaricola*. The type strain is MDM-7^T (CECT 8899^T, KCTC 42722^T).

Description of *Limimaricola*, gen. nov. *Limimaricola* (Li.mi.ma.ri'co.la. L. masc. n. *limus* slime, mud, ooze, silt; L. neut. n. *mare, maris* the sea; L. suff *–cola* (from L. n. *incola*) dweller, inhabitant; N.L. masc. n. *Limimaricola* inhabitant of sea slime, referring to the isolation environment of the type species).

Cells are Gram-negative, aerobic, and rod-shaped. Motility is variable among species. Catalase- and oxidase-positive. Moderately halophilic; most species require NaCl for growth. Nitrate reduction is variable among species. The predominant ubiquinone is Q-10. The major fatty acid (>10% of the total fatty acids) is $C_{18:1}\omega 7c$. The major polar lipids (>10% of the total polar lipids) are phosphatidylglycerol, diphosphatidylglycerol, and phosphatidylcholine. The DNA G+C content is 65.9-69.3 mol%. A member of the family *Rhodobacteraceae*, class *Alphaproteobacteria* according to 16S rRNA gene sequence analysis and phylogenomics. The type species for the genus is *Limimaricola hongkongensis*.

Description of *Limimaricola hongkongensis* comb. nov. *L. hongkongensis* (hong.kong.en'sis. N.L. masc. adj. *hongkongensis* referring to Hong Kong, the isolation source of the type strain). Basonym: *Loktanella hongkongensis* Lau *et al.* 2004.

The description is the same as for *L. hongkongensis* (41). Phylogenetic analysis of the core genome provided strong evidence for the placement of this species in the novel genus *Limimaricola*. The type strain is UST950701-009P^T (DSM 17492^T, JCM 12479 ^{T}, NRRL B-41039 ^{T}).

Description of *Limimaricola aestuariicola* comb. nov. *L. aestuariicola* (aes.tu.a.ri.i'co.la. L. neut. n. *aestuarium* tidal flat; L. suff –*cola* (from L. n. *incola*) dweller, inhabitant; N.L. masc. n. *aestuariicola* an inhabitant of a tidal flat). Basonym: *Loktanella aestuariicola* Park *et al.* 2015.

The description is the same as for *L. aestuariicola* (42). Phylogenetic analysis of 16S rRNA gene sequences provided strong evidence for the placement of this species in the novel genus *Limimaricola*. The type strain is J-TF4^T (KCTC 42135^T, NBRC 110408^T).

Description of *Limimaricola cinnabarinus* comb. nov. *L. cinnabarinus* (cin.na.ba.ri'nus. L. n. *cinnabar -aris* cinnabar; L. suff. *–inus –a – um* suffix used with the sense of belonging to; N.L. masc. adj. *cinnabarinus* belonging to cinnabar, referring to the vermilion color of the cells). Basonym: *Loktanella cinnabarina* Tsubouchi *et al.* 2013.

The description is the same as for *L. cinnabarina* (43). Phylogenetic analysis of the core genome provided strong evidence for the placement of this species in the novel genus *Limimaricola*. The type strain is LL-001^T (DSM 29954^T, JCM 18161^T, CECT 8072^T).

Description of *Limimaricola pyoseonensis* comb. nov. *L. pyoseonensis* (pyo.se.o.nen'sis. N.L. masc. adj. *pyoseonensis* pertaining to Pyoseon Beach, Jeju, Republic of Korea, where the type strain was isolated). Basonym: *Loktanella pyoseonensis* Moon *et al.* 2010.

The description is the same as for *L. pyoseonensis* (44). Phylogenetic analysis of the core genome provided strong evidence for the placement of this species in the novel genus *Limimaricola*. The type strain is JJM85^T (DSM 21424^T, KCTC 22372^T).

Description of *Limimaricola soesokkakensis* comb. nov. *L. soesokkakensis* (so.e.so.kkak.en'sis. N.L. masc. adj. *soesokkakensis* pertaining to Soesokkak, from where the type strain was isolated). Basonym: *Loktanella soesokkakensis* Park *et al.* 2013.

The description is the same as for *L. soesokkakensis* (45). Phylogenetic analysis of the core genome provided strong evidence for the placement of this species in the novel genus *Limimaricola*. The type strain is DSSK1-5^T (CECT 8367^T, KCTC 32425^T).

Description of *Limimaricola variabilis* comb. nov. *L. variabilis* (va.ri.a'bi.lis. L. masc. adj. *variabilis* variable, changeable, referring to the variation in colony color observed between the first two known strains). Basonym: *Loktanella variabilis* Park *et al.* 2013.

The description is the same as for *L. variabilis* (46). Phylogenetic analysis of 16S rRNA gene sequences provided strong evidence for the placement of this species in the novel genus *Limimaricola*. The type strain is J-MR2-Y^T (KCTC 42074^T, CECT 8572^T).

Emended description of the genus *Loktanella* Van Trappen *et al.* 2004 emend. Moon *et al.* 2010 emend. Lee 2012 emend. Tsubouchi *et al.* 2013. The description is as given by Van Trappen *et al.* 2004 (47), Moon *et al.* 2010 (44), Lee 2012 (48) and Tsubouchi *et al.* 2013 (43) with the following amendment. Moderately halophilic, but most species do not require NaCl for growth. Nitrate reduction is variable. The DNA G+C content is 59.1-66.4 mol%. The type species for the genus is *Loktanella salsilacus*.

Emended description of the genus *Phaeobacter* Martens *et al.* 2006 emend. Breider *et al.* 2014. The description is as given by Martens *et al.* 2004 (49) and Breider *et al.* 2014 (6) with the following amendment. Colonies are beige to dark brown. Production of a diffusible brownish pigment has been reported in some species. Moderately halophilic; NaCl is required for growth. The optimum salinity range is 2-3% NaCl. For the species where it has been measured, production of tropodithietic acid is present. Facultative anaerobic growth by reduction of nitrite is variable. The major fatty acid (>10% of the total fatty acids) is $C_{18:1}\omega 7c$. The DNA G+C content is 55.7-61.0 mol%. The type species for the genus is *Phaeobacter gallaeciensis*.

Description of *Phaeobacter italicus* comb. nov. *P. italicus* (i.ta'li.cus. L. masc. adj. *italicus* from Italy, where this species was first isolated). Basonym: *Nautella italica* Vandecandelaere *et al.* 2009.

The description is the same as for *N. italica* (50). Phylogenetic analysis of the core genome provided strong evidence for the placement of this species in the genus *Phaeobacter*. The type strain is LMG 24365^T (CECT 7645^T, CCUG 55857 ^{T}).

Description of *Pseudaestuariivita* gen. nov. *Pseudaestuariivita* (Pseud.aes.tu.a.ri.i.vi'ta. Gr. adj. *pseudes* false; N.L. fem. n. *Aestuariivita* a bacteria generic name; N.L. fem. n. *Pseudaestuariivita* false *Aestuariivita*).

Cells are Gram-negative, aerobic, oval- to rod-shaped, and non-motile. Catalase- and oxidase-positive. Nitrate reduction is negative. The predominant ubiquinone is Q-10. The major fatty acid (>10% of the total fatty acids) is summed feature 8 ($C_{18:1}\omega7c/\omega6c$). The polar lipids are diphosphatidylglycerol, phosphatidylcholine, phosphatidylglycerol, nine unidentified phospholipids, one unidentified aminolipid, and two unidentified lipids. The DNA G+C content is 65.5 mol%. The genus represents a distinct branch within the family *Rhodobacteraceae* of the class *Alphaproteobacteria* based on 16S rRNA gene sequence analysis and phylogenomics. The type species (and sole species) for the genus is *Pseudaestuariivita atlantica.*

Description of *Pseudaestuariivita atlantica* comb. nov. *P. atlantica* (at.lan'ti.ca. L. fem. adj. *atlantica* referring to the Atlantic Ocean, where the strain was isolated). Basonym: *Aestuariivita atlantica* Li *et al.* 2015.

The description is the same as for *A. atlantica* (51). Phylogenetic analysis of the core genome provided strong evidence for the placement of this species in the novel genus *Pseudaestuariivita*. The type strain is 22II-S11-z3^T (KCTC 42276^T, MCCC 1A09432^T).

Emended description of the genus *Ruegeria* Uchino *et al.* 1998 emend. Martens *et al.* 2006 emend. Yi *et al.* 2007. The description is as given by Uchino *et al.* 1998 (52), Martens *et al.* 2006 (49), and Yi *et al.* 2007 (53) with the following amendment. Most species are strict aerobes, but some species can grow facultative anaerobically via nitrate reduction. Accumulation of polyhydroxybutyrate is variable. Motility is variable; motile species are motile by means of polar flagellation or peritrichous flagellation. Some species require sea salts for growth, but others can grow in the presence of Na^+ and/or Mg^{2+}. The major fatty acid (>10% of the total fatty acids) is $C_{18:1}\omega7c$ or summed feature 8 ($C_{18:1}\omega7c/\omega6c$). The type species for the genus is *Ruegeria atlantica*.

Description of *Ruegeria litorea* comb. nov. *R. litorea* (li.to're.a. L. fem. adj. *litorea* of the shore). Basonym: *Tropicibacter litoreus* Lucena *et al.* 2014.

The description is the same as for *T. litoreus* (54). Phylogenetic analysis of the core genome provided strong evidence for the placement of this species in the genus *Ruegeria*. The type strain is R37^T (CECT 7639^T, KCTC 23353^T).

Description of *Ruegeria mediterranea* comb. nov. *R. mediterranea* (me.di.ter.ra'ne.a. L. fem. adj. *mediterranea* pertaining to the Mediterranean Sea). Basonym: *Tropicibacter mediterraneus* Lucena *et al.* 2014.

The description is the same as for *T. mediterraneus* (54). Phylogenetic analysis of 16S rRNA gene sequences and phylogenomics provided strong evidence for the placement of this species in the genus *Ruegeria*. The type strain is M17^T (CECT 7639^T, KCTC 23058^T).

Emended description of the genus *Salipiger* Martinez-Cánovas *et al.* 2004. The description is as given by Martinez-Cánovas *et al.* (55) with the following amendments. Motility is variable; motile species are motile by means of gliding or lateral flagella. Flagellation is variable. Chemoorganoheterotrophic and chemolithoheterotrophic growth is observed. Most

species are aerobic, but some species can grow facultative anaerobically by reducing nitrate. The presence of polyhydroxy acids varies between species. Nutritional and biochemical versatility varies between species. The principal fatty acid (>10% of the total fatty acids) is $C_{18:1}\omega 7c$. The DNA G+C content is 64.5-69.2 mol%. The type species for the genus is *Salipiger mucosus*.

Description of *Salipiger aestuarii* comb. nov. *S. aestuarii* (aes.tu.a'ri.i. L. gen. n. *aestuarii* of a tidal flat, from where the organism was isolated). Basonym: *Citreicella aestuarii* Park *et al.* 2011.

The description is the same as for *C. aestuarii* (56). Phylogenetic analysis of 16S rRNA gene sequences provided strong evidence for the placement of this species in the genus *Salipiger*. The type strain is AD8^T (DSM 22011^T, KACC 13699^T).

Description of *Salipiger bermudensis* comb. nov. *S. bermudensis* (ber.mu.den'sis. N.L. masc. adj. *bermudensis* from Bermuda). Basonym: *Pelagibaca bermudensis* Cho and Giovannoni 2006.

The description is the same as for *P. bermudensis* (57). Phylogenetic analysis of the core genome provided strong evidence for the placement of this species in the genus *Salipiger*. The type strain is HTCC2601^T (DSM 26914^T, JCM 13377^T, KCTC 12554^T).

Description of *Salipiger manganoxidans* comb. nov. *S. manganoxidans* (man.gan.o'xi.dans. N.L. neut. n. *manganum* manganese; N.L. part. adj. *oxidans* oxidizing; N.L. part. adj. *manganoxidans* manganese-oxidizing). Basonym: *Citreicella manganoxidans* Rajasabapathy *et al.* 2016.

The description is the same as for *C. manganoxidans* (58). Phylogenetic analysis of 16S rRNA gene sequences provided strong evidence for the placement of this species in the genus *Salipiger*. The type strain is VSW210^T (KCTC 32497^T, MCC 2286^T).

Description of *Salipiger marinus* comb. nov. *S. marinus* (ma.ri'nus. L. masc. adj. *marinus* of the sea, marine). Basonym: *Citreicella marina* Lai *et al.* 2011.

The description is the same as for *C. marina* (59). Phylogenetic analysis of the core genome provided strong evidence for the placement of this species in the genus *Salipiger*. The type strain is CK-I3-6^T (DSM 26424^T, CCTCC AB 209064^T, LMG 25230^T, MCCC 1A03060^T).

Description of *Salipiger profundus* comb. nov. *S. profundus* (pro.fun'dus. L. masc. adj. *profundus* deep). Basonym: *Thiobacimonas profunda* Li *et al.* 2015.

The description is the same as for *T. profunda* (60). Phylogenetic analysis of the core genome provided strong evidence for the placement of this species in the genus *Salipiger*. The type strain is JLT2016^T (LMG 27365^T, CGMCC 1.12377^T).

Description of *Salipiger thiooxidans* comb. nov. *S. thiooxidans* (thi.o.o'xi'dans). Gr. n. *theion* (Latin transliteration *thium*), sulfur; N.L. v. *oxido* oxidize; N.L. part. adj. *thiooxidans* oxidizing sulfur). Basonym: *Citreicella thiooxidans* Sorokin *et al.* 2006.

The description is the same as for *C. thiooxidans* (61). Phylogenetic analysis of the core genome provided strong evidence for the placement of this species in the genus *Salipiger*. The type strain is CHLG 1^T (DSM 10146^T, UNIQEM U 228^T).

Emended description of the genus *Shimia* Choi and Cho 2006 emend. Hameed *et al.* 2013. The description is as given by Choi and Cho (62) and Hameed *et al.* (63) with the following amendment. The DNA G+C content is 53.8-61.2 mol%. The type species for the genus is *Shimia marina*.

Description of *Shimia abyssi* comb. nov. *S. abyssi* (a.bys'si. L. gen. n. *abyssi* from the abyss). Basonym: *Thalassobius abyssi* Nogi *et al.* 2016.

The description is the same as for *T. abyssi* (64). Phylogenetic analysis of the core genome provided strong evidence for the placement of this species in the genus *Shimia*. The type strain is JAMH 043^T (DSM 100673^T, JCM 30900^T).

Description of *Shimia aestuarii* comb. nov. *S. aestuarii* (aes.tu.a'ri.i. L. gen. n. *aestuarii* of a tidal flat). Basonym: *Thalassobius aestuarii* Yi and Chun 2007.

The description is the same as for *T. aestuarii* (65). Phylogenetic analysis of the core genome provided strong evidence for the placement of this species in the genus *Shimia*. The type strain is JC2049^T (DSM 15283^T, IMSNU 14011^T, KCTC 12049^T).

Description of *Shimia aquaeponti* comb. nov. *S. aquaeponti* (a.quae.pon'ti. L. fem. n. *aqua* water; L. masc. n. *pontus* the sea; N.L. gen. n. *aquaeponti* of the water of the sea, from where the type strain was isolated). Basonym: *Thalassobius aquaeponti* Park *et al.* 2015.

The description is the same as for *T. aquaeponti* (66). Phylogenetic analysis of 16S rRNA gene sequences provided strong evidence for the placement of this species in the genus *Shimia*. The type strain is GJSW-22^T (KCTC 42115^T, NBRC 110378^T).

Description of *Yoonia* gen. nov. *Yoonia* (Yoo'ni.a. N.L. fem. n. *Yoonia* in honor of Jung-Hoon Yoon, for his contributions to the taxonomy of marine *Alphaproteobacteria*).

Cells are Gram-negative, aerobic, and rod-shaped. Motility varies among species; if observed cells are motile via polar flagella. Catalase- and oxidase-positive. Nitrate reduction is negative. Moderately halophilic; most species require NaCl to grow. The predominant ubiquinone is Q-10. The major fatty acid (>10% of the total fatty acids) is $C_{18:1}\omega 7c$. The major polar lipids are phosphatidylcholine and phosphatidylglycerol. The DNA G+C content is 55.0-63.1 mol%. A member of the family *Rhodobacteraceae*, class *Alphaproteobacteria* according to 16S rRNA gene analysis and phylogenomics. The type species for the genus is *Yoonia vestfoldensis*.

Description of *Yoonia vestfoldensis* comb. nov. *Y. vestfoldensis* (vest.fold.en'sis. N.L. fem. adj. *vestfoldensis* referring to the isolation source, lakes Ace and Pendant, Vestfold Hills, Antarctica). Basonym: *Loktanella vestfoldensis* Van Trappen *et al.* 2004.

The description is the same as for *L. vestfoldensis* (47). Phylogenetic analysis of the core genome provided strong evidence for the placement of this species in the novel genus *Yoonia*. The type strain is R-9477^T (DSM 16212^T, LMG 22003^T, CIP 108321^T).

Description of *Yoonia litorea* comb. nov. *Y. litorea* (li.to're.a. L. fem. adj. *litorea* of or belonging to the seashore). Basonym: *Loktanella litorea* Yoon *et al.* 2013.

The description is the same as for *L. litorea* (67). Phylogenetic analysis of the core genome provided strong evidence for the placement of this species in the novel genus *Yoonia*. The type strain is DPG-5^T (DSM 29433^T, KCTC 23883^T, CCUG 62113^T).

Description of *Yoonia maricola* comb. nov. *Y. maricola* (ma.ri'co.la. L. n. *mare* sea; L. suff. -*cola* (from L. n. *incola*) a dweller, inhabitant; N.L. n. *maricola* inhabitant of the sea). Basonym: *Loktanella maricola* Yoon *et al.* 2007.

The description is the same as for *L. maricola* (68). Phylogenetic analysis of the core genome provided strong evidence for the placement of this species in the novel genus *Yoonia*. The type strain is DSW-18^T (DSM 29128^T, KCTC 12863^T, JCM 14564^T).

Description of *Yoonia maritima* comb. nov. *Y. maritima* (ma.ri'ti.ma. L. fem. adj. *maritima* maritime, marine). Basonym: *Loktanella maritima* Tanaka *et al.* 2014.

The description is the same as for *L. maritima* (69). Phylogenetic analysis of the core genome provided strong evidence for the placement of this species in the novel genus *Yoonia*. The type strain is KMM 9530^T (DSM 101533^T, NRIC 0919^T, JCM 19807^T).

Description of *Yoonia rosea* comb. nov. *Y. rosea* (ro'se.a. L. fem. adj. *rosea* rose-colored or rosy, referring to the pinkish color of the colonies). Basonym: *Loktanella rosea* Ivanova *et al.* 2005.

The description is the same as for *L. rosea* (70). Phylogenetic analysis of the core genome provided strong evidence for the placement of this species in the novel genus *Yoonia*. The type strain is Fg36^T (DSM 29591^T, KMM 6003^T, CIP 107851^T, LMG 22534^T).

Description of *Yoonia sediminilitoris* comb. nov. *Y. sediminilitoris* (se.di.mi.ni.li'to.ris. L. n. *sedimen –inis* sediment; L. n. *litus –oris* the seashore, beach; N.L. gen. n. *sediminilitoris* of sediment, of seashore). Basonym: *Loktanella sediminilitoris* Park *et al.* 2013.

The description is the same as for *L. sediminilitoris* (71). Phylogenetic analysis of the core genome provided strong evidence for the placement of this species in the novel genus *Yoonia*. The type strain is D1-W3^T (DSM 29955^T, KCTC 32383^T, CECT 8284^T).

Description of *Yoonia tamlensis* comb. nov. *Y. tamlensis* (tam.len'sis. N.L. fem. adj. *tamlensis* of or belonging to Tamla, the old name of Jeju, Republic of Korea, referring to the site where the type strain was isolated). Basonym: *Loktanella tamlensis* Lee 2012

The description is the same as for *L. tamlensis* (48). Phylogenetic analysis of the core genome provided strong evidence for the placement of this species in the novel genus *Yoonia*. The type strain is SSW-35^T (DSM 26879^T, KCTC 12722^T, JCM 14020^T).

Funding, acknowledgements, and conflicts of interest

Funding. This research was supported in part by a NSF Dimensions of Biodiversity grant OCE-1342694.

Acknowledgements. We acknowledge Aharon Oren for his insightful and helpful comments on the proposed names of the novel genera and novel combinations of genera/species.

Conflicts of Interest. There are no conflicts of interest to declare.

References:

1. Brinkhoff T, Giebel HA, Simon M. 2008. Diversity, ecology, and genomics of the *Roseobacter* clade: a short overview. Archives of Microbiology 189:531-539.
2. Buchan A, González JM, Moran MA. 2005. Overview of the marine roseobacter lineage. Applied and Environmental Microbiology 71:5665-77.
3. Simon M, Scheuner C, Meier-Kolthoff JP, Brinkhoff T, Wagner-Dobler I, Ulbrich M, Klenk HP, Schomburg D, Petersen J, Goker M. 2017. Phylogenomics of *Rhodobacteraceae* reveals evolutionary adaptation to marine and non-marine habitats. ISME Journal 11:1483-1499.
4. Pujalte MJ, Lucena T, Ruvira MA, Arahal DR, Macián MC. 2014. The family *Rhodobacteraceae*, p 439-512. *In* Rosenberg E, DeLong EF, Lory S, Stackebrandt E, Thompson F (ed), The Prokaryotes: *Alphaproteobacteria* and *Betaproteobacteria* doi:10.1007/978-3-642-30197-1_377. Springer Berlin Heidelberg, Berlin, Heidelberg.
5. Luo H, Moran MA. 2014. Evolutionary ecology of the marine *Roseobacter* clade. Microbiology and Molecular Biology Reviews 78:573-587.
6. Breider S, Scheuner C, Schumann P, Fiebig A, Petersen J, Pradella S, Klenk HP, Brinkhoff T, Goker M. 2014. Genome-scale data suggest reclassifications in the *Leisingera-Phaeobacter* cluster including proposals for *Sedimentitalea* gen. nov. and *Pseudophaeobacter* gen. nov. Frontiers in Microbiology 5:416.
7. Yarza P, Richter M, Peplies J, Euzeby J, Amann R, Schleifer KH, Ludwig W, Glockner FO, Rossello-Mora R. 2008. The All-Species Living Tree project: a 16S rRNA-based phylogenetic tree of all sequenced type strains. Systematic and Applied Microbiology 31:241-50.

8. Cole JR, Wang Q, Fish JA, Chai B, McGarrell DM, Sun Y, Brown CT, Porras-Alfaro A, Kuske CR, Tiedje JM. 2014. Ribosomal Database Project: data and tools for high throughput rRNA analysis. Nucleic Acids Research 42:D633-42.

9. Maddison WPM, David R. 2017. Mesqute: a modular system for evolutionary analysis, v3.2. http://mesquiteproject.org.

10. Guindon S, Dufayard JF, Lefort V, Anisimova M, Hordijk W, Gascuel O. 2010. New algorithms and methods to estimate maximum-likelihood phylogenies: assessing the performance of PhyML 3.0. Systematic Biology 59:307-21.

11. Lefort V, Longueville JE, Gascuel O. 2017. SMS: Smart Model Selection in PhyML. Molecular Biology and Evolution doi:10.1093/molbev/msx149.

12. Blom J, Kreis J, Spanig S, Juhre T, Bertelli C, Ernst C, Goesmann A. 2016. EDGAR 2.0: an enhanced software platform for comparative gene content analyses. Nucleic Acids Research 44:W22-8.

13. Goris J, Konstantinidis KT, Klappenbach JA, Coenye T, Vandamme P, Tiedje JM. 2007. DNA-DNA hybridization values and their relationship to whole-genome sequence similarities. International Journal of Systematic and Evolutionary Microbiology 57:81-91.

14. Edgar RC. 2004. MUSCLE: multiple sequence alignment with high accuracy and high throughput. Nucleic Acids Research 32:1792-7.

15. Beukes CW, Palmer M, Manyaka P, Chan WY, Avontuur JR, van Zyl E, Huntemann M, Clum A, Pillay M, Palaniappan K, Varghese N, Mikhailova N, Stamatis D, Reddy TBK, Daum C, Shapiro N, Markowitz V, Ivanova N, Kyrpides N, Woyke T, Blom J, Whitman WB, Venter SN, Steenkamp ET. 2017. Genome data provides high support for generic boundaries in *Burkholderia* sensu lato. Frontiers in Microbiology 8:1154.

16. Capella-Gutierrez S, Silla-Martinez JM, Gabaldon T. 2009. trimAl: a tool for automated alignment trimming in large-scale phylogenetic analyses. Bioinformatics 25:1972-3.

17. Nguyen LT, Schmidt HA, von Haeseler A, Minh BQ. 2015. IQ-TREE: a fast and effective stochastic algorithm for estimating maximum-likelihood phylogenies. Molecular Biology and Evolution 32:268-74.

18. Kalyaanamoorthy S, Minh BQ, Wong TKF, von Haeseler A, Jermiin LS. 2017. ModelFinder: fast model selection for accurate phylogenetic estimates. Nature Methods 14:587-589.

19. Qin QL, Xie BB, Zhang XY, Chen XL, Zhou BC, Zhou J, Oren A, Zhang YZ. 2014. A proposed genus boundary for the prokaryotes based on genomic insights. Journal of Bacteriology 196:2210-5.

20. Schliep KP. 2011. phangorn: phylogenetic analysis in R. Bioinformatics 27:592-3.

21. Sneath PHA, Sokal RR. 1973. Numerical taxonomy; the principles and practice of numerical classification. San Francisco, W. H. Freeman [1973].

22. Keswani J, Whitman WB. 2001. Relationship of 16S rRNA sequence similarity to DNA hybridization in prokaryotes. International Journal of Systematic and Evolutionary Microbiology 51:667-78.

23. Case RJ, Boucher Y, Dahllof I, Holmstrom C, Doolittle WF, Kjelleberg S. 2007. Use of 16S rRNA and *rpoB* genes as molecular markers for microbial ecology studies. Applied and Environmental Microbiology 73:278-88.

24. Vos M, Quince C, Pijl AS, de Hollander M, Kowalchuk GA. 2012. A comparison of *rpoB* and 16S rRNA as markers in pyrosequencing studies of bacterial diversity. PLoS One 7:e30600.

25. Bondoso J, Harder J, Lage OM. 2013. *rpoB* gene as a novel molecular marker to infer phylogeny in *Planctomycetales*. Antonie Van Leeuwenhoek 104:477-88.

26. Aliyu H, Lebre P, Blom J, Cowan D, De Maayer P. 2016. Phylogenomic re-assessment of the thermophilic genus *Geobacillus*. Systematic and Applied Microbiology 39:527-533.

27. Li Y, Xue H, Sang SQ, Lin CL, Wang XZ. 2017. Phylogenetic analysis of family *Neisseriaceae* based on genome sequences and description of *Populibacter corticis* gen. nov., sp. nov., a member of the family *Neisseriaceae*, isolated from symptomatic bark of *Populus* x *euramericana canker*. PLoS One 12:e0174506.

28. Lopes-Santos L, Castro DBA, Ferreira-Tonin M, Correa DBA, Weir BS, Park D, Ottoboni LMM, Neto JR, Destefano SAL. 2017. Reassessment of the taxonomic position of *Burkholderia andropogonis* and description of *Robbsia andropogonis* gen. nov., comb. nov. Antonie Van Leeuwenhoek 110:727-736.

29. Konstantinidis KT, Tiedje JM. 2005. Towards a genome-based taxonomy for prokaryotes. Journal of Bacteriology 187:6258-64.

30. Luo C, Rodriguez RL, Konstantinidis KT. 2014. MyTaxa: an advanced taxonomic classifier for genomic and metagenomic sequences. Nucleic Acids Research 42:e73.

31. Penesyan A, Breider S, Schumann P, Tindall BJ, Egan S, Brinkhoff T. 2013. *Epibacterium ulvae* gen. nov., sp. nov., epibiotic bacteria isolated from the surface of a marine alga. International Journal of Systematic and Evolutionary Microbiology 63:1589-96.

32. Alavi M, Miller T, Erlandson K, Schneider R, Belas R. 2001. Bacterial community associated with *Pfiesteria*-like dinoflagellate cultures. Environmental Microbiology 3:380-96.

33. Miller TR, Hnilicka K, Dziedzic A, Desplats P, Belas R. 2004. Chemotaxis of *Silicibacter* sp. strain TM1040 toward dinoflagellate products. Applied and Environmental Microbiology 70:4692-701.

34. Muramatsu Y, Uchino Y, Kasai H, Suzuki KI, Nakagawa Y. 2007. *Ruegeria mobilis* sp. nov., a member of the *Alphaproteobacteria* isolated in Japan and Palau. International Journal of Systematic and Evolutionary Microbiology 57:1304-1309.

35. Vandecandelaere I, Nercessian O, Segaert E, Achouak W, Faimali M, Vandamme P. 2008. *Ruegeria scottomollicae* sp. nov., isolated from a marine electroactive biofilm. International Journal of Systematic and Evolutionary Microbiology 58:2726-2733.

36. Park S, Lee MH, Lee JS, Oh TK, Yoon JH. 2012. *Thalassobius maritimus* sp. nov., isolated from seawater. International Journal of Systematic and Evolutionary Microbiology 62:8-12.

37. Weon HY, Kim BY, Yoo SH, Kim JS, Kwon SW, Go SJ, Stackebrandt E. 2006. *Loktanella koreensis* sp. nov., isolated from sea sand in Korea. International Journal of Systematic and Evolutionary Microbiology 56:2199-202.

38. Liang J, Zhang Z, Liu Y, Wang M, Zhang XH. 2015. *Loktanella sediminum* sp. nov., isolated from marine surface sediment. International Journal of Systematic and Evolutionary Microbiology 65:686-91.

39. Lucena T, Pujalte MJ, Ruvira MA, Garay E, Macian MC, Arahal DR. 2012. *Tropicibacter multivorans* sp. nov., an aerobic alphaproteobacterium isolated from surface seawater. International Journal of Systematic and Evolutionary Microbiology 62:844-8.

40. Jung YT, Park S, Lee JS, Yoon JH. 2016. *Loktanella marina* sp. nov., isolated from seawater of Yellow Sea in South Korea. International Journal of Systematic and Evolutionary Microbiology 66:2528-2533.

41. Lau SC, Tsoi MM, Li X, Plakhotnikova I, Wu M, Wong PK, Qian PY. 2004. *Loktanella hongkongensis* sp. nov., a novel member of the *α-Proteobacteria* originating from marine biofilms in Hong Kong waters. International Journal of Systematic and Evolutionary Microbiology 54:2281-4.

42. Park S, Jung YT, Won SM, Park JM, Yoon JH. 2014. *Loktanella aestuariicola* sp. nov., an alphaproteobacterium isolated from a tidal flat. Antonie Van Leeuwenhoek 106:707-14.

43. Tsubouchi T, Shimane Y, Mori K, Miyazaki M, Tame A, Uematsu K, Maruyama T, Hatada Y. 2013. *Loktanella cinnabarina* sp. nov., isolated from a deep subseafloor sediment, and emended description of the genus *Loktanella*. International Journal of Systematic and Evolutionary Microbiology 63:1390-5.

44. Moon YG, Seo SH, Lee SD, Heo MS. 2010. *Loktanella pyoseonensis* sp. nov., isolated from beach sand, and emended description of the genus *Loktanella*. International Journal of Systematic and Evolutionary Microbiology 60:785-9.

45. Park S, Lee JS, Lee KC, Yoon JH. 2013. *Loktanella soesokkakensis* sp. nov., isolated from the junction between the North Pacific Ocean and a freshwater spring. Antonie Van Leeuwenhoek 104:397-404.

46. Park JM, Park S, Jung YT, Cho JY, Yoon JH. 2014. *Loktanella variabilis* sp. nov., isolated from a tidal flat. International Journal of Systematic and Evolutionary Microbiology 64:2579-85.

47. Van Trappen S, Mergaert J, Swings J. 2004. *Loktanella salsilacus* gen. nov., sp. nov., *Loktanella fryxellensis* sp. nov. and *Loktanella vestfoldensis* sp. nov., new members of the *Rhodobacter* group, isolated from microbial mats in Antarctic lakes. International Journal of Systematic and Evolutionary Microbiology 54:1263-9.

48. Lee SD. 2012. *Loktanella tamlensis* sp. nov., isolated from seawater. International Journal of Systematic and Evolutionary Microbiology 62:586-90.

49. Martens T, Heidorn T, Pukall R, Simon M, Tindall BJ, Brinkhoff T. 2006. Reclassification of *Roseobacter gallaeciensis* Ruiz-Ponte et al. 1998 as *Phaeobacter gallaeciensis* gen. nov., comb. nov., description of *Phaeobacter inhibens* sp. nov., reclassification of *Ruegeria algicola* (Lafay et al. 1995) Uchino et al. 1999 as *Marinovum algicola* gen. nov., comb. nov., and emended descriptions of the genera *Roseobacter*, *Ruegeria* and *Leisingera*. International Journal of Systematic and Evolutionary Microbiology 56:1293-1304.

50. Vandecandelaere I, Nercessian O, Segaert E, Achouak W, Mollica A, Faimali M, Vandamme P. 2009. *Nautella italica* gen. nov., sp. nov., isolated from a marine electroactive biofilm. International Journal of Systematic and Evolutionary Microbiology 59:811-7.

51. Li G, Lai Q, Du Y, Liu X, Sun F, Shao Z. 2015. *Aestuariivita atlantica* sp. nov., isolated from deep-sea sediment. International Journal of Systematic and Evolutionary Microbiology 65:3281-5.

52. Uchino Y, Hirata A, Yokota A, Sugiyama J. 1998. Reclassification of marine *Agrobacterium* species: proposals of *Stappia stellulata* gen. nov., comb. nov., *Stappia aggregata* sp. nov., nom. rev., *Ruegeria atlantica* gen. nov., comb. nov., *Ruegeria*

gelatinovora comb. nov., *Ruegeria algicola* comb. nov., and *Ahrensia kieliense* gen. nov., sp. nov., nom. rev. Journal of General and Applied Microbiology 44:201-210.

53. Yi H, Lim YW, Chun J. 2007. Taxonomic evaluation of the genera *Ruegeria* and *Silicibacter*: a proposal to transfer the genus *Silicibacter* Petursdottir and Kristjansson 1999 to the genus *Ruegeria* Uchino et al. 1999. International Journal of Systematic and Evolutionary Microbiology 57:815-819.

54. Lucena T, Ruvira MA, Macian MC, Pujalte MJ, Arahal DR. 2013. Description of *Tropicibacter mediterraneus* sp. nov. and *Tropicibacter litoreus* sp. nov. Systematic and Applied Microbiolology 36:325-9.

55. Martinez-Canovas MJ, Quesada E, Martinez-Checa F, del Moral A, Bejar V. 2004. *Salipiger mucescens* gen. nov., sp. nov., a moderately halophilic, exopolysaccharide-producing bacterium isolated from hypersaline soil, belonging to the *α-Proteobacteria*. International Journal of Systematic and Evolutionary Microbiology 54:1735-40.

56. Park MS, Chung BS, Lee HJ, Jin HM, Lee SS, Oh YK, Jeon CO. 2011. *Citreicella aestuarii* sp. nov., isolated from a tidal flat. International Journal of Systematic and Evolutionary Microbiology 61:2595-9.

57. Cho JC, Giovannoni SJ. 2006. *Pelagibaca bermudensis* gen. nov., sp. nov., a novel marine bacterium within the *Roseobacter* clade in the order *Rhodobacterales*. International Journal of Systematic and Evolutionary Microbiology 56:855-9.

58. Rajasabapathy R, Mohandass C, Dastager SG, Liu Q, Li WJ, Colaco A. 2015. *Citreicella manganoxidans* sp. nov., a novel manganese oxidizing bacterium isolated from a shallow water hydrothermal vent in Espalamaca (Azores). Antonie Van Leeuwenhoek 108:1433-9.

59. Lai Q, Fu Y, Wang J, Chen S, Zhong H, Sun F, Shao Z. 2011. *Citreicella marina* sp. nov., isolated from deep-sea sediment. International Journal of Systematic and Evolutionary Microbiology 61:728-31.

60. Li S, Tang K, Liu K, Jiao N. 2015. *Thiobacimonas profunda* gen. nov., sp. nov., a member of the family *Rhodobacteraceae* isolated from deep-sea water. International Journal of Systematic and Evolutionary Microbiology 65:359-64.

61. Sorokin DY, Tourova TP, Muyzer G. 2005. *Citreicella thiooxidans* gen. nov., sp. nov., a novel lithoheterotrophic sulfur-oxidizing bacterium from the Black Sea. Systematic and Applied Microbiology 28:679-87.

62. Choi DH, Cho BC. 2006. *Shimia marina* gen. nov., sp. nov., a novel bacterium of the *Roseobacter* clade isolated from biofilm in a coastal fish farm. International Journal of Systematic and Evolutionary Microbiology 56:1869-73.

63. Hameed A, Shahina M, Lin SY, Lai WA, Hsu YH, Liu YC, Huang YM, Young CC. 2013. *Shimia biformata* sp. nov., isolated from surface seawater, and emended description of the genus *Shimia* Choi and Cho 2006. International Journal of Systematic and Evolutionary Microbiology 63:4533-9.

64. Nogi Y, Mori K, Makita H, Hatada Y. 2015. *Thalassobius abyssi* sp. nov., a marine bacterium isolated from the cold-seep sediment. International Journal of Systematic and Evolutionary Microbiology doi:10.1099/ijsem.0.000758.

65. Yi H, Chun J. 2006. *Thalassobius aestuarii* sp. nov., isolated from tidal flat sediment. Journal of Microbiology 44:171-6.

66. Park S, Jung YT, Won SM, Park JM, Yoon JH. 2014. *Thalassobius aquaeponti* sp. nov., an alphaproteobacterium isolated from seawater. Antonie Van Leeuwenhoek 106:535-42.

67. Yoon JH, Jung YT, Lee JS. 2013. *Loktanella litorea* sp. nov., isolated from seawater. International Journal of Systematic and Evolutionary Microbiology 63:175-80.

68. Yoon JH, Kang SJ, Lee SY, Oh TK. 2007. *Loktanella maricola* sp. nov., isolated from seawater of the East Sea in Korea. International Journal of Systematic and Evolutionary Microbiology 57:1799-802.

69. Tanaka N, Romanenko LA, Kurilenko VV, Svetashev VI, Kalinovskaya NI, Mikhailov VV. 2014. *Loktanella maritima* sp. nov. isolated from shallow marine sediments. International Journal of Systematic and Evolutionary Microbiology 64:2370-5.

70. Ivanova EP, Zhukova NV, Lysenko AM, Gorshkova NM, Sergeev AF, Mikhailov VV, Bowman JP. 2005. *Loktanella agnita* sp. nov. and *Loktanella rosea* sp. nov., from the north-west Pacific Ocean. International Journal of Systematic and Evolutionary Microbiology 55:2203-7.

71. Park S, Jung YT, Yoon JH. 2013. *Loktanella sediminilitoris* sp. nov., isolated from tidal flat sediment. International Journal of Systematic and Evolutionary Microbiology 63:4118-23.

72. Hosoya S, Yokota A. 2007. *Loktanella atrilutea* sp. nov., isolated from seawater in Japan. International Journal of Systematic and Evolutionary Microbiology 57:1966-9.

73. Rüger HJ, Höfle MG. 1992. Marine star-shaped-aggregate-forming bacteria: *Agrobacterium antlanticum* sp. nov.; *Agrobacterium meteori* sp. nov.; *Agrobacterium ferrugineum* sp. nov., nom. rev.; *Agrobacterium gelatinovorum* sp. nov., nom. rev.; and *Agrobacterium stellulatum* sp. nov., nom. rev. International Journal of Systematic Bacteriology 42:133-143.

74. Park S, Yoon JH. 2012. *Ruegeria arenilitoris* sp. nov., isolated from the seashore sand around a seaweed farm. Antonie Van Leeuwenhoek International Journal of General and Molecular Microbiology 102:581-589.

75. Lee J, Whon TW, Shin NR, Roh SW, Kim J, Park SK, Kim MS, Shin KS, Lee JS, Lee KC, Kim YO, Bae JW. 2012. *Ruegeria conchae* sp. nov., isolated from the ark clam *Scapharca broughtonii*. International Journal of Systematic and Evolutionary Microbiology 62:2851-2857.

76. Oh KH, Jung YT, Oh TK, Yoon JH. 2011. *Ruegeria faecimaris* sp. nov., isolated from a tidal flat sediment. International Journal of Systematic and Evolutionary Microbiology 61:1182-1188.

77. Kim YO, Park S, Nam BH, Kang SJ, Hur YB, Lee SJ, Oh TK, Yoon JH. 2012. *Ruegeria halocynthiae* sp. nov., isolated from the sea squirt *Halocynthia roretzi*. International Journal of Systematic and Evolutionary Microbiology 62:925-930.

78. Kämpfer P, Arun AB, Rekha PD, Busse HJ, Young CC, Glaeser SP. 2013. *Ruegeria intermedia* sp. nov., a moderately thermophilic bacterium isolated from a coastal hot spring. International Journal of Systematic and Evolutionary Microbiology 63:2538-2544.

79. Petursdottir SK, Kristjansson JK. 1997. *Silicibacter lacuscaerulensis* gen. nov., sp. nov., a mesophilic moderately halophilic bacterium characteristic of the Blue Lagoon geothermal lake in Iceland. Extremophiles 1:94-99.

80. Huo YY, Xu XW, Li X, Liu C, Cui HL, Wang CS, Wu M. 2011. *Ruegeria marina* sp. nov., isolated from marine sediment. International Journal of Systematic and Evolutionary Microbiology 61:347-350.

81. Kim YO, Park S, Nam BH, Jung YT, Kim DG, Yoon JH. 2014. *Ruegeria meonggei* sp. nov., an alphaproteobacterium isolated from ascidian *Halocynthia roretzi*. Antonie Van Leeuwenhoek International Journal of General and Molecular Microbiology 105:551-558.

82. González JM, Covert JS, Whitman WB, Henriksen JR, Mayer F, Scharf B, Schmitt R, Buchan A, Fuhrman JA, Kiene RP, Moran MA. 2003. *Silicibacter pomeroyi* sp. nov. and *Roseovarius nubinhibens* sp. nov., dimethylsulfoniopropionate-demethylating bacteria from marine environments. International Journal of Systematic and Evolutionary Microbiology 53:1261-1269.

83. Harwati TU, Kasai Y, Kodama Y, Susilaningsih D, Watanabe K. 2009. *Tropicibacter naphthalenivorans* gen. nov., sp. nov., a polycyclic aromatic hydrocarbon-degrading bacterium isolated from Semarang Port in Indonesia. International Journal of Systematic and Evolutionary Microbiology 59:392-6.

84. Iwaki H, Nishimura A, Hasegawa Y. 2012. *Tropicibacter phthalicus* sp. nov., a phthalate-degrading bacterium from seawater. Current Microbiology 64:392-6.

85. Arahal DR, Macian MC, Garay E, Pujalte MJ. 2005. *Thalassobius mediterraneus* gen. nov., sp. nov., and reclassification of *Ruegeria gelatinovorans* as *Thalassobius gelatinovorus* comb. nov. International Journal of Systematic and Evolutionary Microbiology 55:2371-2376.

86. Hyun DW, Kim MS, Shin NR, Kim JY, Kim PS, Whon TW, Yun JH, Bae JW. 2013. *Shimia haliotis* sp. nov., a bacterium isolated from the gut of an abalone, *Haliotis discus hannai*. International Journal of Systematic and Evolutionary Microbiology 63:4248-53.

87. Nogi Y, Mori K, Uchida H, Hatada Y. 2015. *Shimia sagamensis* sp. nov., a marine bacterium isolated from cold-seep sediment. International Journal of Systematic and Evolutionary Microbiology 65:2786-90.

88. Chen MH, Sheu SY, Chen CA, Wang JT, Chen WM. 2011. *Shimia isoporae* sp. nov., isolated from the reef-building coral *Isopora palifera*. International Journal of Systematic and Evolutionary Microbiology 61:823-7.

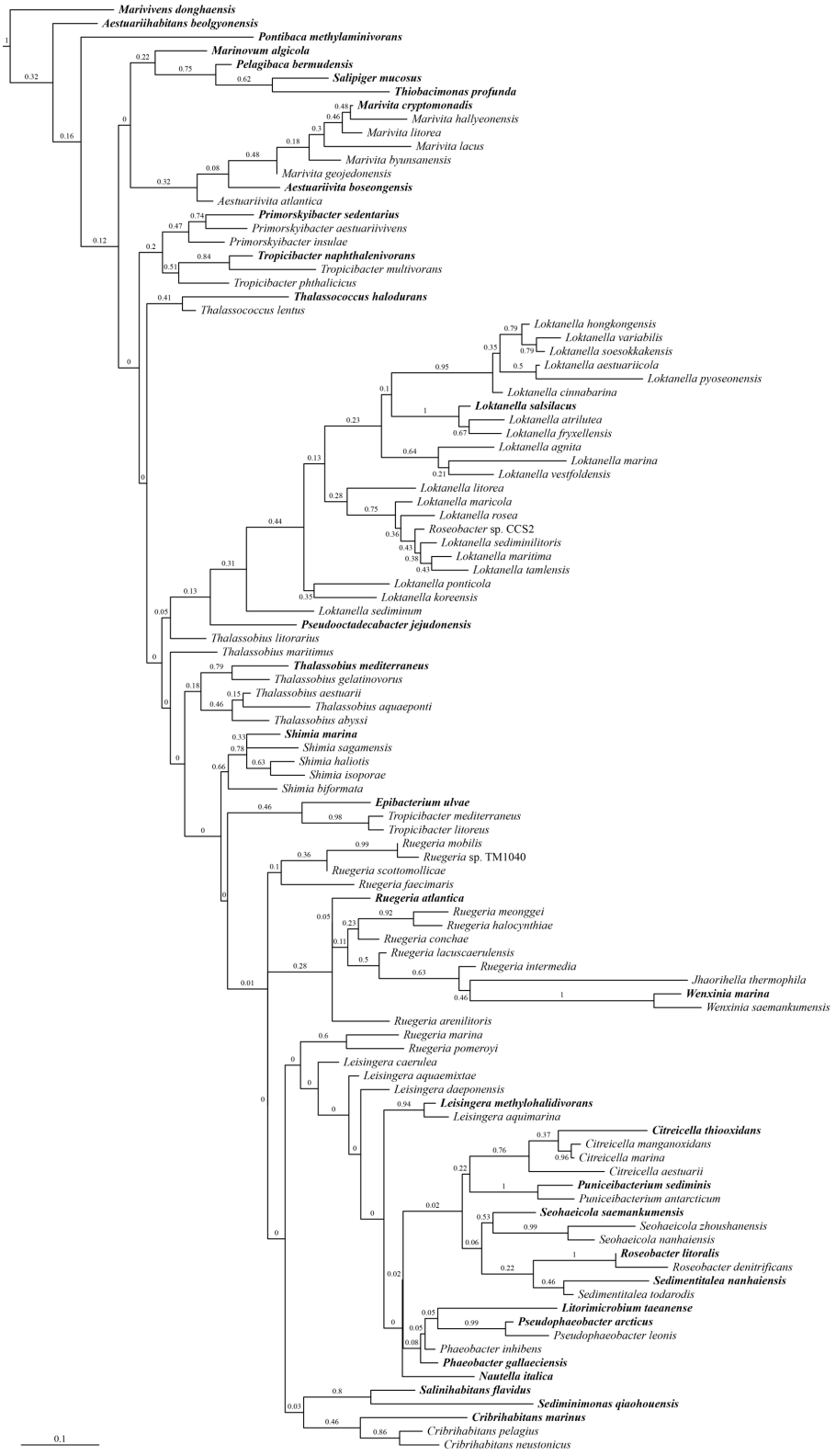

Figure 2-1. 16S rRNA maximum likelihood tree for all species included in this analysis.

Tree was generated using PhyML server 3.0 (http://www.atgc-montpellier.fr/phyml/) with smart

model selection (10, 11). Bolded taxa indicate the type species of each genus based on current taxonomic assignments. Numbers on branches indicate the percentage of bootstrap supports after 1000 replicates. The scale bar indicates the number of substitutions per site. The tree is rooted on the genus "*Ketogulonicigenium"* (omitted from tree) and includes all species included in the final analysis. Strain information and accession numbers can be found in Table S2-1.

Table 2-1. Cophenetic correlation coefficients. For 16S rRNA gene sequence similarity (16S ID), values are the cophenetic correlation coefficients for all 108 taxa included in the expanded data set. For ANI, cAAI, POCP, and RpoC protein sequence similarity (RpoC ID), values are the cophenetic correlation coefficients for the 81 taxa with whole-genome sequences available.

Metric	Cophenetic Correlation Coefficient
16S ID	0.72
ANI	0.92
cAAI	0.98
POCP	0.89
RpoC ID	0.94

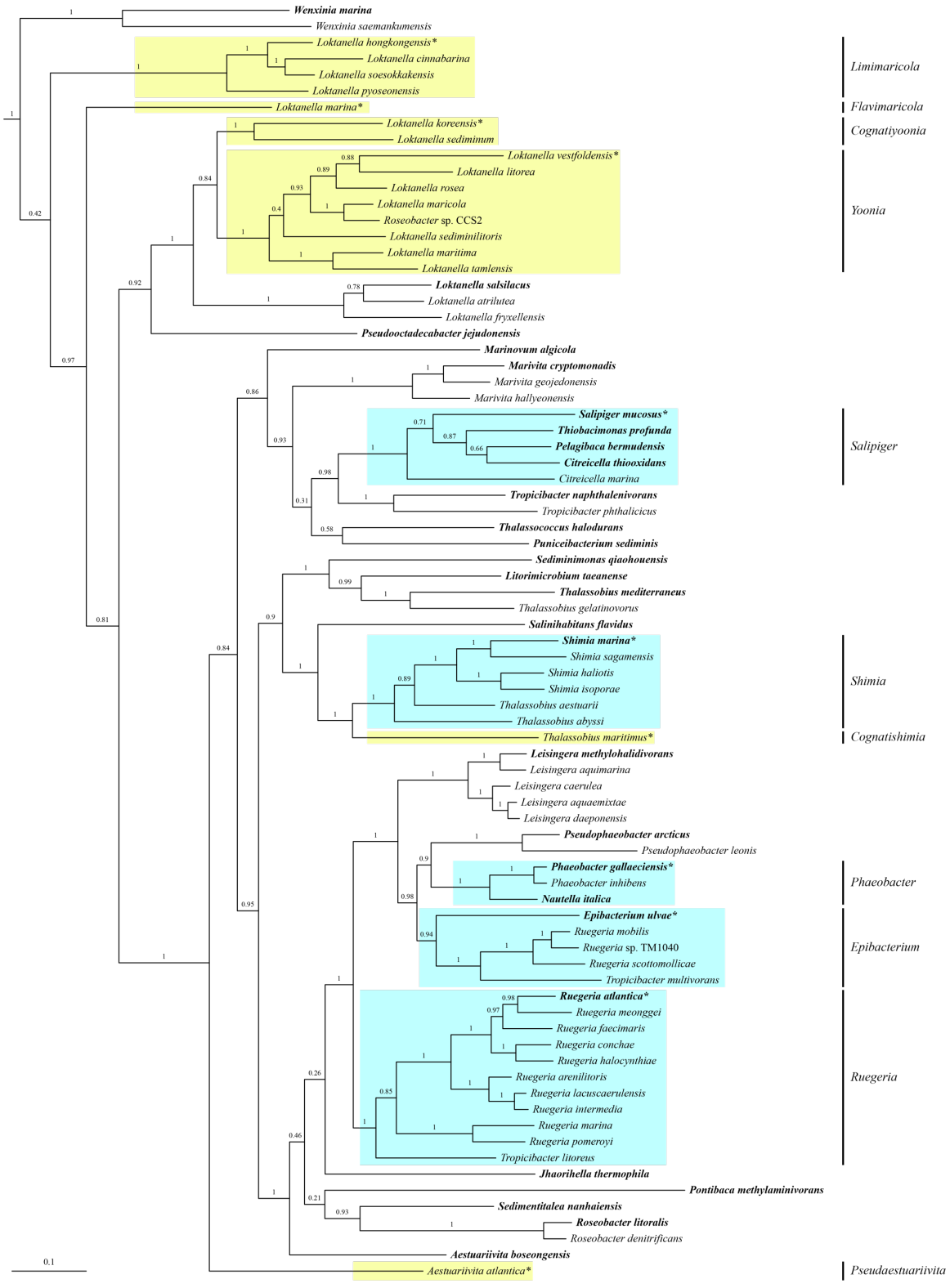

Figure 2-2. Curated core gene maximum likelihood tree. Tree was generated using PhyML server 3.0 (http://www.atgc-montpellier.fr/phyml/) with smart model selection (10, 11). Bolded

taxa indicate the type species of each genus based on current taxonomic assignments. Numbers on branches indicate the fraction of bootstrap support after 100 replicates. The scale bar indicates the number of substitutions per site. Blue indicates the addition of taxa to an existing genus, yellow indicates the addition of taxa to a novel genus, asterisks indicate the type species for the proposed changes, and the labels to the right of the tree indicate the proposed name for each clade (see text for details). The tree is rooted on the genus "*Ketogulonicigenium"* (omitted from tree). Strain and genome information can be found in Table S2-1.

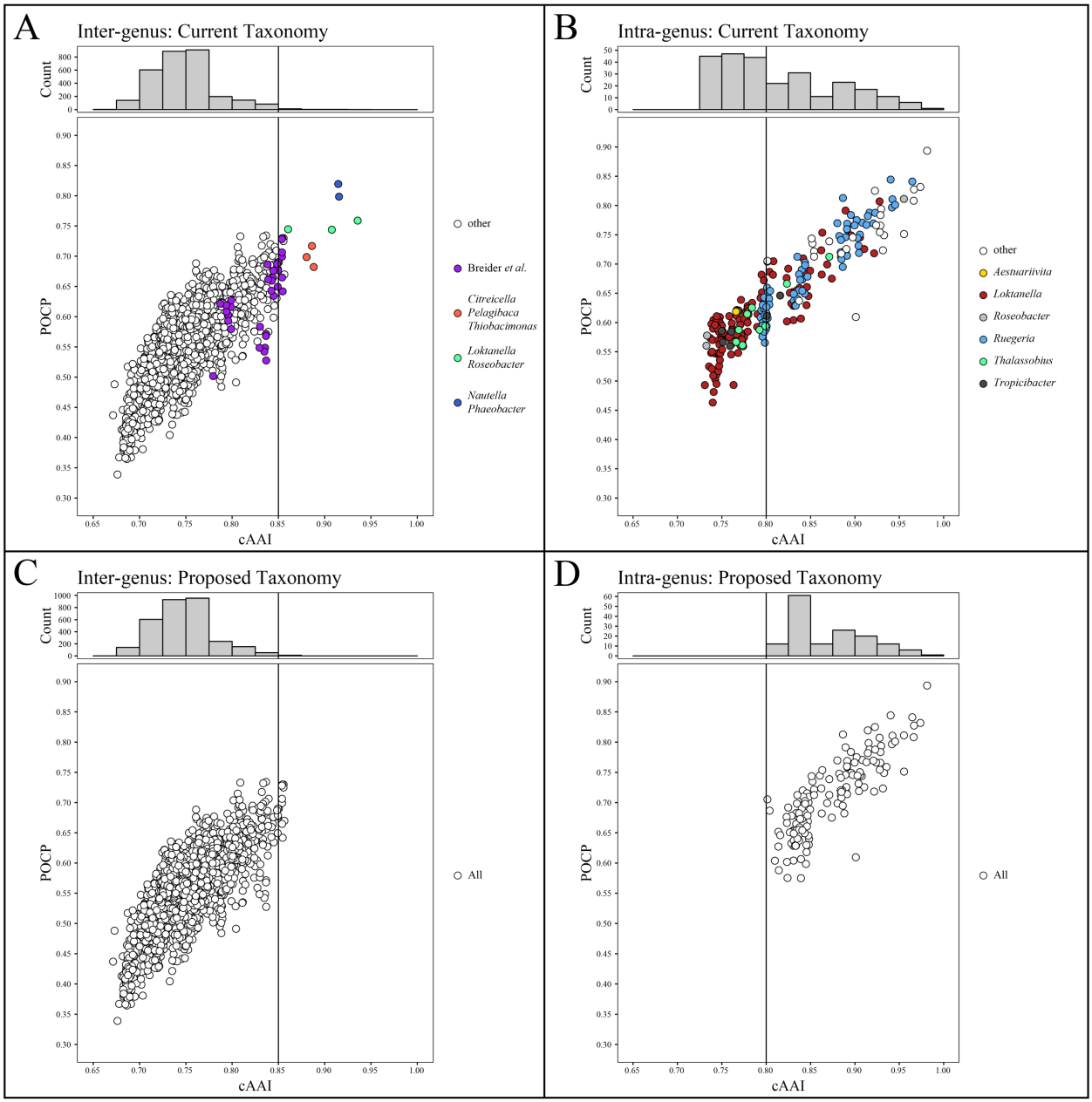

Figure 2-3. cAAI and POCP distribution within and between genera. Plots depict the relationship between cAAI and POCP for all 3,240 pairwise comparisons in the data set. Histograms at the top of each plot indicate the distribution of all cAAI values in the corresponding data set. The proposed cAAI values for delimiting genera are depicted as vertical lines on the plots (see text for details). Unless noted, comparisons are shown as empty circles. (**a**) Pairwise comparisons between genera based on the current taxonomy. The pairwise comparisons

between the genera proposed by Breider *et al.* (6) are shown in purple, the pairwise comparisons between *Citreicella thiooxidans*, *Pelagibaca bermudensis*, and *Thiobacimonas profunda* are shown in orange, the comparisons of *Roseobacter* sp. CCS2 against *Loktanella litorea*, *Loktanella maricola*, and *Loktanella rosea* are shown in green, and the comparisons of *Nautella italica* against *Phaeobacter gallaeciensis* and *Phaeobacter inhibens* are shown in blue. (**b**) Pairwise comparisons within genera based on the current taxonomy. The pairwise comparisons within *Aestuariivita* are shown in yellow, the pairwise comparisons within *Loktanella* are shown in red, the pairwise comparisons within *Roseobacter* are shown in light grey, the pairwise comparisons within *Ruegeria* are shown in light blue, the pairwise comparisons within *Thalassobius* are shown in green, and the pairwise comparisons within *Tropicibacter* are shown in dark grey. (**c**) All comparisons between genera based on the proposed taxonomy. (**d**) All comparisons within genera based on the proposed taxonomy.

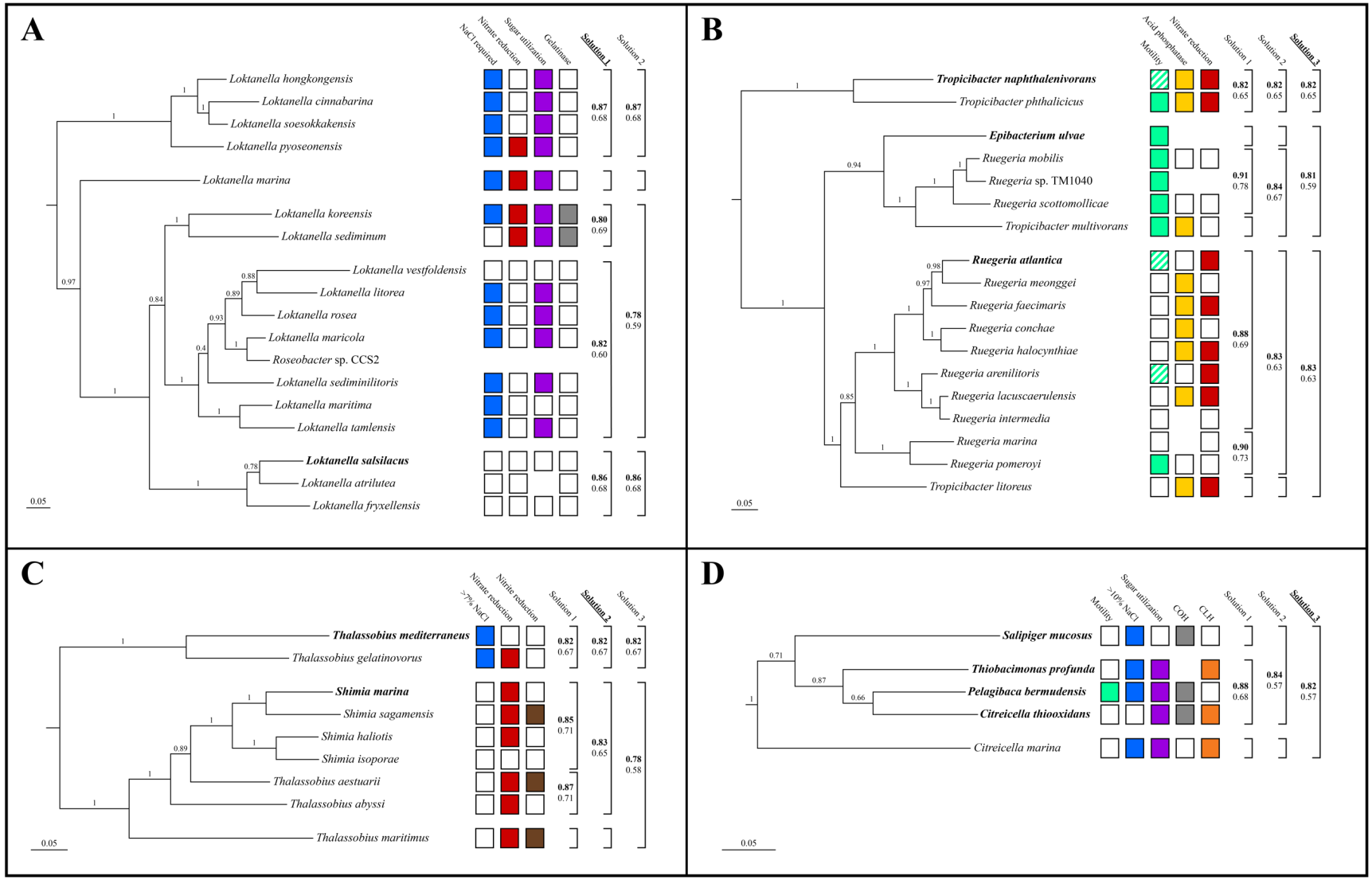

Figure 2-4. Phenotypic characteristics of ambiguous taxa. Trees were constructed by pruning the curated core-gene maximum likelihood tree to show the taxa being compared (Fig. 2-2). Bolded taxa indicate the type species of each genus based on current

taxonomic assignments. Phenotypes are shown in boxes adjacent to the tree. White boxes indicate the absence of the respective phenotype, red boxes indicate the ability to reduce nitrate to nitrite, purple boxes indicate the ability to utilize sugars as a sole carbon source, and spaces without boxes indicate missing data. Possible taxonomic solutions are shown on the far right of each figure. The bolded, underlined solutions indicate the proposed taxonomic reassignments. The numbers within each bracket indicates the minimum cAAI (bold) and POCP values for all comparisons within the bracketed clade. (**a**) Delimiting genera within the *Loktanella* genus. Blue boxes indicate a requirement for NaCl for growth, and grey boxes indicate the ability to hydrolyze gelatin (37, 38, 40, 41, 43-48, 67-72). (**b**) Delimiting genera within the *Epibacterium*, *Ruegeria*, and *Tropicibacter* genera. Solid green boxes indicate motility via polar flagella, striped green boxes indicate motility via peritrichous flagella, and yellow boxes indicate the presence of acid phosphatase activity (31-35, 39, 53, 54, 73-84). (**c**) Delimiting genera within the *Shimia* and *Thalassobius* genera. Blue boxes indicate the ability to grow in the presence of >7% NaCl (*w/v*), and brown boxes indicate the ability to reduce nitrate to gas (36, 62-65, 73, 85-88). (**d**) Delimiting the genus boundary within the *Citreicella*, *Pelagibaca*, *Salipiger*, and *Thiobacimonas* genera. Green boxes indicate motility via gliding, blue boxes indicate the ability to grow in the presence of >10% NaCl (*w/v*), grey boxes indicate chemoorganoheterotrophic (COH) growth, and orange boxes indicate chemolithoheterotrophic (CLH) growth (4, 55, 57, 59-61).

CHAPTER 3

THE GENUS *RUEGERIA*[2]

[2] Wirth, J.S. and W.B. Whitman. 2019. Accepted by *Bergey's Manual of Systematics of Archaea and Bacteria*.

Abstract

Gram-negative, aerobic, catalase- and oxidase-positive rods. Reproduces by normal cell division. Optimal growth typically occurs between 25–37 ˚C, 2–3 % (*w/v*) NaCl, and pH 6.5–8.5. Capable of utilizing a large variety of organic carbon sources. Every species tested can utilize L-tyrosine as a sole source of carbon and energy. Most species can utilize at least one organic acid and at least one carbohydrate as a sole source of carbon and energy. Most species utilize acetate, citrate, malate, pyruvate, succinate, cellobiose, fructose, D-galactose, D-glucose, and D-mannose as sole carbon and energy sources. The major fatty acid is $C_{18:1}$ *ω7c* or summed feature 8 ($C_{18:1}$ *ω7c*/*ω6c*). The major quinone is ubiquinone 10. Abundant in the surface layers of the ocean. Species have been isolated from marine sand, marine sediment, rhizosphere soil of mangrove trees, hot springs, the upper 3000 m of marine environments, the brine-seawater interface, and the interiors of ark clams (*Scapharca broughtonii*), oysters, and sea squirts (*Halocynthia roretzi*). Most species are non-motile. Members of the class *Alphaproteobacteria* (cbm00041), family *Rhodobacteraceae* (fbm00173). The type species is *Ruegeria atlantica*.

Etymology

Rue.ger'ia. M.L. ending *–ia*; M.L fem. n. *Ruegeria*, honoring Hans-Jürgen Rüger, a German microbiologist, for his contribution to the taxonomy of marine species of *Agrobacterium*.

Abridged description of the genus

Rod-shaped, Gram negative staining, polar, peritrichous, or unflagellated. No photosynthetic growth occurs. All species are aerobes, most species are strict aerobes but some facultative anaerobes exist. All facultatively anaerobic species reduce nitrate, but some strictly aerobic species also reduce nitrate. Only five species are known to reduce nitrate to nitrogen gas: *R. atlantica*, *R. denitrificans*, *R. lacuscaerulensis*, *R. litorea*, and *R. mediterranea*. Cells occur singly, and sometimes form star-shaped aggregates. Catalase- and oxidase-positive. Reproduces by normal cell division. Growth temperatures range from 4 ˚C to 55 ˚C, but most species grow optimally between 25–37 ˚C. Some species grow optimally at 45 ˚C. All species require NaCl and/or sea salts for growth except for *R. kandeliae* and *R. marina*. Optimal NaCl concentrations are typically between 2 % and 3 % (*w/v*) NaCl, but some species can tolerate salinities as low as 0 % and as high as 17 % (*w/v*) NaCl. All species have an optimal pH between 6.5 and 8.0, but some species tolerate pHs as low as 5 or as high as 11.

All species except for *R.intermedia* are capable of utilizing one or more organic acids as sole carbon and energy sources. All species except for *R. litorea* are capable of utilizing one or more sugars as sole carbon and energy sources. Every species tested is capable of utilizing L-tyrosine as a sole carbon and energy source. Most species can utilize acetate, citrate, malate, pyruvate, succinate, D-fructose, D-galactose, D-glucose, and D-mannose.

The major fatty acid is $C_{18:1}$ *ω7c* or summed feature 8 ($C_{18:1}$ *ω7c*/*ω6c*). The major quinone is ubiquinone 10. The polar lipids ≥1.0 % of the total lipids are diphosphatidylglycerol,

phosphatidylcholine, phosphatidylethanolamine, phosphatidylglycerol, at least three unidentified aminolipids, at least five unidentified lipids, and at least three unidentified phospholipids. The fatty acids observed with ≥1.0 % of the total fatty acids in at least one species comprise $C_{9:0}$, $C_{10:0}$, $C_{11:0}$, $C_{12:0}$, $C_{14:0}$, $C_{16:0}$, $C_{18:0}$, $C_{14:1}$ *ω7c*, $C_{17:1}$ *ω7c*, $C_{17:1}$ *ω8c*, $C_{18:0}$ iso, $C_{18:1}$ *ω6c*, $C_{18:1}$ *ω7c*, $C_{18:1}$ *ω9c*, $C_{19:0\ cy}$ *ω8c*, $C_{20:1}$ *ω7c*, $C_{18:1}$ 11-CH3, $C_{18:1}$ *ω7c* 11-CH3, $C_{10:0}$ 3-OH, $C_{12:0}$ 2-OH, $C_{12:0}$ 3-OH, $C_{16:0}$ 2-OH, $C_{16:1}$ 2-OH, and $C_{18:1}$ 2-OH. The 2-OH 16:0 fatty acid is ester-linked, the 3-OH 12:0 fatty acid appears to be both ester- and amide-linked, while the 3-OH 10:0 and 3-OH 14:1/3-oxo-14:0 fatty acids are amide-linked (1).

Abundant in the surface layers of the ocean. Species have been isolated from marine sand, marine sediment, the rhizospheres of mangrove trees (*Kandelia candel*), hot springs, the upper 3000 m of marine environments, the brine-seawater interface, and the interiors of ark clams (*Scapharca broughtonii*), oysters, and sea squirts (*Halocynthia roretzi*). Most species are non-motile, but three species are motile via either peritrichous or polar flagellation. Capable of degrading a variety of carbon sources including carbohydrates, alcohols, carboxylic acids, and amino acids. Members of the class *Alphaproteobacteria* (cbm00041), family *Rhodobacteraceae* (fbm00173). The type species is *Ruegeria atlantica*.DNA G+C content (mol %) is 55–66.15 as determined by HPLC, thermal denaturation, and/or genome sequencing. There are 16 species with validly published names.

Further descriptive information

Cell morphology. The cells of all sixteen species in *Ruegeria* are Gram negative staining rods and were isolated from marine environments (2-15). A collection of all characters in the *Ruegeria* can be found in **Table 3-1**, and the distinguishing characteristics of the *Ruegeria* species can be found in **Table 3-2**. Cell length varies from 0.5 μm to 18 μm, while cell diameter ranges between 0.2 μm and 1.2 μm. Flagellation varies between species. *R. kandeliae* and *R.*

pomeroyi possess a single polar flagellum, *R. arenilitoris* and *R. atlantica* possess peritrichous flagella, but the remaining species where it was tested were unflagellated (**Table 3-1**). Moreover, only *R. arenilitoris*, *R. kandeliae*, and *R. pomeroyi* were motile. Two of the species, *R. atlantica* and *R. litorea*, form star-shaped rosettes.

Colonial and cultural characteristics. On agar media, colonies can typically be observed after 1–3 days. Colonies range from 0.4 mm to 4.0 mm in diameter, are circular, flat to raised, and are cream-colored. Colonies of *Ruegeria arenilitoris* and *Ruegeria profundi* are slightly irregular (8, 13). Colonies of *Ruegeria atlantica* can be colorless, translucent, beige, or yellow (2). Colonies of *Ruegeria conchae* and *Ruegeria kandeliae* possess an entire margin (9, 15). Colonies of *Ruegeria denitrificans* are not pigmented (14). Colonies of *Ruegeria faecimaris* can be observed after 5 days at 30 ˚C (6). Colonies of *Ruegeria intermedia* and *Ruegeria marisrubri* possess a spreading edge (11, 13). Colonies of *Ruegeria lacuscaerulensis* are tan colored (3). Colonies of *Ruegeria litorea* possess an irregular margin. Colonies of *Ruegeria litorea* and *Ruegeria mediterranea* and become brownish with aging at 28 ˚C (10). Colonies of *Ruegeria marina* are rough (5).

Nutrition and growth conditions. Although pH optima vary between species, all species which have been tested grow optimally between pH 6 and pH 8 (**Table 3-1**). Most species grow optimally at sodium chloride concentrations between 0.5 % (*w/v*) and 3.5 % (*w/v*), but there are two exceptions. *R. marisrubri* grows optimally at 8.8–11.7 % (*w/v*), and *R. profundi* grows optimally at 5.8–8.8 % (*w/v*) (13). Only *R. kandeliae* and *R. marina* can grow in the absence of NaCl (5, 15). Most species grow optimally around 25–30 ˚C, but there are some exceptions. *R. lacuscaerulensis* grows optimally at 45 ˚C, *R. marina* grows optimally at 35–37 ˚C, and *R. intermedia* grows optimally at 37–45 ˚C (3, 5, 11).

Various carbon sources are utilized by *Ruegeria* as a sole source of carbon and energy (**Tables 3-1 and 3-2**). All species tested can utilize L-tyrosine. Except for *R. intermedia*, all species can utilize one or more organic acids. Although there are conflicting or no data for some species, most species utilize acetate, succinate, malate, citrate, and pyruvate (**Table 3-1**). All species can utilize one or more sugars except for *R. litorea*. Most species can utilize D-glucose. Although there have been several reports that *R. lacuscaerulensis* does not utilize glucose, we routinely obtain good growth on glucose as a sole source of carbon and energy (Petursdottir and Kristjansson, 1997; Lee *et al.*, 2007; Kämpfer *et al.*, 2013). With a few exceptions and some missing data, species do not use L-arabinose, maltose, salicin or sucrose (**Table 3-1**). *Ruegeria* species are susceptible to a variety of antibiotics, but not all species have been tested for the same antibiotics (**Table 3-3**). There are no data for antibiotic susceptibility in *R. denitrificans*, *R. intermedia*, *R. litorea*, or *R. mediterranea*. All species tested are resistant to bacitracin, clindamycin, lincomycin, nystatin, and trimethoprim, but are susceptible to amoxicillin, ampicillin, carbenicillin, cefotaxime, cefoxitin, cephalothin, erythromycin, furazolidone, nitrofurantoin, oxytetracycline, polymyxin B, rifampicin, and tobramycin. All species tested are susceptible to chloramphenicol except for *R. pomeroyi* (unpublished data). All species tested are susceptible to neomycin except for *R. meonggei*. All species tested are susceptible to penicillin-G except for *R. atlantica*. All species tested are susceptible to streptomycin except for *R. halocynthiae* and *R. lacuscaerulensis*. Susceptibility to gentamycin, kanamycin, novobiocin, oleandomycin, tetracycline, and vancomycin is variable within *Ruegeria*.

Chemotaxonomic characteristics. The major fatty acid in *Ruegeria* is $C_{18:1}$ *ω7c*. Every species possesses $C_{18:1}$ *ω7c*, but its percentage ranges from 36 % to 82 %. The following fatty acids have been observed in all *Ruegeria* species: $C_{16:0}$ (1.6–14.0 %), $C_{18:1}$ *ω7c* 11-CH_3 (1.0–

30.0 %), $C_{12:0}$ 3-OH (<0.5–7.5 %), and $C_{16:0}$ 2-OH (<0.5%–11.6 %). The 2-OH 16:0 fatty acid is ester-linked; the 3-OH 12:0 fatty acid appears to be both ester- and amide-linked, while the 3-OH 10:0 and 3-OH $C_{14:1/3}$-oxo-$_{14:0}$ are amide-linked (1). A complete list of the fatty acids in *Ruegeria* species can be found in **Table 3-4**.

Genome features and genetic methods available. Whole-genome sequences are available for the type strains of all the *Ruegeria* species (**Table 3-5**). Using the EDGAR server 2.3, the core genome of the *Ruegeria* species consists of 1,960 predicted protein coding sequences (16). The average amino acid identity of the core genes (cAAI) within the genus ranges from 0.83 to 0.96 with a mean of 0.87 (**Fig. 3-1**). Only one strain has a closed genome sequence: *R. pomeroyi* DSS-3^T. It possesses one chromosome and one extra-chromosomal replicon of 0.49 megabase pairs. Because of its size, the extra-chromosomal replicon is referred to as a "megaplasmid" (17).

A genetics system has been developed for *R. pomeroyi* that allows for targeted gene disruptions by homologous recombination (18). First, regions of homology (1,000-1,500 base pairs in length) flanking the target site and the *tetAR* genes from pRK415 are PCR amplified. The PCR products are then cloned into the pCR2.1 vector such that the *tetAR* genes are sandwiched between the upstream and downstream regions of homology. The pCR2.1 vector contains a kanamycin marker and cannot replicate in *R. pomeroyi*. Because of this, a double recombination event is required for acquisition of tetracycline resistance and kanamycin sensitivity. Once constructed, plasmid DNA is methylated using a CpG methyltransferase as recommended by New England Biolabs to avoid the very active restriction system. The methylated plasmid can then be desalted and electroporated into *R. pomeroyi*. Mutants are selected by growing cells in the presence of tetracycline (25 μg/mL) and then screened for

sensitivity to kanamycin (100 µg/mL). Confirmation of the gene replacement is accomplished with PCR and/or sequencing (18, 19).

Several vectors are available that replicate in *R. pomeroyi* and can be used for complementation of a deletion or expression of recombinant genes. The vectors pBBR1MCS-2 (Km^R), pBBR1MCS-3 (Tc^R), and pBBR1MCS-5 (Gm^R) are all compatible with *R. pomeroyi* (20). pRK415 (Tc^R) is another vector that is compatible with *R. pomeroyi* (21).

Ecology. *Ruegeria* species are found in aerobic, marine environments such as seawater, marine sediment, and marine sand from the surface of the seashore. One species was isolated from the rhizosphere of a mangrove tree. Marine invertebrates, including ascidians, sponges, clams, and oysters also provide suitable habitats for *Ruegeria*. With a pH of 7.5, an average temperature of 37 ˚C, a salinity of 2.5 %, and saturated silica, the Blue Lagoon in Iceland is the most unique environment from which a *Ruegeria* species was isolated.

Enrichment and isolation procedures

Several techniques have been published for isolating and enriching *Ruegeria* species. Because they are often the most abundant, culturable bacteria in seawater and marine sediments, serial dilution, plating onto some form of sea water-based medium, and aerobic incubation for several days at a temperature near that of the isolation environment is often sufficient.

Ruegeria arenilitoris, *Ruegeria faecimaris*, *Ruegeria intermedia*, *Ruegeria kandeliae*, *Ruegeria litorea*, and *Ruegeria mediterranea* were all isolated using the standard, serial dilution, plating technique on marine agar 2216. *R. arenilitoris* and *R. faecimaris* isolation plates were incubated at 25 ˚C, *R. litorea* and *R. mediterranea* isolation plates were incubated at 28 ˚C, and *R. intermedia* isolation plates were incubated at 45 ˚C (6, 8, 10, 11, 14, 15).

Ruegeria atlantica was isolated by collecting marine sediment from depths of approximately 3000 m using a Van Veen grab sampler. The sediment samples were immediately

serially diluted and plated onto modified ZoBell seawater agar. Plates were incubated at 15 ˚C for 8–17 days (2).

Ruegeria conchae was isolated from an ark clam that was harvested from the intertidal zone of an ark clam farm. The clam tissue was homogenized and suspended in sterile PBS. The suspension was serially diluted, and the dilutions were plated onto marine agar 2216. Plates were incubated at 25 ˚C for 3 days (9).

Ruegeria denitrificans was isolated from the inner contents of an oyster that was harvested on the coast of Vinaroz, Spain. The oyster tissue was homogenized and diluted with sterile seawater. The dilution was plated onto marine agar and incubated at 28 ˚C for 10 days (14).

Ruegeria halocynthiae and *Ruegeria meonggei* were isolated from the inner contents of an ascidian (*Halocynthia roretzi*). The inner contents were serially diluted with a 0.85 % (*w/v*) NaCl solution, and these dilutions were spread onto marine agar 2216 plates. Plates were then incubated at 25 ˚C for 10 days (7, 12).

Ruegeria lacuscaerulensis was isolated from water collected 1 m from the shore at Blue Lagoon in Iceland, at a depth of approximately 20 cm. The samples were serially diluted with autoclaved Blue Lagoon water, and the dilutions were plated onto plate count agar with different proportions of Blue Lagoon water (0 %, 25 %, 50 %; 100 %). Plates were incubated at 37 ˚C for 3 days (3, 22).

Ruegeria marina was isolated from marine sediment. Approximately 100 mg of sediment was added to 3 mL of sterile seawater and vortexed for 15 min to form a suspension. The sediment suspension was serially diluted, the dilutions were plated onto modified ZoBell medium, and the plates were incubated at 37 ˚C for 3 days (5).

Ruegeria marisrubri and *Ruegeria profundi* were isolated from the brine-seawater interface of the Erba Deep in the Red Sea in Saudi Arabia. Samples were enriched by inoculating 30 mL of enrichment medium composed of 50 % marine 2216 broth and 50 % sterilized *in situ* brine water with 5 mL of brine and incubating at 28 ˚C for 1 week. The enrichment cultures were then plated onto marine 2216 agar plates amended to contain 10 % (*w/v*) NaCl. Bacterial growth was purified to single colonies on marine 2216 agar plates (13).

Ruegeria pomeroyi was isolated by first passing seawater through a 1 µm filter to remove non-bacterial particulates. The filtered seawater was then enriched in filter-sterilized seawater with 10 µM dimethylsulfoniopropionate at 25 ˚C for 2 weeks. The enrichment culture was spread onto low-nutrient seawater medium plates, and the plates were incubated at 25 ˚C for 15 days in the dark (4).

Maintenance procedures

Strains of *Ruegeria* can be maintained on solid media or in liquid cultures. For growth in liquid cultures, shaking or stirring is recommended to provide enough oxygen for growth and homogenization of the available nutrients for non-motile strains.

Several types of rich media are available for cultivating *Ruegeria* species. Bacto marine agar/broth (Difco 2216 / DSMZ Medium 514) is the most common rich medium used for cultivating *Ruegeria* species. Half-strength yeast extract tryptone sea-salts (½ YTSS) medium (DSMZ Medium 974) is also used (4). Another alternative is B2 agar, which has a pH of 7.7 and is composed of 75 % (*v/v*) seawater, 0.5 % (*w/v*) peptone, 0.1 % (*w/v*) yeast extract, 40 µg/mL iron (III) phosphate *n*-hydrate, and 1.5 % (*w/v*) agar (23).

There are two minimal media used to cultivate *Ruegeria* species: basal medium (BM) and marine basal medium (MBM). BM contains 200 mM NaCl, 50 mM $MgSO_4$, 10 mM KCl, 10 mM $CaCl_2$, 50–100 mM Tris-HCl (pH 7.5), 19 mM NH_4Cl, 330 µM K_2HPO_4, and 100 µM

$FeSO_4$. The sole carbon source is usually added to a final concentration of 0.1–0.2 % (*w/v* for solids and *v/v* for liquids). If amino acid supplementation is required, all twenty amino acids are provided at a concentration of 1 mg/L. The amino acid stock solution should be filter-sterilized and added to media that has been autoclaved and allowed to cool (24).

MBM is composed of 80 mM HEPES (pH 6.8-6.9), 290 µM KH_2PO_4, 7.1 mM NH_4Cl, 68 µM iron (III) EDTA sodium salt (FeEDTA), 2 % (*w/v*) sea salts (Sigma), and 0.1 % (*v/v*) vitamin solution (25). The vitamin solution consists of 20 µg/mL biotin, 20 µg/mL folic acid, 100 µg/mL pyridoxine-HCl, 50 µg/mL riboflavin, 50 µg/mL thiamine, 50 µg/mL nicotinic acid, 50 µg/mL pantothenic acid, 1 µg/mL cyanocobalamin, and 50 µg/mL *p*-aminobenzoic acid (26). Its pH is adjusted to 7 before filter-sterilization. A 1.36 mM (20x) FeEDTA stock solution should be autoclaved separately and stored at 4 ˚C. Both the vitamins and the FeEDTA stock solutions should be added to medium that has been autoclaved and allowed to cool. The sole carbon source is usually added to a concentration of 12 mM total carbon.

In order to store *Ruegeria* species, mid-log phase cultures in a rich medium are mixed with a sterile glycerol solution for a final concentration of 40–50 % (*v/v*) glycerol. The freezer stock can then be stored at -80 ˚C indefinitely. To revive the frozen strain, transfer a small portion of the frozen stock into rich medium and incubate for several days or until growth occurs.

Differentiation of the genus *Ruegeria* from other genera

Over 40 phenotypic and chemotaxonomic characters were examined, but the absence of polar flagella is the only character that distinguishes most *Ruegeria* from the closely related genera *Cribrihabitans*, *Epibacterium*, *Leisingera*, *Phaeobacter*, and *Pseudophaeobacter* (**Table 3-6**). However, two species of *Ruegeria, R. pomeroyi* and *R. kandeliae*, possesses a single, polar flagellum (4). Many of the other characters were not conserved within the genera or there were

conflicting data between various reports. Currently, the best way to distinguish *Ruegeria* from other genera is through the use of whole-genome or other, sequence-based approaches.

Taxonomic comments

The genus *Ruegeria* was first proposed by Uchino *et al.* to accommodate a distinct phylogenetic group (based on 16S rRNA gene sequences) of oxidase-positive, catalase-positive, non-photosynthetic organisms that require NaCl and/or sea salts for growth (27, 28). This resulted in the reclassification of *Agrobacterium atlanticum* as the type species *Ruegeria atlantica*. Uchino *et al.* also reclassified *Agrobacterium gelatinovorum* and *Roseobacter algicola* into the genus as *Ruegeria gelatinovorans* and *Ruegeria algicola* (27, 28). These two species were later reclassified as *Thalassobius gelatinovorus* and *Marinovum algicola* by Arahal *et al.* and Martens *et al.*, respectively (1, 29). Yi *et al.* then reclassified *Silicibacter lacuscaerulensis* and *Silicibacter pomeroyi* into the genus as *Ruegeria lacuscaerulensis* and *Ruegeria pomeroyi*, respectively (30). Shortly after, three more species were isolated and added to the genus: *Ruegeria mobilis*, *Ruegeria pelagia*, and *Ruegeria scottomollicae* (31-33). Lai *et al.* later reclassified *R. pelagia* as a heterotypic synonym of *R. mobilis* (34). Since then, nine species have been isolated and added to the genus *Ruegeria* (listed in order of publication): *R. marina*, *R. faecimaris*, *R. arenilitoris*, *R. halocynthiae*, *R. conchae*, *R. intermedia*, *R. meonggei*, *R. marisrubri*, and *R. profundi* (5-9, 11-13, 35, 36). After an extensive taxonomic re-evaluation based on whole-genome sequences, *Ruegeria mobilis*, *Ruegeria scottomollicae*, and *Ruegeria* sp. TM1040 were reclassified as *Epibacterium mobile*, *Epibacterium scottomollicae*, and *Epibacterium* sp. TM1040, respectively (37). This reclassification also moved *Tropicibacter litoreus* and *Tropicibacter mediterraneus* into the genus as *Ruegeria litorea* and *Ruegeria mediterranea*, respectively (37). At the time, only the 16S rRNA gene sequence was available

for *R. mediterranea* (37). Finally, *Ruegeria denitrificans* and *Ruegeria kandeliae* were isolated and added to the genus (14, 15).

After these reclassifications, the resulting genus of *Ruegeria* was monophyletic in a maximum likelihood tree based on the highly conserved core genes (37). Since that time, the whole-genome sequences of additional species became publicly available, including *Ruergeria denitrificans*, *Ruegeria kandeliae*, *Ruegeria marisrubri*, *Ruegeria mediterranea*, *Ruegeria profundi*, and *Cribrihabitans marinus* (13-15). Using the methodology of Wirth and Whitman (2018), a maximum likelihood tree based on 49 of the most conserved core genes was constructed using IQTree v. 1.6.3 (**Fig. 3-2**). This tree validated the taxonomic placement of *R. denitrificans*, *R. marisrubri*, *R. mediterranea*, and *R. profundi*. However, *Cribrihabitans marinus* was placed within the *Ruegeria* clade (**Fig. 3-2**).

To investigate this further, the average amino acid identity of the core genes (cAAI) was examined. Compared to the *Ruegeria* species, cAAI values with *C. marinus* ranged between 0.82 and 0.84 (**Fig. 3-1**). Compared with the closely related genus *Epibacterium*, the cAAI values ranged between 0.78 and 0.79. Previously, cAAI values above 0.85 were considered evidence for inclusion of species in the same genus and values below 0.80 as evidence for exclusion of species from the same genus (37, 38). Thus, *C. marinus* was not clearly excluded from *Ruegeria* by cAAI values, but inclusion in this genus was strongly supported by the topology of the maximum likelihood tree. These results support reclassification of *C. marinus* within *Ruegeria*. However, there are two *Cribrihabitans* species whose whole-genome sequences are not currently available. Because of this, the taxonomic placement of these organisms should be re-evaluated once these sequences become available.

The taxonomic placement of the most recent addition to the genus, *R. kandeliae*, is not supported by the cAAI (**Fig. 3-1**) or the phylogenetic tree (**Fig. 3-2**). This is likely due to the fact

that this species taxonomic placement was primarily done on the basis of 16S rRNA sequences, a metric that has been shown to be poorly correlated with the evolution of this group (37, 39-43). Because of this, an in-depth analysis of the phylogenetic placement of *R. kandeliae* is required to accurately assign *R. kandeliae* in the roseobacter group.

List of species of the genus *Ruegeria*

Ruegeria arenilitoris Park and Yoon 2013, 3^{VP} (Effective publication: Park and Yoon 2012, 586). *a.re.ni.li.to'ris*. L. n. *arena* sand; L. n. *litus -oris* the seashore, coast; N.L. gen. n. *arenilitoris* of sand of seashore, from which the type strain was isolated.

Description as for the genus and the following characteristics (2, 4, 6, 7, 9, 12-14, 29-33, 35). Cells are 0.2–0.6 μm in diameter and 0.8–4.0 μm long. Motile by means of peritrichous flagella. Colonies on marine agar are circular to slightly irregular, flat to raised, glistening, smooth, grayish yellow in color and 2.0–3.0 mm after incubation for 3 days at 30 °C. Anaerobic growth occurs on marine agar. Growth occurs between 4 ˚C and 45 ˚C (optimum, 30–37 ˚C). Growth does not occur at 50 ˚C. Growth occurs between pH 5.5 and pH 8.0 (optimum, pH 7.0–8.0). Growth does not occur at pH 5.0. Growth occurs between 0.5 % (*w/v*) NaCl and 6.0 % (*w/v*) NaCl (optimum, 2.0 % (*w/v*) NaCl). Mg^{2+} ions are required for growth but K^{+} ions are not. Nitrate is reduced to nitrate. Hydrolyzes hypoxanthine and L-tyrosine, but not casein, esculin, gelatin, starch, Tweens 20, 40, 60, and 80, urea, or xanthine. Utilizes D-cellobiose, D-fructose, D-galactose, D-glucose, D-mannose, D-xylose, acetate, citrate, malate, pyruvate, and succinate as sole carbon sources, but not L-arabinose, maltose, sucrose, D-trehalose, benzoate, formate, or L-glutamate. Produces acid from L-arabinose, D-cellobiose, and D-galactose, but not from D-fructose, D-glucose, *myo*-inositol, lactose, maltose, D-mannitol, D-mannose, D-melezitose, melibiose, D-raffinose, L-rhamnose, D-ribose, D-sorbitol, sucrose, D-trehalose, or D-xylose. In assays with the API-ZYM system, reactions for alkaline phosphatase activity are positive;

reactions for esterase (C4) and leucine arylamidase activities are weakly positive; but reactions for esterase lipase (C8), lipase (C14), valine arylamidase, cystine arylamidase, trypsin, α-chymotrypsin, acid phosphatase, α-galactosidase, β-galactosidase, β-glucuronidase, α-glucosidase, β-glucosidase, *N*-acetyl-β-glucosaminidase, α-mannosidase and α-fucosidase activities are negative. There are conflicting reports naphthol-AS-BI-phosphohydrolase activity (Table 3-1). The susceptibilities to antibiotics are summarized in Table 3-3. The fatty acid composition is summarized in Table 3-4. Isolated from seashore sand around a seaweed farm at Geoje island, South Korea. The DNA G+C content (mol %) is 66.4 and 61.3 as determined by HPLC and genome sequencing, respectively. The type strain is G-M8^{T} (=KCTC 23960^{T} =CCUG 62412^{T}). The GenBank accession numbers are JQ807219 (16S rRNA gene) and GCA_900185035 (genome).

Ruegeria atlantica (Rüger and Hölfe 1992) Uchino, Hirata, and Yokota 1999, 2^{VP} (Effective publication: Uchino, Hirata, and Yokota 1998, 208) (*Agrobacterium atlanticum* Rüger and Hölfe 1992, 141^{VP}). *at.lan'ti.ca* M.L. adj. *atlantica*, pertaining to the Atlantic Ocean.

Description as for the genus and the following characteristics (2, 4, 6, 7, 9, 12-14, 29-33). Cells are 0.6–1.0 μm in diameter and 1.5–2.0 μm long. Nonmotile but possess peritrichous flagella. Colonies are circular; flat to raised; translucent; colorless, beige, or yellowish; with a mean diameter of 2–3 mm. Growth occurs between 5 ˚C and 35 ˚C (optimum, 25–30 ˚C). Growth occurs between pH 6 and pH 11 (optimum, pH 7). Growth occurs between 3 % (*w/v*) NaCl and 10 % (*w/v*) NaCl (optimum, 3 % (*w/v*) NaCl). Reduces nitrate to nitrite and gas. Hydrolyzes esculin, hypoxanthine, L-tyrosine, and xanthine, but not casein, carboxymethylcellulose, gelatin, or starch. There are conflicting reports for the hydrolysis of Tween-80. Utilizes citrate, fumarate, malate, pyruvate, succinate, L-alanine, and L-tyrosine as sole carbon and energy sources, but not L-arabinose, D-fucose, lactose, adipate, benzoate,

formate, *p*-hydroxybenzoate, quinate, arabitol, adonitol, sorbitol, xylitol, or L-histidine. The ability to utilize cellobiose, D-galactose, gluconate, D-glucose, maltose, D-mannose, D-ribose, sucrose, trehalose, D-xylose, acetate, DL-3-hydroxybutyrate, lactate, propionate, glycerol, mannitol, L-arginine, L-aspartate, L-hisitidine, L-lysine, L-ornithine, and putrescine varies between strains. There are conflicting reports for the utilization of fructose, maltose, sucrose, trehalose, and L-glutamate. Produces acid from amygdalin, esculin, dulcitol, glycerol, glycogen, and xylitol, but not from D-adonitol, D-arabinose, arbutin, erythritol, D-fructose, D-fucose, gentiobiose, gluconate, 5-ketogluconate, *N*-acetylglucosamine, glucose, methyl α-D-glucoside, lactose, D-lyxose, D-mannose, melezitose, melibiose, methyl α-D-mannoside, L-rhamnose, salicin, L-sorbose, sucrose, D-tagatose, or methyl β-D-xyloside. There are conflicting reports for acid production from L-arabinose, D-cellobiose, galactose, *myo*-inositol, maltose, mannitol, raffinose, D-ribose, D-sorbitol, trehalose, and D-xylose. In assays with the API-ZYM system, reactions for alkaline phosphatase and leucine arylamidase are positive; reactions α-glucosidase are weakly positive; but reactions for esterase lipase (C8), lipase (C14), cystine arylamidase, trypsin, α-chymotrypsin, acid phosphatase, naphthol-AS-BI-phosphohydrolase, α-galactosidase, β-galactosidase, β-glucuronidase, β-glucosidase, *N*-acetyl-β-glucosaminidase, α-mannosidase and α-fucosidase are negative. There are conflicting reports for esterase (C4) and α-glucosidase activities (Table 1). Negative reactions for arginine dihydrolase and urease. Does not produce indole from tryptophan. Capable of demethylation/demethiolation of dimethylsulfoniopropionate to methanethiol and cleavage of dimethylsulfoniopropionate to dimethyl sulfide. Susceptible to furazolidone and oxytetracyline, but resistant to clindamycin and trimethoprim. The susceptibilities to other antibiotics are summarized in Table 3-3. The fatty acid composition is summarized in Table 3-4. Isolated from marine sediments of the eastern Atlantic Ocean. The DNA G+C content (mol %) is 55 and 56.4 as determined by thermal denaturation and genome

sequencing, respectively. The type strain is 1480^{T} (=IAM 14463^{T} = DSM 5823^{T}). The GenBank accession numbers are D88526 (16S rRNA gene) and GCA_001458195 (genome).

Ruegeria conchae Lee, Whon, Shin, Roh, Kim, Park, Kim, Shin, Lee, Lee, Kim, and Bae 2012, 2853^{VP}. *con'chae*. L. gen. n. *conchae* of/from a bivalve, shellfish.

Description as for the genus and the following characteristics (9, 12, 13). Cells are 0.3–0.5 μm in diameter and 0.5–1.0 μm long. Cells are non-motile and are not flagellated. Colonies are yellow, circular with entire margins and 1.0–2.5 mm in diameter after incubation for 3 days on marine agar at 30 ˚C. Strict aerobes. Growth occurs between 10 ˚C and 37 ˚C (optimum, 25–30 ˚C). Growth occurs between pH 7.0 and pH 10.0 (optimum pH 8.0). Growth occurs between 1 % (*w/v*) NaCl and 5 % (*w/v*) NaCl (optimum, 2 % (*w/v*) NaCl). Does not reduce nitrate to nitrite. Hydrolyzes esculin, but does not hydrolyze casein, starch, or xanthine. Utilizes gluconate, D-glucose, D-mannose, D-ribose, D-xylose, acetate, citrate, malate, pyruvate, succinate, arabitol, and glycerol as sole carbon and energy sources, but not L-arabinose, D-fucose, lactose, rhamnose, salicin, sucrose, benzoate, formate, adonitol, mannitol, sorbitol, xylitol, or L-glutamate. There are conflicting reports for the utilization of D-cellobiose, D-fructose, D-galactose, maltose, and trehalose. Produces acid from arbutin, erythritol, esculin, gentiobiose, gluconate, 5-ketogluconate, methyl α-D-glucoside, salicin, and xylitol, but not from D-adonitol, amygdalin, D-arabinose, L-arabinose, D-arabitol, D-cellobiose, dulcitol, D-fucose, D-galactose, *N*-acetylglucosamine, glycerol, glycogen, *myo*-inositol, D-lyxose, methyl α-D-mannoside, melezitose, melibiose, raffinose, L-rhamnose, D-sorbitol, L-sorbose, sucrose, D-tagatose, trehalose, D-xylose, or methyl β-D-xyloside. There are conflicting reports for acid production from D-fructose, D-glucose, lactose, maltose, mannitol, D-mannose, and D-ribose. In assays with the API-ZYM system, reactions for alkaline phosphatase, acid phosphatase, esterase (C4), esterase (C8), and leucine aryamidase are positive; reactions for β-galactosidase and α-

glucosidase are weakly positive; but reactions for lipase (C14), valine arylamidase, cystine arylamidase, trypsin, α-chymotrypsin, α-galactosidase, β-glucuronidase, *N*-acetyl-β-glucosaminidase, α-mannosidase, α-fucosidase are negative. There are conflicting reports for naphthol-AS-BI-phosphohydrolase activity (Table 3-1). Negative for reactions of L-arginine dihyrolase, protease, and urease. Does not produce indole from tryptophan. The susceptibilities to antibiotics are summarized in Table 3-3. The fatty acid composition is summarized in Table 3-4. Isolated from an ark clam from the South Sea of Korea. The DNA G+C content (mol %) is 55.7 as determined by genome sequencing. The type strain is TW15^{T} (=KACC 15115^{T} =JCM 17315^{T}). The GenBank accession numbers are HQ171439 (16S rRNA gene) and GCA_000192475 (genome).

Ruegeria denitrificans Arahal, Lucena, Rodrigo-Torres, and Pujalte 2018, 2521^{VP}. *de.ni.tri'fi.cans*. N.L. part. adj. *denitificans* denitrifying.

Description as for the genus and the following characteristics (14). Cells are non-motile. Colonies on marine agar are smooth, circular, convex, have regular borders, and are not pigmented. Aerobic chemoorganotroph. Growth occurs between 15 ˚C and 26 ˚C (optimum, 26 ˚C), but not at 4 ˚C or 37 ˚C. Growth occurs between pH 6 and pH 9 (optimum, pH 7). Growth occurs between 1.5 % (*w/v*) total salinity and 6 % (*w/v*) total salinity (optimum, 3 % (*w/v*) total salinity), but not at total salinities of 1.0 % (*w/v*) or less or 7 % (*w/v*) or more. Requires Na^{+} and Mg^{2+} ions for growth. Reduces nitrate to dinitrogen. Hydrolyzes *p*-nitrophenyl β-D-glucopyranoside, but not casein, DNA, esculin, gelatin, starch, or Tween-80. Utilizes D-fructose, D-galactose, *N*-acetyl-D-glucosamine, D-glucose, maltose, D-mannose, melibiose, L-rhamnose, D-ribose, sucrose, acetate, t-aconitate, 4-aminobutyrate, butyrate, citrate, D-glycerate, 3-hydroxybutyrate, lactate, malate, 2-oxoglutarate, propionate, pyruvate, succinate, D-glycerol, *myo*-inositol, mannitol, sorbitol, L-alanine, L-arginine, L-aspartate, L-citrulline, L-glutamate,

glycine, L-leucine, L-lysine, L-ornithine, putrescine, L-sarcosine, L-serine, L-threonine, and L-tyrosine as sole carbon and energy sources, but not amygdalin, L-arabinose, D-cellobiose, lactose, salicin, trehalose, D-xylose, D-galacturonate, D-gluconate, D-glucuronate, D-saccharate, or L-histidine. In assays with the API-ZYM system, reactions for acid phosphatase and alkaline phosphatase activities are positive; but reactions for α-chymotrypsin, cystine arylamidase, esterase (C4), esterase lipase (C8), α-fucosidase, α-galactosidase, β-galactosidase, *N*-acetyl-β-glucosaminidase, α-glucosidase, β-glucosidase, β-glucuronidase, leucine arylamidase, lipase (C14), α-mannosidase, naphthol-AS-BI-phosphohydrolase, trypsin, and valine arylamidase activities are negative (Table 3-1). The fatty acid composition is summarized in Table 3-4. Isolated from an oyster harvested from the coast of Vinaroz, Spain. The DNA G+C content (mol %) is 56.7 as determined by genome sequencing. The type strain is CECT 5091^{T} (=50M10^{T} =LMG 29896^{T}). The GenBank accession numbers are MH023307 (16S rRNA gene) and GCA_001458295 (genome).

Ruegeria faecimaris Oh, Jung, Oh, and Yoon 2011, 1186^{VP}. *fae.ci.ma'ris*. L. n. *faex faecis* sediment; L. gen. n. *maris* of the sea; N.L. gen. n. *faecimaris* of the sediment of the sea.

Description as for the genus and the following characteristics (6, 9). Cells are 0.3–0.6 µm in diameter and 1.0–8.0 µm long. A few cells longer than 10 µm may occur. Cells are non-motile and are not flagellated. Colonies on marine agar are circular, glistening, convex, smooth, greyish yellow in color, and 0.5–2.0 mm in diameter after incubation for 5 days at 30 ˚C. Growth occurs between 4 ˚C and 37 ˚C (optimum, 30 ˚C) but not at 40 ˚C. Growth occurs between pH 5.0 and pH 8.0 (optimum, pH 7–8) but not at pH 4.5. Growth occurs between 0.5 % (*w/v*) NaCl and 7.0 % (*w/v*) NaCl (optimum 2–3 % (*w/v*) NaCl), but not in the absence of NaCl or in the presence of more than 8.0 % (*w/v*) NaCl. Hydrolyzes esculin, hypoxanthine, L-tryrosine, and Tweens 20, 40, 60, and 80, but not casein, starch, urea, or xanthine. There are conflicting reports for the

hydrolysis of gelatin. Utilizes D-cellobiose, D-fructose, D-galactose, D-glucose, D-mannose, L-rhamnose, acetate, citrate, malate, pyruvate, succinate, and L-tyrosine as sole carbon and energy sources, but not L-arabinose, maltose, sucrose, trehalose, D-xylose, benzoate, formate, or L-glutamate. Produces acid from erythritol, esculin, D-galactose, 5-ketogluconate, *N*-acetylglucosamine, glycogen, methyl α-D-mannoside, L-rhamnose, sucrose, D-tagatose, xylitol, and methyl β-D-xyloside, but not from D-adonitol, amygdalin, D-arabinose, L-arabinose, D-arabitol, arbutin, D-cellobiose, dulcitol, D-fructose, D-fucose, gentiobiose, gluconate, D-glucose, methyl α-D-glucoside, glycerol, *myo*-inositol, lactose, D-lyxose, maltose, mannitol, D-mannose, melibiose, raffinose, salicin, D-sorbitol, L-sorbose, trehalose, or D-xylose. There are conflicting data for acid production from melezitose and D-ribose. In assays with the API-ZYM system, reactions for alkaline phosphatase and acid phosphatase are positive; reactions for esterase (C4) are weakly positive; but reactions for esterase lipase (C8), lipase (C14), leucine arylamidase, valine arylamidase, cystine arylamidase, trypsin, α-chymotrypsin, naphthol-AS-BI-phosphohydrolase, α-galactosidase, β-galactosidase, β-glucuronidase, α-glucosidase, β-glucosidase, *N*-acetyl-β-glucosaminidase, α-mannosidase and α-fucosidase are negative (Table 3-1). Susceptible to cephalothin. The susceptibilities to other antibiotics are summarized in Table 3-3. The fatty acid composition is summarized in Table 3-4. Isolated from a tidal flat of Hwang-do, Korea. The DNA G+C content (mol %) is 57.9 and 56.7 as determined by HPLC and genome sequencing, respectively. The GenBank accession number is GU057915 (16S rRNA gene). The IMG taxon ID is 2724679780.

Ruegeria halocynthiae Kim, Park, Nam, Kang, Hur, Lee, Oh, and Yoon 2012, 928^{VP}. *ha.lo.cyn.thi'a.e*. N.L. gen. n. *halocynthiae* of *Halocynthia*, named after the generic name of the sea squirt *Halocynthia roretzi*, from which the type strain was isolated.

Description as for the genus and the following characteristics (7, 9, 12). Cells are 0.2–0.6 μm in diameter and 1.0–10 μm long. A few cells longer than 10 μm may occur. Cells are non-motile and are not flagellated. Colonies on marine agar are circular to slightly irregular, flat, glistening, smooth, cream-colored, and 2.0–3.0 mm in diameter after incubation for 3 days at 30 ˚C. Anaerobic growth does not occur on marine agar but does occur on marine agar supplemented with nitrate. Growth occurs between 10 ˚C and 37 ˚C (optimum, 30 ˚C), but not 4 ˚C or 40 ˚C. Growth occurs between pH 5.5 and pH 8.0 (optimum, pH 7.0-8.0), but not at pH 5.0. Growth occurs between 0.5 % (*w/v*) NaCl and 6.0 % (*w/v*) NaCl (optimum, 2–3 % (*w/v*) NaCl), but not in the absence of NaCl or in the presence of more than 7.0 % (*w/v*) NaCl. Reduces nitrate to nitrite. Hydrolyzes hypoxanthine, L-tyrosine, and xanthine, but not casein, starch, Tween 80, or urea. There are conflicting reports for the hyrdolysis of esculin and gelatin. Utilizes D-cellobiose, D-galactose, D-glucose, D-mannose, acetate, citrate, malate, succinate, and L-tyrosine as sole carbon and energy sources, but not L-arabinose, D-fructose, maltose, salicin, sucrose, trehalose, D-xylose, benzoate, formate, pyruvate, or L-glutamate. Produces acid from esculin, 5-ketogluconate, D-mannose, D-ribose, L-sorbose, and D-tagatose, but not from D-adonitol, amygdalin, D-arabinose, L-arabinose, D-arabitol, arbutin, D-cellobiose, dulcitol, erythritol, D-fucose, gentiobiose, gluconate, *N*-acetylglucosamine, methyl α-D-glucoside, glycerol, glycogen, *myo*-inositol, lactose, D-lyxose, maltose, mannitol, methyl α-D-mannoside, melezitose, melibiose, raffinose, L-rhamnose, salicin, D-sorbitol, sucrose, trehalose, xylitol, D-xylose, or methyl β-D-xyloside. There are conflicting reports for acid production from D-fructose, D-galactose, and D-glucose. In assays with the API-ZYM system, reactions for acid phosphatase, alkaline phosphatase, esterase lipase (C8), leucine arylamidase, and α-glucosidase are positive; reactions for, esterase (C4) is weakly positive; but reactions for lipase (C14), valine arylamidase, cystine arylamidase, trypsin, α-chymotrypsin, naphthol-AS-BI-phosphohydrolase,

α-galactosidase, β-galactosidase, β-glucuronidase, β-glucosidase, *N*-acetyl-β-glucosaminidase, α-mannosidase, and α-fucosidase are negative (Table 3-1). Susceptible to cephalothin. The susceptibilities to other antibiotics are summarized in Table 3-3. The fatty acid composition is summarized in Table 3-4. Isolated from a sea squirt (*Halocynthia roretzi*) collected in the South Sea, Korea. The DNA G+C content (mol %) is 58.6 and 57.4 as determined by HPLC and genome sequencing, respectively. The type strain is MA1-6^{T} (=KCTC 23463^{T} =CCUG 60744^{T}). The GenBank accession numbers are HQ852038 (16S rRNA gene) and GCA_900106805 (genome).

Ruegeria intermedia Kämpfer, Arun, Rekha, Busse, Young, and Glaeser 2013, 2542^{VP}. *in.ter.me'di.a*. L. fem. adj. *intermedia* that is between, intermediate, referring to the fact that the species is grouped between the genera *Ruegeria*, *Lutimaribacter* and *Pseudoruegeria* on the basis of 16S rRNA gene sequence similarities.

Description as for the genus and the following characteristics (11, 13). Cells are 1.0–1.2 μm in diameter and 2.0–5.0 μm long. Some cells are irregularly rod-shaped. Non-motile. Colonies on marine agar are cream colored, circular with a spreading edge, and visible after 24 hours at 37 ˚C. Growth does not occur on tryptic soy, nutrient, and yeast extract agars. Growth occurs between 15 ˚C and 55 ˚C (optimum, 37–45 ˚C), but not at 10 ˚C or 60 ˚C. Growth occurs between pH 5.0 and pH 10.0 (optimum, pH 8.0). Growth occurs between 1 % (*w/v*) NaCl and 4 % (*w/v*) NaCl (optimum, 1–2 % (*w/v*) NaCl). Hyrdolyzes esculin, bis-*p*-nitrophenylphosphate, bis-*p*-nitrophenylphenylphosphonate, and bis-*p*-nitrophenylphosphorylcholine, but not gelatin, *p*-nitrophenyl-α-D-glucopyranoside, *p*-nitrophenyl-β-D-galactopyranoside, *p*-nitrophenyl-β-D-xylopyranoside, *p*-nitrophenyl-β-D-glucopyranoside, *p*-nitrophenyl-β-D-glucuronide, 2-deoxythymidine-2′-*p*-nitrophenylphosphate, L-alanine-*p*-nitroanilide, γ-L-glutamate-*p*-nitroanilide, or L-proline-*p*-nitroanilide. Utilizes D-galactose and D-glucose as sole carbon and

energy sources, but not L-arabinose, D-cellobiose, gluconate, maltose, D-mannose, melibiose, D-ribose, salicin, sucrose, D-xylose, acetate, adipate, 4-aminobutyrate, azelate, citrate, fumarate, glutarate, 3-hydroxybenzoate, 4-hydroxybenzoate, DL-3-hydrxoybutyrate, itaconate, lactate, mesaconate, phenylacetate, propionate, pyruvate, suberate, adonitol, glycerol, *myo*-inositol, malitol, mannitol, sorbitol, L-alanine, β-alanine, L-aspartate, L-histidine, L-leucine, L-ornithine, L-phenylalanine, L-proline, L-serine, L-tryptophan, *N*-acetyl-D-glucosamine, *N*-acetylgalactosamine, or L-arbutin (Table 3-1). The polyamine pattern is characterized by the major compound spermidine. The fatty acid composition is summarized in Table 3-4. Isolated from a coastal hot spring of Green Island (Lutao), Taiwan. The DNA G+C content (mol %) is 64.0 as determined by genome sequencing. The type strain is CC-GIMAT-2^T (=CCUG 59209^T =LMG 25539^T =CCM 7758^T). The GenBank accession number is FR832879 (16S rRNA gene). The IMG taxon ID is 2695420938.

Ruegeria kandeliae Xhang, Wang, Yin, Liang, and Xu 2018, 2657^{VP}. *kan.de'li.ae*. N.L. gen. n. *kandeliae* of *Kandelia*, referring to a genus of mangrove plant.

Although the taxonomic analysis described above suggests that *R. kandeliae* is not a member of the genus *Ruegeria stricto sensu*, the species description is included here for completeness, and future work is expected to reassign this species to another genus. Description of the species is as for the genus and the following charactertistics (15). Cells are 0.5–0.7 μm in diameter and 1.3–3.3 μm long. Cells are motile by means of one polar flagellum. Colonies are circular, cream-coloured, and 0.4–0.8 mm in diameter. Growth occurs between 10 ˚C and 40 ˚C (optimum, 30–37 ˚C). Growth occurs between pH 5 and 8.5 (optimum, pH 6–7). Growth occurs between 0 % (*w/v*) NaCl and 9 % (*w/v*) NaCl (optimum, 0.5–3 % (*w/v*) NaCl). Does not reduce nitrate to nitrite. Hydrolyzes L-arginine and urea, but not esculin, gelatin, or Tweens 20, 40, 60, or 80. Utilizes L-arabinose, gluconate, D-glucose, adipate, citrate, malate, and phenylacetate as

sole carbon and energy sources, but not maltose, D-mannose, *N*-acetyl-glucosamine, or caprate. Does not produce acid from glucose. In assays with the API ZYM system, reactions for acid phosphatase, alkaline phosphatase, esterase (C4), esterase lipase (C8), leucine arylamidase, and naphthol-AS-BI-phosphohydrolase are positive; reactions for α-galactosidase and valine arylamidase are weakly positive; but reactions for α-chymotrypsin, cystine arylamidase, α-fucosidase, β-galactosidase, *N*-acetyl-β-glucosaminidase, α-glucosidase, β-glucosidase, β-glucuronidase, lipase (C14), α-mannosidase, and trypsin are negative (Table 3-1). Does not produce indole from tryptophan. Susceptible to amikacin, cephalexin, norfloxacin, rifampicin, and tobramycin, but resistant to ciprofloxacin, clindamycin, and nalidixic acid. The susceptibilities to other antibiotics are summarized in Table 3-3. The fatty acid composition is summarized in Table 3-4. Isolated from the rhizosphere soil of a mangrove (*Kandelia candel*) in Mai Po Natur Reserve (Hong Kong, China) in December of 2016. The DNA G+C content (mol %) is 65.7 as determined by genome sequencing. The type strain is J95^{T} (=MCC 1K03284^{T} =DSM 104293^{T}). The GenBank accession numbers are KY038376 (16S rRNA gene) and GCA_003116585 (genome).

Ruegeria lacuscaerulensis (Petursdottir and Kristjansson 1997) Yi, Lim, and Chun 2007, 818^{VP} (*Silicibacter lacuscaerulensis* Petursdottir and Kristjansson 1999, 1325). *la.cus.cae.ru.len' sis*. L. masc. n. *lacus*, lake; L. adj. *caeruleus*, blue; M.L. adj. *lacuscaerulensis*, pertaining to the blue lake.

Description as for the genus and the following characteristics (3, 4, 6, 9, 11, 13, 14, 29, 30, 32, 33, 44). Cells are 0.6–0.8 μm in diameter and 9–18 μm long. Unicellular and non-sporeforming. Cells are non-motile and are not flagellated. Contains intracellular poly-β-hydroxybutyrate granules. Colonies are tan colored, opaque, and 2–4 mm in diameter. Strict aerobe. Growth occurs between 10 ˚C and 45 ˚C (optimum, 35–40 ˚C). Growth occurs between

pH 6.5 and 8.5 (optimum, pH 7.0-7.5). Growth occurs between 1.5 % (*w/v*) NaCl and 7 % (*w/v*) NaCl (optimum 3.5 % (*w/v*) NaCl). Requires sea salts for growth. Reduces nitrate to dinitrogen. Hydrolyzes hypoxanthine and L-tyrosine, but not carboxymethylcellulose, casein, gelatin, or starch. There are conflicting reports for the hydrolysis of esculin and gelatin. Utilizes D-cellobiose, D-fructose, D-galactose, saccharose, malate, pyruvate, succinate, L-arginine, L-lysine, and L-tyrosine as sole carbon and energy sources, but not L-arabinose, gluconate, maltose, salicin, sucrose, trehalose, D-xylose, benzoate, formate, or L-glutamate. There are conflicting reports for the utilization of D-glucose, D-mannose, acetate, citrate, and mannitol. Produces acid from D-arabitol, dulcitol, esculin, D-fucose, methyl α-D-glucoside, D-lyxose, methyl α-D-mannoside, D-tagatose, and xylitol, but not from D-adonitol, amygdalin, D-arabinose, L-arabinose, arbutin, erythritol, D-galactose, gentiobiose, gluconate, 5-ketogluconate, *N*-acetylglucosamine, glucose, glycogen, glycerol, *myo*-inositol, lactose, mannitol, D-mannose, melibiose, raffinose, L-rhamnose, salicin, D-sorbitol, L-sorbose, D-xylose, or methyl β-D-xyloside. There are conflicting reports for the production of acid from D-cellobiose, D-fructose, maltose, melezitose, D-ribose, sucrose, and trehalose. In assays with the API-ZYM system, reactions for alkaline phosphatase and leucine arylamidase; reactions for β-galactosidase are weakly positive; but reactions for lipase (C14), cystine arylamidase, trypsin, α-chymotrypsin, α-galactosidase, β-glucuronidase, β-glucosidase, *N*-acetyl-β-glucosaminidase, α-mannosidase and α-fucosidase are negative. There are conflicting reports for acid phosphatase, esterase (C4), esterase (C8), α-glucosidase, naphthol-AS-BI-phosphohydrolase, and valine arylamidase activities (Table 3-1). Negative reactions for arginine dihydrolase and urease. Does not produce indole from tryptophan. Capable of demethylation/demethiolation of dimethylsulfoniopropionate to methanethiol, but not cleavage of dimethylsulfoniopropionate to dimethylsulfide. Resistant to clindamycin and trimethoprim. The susceptibilities to other antibiotics are summarized in Table

3-3. The fatty acid composition is summarized in Table 3-4. Bacteriochlorophyll A is absent. Does not utilize tetramethylammonium chloride but tolerates up to 0.2%. Membrane-bound cytochrome C with a distinctive peak at 549 nm. Isolated from Blue Lagoon, near Svartsengi geothermal powerplant, Iceland. The DNA G+C content (mol %) is 66.2 and 63.0 as determined by HPLC and genome sequencing, respectively. The type strain is ITI-1157^{T} (=DSM 11314^{T} =KCTC 2953^{T}). The GenBank accession numbers are U77644 (16S rRNA gene) and GCA_000161775 (genome).

Ruegeria litorea (Lucena, Ruvira, Macián, Pujalte, and Arahal 2013) Wirth and Whitman 2018, 2406^{VP} (*Tropicibacter litoreus* Lucena, Ruvira, Macián, Pujalte, Arahal 2014, 3). *li.to're.a.* L. fem. adj. *litorea* of the shore.

Description as for the genus and the following characteristics (10, 45). Cells are 0.7 µm in diameter and 1.0–3.0 µm long. Cells are non-motile and are not flagellated. Cells do not accumulate poly-β-hydroxybutyrate. Colonies on marine agar are creamy with an irregular margin and become brownish with aging after 2 days at 28 ˚C. Strict aerobe. Growth occurs between 15 ˚C and 30 ˚C (optimum 28 ˚C). Growth occurs between 1.7 % (*w/v*) NaCl and 7.0 % (*w/v*) NaCl. Reduces nitrate to nitrite and dinitrogen. Does not hydrolyze agar, alginate, casein, DNA, esculin, gelatin, lecithin, starch, Tween 80, or urea. Does not produce acid from glucose or trehalose. Utilizes acetate, 4-aminobutyrate, butyrate, citrate, fumarate, 3-hydroxybutyrate, lactate, malate, 2-oxoglutarate, propionate, pyruvate, succinate, glycerol, L-alanine, L-arginine, L-citrulline, L-glutamate, L-leucine, L-ornithine, L-threonine, and L-tyrosine as sole carbon and energy sources, but not amygdalin, L-arabinose, D-cellobiose, D-fructose, D-galactose, galacturonate, gluconate, D-glucose, glucuronate, D-glycerate, lactose, maltose, D-mannose, D-melibiose, L-rhamnose, D-saccharate, salicin, sucrose, trehalose, D-xylose, *myo*-inositol, mannitol, sorbitol, L-histidine, L-lysine, or putrescine. In assays with the API-ZYM system,

reactions for acid phosphatase, alkaline phosphatase, and leucine arylamidase are positive; but reactions for α-chymotrypsin, cystine arylamidase, esterase (C4), esterase lipase (C8), α-galactosidase, β-galactosidase, *N*-acetyl-β-glucosaminidase, α-glucosidase, β-glucosidase, β-fucosidase, β-glucuronidase, lipase (C14), α-mannosidase, naphthol-AS-BI-phosphohydrolase, trypsin, and valine arylamidase are negative (Table 3-1). Negative reaction for arginine dihydrolase. Does not produce indole from tryptophan. The susceptibilities to antibiotics are summarized in Table 3-3. The fatty acid composition is summarized in Table 3-4. Isolated from Mediterranean seawater at Malvarrosa beach, Valencia, Spain. The DNA G+C content (mol %) is 59.0 and 59.2 as determined by HPLC and genome sequencing, respectively. The type strain is R37^{T} (=CECT 7639 ^{T} =KCTC 23353 ^{T}). The GenBank accession numbers are FJ872535 (16S rRNA gene) and GCA_900172225 (genome).

Ruegeria marina Huo, Xu, Li, Liu, Cui, Wang, and Wu 2011, 349^{VP}. *ma.ri'na*. L. fem. adj. *marina* marine, of the sea, where the type strain was isolated.

Description as for the genus and the following characteristics (5, 9, 15). Cells are 0.5–1.0 μm in diameter and 2.0–4.5 μm long. Cells are non-motile and are not flagellated. Colonies on marine agar are 1.5–2 mm in diameter, rough, slightly elevated, and cream-colored with regular edges after 3 days at 35 ˚C. Growth occurs between 10 ˚C and 42 ˚C (optimum, 35–37 ˚C). Growth occurs between pH 6.5 and pH 9.0 (optimum, pH 7.5). Growth occurs between 0 % (*w/v*) NaCl and 7.5 % (*w/v*) NaCl (optimum, 0.5–3.0 % (*w/v*) NaCl). Does not reduce nitrate to nitrite. Hydrolyzes casein, Tween 20, and L-tyrosine, but not starch, Tween-40, Tween-60, Tween-80, or urea. There are conflicting reports for the hydrolysis of esculin and gelatin. Utilizes D-glucose, D-xylose, acetate, citrate, lactate, malate, propionate, pyruvate, succinate, ethanol, glycerol, L-alanine, L-arginine, L-cysteine, L-glutamate, L-isoleucine, L-histidine, L-lysine, L-ornithine, L-serine, and L-tyrosine as sole carbon and energy sources, but not L-

arabinose, D-cellobiose, D-fructose, D-galactose, gluconate, lactose, maltose, D-mannose, L-rhamnose, salicin, sucrose, trehalose, formate, fumarate, mannitol, or sorbitol. Produces acid from 5-ketogluconate, D-glucose, D-sorbitol, D-tagatose, and methyl β-D-xyloside, but not from D-adonitol, amygdalin, D-arabinose, L-arabinose, D-arabitol, arbutin, D-cellobiose, dulcitol, erythritol, esculin, D-fructose, D-fucose, D-galactose, gentiobiose, gluconate, *N*-acetylglucosamine, methyl α-D-glucoside, glycerol, glycogen, *myo*-inositol, lactose, D-lyxose, maltose, mannitol, D-mannose, methyl α-D-mannoside, melezitose, raffinose, D-ribose, salicin, L-sorbose, starch, sucrose, trehalose, xylitol, or D-xylose. In assays with the API ZYM system, reactions for acid phosphatase, alkaline phosphatase, esterase (C4), esterase lipase (C8), leucine arylamidase, naphthol-AS-BI-phosphohydrolase and valine arylamidase are positive; but reactions for α-chymotrypsin, cystine arylamidase, α-galactosidase, β-galactosidase, *N*-acetyl-β-glucosaminidase, α-glucosidase, β-glucosidase, β-fucosidase, β-glucuronidase, lipase (C14), α-mannosidase, and trypsin are negative (Table 3-1). Negative reactions also for arginine dihydrolase, *o*-nitrophenyl-β-D-galactopyranosidase, lysine decarboxylase, ornithine decarboxylase, and tryptophan deaminase. Does not produce indole from tryptophan. Susceptible to amoxicillin, cefotaxime, nitrofurantoin, rifampicin, and tobramycin, but resistant to bacitracin and nystatin. The susceptibilities to other antibiotics are summarized in Table 3-3. The fatty acid composition is summarized in Table 3-4. Isolated from a marine sediment of the East China Sea. The DNA G+C content (mol %) is 63.5 and 62.8 as determined by HPLC and genome sequencing, respectively. The type strain is ZH17^{T} (=CGMCC 1.9108^{T} =JCM 16262^{T}). The GenBank accession numbers are FJ872535 (16S rRNA gene) and GCA_900101475 (genome).

Ruegeria marisrubri Zhang, Haroon, Zhang, Dong, Wang, Liu, Xun, Dong, and Stingl 2017, 4630^{VP}. *ma.ris.ru'bri.* L. n. *mare*, *maris* sea; L. adj. *ruber* red; N.L. gen. n. *marisrubri* of the Red Sea.

Description as for the genus and the following characteristics (13). Cells are 0.6–1.2 μm in diameter and 2.0–5.0 μm long. Unicellular and non-sporeforming. Cells are non-motile and are not flagellated. Colonies are beige colored with a spreading edge and approximately 3.0 mm in diameter. Growth occurs between 20 ˚C and 50 ˚C (optimum, 37–40 ˚C). Growth occurs between pH 6.0 and 8.5 (optimum, pH 7.0–7.5). Growth occurs between 2.9 % (*w/v*) NaCl and 15.2 % (*w/v*) NaCl (optimum 8.8–11.7 % (*w/v*) NaCl). Reduces nitrate to nitrite. Hydrolyzes esculin and gelatin, but not Tween 80. Utilizes D-cellobiose, dextrin, D-fructose, D-fructose-6-phosphate, gentiobiose, D-glucose, β-methyl D-glucoside, lactose, maltose, D-mannose, melibiose, pectin, raffinose, salicin, sucrose, *N*-acetyl-D-glucosamine, *N*-acetyl-β-D-mannosamine, *N*-acetyl neuraminic acid, γ-aminobutryric acid, fusidic acid, L-galactonic acid lactone, D-glucuronic acid, α-hydroxybutyric acid, α-ketobutyric acid, lactate, D-lactic acid methyl ester, nalidixic acid, methyl pyruvate, arabitol, glycerol, L-arginine, L-aspartic acid, L-glutamate, glycyl-L-proline, D-serine, and L-serine as sole carbon and energy sources, but not D-fucose, D-galactose, acetate, citrate, or mannitol. In assays with the API-ZYM system, reactions for alkaline phosphatase, esterase lipase (C8), α-fucosidase, α-glucosidase, α-mannosidase, and valine arylamidase are positive; reactions for esterase (C4), β-galactosidase, leucine arylamidase, and trypsin are weakly positive; but reactions for acid phosphatase, α-chymotrypsin, cystine arylamidase, α-galactosidase, *N*-acetyl-β-glucosaminidase, β-glucuronidase, lipase (C14), and naphthol-AS-BI-phosphohydrolase are negative (Table 3-1). Does not produce indole from tryptophan. Negative for urease. The susceptibilities to antibiotics are summarized in Table 3-3. The fatty acid composition is summarized in Table 3-4. Isolated from the brine–seawater interface at Erba Deep in the Red Sea, Saudi Arabia. The DNA G+C content (mol %) is 62.94 as determined by genome sequencing. The type strain is ZGT118^{T} (=JCM 1959^{T} =ACCC 19862^{T}).

The GenBank accession numbers are KP726356 (16S rRNA gene) and GCA_001507595 (genome).

Ruegeria mediterranea (Lucena, Ruvira, Macián, Pujalte, Arahal 2013) Wirth and Whitman 2018, 2406^{VP} (*Tropicibacter mediterraneus* Lucena, Ruvira, Macián, Pujalte, Arahal 2014, 3). *me.di.ter.ra'ne.a.* L. fem. adj. *mediterranea* pertaining to the Mediterranean Sea.

Description as for the genus and the following characteristics (10, 45). Cells are 0.6–0.7 µm in diameter and 1.0–5.0 µm long. Cells are non-motile and are not flagellated. Cells do not accumulate poly-β-hydroxybutyrate. Colonies on marine agar are regular and cream colored after incubation for 24 hours at 28 ˚C and develop a brown pigmentation in the center and border of colonies after incubation for 72 hours at 28 ˚C. Growth occurs between 15 ˚C and 30 ˚C (optimum, 28 ˚C), but not at 4 ˚C. Growth occurs between 0.9 % (*w/v*) total salinity and 5.0 % (*w/v*) total salinity, but not at total salinities below 0.9 % (*w/v*) or above 7.0 % (*w/v*). Reduction of nitrate and nitrite varies between strains. Does not hydrolyze agar, alginate, casein, DNA, esculin, gelatin, lecithin, starch, Tween 80, or urea. Utilizes D-fructose, D-galactose, D-glucose, D-xylose, acetate, 4-aminobutyrate, butyrate, citrate, fumarate, DL-3-hydroxybutyrate, lactate, malate, 2-oxoglutarate, propionate, pyruvate, succinate, glycerol, mannitol, L-alanine, L-arginine, L-glutamate, L-histidine, and L-tyrosine as sole carbon and energy sources, but not L-arabinose, D-cellobiose, gluconate, lactose, maltose, D-mannose, L-rhamnose, salicin, sucrose, trehalose, or sorbitol. Does not produce acid from glucose. In assays with the API-ZYM system, reactions for acid phosphatase, alkaline phosphatase, and leucine arylamidase activities are positive; but reactions for α-chymotrypsin, cystine arylamidase, esterase (C4), esterase lipase (C8), α-fucosidase, α-galactosidase, *N*-acetyl-β-glucosaminidase, β-glucuronidase, lipase (C14), α-mannosidase, trypsin, and valine arylamidase activities are negative. Reactions for naphthol-AS-BI-phosphohydrolase, β-galactosidase, and α-glucosidase varies between strains (Table 3-1).

The susceptibilities to antibiotics are summarized in Table 3-3. The fatty acid composition is summarized in Table 3-4. Isolated from coastal seawater in the western Mediterranean Sea. The DNA G+C content (mol %) is 58.5–59.0 and 58.9 as determined by HPLC and genome sequencing, respectively. The type strain is M17^{T} (=CECT 7615^{T} =KCTC 23058^{T}). The GenBank accession numbers are HE860710 (16S rRNA gene) and GCA_900302455 (genome).

Ruegeria meonggei Kim, Park, Nam, Jung, Kim and Yoon 2014, 3604^{VP} (Effective publication: Kim, Park, Nam, Jung, Kim and Yoon 2014, 557). *me.ong.ge'i*. N.L. gen. n. *meonggei* of meongge, the Korean name for ascidian *Halocynthia roretzi*, from which the type strain was isolated.

Description as for the genus and the following characteristics (12, 14, 36). Cells are 0.2–0.8 μm in diameter and 0.5–10 μm long. Some cells longer than 10 μm occur. Cells are non-motile and are not flagellated. Colonies on marine agar are circular, slightly convex, glistening, smooth, grayish yellow in color, and 1.0–1.5 mm after incubation for 3 days at 30 °C. Strict aerobe. Anaerobic growth does not occur on marine agar or on marine agar supplemented with nitrate. Growth occurs between 4 ˚C and 30 ˚C (optimum, 30 ˚C), but not at 35 ˚C. Growth occurs between pH 6.5 and 8.0 (optimum, pH 7.0–8.0), but not at pH 6.0. Growth occurs between 1.0 % (*w/v*) NaCl and 6.0 % (*w/v*) NaCl (optimum, 2–3 % (*w/v*) NaCl). Reduces nitrate to dinitrogen. There are conflicting reports for the reduction of nitrate to nitrite. Hydrolyzes hypoxanthine and L-tyrosine, but not casein, esculin, gelatin, starch, Tween 80, urea, or xanthine. Utilizes D-cellobiose, D-fructose, D-galactose, D-glucose, D-mannose, D-xylose, acetate, pyruvate, and L-tyrosine as sole carbon and energy sources, but not L-arabinose, maltose, salicin, sucrose, trehalose, benzoate, citrate, malate, succinate, or L-glutamate. In assays with the API-ZYM system, reactions for alkaline phosphatase, esterase (C4), and leucine arylamidase activities are positive; reactions for esterase lipase (C8) and acid phosphatase

activities are weakly positive; but reactions for lipase (C14), valine arylamidase, cystine arylamidase, trypsin, α-chymotrypsin, naphthol-AS-BI-phosphohydrolase, α-galactosidase, β-galactosidase, β-glucuronidase, α-glucosidase, β-glucosidase, *N*-acetyl-β-glucosaminidase, α-mannosidase, and α-fucosidase activities are negative (Table 3-1). The susceptibilities to antibiotics are summarized in Table 3-3. The fatty acid composition is summarized in Table 3-4. Isolated from an ascidian (*Halocynthia roretzi*) collected from the South Sea, South Korea. The DNA G+C content (mol %) is 58.0 and 57.3 as determined by HPLC and genome sequencing, respectively. The type strain is MA-E2-3^{T} (=KCTC 32450^{T} = CECT 8411^{T}). The GenBank accession numbers are KF740534 (16S rRNA gene) and GCA_900172215 (genome).

Ruegeria pomeroyi (González, Covert, Whitman, Henrikson, Mayer, Scharf, Schmitt, Buchan, Fuhrman, Kiene, and Moran 2003) Yi, Lim, and Chun 2007, 818^{VP} (*Silicibacter pomeroyi* González, Covert, Whitman, Henrikson, Mayer, Scharf, Schmitt, Buchan, Fuhrman, Kiene, and Moran 2003, 1267). *po.me.roy'i*. N.L. masc. gen. n. *pomeroyi* of Lawrence R. Pomeroy, marine microbial ecologist who first elucidated the role of bacteria in the marine food web.

Description as for the genus and the following characteristics (4-6, 9, 14, 18, 30, 32, 33). Cells are 0.4–0.6 μm in diameter and 1.9–3.5 μm long. Cells contain poly-β-hydroxybutyrate granules and outer-membrane blebs. Cells are motile by means of one polar, complex flagellum. Colonies are circular, cream-colored, and convex. Growth occurs between 10 ˚C and 40 ˚C (optimum, 30 ˚C). Optimum growth occurs between 0.6–2.3 % (*w/v*) NaCl. Requires sea salts for growth. Vitamins are stimulatory but not essential for growth. Does not reduce nitrate to nitrite or gas. Hydrolyzes gelatin, hypoxanthine, and xanthine, but not casein, cellulose, starch, or xylan. There are conflicting reports for the hydrolysis of esculin and Tween-80. Utilizes gluconate, D-glucose, D-xylose, acetate, acrylate, citrate, cysteic acid,

dimethylsulfoniopropionate, DL-3-hydroxybutyrate, malate, pyruvate, ethanol, glycerol, L-alanine, L-arginine, L-methionine, L-serine, L-taurine, and L-tyrosine as sole sources of carbon and energy, but not L-arabinose, D-cellobiose, D-fructose, D-galactose, maltose, D-mannose, L-rhamnose, salicin, sucrose, trehalose, benzoate, formate, mannitol, or L-glutamate. There are conflicting reports for the utilization of succinate. Produces acid from D-adonitol, arbutin, esculin, D-tagatose, D-xylose, and methyl β-D-xyloside, but not from amygdalin, D-arabinose, L-arabinose, D-cellobiose, dulcitol, erythritol, D-fucose, D-galactose, gentiobiose, gluconate, 5-ketogluconate, *N*-acetylglucosamine, methyl α-D-glucoside, glycerol, glycogen, lactose, D-lyxose, maltose, mannitol, D-mannose, methyl α-D-mannoside, melezitose, melibiose, raffinose, L-rhamnose, salicin, D-sorbitol, L-sorbose, sucrose, trehalose, or xylitol. There are conflicting reports for the production of acid from D-fructose, D-glucose, *myo*-inositol, and D-ribose. In assays with the API-ZYM system, reactions for alkaline phosphatase and leucine arylamidase are positive; reactions for esterase lipase (C8) are weakly positive; but reactions for acid phosphatase, lipase (C14), valine arylamidase, cystine arylamidase, trypsin, α-chymotrypsin, α-galactosidase, β-galactosidase, β-glucuronidase, α-glucosidase, β-glucosidase, *N*-acetyl-β-glucosaminidase, α-mannosidase, naphthol-AS-BI-phosphohydrolase, and α-fucosidase are negative. There are conflicting reports for esterase (C4) activities (Table 3-1). Negative reactions for arginine dihydrolase and urease. Does not produce indole from tryptophan. Capable of demethylation/demethiolation of dimethylsulfoniopropionate to methanethiol and cleavage of dimethylsulfoniopropionate to dimethyl sulfide. Resistant to clindamycin and trimethoprim. The susceptibilities to other antibiotics are summarized in Table 3-3. The fatty acid composition is summarized in Table 3-4. Isolated from seawater in coastal Georgia, USA. The DNA G+C content (mol %) is 68.0±0.1 and 64.1 as determined by HPLC and genome sequencing,

respectively. The type strain is DSS-3^T (=ATCC 700808^T =DSM 15171^T). The GenBank accession numbers are AF098491 (16S rRNA gene) and GCA_000011965 (genome).

Ruegeria profundi Zhang, Haroon, Zhang, Dong, Wang, Liu, Xun, Dong, and Stingl 2017, 4629^{VP}. *pro.fun'di.* L. gen. n. *profundi* from the depths of the sea.

Description as for the genus and the following characteristics (13). Cells are 0.5–1.0 µm in diameter and 1.0–3.0 µm long with a few cells longer than 5.0 µm. Cells are non-motile and are not flagellated. Colonies on marine agar are circular to slightly irregular, flat, smooth, cream colored, and 2.0–3.0 mm in diameter after incubation at 33 ˚C for 3 days. Growth occurs between 15–42 ˚C (optimum, 33–35 ˚C). Growth occurs between pH 5.5 and pH 9 (optimum, pH 7.5–8). Growth occurs between 2.9 % (*w/v*) NaCl and 16.9 % (*w/v*) NaCl (optimum, 5.8–8.8 % (*w/v*) NaCl). Does not reduce nitrate to nitrite. Hydrolyzes esculin, but not acetate, casein, gelatin, or Tween-80. Utilizes D-fructose, D-mannose, sucrose, lactate, arabitol, and mannitol as sole carbon and energy sources, but not D-cellobiose, D-fucose, D-galactose, D-glucose, maltose, salicin, acetate, citrate, or glycerol. In assays with the API-ZYM system, reactions for alkaline phosphatase, esterase (C4), esterase lipase (C8), and leucine arylamidase activities are positive; reactions for acid phosphatase and α-glucosidase activities are weakly positive; but reactions for α-chymotrypsin, cystine arylamidase, α-fucosidase, α-galactosidase, β-galactosidase, *N*-acetyl-β-glucosaminidase, β-glucuronidase, lipase (C14), α-mannosidase, naphthol-AS-BI-phosphohydrolase, trypsin, and valine arylamidase are negative. The susceptibilities to antibiotics are summarized in Table 3-3. The fatty acid composition is summarized in Table 3-4. Isolated from the brine–seawater interface at Erba Deep in the Red Sea, Saudi Arabia. The DNA G+C content (mol %) is 56.7 as determined by genome sequencing. The type strain is ZGT108^T (=JCM 19518^T =ACCC 19861^T). The GenBank accession numbers are KP726355 (16S rRNA gene) and GCA_001507545 (genome).

References:

1. Martens T, Heidorn T, Pukall R, Simon M, Tindall BJ, Brinkhoff T. 2006. Reclassification of *Roseobacter gallaeciensis* Ruiz-Ponte *et al.* 1998 as *Phaeobacter gallaeciensis* gen. nov., comb. nov., description of *Phaeobacter inhibens* sp. nov., reclassification of *Ruegeria algicola* (Lafay *et al.* 1995) Uchino *et al.* 1999 as *Marinovum algicola* gen. nov., comb. nov., and emended descriptions of the genera *Roseobacter*, *Ruegeria* and *Leisingera*. International Journal of Systematic and Evolutionary Microbiology 56:1293-1304.
2. Rüger HJ, Höfle MG. 1992. Marine star-shaped-aggregate-forming bacteria: *Agrobacterium antlanticum* sp. nov.; *Agrobacterium meteori* sp. nov.; *Agrobacterium ferrugineum* sp. nov., nom. rev.; *Agrobacterium gelatinovorum* sp. nov., nom. rev.; and *Agrobacterium stellulatum* sp. nov., nom. rev. International Journal of Systematic Bacteriology 42:133-143.
3. Petursdottir SK, Kristjansson JK. 1997. *Silicibacter lacuscaerulensis* gen. nov., sp. nov., a mesophilic moderately halophilic bacterium characteristic of the Blue Lagoon geothermal lake in Iceland. Extremophiles 1:94-99.
4. González JM, Covert JS, Whitman WB, Henriksen JR, Mayer F, Scharf B, Schmitt R, Buchan A, Fuhrman JA, Kiene RP, Moran MA. 2003. *Silicibacter pomeroyi* sp. nov. and *Roseovarius nubinhibens* sp. nov., dimethylsulfoniopropionate-demethylating bacteria from marine environments. International Journal of Systematic and Evolutionary Microbiology 53:1261-1269.
5. Huo YY, Xu XW, Li X, Liu C, Cui HL, Wang CS, Wu M. 2011. *Ruegeria marina* sp. nov., isolated from marine sediment. International Journal of Systematic and Evolutionary Microbiology 61:347-350.

6. Oh KH, Jung YT, Oh TK, Yoon JH. 2011. *Ruegeria faecimaris* sp. nov., isolated from a tidal flat sediment. International Journal of Systematic and Evolutionary Microbiology 61:1182-1188.

7. Kim YO, Park S, Nam BH, Kang SJ, Hur YB, Lee SJ, Oh TK, Yoon JH. 2012. *Ruegeria halocynthiae* sp. nov., isolated from the sea squirt *Halocynthia roretzi*. International Journal of Systematic and Evolutionary Microbiology 62:925-930.

8. Park S, Yoon JH. 2012. *Ruegeria arenilitoris* sp. nov., isolated from the seashore sand around a seaweed farm. Antonie Van Leeuwenhoek International Journal of General and Molecular Microbiology 102:581-589.

9. Lee J, Whon TW, Shin NR, Roh SW, Kim J, Park SK, Kim MS, Shin KS, Lee JS, Lee KC, Kim YO, Bae JW. 2012. *Ruegeria conchae* sp. nov., isolated from the ark clam *Scapharca broughtonii*. International Journal of Systematic and Evolutionary Microbiology 62:2851-2857.

10. Lucena T, Ruvira MA, Macian MC, Pujalte MJ, Arahal DR. 2013. Description of *Tropicibacter mediterraneus* sp. nov. and *Tropicibacter litoreus* sp. nov. Systematic and Applied Microbiolology 36:325-9.

11. Kämpfer P, Arun AB, Rekha PD, Busse HJ, Young CC, Glaeser SP. 2013. *Ruegeria intermedia* sp. nov., a moderately thermophilic bacterium isolated from a coastal hot spring. International Journal of Systematic and Evolutionary Microbiology 63:2538-2544.

12. Kim YO, Park S, Nam BH, Jung YT, Kim DG, Yoon JH. 2014. *Ruegeria meonggei* sp. nov., an alphaproteobacterium isolated from ascidian *Halocynthia roretzi*. Antonie Van Leeuwenhoek International Journal of General and Molecular Microbiology 105:551-558.

13. Zhang G, Haroon MF, Zhang R, Dong X, Wang D, Liu Y, Xun W, Dong X, Stingl U. 2017. *Ruegeria profundi* sp. nov. and *Ruegeria marisrubri* sp. nov., isolated from the brine-seawater interface at Erba Deep in the Red Sea. International Journal of Systematic and Evolutionary Microbiology 67:4624-4631.

14. Arahal DR, Lucena T, Rodrigo-Torres L, Pujalte MJ. 2018. *Ruegeria denitrificans* sp. nov., a marine bacterium in the family *Rhodobacteraceae* with the potential ability for cyanophycin synthesis. International Journal of Systematic and Evolutionary Microbiology 68:2515-2522.

15. Zhang L, Wang KL, Yin Q, Liang JY, Xu Y. 2018. *Ruegeria kandeliae* sp nov., isolated from the rhizosphere soil of a mangrove plant *Kandelia candel*. International Journal of Systematic and Evolutionary Microbiology 68:2653-2658.

16. Blom J, Kreis J, Spanig S, Juhre T, Bertelli C, Ernst C, Goesmann A. 2016. EDGAR 2.0: an enhanced software platform for comparative gene content analyses. Nucleic Acids Research 44:W22-W28.

17. Moran MA, Buchan A, Gonzalez JM, Heidelberg JF, Whitman WB, Kiene RP, Henriksen JR, King GM, Belas R, Fuqua C, Brinkac L, Lewis M, Johri S, Weaver B, Pai G, Eisen JA, Rahe E, Sheldon WM, Ye W, Miller TR, Carlton J, Rasko DA, Paulsen IT, Ren Q, Daugherty SC, Deboy RT, Dodson RJ, Durkin AS, Madupu R, Nelson WC, Sullivan SA, Rosovitz MJ, Haft DH, Selengut J, Ward N. 2004. Genome sequence of *Silicibacter pomeroyi* reveals adaptations to the marine environment. Nature 432:910-3.

18. Henriksen JR. 2008. Physiology of dimethylsulfoniopropionate metabolism in a model marine roseobacer, *Silicibacter pomeroyi*. Doctor of Philosophy. University of Georgia, Athens, GA.

19. Reisch CR, Stoudemayer MJ, Varaljay VA, Amster IJ, Moran MA, Whitman WB. 2011. Novel pathway for assimilation of dimethylsulphoniopropionate widespread in marine bacteria. Nature 473:208-11.

20. Kovach ME, Elzer PH, Hill DS, Robertson GT, Farris MA, Roop RM, Peterson KM. 1995. Four new derivatives of the broad-host-range cloning vector pBBR1MCS, carrying different anitbiotic-resistance cassettes. Gene 166:175-176.

21. Keen NT, Tamaki S, Kobayashi D, Trollinger D. 1988. Improved broad-host-range plasmids for DNA cloning in Gram-negative bacteria. Gene 70:191-197.

22. Pétursdóttir SK, Kristjánsson JK. 1996. The relationship between physical and chemical conditions and low microbial diversity in the Blue Lagoon geothermal lake in Iceland. Fems Microbiology Ecology 19:39-45.

23. Yokoyama A, Izumida H, Miki W. 1994. Production of astaxanthin and 4-ketozeaxanthin by the marine bacterium, *Agrobacterium aurantiacum*. Bioscience Biotechnology and Biochemistry 58:1842-1844.

24. Baumann P, Baumann L. 1981. The marine Gram-negative eubacteria: genera *Photobacterium*, *Beneckea*, *Alteromonas*, *Pseudomonas*, and *Alcaligenes*. The Prokaryotes 2:1302-1331.

25. Reisch CR, Moran MA, Whitman WB. 2008. Dimethylsulfoniopropionate-dependent demethylase (DmdA) from *Pelagibacter ubique* and *Silicibacter pomeroyi*. Journal of Bacteriology 190:8018-8024.

26. Gonzalez JM, Mayer F, Moran MA, Hodson RE, Whitman WB. 1997. *Microbulbifer hydrolyticus* gen. nov., sp. nov., and *Marinobacterium georgiense* gen. nov., sp. nov., two marine bacteria from a lignin-rich pulp mill waste enrichment community. International Journal of Systematic Bacteriology 47:369-376.

27. Uchino Y, Hirata A, Yokota A, Sugiyama J. 1998. Reclassification of marine *Agrobacterium* species: proposals of *Stappia stellulata* gen. nov., comb. nov., *Stappia aggregata* sp. nov., nom. rev., *Ruegeria atlantica* gen. nov., comb. nov., *Ruegeria gelatinovora* comb. nov., *Ruegeria algicola* comb. nov., and *Ahrensia kieliense* gen. nov., sp. nov., nom. rev. Journal of General and Applied Microbiology 44:201-210.

28. Uchino Y, Hirata A, Yokota A, Sugiyama J. 1999. Validation List no. 68. International Journal of Systematic Bacteriology 49:1-3.

29. Arahal DR, Macian MC, Garay E, Pujalte MJ. 2005. *Thalassobius mediterraneus* gen. nov., sp. nov., and reclassification of *Ruegeria gelatinovorans* as *Thalassobius gelatinovorus* comb. nov. International Journal of Systematic and Evolutionary Microbiology 55:2371-2376.

30. Yi H, Lim YW, Chun J. 2007. Taxonomic evaluation of the genera *Ruegeria* and *Silicibacter*: a proposal to transfer the genus *Silicibacter* Petursdottir and Kristjansson 1999 to the genus *Ruegeria* Uchino *et al.* 1999. International Journal of Systematic and Evolutionary Microbiology 57:815-819.

31. Muramatsu Y, Uchino Y, Kasai H, Suzuki KI, Nakagawa Y. 2007. *Ruegeria mobilis* sp. nov., a member of the *Alphaproteobacteria* isolated in Japan and Palau. International Journal of Systematic and Evolutionary Microbiology 57:1304-1309.

32. Lee K, Choo YJ, Giovannoni SJ, Cho JC. 2007. *Ruegeria pelagia* sp. nov., isolated from the Sargasso Sea, Atlantic ocean. International Journal of Systematic and Evolutionary Microbiology 57:1815-1818.

33. Vandecandelaere I, Nercessian O, Segaert E, Achouak W, Faimali M, Vandamme P. 2008. *Ruegeria scottomollicae* sp. nov., isolated from a marine electroactive biofilm. International Journal of Systematic and Evolutionary Microbiology 68:2726-2733.

34. Lai QL, Yuan J, Li FY, Zheng TL, Shao ZZ. 2010. *Ruegeria pelagia* is a later heterotypic synonym of *Ruegeria mobilis*. International Journal of Systematic and Evolutionary Microbiology 60:1918-1920.

35. Park S, Yoon JH. 2013. Validation List no. 149. International Journal of Systematic and Evolutionary Microbiology 63:1-5.

36. Kim YO, Park S, Nam BH, Jung YT, Kim DG, Yoon JH. 2014. Validation List no. 160. International Journal of Systematic and Evolutionary Microbiology 64:3603-3606.

37. Wirth JS, Whitman WB. 2018. Phylogenomic analyses of a clade within the roseobacter group suggest taxonomic reassignments of species of the genera *Aestuariivita*, *Citreicella*, *Loktanella*, *Nautella*, *Pelagibaca*, *Ruegeria*, *Thalassobius*, *Thiobacimonas* and *Tropicibacter*, and the proposal of six novel genera. Internationl Journal of Systematic and Evolutionary Microbiology 68:2393-2411.

38. Luo C, Rodriguez RL, Konstantinidis KT. 2014. MyTaxa: an advanced taxonomic classifier for genomic and metagenomic sequences. Nucleic Acids Research 42:e73.

39. Buchan A, González JM, Moran MA. 2005. Overview of the marine *Roseobacter* lineage. Applied and Environmental Microbiology 71:5665-77.

40. Brinkhoff T, Giebel HA, Simon M. 2008. Diversity, ecology, and genomics of the *Roseobacter* clade: a short overview. Archives of Microbiology 189:531-539.

41. Breider S, Scheuner C, Schumann P, Fiebig A, Petersen J, Pradella S, Klenk HP, Brinkhoff T, Goker M. 2014. Genome-scale data suggest reclassifications in the *Leisingera-Phaeobacter* cluster including proposals for *Sedimentitalea* gen. nov. and *Pseudophaeobacter* gen. nov. Frontiers in Microbiology 5:416.

42. Luo H, Moran MA. 2014. Evolutionary ecology of the marine *Roseobacter* clade. Microbiology and Molecular Biology Reviews 78:573-587.

43. Simon M, Scheuner C, Meier-Kolthoff JP, Brinkhoff T, Wagner-Dobler I, Ulbrich M, Klenk HP, Schomburg D, Petersen J, Goker M. 2017. Phylogenomics of *Rhodobacteraceae* reveals evolutionary adaptation to marine and non-marine habitats. ISME Journal 11:1483-1499.

44. Petursdottir SK, Kristjansson JK. 1999. Validation List no. 71. International Journal of Systematic Bacteriology 49:1325-1326.

45. Lucena T, Ruvira MA, Macian MC, Pujalte MJ, Arahal DR. 2014. Validation List no. 155. International Journal of Systematic and Evolutionary Microbiology 64:1-5.

46. Nguyen LT, Schmidt HA, von Haeseler A, Minh BQ. 2015. IQ-TREE: a fast and effective stochastic algorithm for estimating maximum-likelihood phylogenies. Molecular Biology and Evolution 32:268-274.

47. Kalyaanamoorthy S, Minh BQ, Wong TKF, von Haeseler A, Jermiin LS. 2017. ModelFinder: fast model selection for accurate phylogenetic estimates. Nature Methods 14:587-589.

Table 3-1. Phenotypes of the *Ruegeria* species. Species: 1, *R. atlantica*; 2, *R. arenilitoris*; 3, *R. conchae*; 4, *R. denitrificans*; 5, *R. faecimaris*; 6, *R. halocynthiae*; 7, *R. intermedia*; 8, *R. kandeliae*; 9, *R. lacuscaerulensis*; 10, *R. litorea*; 11, *R. marina*; 12, *R. marisrubri*; 13, *R. mediterranea*; 14, *R. meonggei*; 15, *R. pomeroyi*; 16, *R. profundi*. All species are positive for oxidase, catalase, the utilization of L-arginine as a sole carbon and energy source (no data for *R. arenilitoris*, *R. conchae*, *R. faecimaris*, *R. halocynthiae*, *R. intermedia*, *R. kandeliae*, *R. meonggei*, and *R. profundi*), and the utilization of L-tyrosine as a sole carbon and energy source (no data for *R. conchae*, *R. intermedia*, *R. kandeliae*, *R. marisrubri*, and *R. profundi*). All species are negative for Gram staining, aerobic acid production from D-arabinose (no data for *R. arenilitoris*, *R. denitrificans*, *R. intermedia*, *R. kandeliae*, *R. litorea*, *R. marisrubri*, *R. mediterranea*, *R. meonggei*, and *R. profundi*), aerobic acid production from melibiose (no data for *R. denitificans*, *R. intermedia*, *R. kandeliae*, *R. litorea*, *R. marisrubri*, *R. mediterranea*, and *R. profundi*), the utilization of benzoate as a sole carbon and energy source (no data for *R. denitirificans*, *R. intermedia*, *R. kandeliae*, *R. litorea*, *R. marina*, *R. marisrubri*, *R. mediterranea*, and *R. profundi*), and the utilization of formate as a sole carbon and energy source (no data for *R. denitrificans*, *R. intermedia*, *R. kandeliae*, *R. litorea*, *R. marisrubri*, *R. mediterranea*, and *R. profundi*). "+" indicates a positive result; "-" indicates a negative result; "d" indicates different results between strains; "v" indicates conflicting reports; "ND" indicates no data available in the literature.

Characteristic	**1**	**2**	**3**	**4**
Morphology				
Shape	rod	rod	rod	rod
Diameter	0.6-0.8	0.2-0.6 µm	0.3-0.5 µm	ND
Length	1.5-2	0.8-4.0 µm	0.5-1.0 µm	ND
Motility	-	+	-	-
Flagellation				
Peritrichous	+	+	-	ND
Polar	-	-	-	ND
Facultatively anaerobic	-	+	-	ND
Growth range (optimum)				
Temperature (˚C)	5-30 (25)	4-45 (30-37)	10-37 (25-30)	15-26 (26)
% NaCl (*w/v*)	3-10 (3)	0.5-6 (2)	1-5 (2)	1.5-6 (3)
pH	6-11 (7)	5.5-8 (7-8)	7-10 (8)	6-9 (7)
Enzymatic activity (API-ZYM)				
acid phosphatase	-	-	+	+
esterase (C4)	v	+	+	-
esterase lipase (C8)	-	-	+	-

α-fucosidase	-	-	-	-
β-galactosidase	-	-	+	-
α-glucosidase	v	-	+	-
leucine arylamidase	+	+	+	-
α-mannosidase	-	-	-	-
naphthol-AS-BI-phosphohydrolase	v	-	v	-
trypsin	-	-	-	-
valine arylamidase	v	-	-	-
Nitrate reduction				
to nitrite	+	+	v	-
to gas	+	+	ND	+
Aerobic acid production				
D-adonitol	-	ND	-	ND
amygdalin	+	ND	-	ND
L-arabinose	v	+	-	ND
D-arabitol	-	ND	-	ND
arbutin	-	ND	+	ND
cellobiose	v	+	-	ND
erythritol	-	ND	+	ND
esculin	+	ND	+	ND
dulcitol	+	ND	-	ND
fructose	-	-	v	ND
D-fucose	-	ND	-	ND
galactose	v	+	-	ND
gentiobiose	-	ND	+	ND
gluconate	-	ND	+	ND
5-ketogluconate	-	ND	+	ND
N-acetylglucosamine	-	ND	-	ND
glucose	-	-	v	ND

methyl α-D-glucoside	-	ND	+	ND
glycogen	+	ND	-	ND
glycerol	+	ND	-	ND
myo-inositol	v	-	-	ND
lactose	-	-	v	ND
D-lyxose	-	ND	-	ND
maltose	v	-	v	ND
mannitol	v	-	v	ND
D-mannose	-	-	v	ND
melezitose	-	-	-	ND
methyl α-D-mannoside	-	ND	-	ND
raffinose	v	-	-	ND
L-rhamnose	-	-	-	ND
D-ribose	v	-	v	ND
salicin	-	ND	+	ND
D-sorbitol	v	-	-	ND
L-sorbose	-	ND	-	ND
sucrose	-	-	-	ND
D-tagatose	-	ND	-	ND
trehalose	v	-	-	ND
xylitol	+	ND	+	ND
D-xylose	v	-	-	ND
methyl β-D-xyloside	-	ND	-	ND
Carbohydrate utilization				
L-arabinose	-	-	-	-
cellobiose	d	+	v	-
D-fructose	v	+	v	+
D-galactose	d	v	v	+
gluconate	d	ND	+	-

D-glucose	d	+	+	+
maltose	d	v	v	+
D-mannose	d	+	+	+
L-rhamnose	-	-	-	+
salicin	-	v	v	-
sucrose	d	-	-	+
trehalose	d	-	v	-
D-xylose	d	+	+	-
Carboxylic acid utilization				
acetate	d	+	+	+
citrate	+	+	v	+
lactate	d	+	+	+
malate	+	+	+	+
pyruvate	+	+	+	+
succinate	+	+	+	+
Alcohol utilization				
glycerol	d	-	v	+
mannitol	d	-	v	+
Amino acid utilization				
L-glutamate	v	-	-	+
Hydrolysis of:				
esculin	+	-	+	-
gelatin	-	v	v	-
Tween-80	v	-	-	-
xanthine	+	-	-	ND
DNA G+C content (mol%)	55	64.6	55.7	56.7
Isolation habitat	marine sediment	marine sediment	ark clam	oyster
References	(2, 4, 6, 9, 13, 14, 29-32)	(8, 12-14)	(9, 12, 13)	(14)

Table 3-1 (continued).

Characteristic	5	6	7	8
Morphology				
Shape	rod	rod	irregular rod	rod
Diameter	0.3-0.6 µm	0.2-0.6 µm	1.0-1.2 µm	0.5-0.7 µm
Length	1.0-8.0 µm	1.0-10µm	2.0-5.0 µm	1.3-3.3 µm
Motility	-	-	-	+
Flagellation				
Peritrichous	-	-	ND	-
Polar	-	-	ND	+
Facultatively anaerobic	-	+*	ND	ND
Growth range (optimum)				
Temperature (˚C)	4-37 (30)	10-37 (30)	15-55 (37-45)	10-40 (30-37)
% NaCl (*w/v*)	0.5-7 (2-3)	0.5-6 (2-3)	1-4 (1-2)	0-9 (0.5-3)
pH	5-8 (7-8)	5.5-8 (7-8)	5-10 (8)	5-8.5 (6-7)
Enzymatic activity (API-ZYM)				
acid phosphatase	+	+	+	+
esterase (C4)	+	+	+	+
esterase lipase (C8)	-	+	ND	+
α-fucosidase	-	-	ND	-
β-galactosidase	-	-	+	-
α-glucosidase	-	+	ND	-
leucine arylamidase	-	+	ND	+
α-mannosidase	-	-	ND	-
naphthol-AS-BI-phosphohydrolase	-	-	-	+
trypsin	-	-	ND	-
valine arylamidase	-	-	-	+
Nitrate reduction				

to nitrite	+	+	-	-
to gas	ND	ND	ND	ND
Aerobic acid production				
D-adonitol	-	-	ND	ND
amygdalin	-	-	ND	ND
L-arabinose	-	-	ND	ND
D-arabitol	-	-	ND	ND
arbutin	-	-	ND	ND
cellobiose	-	-	ND	ND
erythritol	+	-	ND	ND
esculin	+	+	ND	ND
dulcitol	-	-	ND	ND
fructose	-	v	ND	ND
D-fucose	-	-	ND	ND
galactose	+	v	ND	ND
gentiobiose	-	-	ND	ND
gluconate	-	-	ND	ND
5-ketogluconate	+	+	ND	ND
N-acetylglucosamine	+	-	ND	ND
glucose	-	v	ND	-
methyl α-D-glucoside	-	-	ND	ND
glycogen	+	-	ND	ND
glycerol	-	-	ND	ND
myo-inositol	-	-	ND	ND
lactose	-	-	ND	ND
D-lyxose	-	-	ND	ND
maltose	-	-	ND	ND
mannitol	-	-	ND	ND
D-mannose	-	+	ND	ND

melezitose	v	-	ND	ND
methyl α-D-mannoside	+	-	ND	ND
raffinose	-	-	ND	ND
L-rhamnose	+	-	ND	ND
D-ribose	v	+	ND	ND
salicin	-	-	ND	ND
D-sorbitol	-	-	ND	ND
L-sorbose	-	+	ND	ND
sucrose	+	-	ND	ND
D-tagatose	+	+	ND	ND
trehalose	-	-	ND	ND
xylitol	+	-	ND	ND
D-xylose	-	-	ND	ND
methyl β-D-xyloside	+	-	ND	ND
Carbohydrate utilization				
L-arabinose	-	-	-	+
cellobiose	+	+	-	ND
D-fructose	+	-	-	ND
D-galactose	+	+	+	ND
gluconate	ND	ND	-	+
D-glucose	+	+	+	+
maltose	-	-	-	-
D-mannose	+	+	-	-
L-rhamnose	+	ND	ND	ND
salicin	-	-	-	ND
sucrose	-	-	-	ND
trehalose	-	-	ND	ND
D-xylose	-	-	-	ND
Carboxylic acid utilization				

acetate	+	+	-	ND
citrate	+	+	-	+
lactate	ND	ND	v	ND
malate	+	+	ND	+
pyruvate	+	-	-	ND
succinate	+	+	ND	ND
Alcohol utilization				
glycerol	ND	ND	-	ND
mannitol	ND	ND	-	+
Amino acid utilization				
L-glutamate	-	-	ND	ND
Hydrolysis of:				
esculin	+	v	+	-
gelatin	v	v	-	-
Tween-80	+	-	-	-
xanthine	-	+	ND	ND
DNA G+C content (mol%)	57.9	58.6	ND	65.7
Isolation habitat	marine sediment	sea squirt	marine hot spring	rhizosphere soil of mangrove
References	(6, 9)	(7, 9)	(11, 13)	(15)

Table 3-1 (continued).

Characteristic	**9**	**10**	**11**	**12**
Morphology				
Shape	rod	ovoid rod	rod	rod
Diameter	0.6-0.8 µm	0.7 µm	0.5-1 µm	0.6-1.2 µm
Length	9.0-18.0 µm	1.0-3.0 µm	2-4.5 µm	2.0-5.0 µm
Motility	-	-	-	-
Flagellation				

Peritrichous	-	-	-	-
Polar	-	-	-	-
Facultatively anaerobic	-	ND	ND	ND
Growth range (optimum)				
Temperature (˚C)	10-50 (35-45)	15-30 (28)	10-42 (35-37)	20-50 (37-40)
% NaCl (*w/v*)	1.5-7 (3.5)	1.7-7.0 (ND)	0-7.5 (0.5-3)	2.9-15.2 (8.8-11.7)
pH	6.5-8.5 (7-7.5)	ND (ND)	6.5-9 (7.5)	6-8.5 (7-7.5)
Enzymatic activity (API-ZYM)				
acid phosphatase	v	+	+	-
esterase (C4)	v	-	+	+
esterase lipase (C8)	v	-	+	+
α-fucosidase	-	-	-	+
β-galactosidase	+	-	-	+
α-glucosidase	v	-	-	+
leucine arylamidase	+	+	+	+
α-mannosidase	-	-	-	+
naphthol-AS-BI-phosphohydrolase	v	-	+	-
trypsin	-	-	-	+
valine arylamidase	v	-	+	+
Nitrate reduction				
to nitrite	+	-	-	+
to gas	+	+	ND	ND
Aerobic acid production				
D-adonitol	-	ND	-	ND
amygdalin	-	ND	-	ND
L-arabinose	-	ND	-	ND
D-arabitol	+	ND	-	ND
arbutin	-	ND	-	ND
cellobiose	v	ND	-	ND

erythritol	-	ND	-	ND
esculin	+	ND	-	ND
dulcitol	+	ND	-	ND
fructose	v	ND	-	ND
D-fucose	+	ND	-	ND
galactose	-	ND	-	ND
gentiobiose	-	ND	-	ND
gluconate	-	ND	-	ND
5-ketogluconate	-	ND	+	ND
N-acetylglucosamine	-	ND	-	ND
glucose	-	-	+	ND
methyl α-D-glucoside	+	ND	-	ND
glycogen	-	ND	-	ND
glycerol	-	ND	-	ND
myo-inositol	-	ND	-	ND
lactose	-	ND	-	ND
D-lyxose	+	ND	-	ND
maltose	v	ND	-	ND
mannitol	-	ND	-	ND
D-mannose	-	ND	-	ND
melezitose	v	ND	-	ND
methyl α-D-mannoside	+	ND	-	ND
raffinose	-	ND	-	ND
L-rhamnose	-	ND	ND	ND
D-ribose	v	ND	-	ND
salicin	-	ND	-	ND
D-sorbitol	-	ND	+	ND
L-sorbose	-	ND	-	ND
sucrose	v	ND	-	ND

D-tagatose	+	ND	+	ND
trehalose	v	ND	-	ND
xylitol	+	ND	-	ND
D-xylose	-	ND	-	ND
methyl β-D-xyloside	-	ND	+	ND
Carbohydrate utilization				
L-arabinose	-	-	-	ND
cellobiose	+	-	-	+
D-fructose	+	-	-	+
D-galactose	v	-	-	-
gluconate	-	-	-	ND
D-glucose	v	-	+	+
maltose	v	-	-	+
D-mannose	v	-	-	+
L-rhamnose	ND	-	-	ND
salicin	v	-	-	+
sucrose	-	-	-	+
trehalose	-	-	-	ND
D-xylose	-	-	+	ND
Carboxylic acid utilization				
acetate	v	+	+	-
citrate	v	+	+	-
lactate	+	+	+	+
malate	+	+	+	ND
pyruvate	+	+	+	ND
succinate	+	+	+	ND
Alcohol utilization				
glycerol	+	+	+	+
mannitol	v	-	-	-

Amino acid utilization				
L-glutamate	-	+	+	+
Hydrolysis of:				
esculin	v	-	v	+
gelatin	-	-	v	+
Tween-80	v	-	-	-
xanthine	+	ND	ND	ND
DNA G+C content (mol%)	66.15	59	63.5	62.94
Isolation habitat	geothermal lake	seawater	marine sediment	brine-seawater interface
References	(3, 4, 6, 9, 11, 13, 14, 29, 30, 32)	(10)	(5, 9, 15)	(13)

Table 3-1 (continued).

Characteristic	**13**	**14**	**15**	**16**
Morphology				
Shape	ovoid rod	rod	toga-like rod	rod
Diameter	0.6-0.7 µm	0.2-0.8 µm	0.4-0.6 µm	0.5-1.0 µm
Length	1.0-5.0 µm	0.5-10 µm	1.9-3.5 µm	1.0-3.0 µm
Motility	-	-	+	-
Flagellation				
Peritrichous	-	-	-	-
Polar	-	-	+	-
Facultatively anaerobic	ND	-	-	ND
Growth range (optimum)				
Temperature (˚C)	15-30 (28)	4-30 (30)	10-40 (30)	15-42 (33-35)
% NaCl (*w/v*)	0.9-5.0 (ND)	1-6 (2-3)	ND (0.6-2.3)	2.9-16.9 (5.8-8.8)
pH	ND (ND)	6.5-8 (7-8)	ND (ND)	5.5-9 (7.5-8)
Enzymatic activity (API-ZYM)				
acid phosphatase	+	+	-	+

esterase (C4)	-	+	v	+
esterase lipase (C8)	-	+	+	+
α-fucosidase	-	-	-	-
β-galactosidase	d	-	-	-
α-glucosidase	d	-	-	+
leucine arylamidase	+	+	+	+
α-mannosidase	-	-	-	-
naphthol-AS-BI-phosphohydrolase	d	-	-	-
trypsin	-	-	-	-
valine arylamidase	-	-	-	-
Nitrate reduction				
to nitrite	d	-	-	-
to gas	d	+	-	ND
Aerobic acid production				
D-adonitol	ND	ND	+	ND
amygdalin	ND	ND	-	ND
L-arabinose	ND	-	-	ND
D-arabitol	ND	ND	-	ND
arbutin	ND	ND	+	ND
cellobiose	ND	-	-	ND
erythritol	ND	ND	-	ND
esculin	ND	ND	+	ND
dulcitol	ND	ND	-	ND
fructose	ND	-	v	ND
D-fucose	ND	ND	-	ND
galactose	ND	-	-	ND
gentiobiose	ND	ND	-	ND
gluconate	ND	ND	-	ND
5-ketogluconate	ND	ND	-	ND

N-acetylglucosamine	ND	ND	-	ND
glucose	-	-	v	ND
methyl α-D-glucoside	ND	ND	-	ND
glycogen	ND	ND	-	ND
glycerol	ND	ND	-	ND
myo-inositol	ND	-	v	ND
lactose	ND	-	-	ND
D-lyxose	ND	ND	-	ND
maltose	ND	-	-	ND
mannitol	ND	-	-	ND
D-mannose	ND	-	-	ND
melezitose	ND	-	-	ND
methyl α-D-mannoside	ND	ND	-	ND
raffinose	ND	-	-	ND
L-rhamnose	ND	-	-	ND
D-ribose	ND	-	v	ND
salicin	ND	ND	-	ND
D-sorbitol	ND	-	-	ND
L-sorbose	ND	ND	-	ND
sucrose	ND	-	-	ND
D-tagatose	ND	ND	+	ND
trehalose	ND	-	-	ND
xylitol	ND	ND	-	ND
D-xylose	ND	-	+	ND
methyl β-D-xyloside	ND	ND	+	ND
Carbohydrate utilization				
L-arabinose	-	-	-	ND
cellobiose	-	+	-	-
D-fructose	+	+	-	+

D-galactose	+	+	-	-
gluconate	-	ND	+	ND
D-glucose	+	+	+	-
maltose	-	-	-	-
D-mannose	-	+	-	+
L-rhamnose	-	ND	-	ND
salicin	-	-	-	-
sucrose	-	-	-	+
trehalose	-	-	-	ND
D-xylose	+	+	+	ND
Carboxylic acid utilization				
acetate	+	+	+	-
citrate	+	-	+	-
lactate	+	ND	ND	+
malate	+	-	+	ND
pyruvate	+	+	+	ND
succinate	+	-	v	ND
Alcohol utilization				
glycerol	+	ND	+	-
mannitol	+	ND	-	+
Amino acid utilization				
L-glutamate	+	-	-	-
Hydrolysis of:				
esculin	-	-	-	+
gelatin	-	-	+	-
Tween-80	-	-	v	-
xanthine	ND	-	+	ND
DNA G+C content (mol%)	58.5-59.0	58	68	56.68

Isolation habitat	seawater	sea squirt	sea water	brine-seawater interface
References	(10)	(12, 14)	(4-6, 9, 14, 30, 32)	(13)

* Nitrate required for facultative growth.

Table 3-2. Distinguishing characteristics of the *Ruegeria* species. Species: 1, *R. atlantica*; 2, *R. arenilitoris*; 3, *R. conchae*; 4, *R. denitrificans*; 5, *R. faecimaris*; 6, *R. halocynthiae*; 7, *R. intermedia*; 8, *R. kandeliae*; 9, *R. lacuscaerulensis*; 10, *R. litorea*; 11, *R. marina*; 12, *R. marisrubri*; 13, *R. mediterranea*; 14, *R. meonggei*; 15, *R. pomeroyi*; 16, *R. profundi*. "+" indicates positive for the character; "-" indicates negative for the character; "d" indicates different results between strains; "v" indicates conflicting reports; "ND" indicates no data available in the literature.

Characteristic	**1**	**2**	**3**	**4**	**5**	**6**	**7**	**8**
Motility	-	+	-	-	-	-	-	+
Flagellation								
Peritrichous	+	+	-	ND	-	-	ND	-
Polar	-	-	-	ND	-	-	ND	+
Growth range (optimum)								
≤5 ˚C	+	+	-	-	+	-	-	-
≥40 ˚C	-	+	-	-	-	-	+	+
<1 % (*w/v*) NaCl	-	+	-	-	+	+	-	+
>5 % (*w/v*) NaCl	+	+	-	+	+	+	-	+
pH <6	-	+	-	-	+	+	+	+
pH >8	+	-	+	+	-	-	+	+
Facultatively anaerobic	-	+	-	ND	-	+*	ND	ND
Nitrate reduction								
to nitrite	+	+	v	-	+	+	-	-
Enzymatic activity (API-ZYM)								
acid phosphatase	-	-	+	+	+	+	+	+
esterase (C4)	v	+	+	-	+	+	+	+
esterase lipase (C8)	-	-	+	-	-	+	ND	+
α-fucosidase	-	-	-	-	-	-	ND	-
β-galactosidase	-	-	+	-	-	-	+	-
α-glucosidase	v	-	+	-	-	+	ND	-
leucine arylamidase	+	+	+	-	-	+	ND	+
α-mannosidase	-	-	-	-	-	-	ND	-

naphthol-AS-BI-phosphohydrolase	v	-	v	-	-	-	-	+
trypsin	-	-	-	-	-	-	ND	-
valine arylamidase	v	-	-	-	-	-	-	+
Carbohydrate utilization								
L-arabinose	-	-	-	-	-	-	-	+
cellobiose	d	+	v	-	+	+	-	ND
D-galactose	d	v	v	+	+	+	+	ND
D-glucose	d	+	+	+	+	+	+	+
maltose	d	-	v	+	-	-	-	-
D-mannose	d	+	+	+	+	+	-	-
salicin	-	-	-	-	-	-	-	ND
DNA G+C content (mol%)	55	64.6	55.7	56.7	57.9	58.6	ND	65.7

Table 3-2 (continued).

Characteristic	**9**	**10**	**11**	**12**	**13**	**14**	**15**	**16**
Motility	-	-	-	-	-	-	+	-
Flagellation								
Peritrichous	-	-	-	-	-	-	-	-
Polar	-	-	-	-	-	-	+	-
Growth range (optimum)								
≤5 ˚C	-	-	-	-	-	+	-	-
≥40 ˚C	+	-	+	+	-	-	+	+
<1 % (*w/v*) NaCl	-	-	+	-	+	-	+	-
>5 % (*w/v*) NaCl	+	+	+	+	-	+	-	+
pH <6	-	ND	-	-	ND	-	ND	+
pH >8	+	ND	+	+	ND	-	ND	+
Facultatively anaerobic	-	ND	ND	ND	ND	-	-	ND
Nitrate reduction								
to nitrite	+	-	-	+	d	-	-	-

Enzymatic activity (API-ZYM)								
acid phosphatase	v	+	+	-	+	+	-	+
esterase (C4)	v	-	+	+	-	+	v	+
esterase lipase (C8)	v	-	+	+	-	+	+	+
α-fucosidase	-	-	-	+	-	-	-	-
β-galactosidase	+	-	-	+	d	-	-	-
α-glucosidase	v	-	-	+	d	-	-	+
leucine arylamidase	+	+	+	+	+	+	+	+
α-mannosidase	-	-	-	+	-	-	-	-
naphthol-AS-BI-phosphohydrolase	v	-	+	-	d	-	-	-
trypsin	-	-	-	+	-	-	-	-
valine arylamidase	v	-	+	+	-	-	-	-
Carbohydrate utilization								
L-arabinose	-	-	-	ND	-	-	-	ND
cellobiose	+	-	-	+	-	+	-	-
D-galactose	v	-	-	-	+	+	-	-
D-glucose	v	-	+	+	+	+	+	-
maltose	v	-	-	+	-	-	-	-
D-mannose	v	-	-	+	-	+	-	+
salicin	v	-	-	+	-	-	-	-
DNA G+C content (mol %)	66.15	59	63.5	62.94	58.5-59.0	58	68.0±0.1	56.68

Table 3-3. Antibiotic susceptibility in the *Ruegeria*. Species: 1, *R. atlantica*; 2, *R. arenilitoris*; 3, *R. conchae*; 4, *R. faecimaris*; 5, *R. halocynthiae*; 6, *R. kandeliae*; 7, *R. lacuscaerulensis*; 8, *R. marina*; 9, *R. marisrubri*; 10, *R. meonggei*; 11, *R. pomeroyi*; 12, *R. profundi*. No data available for *R. intermedia*, *R. litorea*, and *R. mediterranea*. All species are sensitive to ampicillin (no data for *R. atlantica*, *R. halocynthiae*, or *R. lacuscaerulensis*), carbenicillin (no data for *R. atlantica*, *R. conchae*, *R. kandeliae*, *R. lacuscaerulensis*, *R. marisrubri*, *R. pomeroyi*, or *R. profundi*), cefoxitin (no data for *R. arenilitoris*, *R. conchae*, *R. faecimaris*, *R. halocynthiae*, *R. kandeliae*, *R. marisrubri*, or *R. profundi*), erythromycin (no data for *R. arenilitoris*, *R. conchae*, *R. faecimaris*, *R. halocynthiae*, or *R. meonggei*), or polymyxin B (no data for *R. atlantica*). "+" indicates that a species is susceptible to the antibiotic. "-" indicates that a species is resistant to an antibiotic. "ND" indicates no data available.

Antibiotic	**1**	**2**	**3**	**4**	**5**	**6**
Chloramphenicol	+	+	+	+	+	+
Gentamycin	-	-	-	+	+	+
Kanamycin	ND	-	+	+	-	+
Lincomycin	ND	-	ND	-	-	ND
Neomycin	ND	+	ND	+	+	+
Novobiocin	ND	-	+	-	-	-
Oleandomycin	ND	+	ND	-	-	ND
Penicillin-G	-	+	+	+	+	+
Streptomycin	+	+	+	+	-	+
Tetracycline	-	-	+	-	-	+
Vancomycin	+	ND	ND	ND	ND	-
References	(2, 33)	(8)	(9)	(6)	(7)	(15)

Table 3-3 (continued).

Antibiotic	**7**	**8**	**9**	**10**	**11**	**12**
Chloramphenicol	+	+	+	+	-*	+
Gentamycin	-	+	-	-	+	-
Kanamycin	ND	+	+	-	+	+
Lincomycin	ND	ND	ND	-	ND	ND
Neomycin	ND	ND	ND	-	+	ND
Novobiocin	ND	+	ND	-	ND	ND
Oleandomycin	ND	ND	ND	+	ND	ND
Penicillin-G	+	+	+	+	ND	+
Streptomycin	-	+	+	+	+	+
Tetracycline	+	+	+	-	+	+
Vancomycin	-	+	-	ND	-	+
References	(3, 33)	(5, 15)	(13)	(12)	(5, 18, 33)	(13)

*: unpublished data

Table 3-4. Fatty acids in the *Ruegeria* species. Species: 1, *R. atlantica*; 2, *R. arenilitoris*; 3, *R. conchae*; 4, *R. denitrificans*; 5, *R. faecimaris*; 6, *R. halocynthiae*; 7, *R. intermedia*; 8, *R. kandeliae*; 9, *R. lacuscaerulensis*; 10, *R. litorea*; 11, *R. marina*; 12, *R. marisrubri*; 13, *R. mediterranea*; 14, *R. meonggei*; 15, *R. pomeroyi*; 16, *R. profundi*. Values indicate the observed ranges for the percentage of total fatty acids in the cells. "—" indicates not detected, "tr" indicates trace (<1.0 %), and "ND" indicates no data available.

Fatty Acid	1	2	3	4
$C_{9:0}$	ND	ND	ND	ND
$C_{10:0}$	1.7 - 3.0	2.9 - 4.4	3.1 - 3.2	2.3
$C_{11:0}$	—	ND	—	ND
$C_{12:0}$	2.6 - 4.3	2.8 - 3.7	3.6 - 3.9	2.9
$C_{14:0}$	tr	tr	—	ND
$C_{16:0}$	3.2 - 11.5	3.1 - 3.9	5.3 - 6.3	2.9
$C_{17:0}$	tr	tr	tr	ND
$C_{18:0}$	tr - 3.3	tr - 1.8	1.8 - 4.2	1.2
$C_{14:1}$ ω5c	tr	tr	—	ND
$C_{17:1}$ ω7c	—	tr	ND	ND
$C_{17:1}$ ω8c	—	—	tr	ND
$C_{18:0}$ iso	ND	ND	ND	ND
$C_{18:1}$ ω6c	—	ND	ND	ND
$C_{18:1}$ ω7c	41.8 - 71.2*	46.0 - 72.0*	54.2 - 56.3*	70.3*
$C_{18:1}$ ω9c	—	—	tr - 1.1	ND
$C_{20:1}$ ω7c	0 - 1.7	tr	—	—
$C_{18:1}$ 11-CH3	0 - 8.7	4.1	ND	ND
$C_{18:1}$ ω7c 11-CH3	7.1 - 30.0	14.6 - 18.6	13.7 - 15.2	3.5
$C_{19:0\ cy}$ω8c	—	4.7 - 7.8	—	ND
$C_{10:0}$ 3-OH	tr - 1.6	tr	tr	tr
$C_{12:0}$ 2-OH	ND	ND	ND	ND

$C_{12:0}$ 3-OH	4.7 - 6.5	5.6 - 6.9	5.0 - 7.2	5.8
$C_{12:1}$ 3-OH	ND	ND	ND	ND
$C_{16:0}$ 2-OH	3.4 - 10.7	4.6 - 7.8	5.0 - 7.3	8.1
$C_{16:1}$ ω7c/15 iso 2-OH	tr	tr	—	ND
iso-$C_{17:0}$ 3-OH	tr - 1.5	tr - 1.8	—	1.2
$C_{18:1}$ 2-OH	tr - 2.2	1.1 - 1.4	tr	ND
anteiso-$C_{15:0}$	tr	tr	tr	ND
$C_{16:0}$ N alcohol	tr	tr	tr	ND
References	(4, 6, 9, 12-14, 30, 31)	(8, 12-14)	(9, 12, 13)	(14)

Table 3-4 (continued).

Fatty Acid	**5**	**6**	**7**	**8**
$C_{9:0}$	ND	ND	ND	ND
$C_{10:0}$	3.1	3.0 - 3.2	2.9 - 3.4	—
$C_{11:0}$	ND	—	ND	ND
$C_{12:0}$	3.4	2.9 - 3.0	2.3 - 2.6	ND
$C_{14:0}$	ND	—	tr	ND
$C_{16:0}$	4.4	2.2 - 6.0	4.2	3.8
$C_{17:0}$	ND	tr	tr	ND
$C_{18:0}$	tr	tr - 2.4	3.4	tr
$C_{14:1}$ ω5c	ND	tr	tr	ND
$C_{17:1}$ ω7c	—	tr	—	ND
$C_{17:1}$ ω8c	ND	—	—	ND
$C_{18:0}$ iso	ND	ND	ND	ND
$C_{18:1}$ ω6c	ND	ND	ND	ND
$C_{18:1}$ ω7c	73.6	40.9 - 60.5*	56.9 - 59.2*	43.9

$C_{18:1}$ ω9c	ND	—	—	ND
$C_{20:1}$ ω7c	—	tr	—	ND
$C_{18:1}$ 11-CH3	ND	ND	ND	ND
$C_{18:1}$ ω7c 11-CH3	2.1	8.9 - 29.0	12.7 - 13.0	1.0
$C_{19:0\ cy}$ω8c	—	—	4.7 - 5.5	29.9
$C_{10:0}$ 3-OH	0.9	tr	tr	2.3
$C_{12:0}$ 2-OH	ND	ND	ND	ND
$C_{12:0}$ 3-OH	4.8	4.8 - 6.9	5.6 - 7.0	1.8
$C_{12:1}$ 3-OH	ND	ND	ND	ND
$C_{16:0}$ 2-OH	3.9	9.3 - 11.6	2.2 - 3.1	ND
$C_{16:1}$ ω7c/15 iso 2-OH	ND	tr	tr	1.1
iso-$C_{17:0}$ 3-OH	ND	—	tr	ND
$C_{18:1}$ 2-OH	1.1	tr - 1.7	tr	tr
anteiso-$C_{15:0}$	ND	—	tr	ND
$C_{16:0}$ N alcohol	ND	ND	tr	ND
References	(6)	(7, 9, 12)	(11, 13)	(15)

Table 3-4 (continued).

Fatty Acid	**9**	**10**	**11**	**12**
$C_{9:0}$	ND	1.2	ND	ND
$C_{10:0}$	2.5 - 6.3	ND	2.0 - 2.4	4.1
$C_{11:0}$	tr	ND	ND	ND
$C_{12:0}$	1.8 - 4.5	1.3	2.4	tr
$C_{14:0}$	tr	1.7	ND	tr
$C_{16:0}$	1.6 - 4.2	8.4	8.3 - 8.5	6.4
$C_{17:0}$	tr	ND	ND	tr

$C_{18:0}$	2.0 - 4.8	3.6	1.9 - 2.0	1.8
$C_{14:1}$ ω5c	tr	ND	ND	tr
$C_{17:1}$ ω7c	—	ND	ND	ND
$C_{17:1}$ ω8c	0 - 2.3	ND	ND	tr
$C_{18:0}$ iso	ND	2.1	ND	ND
$C_{18:1}$ ω6c	ND	ND	ND	ND
$C_{18:1}$ ω7c	56.3 - 81.7*	68.0*	54.8 - 59.2	52.6*
$C_{18:1}$ ω9c	—	—	ND	—
$C_{20:1}$ ω7c	0 - 2.6	ND	ND	tr
$C_{18:1}$ 11-CH3	2.2	ND	ND	ND
$C_{18:1}$ ω7c 11-CH3	1.8 - 10.1	5	10.4 - 17.5	10.9
$C_{19:0\ cy}$ω8c	tr - 5.2	ND	—	5.6
$C_{10:0}$ 3-OH	tr - 3.3	4.8	tr	tr
$C_{12:0}$ 2-OH	ND	1.2	ND	ND
$C_{12:0}$ 3-OH	4.0 - 8.7	tr	4.4 - 5.3	3.5
$C_{12:1}$ 3-OH	ND	—	ND	ND
$C_{16:0}$ 2-OH	tr	1.6	5	6.7
$C_{16:1}$ ω7c/15 iso 2-OH	tr	ND	ND	tr
iso-$C_{17:0}$ 3-OH	tr	ND	ND	tr
$C_{18:1}$ 2-OH	—	ND	tr	tr
anteiso-$C_{15:0}$	tr	ND	ND	tr
$C_{16:0}$ N alcohol	tr	ND	ND	tr
References	(4, 6, 9, 11-14, 30)	(10)	(5)	(13)

Table 3-4 (continued).

Fatty Acid	13	14	15	16
$C_{9:0}$	—	ND	ND	ND
$C_{10:0}$	ND	2.7	2.8 - 3.7	3.3
$C_{11:0}$	ND	ND	ND	ND
$C_{12:0}$	tr	3.8	1.1 - 1.5	1.8
$C_{14:0}$	tr	ND	ND	tr
$C_{16:0}$	5.4	2.7	6.7 - 14.0	4.7
$C_{17:0}$	ND	ND	—	tr
$C_{18:0}$	1.6	1.2 - 1.3	1.4 - 3.6	1.3
$C_{14:1}$ ω5c	ND	ND	ND	tr
$C_{17:1}$ ω7c	ND	ND	tr	ND
$C_{17:1}$ ω8c	ND	ND	ND	—
$C_{18:0}$ iso	1.5	ND	ND	ND
$C_{18:1}$ ω6c	ND	ND	ND	ND
$C_{18:1}$ ω7c	75.6*	59.1 - 73.0*	36.1 - 76.3*	50.7*
$C_{18:1}$ ω9c	—	ND	ND	tr
$C_{20:1}$ ω7c	ND	tr	tr	tr
$C_{18:1}$ 11-CH3	ND	2.7	tr - 1.9	ND
$C_{18:1}$ ω7c 11-CH3	6.2	12.3	5.4 - 25.5	9.4
$C_{19:0\ cy}$ω8c	ND	—	—	1.3
$C_{10:0}$ 3-OH	3.5	tr	tr - 1.6	1
$C_{12:0}$ 2-OH	1.3	ND	ND	ND
$C_{12:0}$ 3-OH	tr	6.1 - 7.2	4.9 - 6.6	6.4
$C_{12:1}$ 3-OH	—	ND	ND	ND
$C_{16:0}$ 2-OH	2.6	3.7 - 7.9	2.8 - 7.6	11.9
$C_{16:1}$ ω7c/15 iso 2-OH	ND	ND	—	tr

iso-$C_{17:0}$ 3-OH	ND	ND	—	tr
$C_{18:1}$ 2-OH	ND	tr	5.4	1.4
anteiso-$C_{15:0}$	ND	ND	ND	tr
$C_{16:0}$ N alcohol	ND	ND	ND	tr
References	(10)	(12, 14)	(4-6, 14)	(13)

*: one or more measurements performed on summed feature 8 ($C_{18:1}$ *ω6c* and/or $C_{18:1}$ *ω7c*)

Table 3-5. Genome sequences for the *Ruegeria* species. All genomes represent the type strain of the respective species and were downloaded from NCBI (https://www.ncbi.nlm.nih.gov).

Organism	Assembly level	Genome size (Mbp)	Number of PEG*	Number of REG†	Assembly gap length (bp)
Ruegeria atlantica	Contig	4.82	4736	46	0
Ruegeria arenilitoris	Contig	3.87	3791	63	0
Ruegeria conchae	Contig	4.49	4263	46	0
Ruegeria denitrificans	Contig	4.62	4541	47	0
Ruegeria faecimaris‡	Scaffold	4.12	4072	58	0
Ruegeria halocynthiae	Contig	4.24	4071	63	0
Ruegeria intermedia‡	Scaffold	3.86	3846	56	0
Ruegeria kandeliae	Contig	5.48	5156	51	0
Ruegeria lacuscaerulensis	Scaffold	3.52	3324	63	7844
Ruegeria litorea	Contig	4.69	4494	73	0
Ruegeria marina	Scaffold	5.00	4735	56	200
Ruegeria marisrubri	Contig	4.01	3730	48	0
Ruegeria mediterranea	Contig	5.28	5006	82	0
Ruegeria meonggei	Contig	4.54	4471	59	0
Ruegeria pomeroyi	Complete	4.60	4306	64	0
Ruegeria profundi	Contig	4.26	4008	47	0

Table 3-5 (continued).

Organism	Number of replicons	Number of scaffolds	Number of contigs	Genbank assembly
Ruegeria atlantica	—	—	75	GCA_001458195
Ruegeria arenilitoris	—	—	11	GCA_900185035
Ruegeria conchae	—	—	28	GCA_000192475
Ruegeria denitrificans	—	—	42	GCA_001458295

Ruegeria faecimaris‡	—	38	—	—
Ruegeria halocynthiae	—	—	35	GCA_900106805
Ruegeria intermedia‡	—	86	—	—
Ruegeria kandeliae	—	—	30	GCA_003116585
Ruegeria lacuscaerulensis	—	2	47	GCA_000161775
Ruegeria litorea	—	—	18	GCA_900172225
Ruegeria marina	—	51	53	GCA_900101475
Ruegeria marisrubri	—	—	39	GCA_001507595
Ruegeria mediterranea	—	—	49	GCA_900302455
Ruegeria meonggei	—	—	33	GCA_900172215
Ruegeria pomeroyi	2	—	—	GCA_000011965
Ruegeria profundi	—	—	33	GCA_001507545

* Predicted protein-encoding genes (PEG)
† Predicted RNA-encoding genes (REG)
‡ Genome sequences for *R. faecimaris* and *R. intermedia* were not available from NCBI and were downloaded from IMG (https://img.jgi.doe.gov). The IMG taxon IDs for these strains are 2724679780 and 2695420938, respectively.

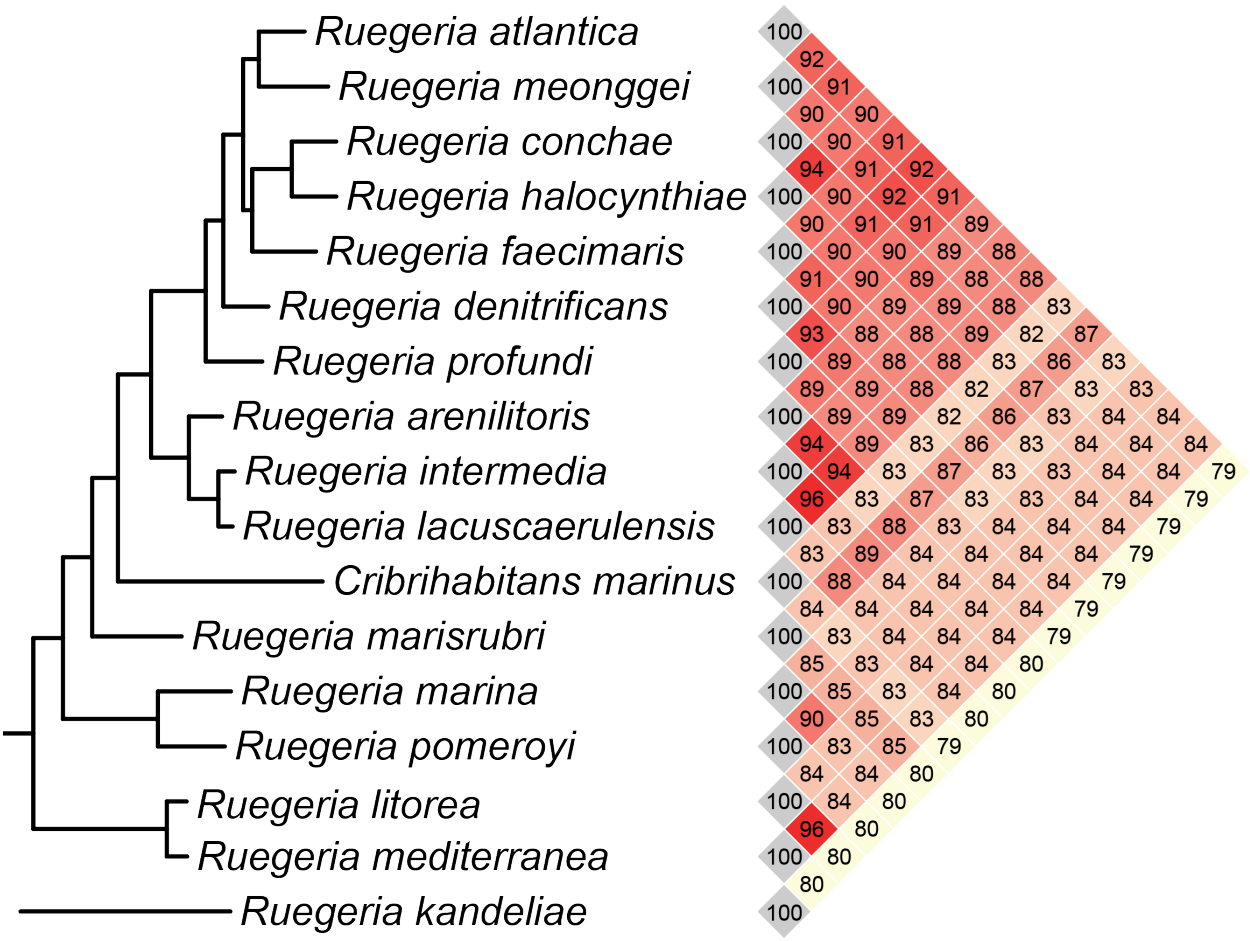

Figure 3-1. Heatmap of the average amino acid identity of the core genes (cAAI) for the *Ruegeria* species. cAAI values are shown in the grid on the right-hand side. A sub-tree from the maximum likelihood tree (Fig. 3-2) is shown on the left-hand side. *Ruegeria kandeliae* J95^{T} is not in the same clade but has been included.

Table 3-6. Distinguishing characteristics of *Ruegeria* from other, closely-related genera. Genera: 1, *Ruegeria*; 2, *Cribrihabitans*; 3, *Epibacterium*; 4, *Leisingera*; 5, *Phaeobacter*; 6, *Pseudophaeobacter*.

Characteristic	**1**	**2**	**3**	**4**	**5**	**6**
Polar flagellum(a)*	-	+	+	D	+	ND
Oxidase	+	-	+	+	+	+
API ZYM†						
α-glucosidase	D	-	D	-	+	-
naphthol-AS-BI-phosphohydrolase	-	+	D	D	D	-
diphosphatidylglycerol‡	D	+	-	-	D	D

*: No data available for polar flagellation of *Leisingera methylohalidivorans*, *Pseudophaeobacter arcticus*, *Pseudophaeobacter leonis*, *Ruegeria denitrificans*, or *Ruegeria intermedia*.

†: No data available for API-ZYM tests of *Epibacterium ulvae*, *Phaeobacter porticola*, or *Ruegeria intermedia*.

‡: No data available for the presence of diphosphatidylglycerol in *Epibacterium mobile*, *Epibacterium scottomollicae*, *Leisingera aquimarina*, *Leisingera caerulea*, *Phaeobacter italicus*, *Ruegeria denitrificans*, or *Ruegeria litorea*.

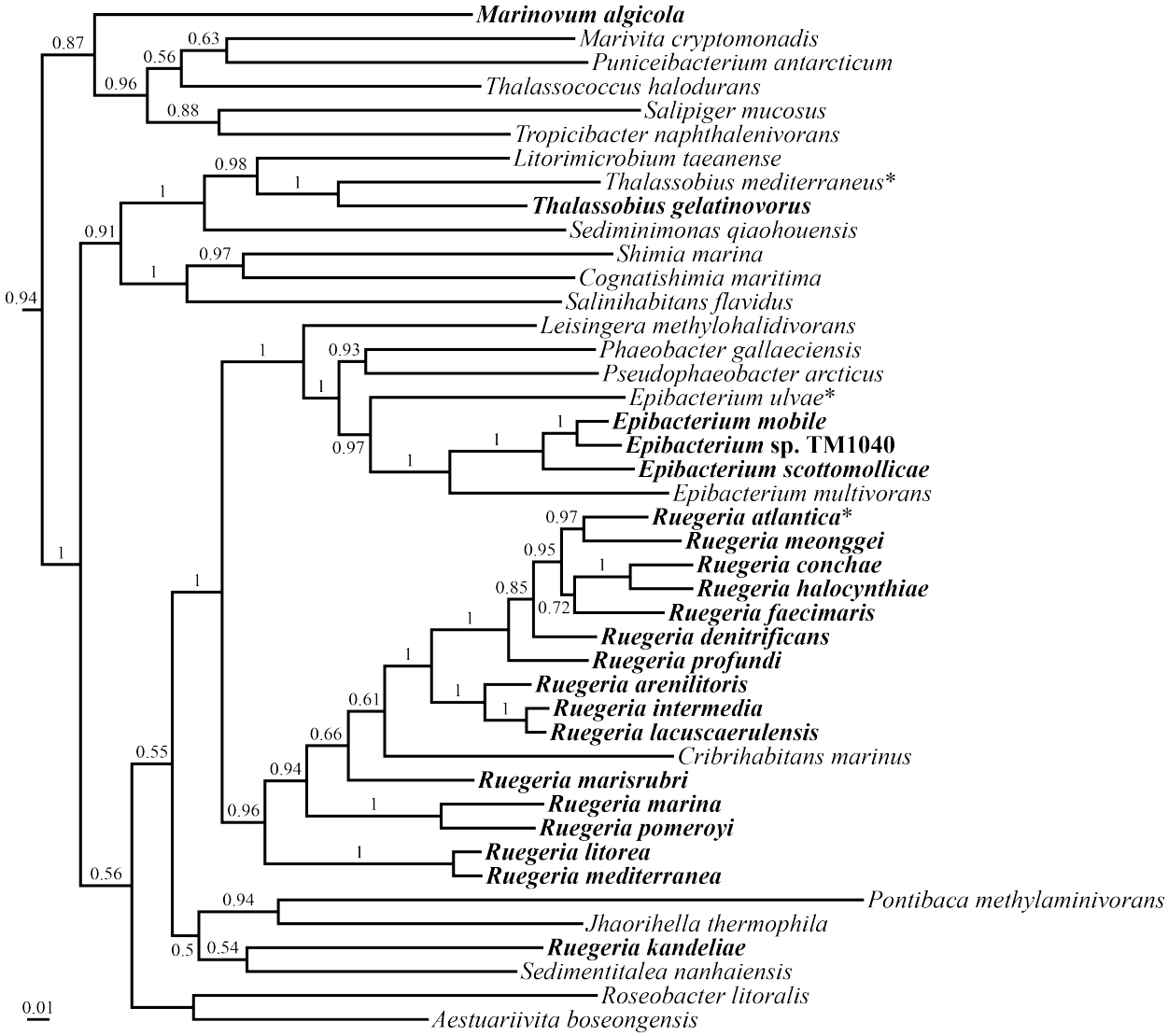

Figure 3-2. Maximum likelihood phylogeny of the *Ruegeria* species and its relatives. The tree was based on the concatenated multiple alignment of 49 of the most conserved genes present in the whole-genome sequences examined by Wirth and Whitman (2018) with the addition of the recently published genomes for *Cribrihabitans marinus* CZ-AM5^T (GCA_900109035), *Phaeobacter piscinae* 27-4^T (GCA_002407245), *Phaeobacter porticola* P97^T (GCA_001888185), *Primorskyibacter insulae* SSK3-2^T (GCA_900302505), *Puniceibacterium antarcticum* SM1211^T (GCA_002760615), *Ruegeria denitrificans* CECT 5091^T (GCA_001458295), *Ruegeria kandeliae* J95^T (GCA_003116585), *Ruegeria marisrubri* ZGT118^T (GCA_001507595), *Ruegeria mediterranea* M17^T (GCA_900302455), and *Ruegeria profundi* ZGT108^T (GCA_001507545). The tree was constructed using IQTree version 1.6.3 with the best model (LG+F+I+G4) identified by Bayesian information criterion and 100 bootstrap replicates (46, 47). The tree was rooted on the genus "*Ketogulonicigenium*", and the following genera were pruned from the tree: *Cognatiyoonia*, *Flavimaricola*, *Limimaricola*, *Loktanella*, "*Ketogulonicigenium*", *Pseudaestuariivita*, *Pseudoctadecabacter*, and *Wenxinia*. For the remaining genera, all species except for the type species were pruned from the tree with three exceptions: *Epibacterium*, *Ruegeria*, and *Thalassobius*. Bolded taxa indicate the current and former members of the genus *Ruegeria*. All genomic sequences were taken from the type strain

of their respective species. The numbers on the branches indicate the fraction of bootstrap support after 100 replicates. The scale bar indicates the number of substitutions per site.

*: Type species of *Epibacterium*, *Ruegeria*, and *Thalassobius*, respectively

CHAPTER 4

THE GENUS *EPIBACTERIUM*[3]

[3] Wirth, J.S. and W.B. Whitman. 2018. Accepted by *Bergey's Manual of Systematics of Archaea and Bacteria*.

Reprinted here with permission of the publisher.

Abstract

Gram-negative staining, aerobic, catalase- and oxidase-positive rods. Reproduces by normal cell division. Optimal growth typically occurs between 24–37 ˚C, 1–3.5 % (*w/v*) NaCl, and pH 7–8. Capable of utilizing a large variety of organic carbon sources. Every species can utilize D-cellobiose, D-fructose, D-galactose, acetate, pyruvate, succinate, and L-tyrosine as sole carbon and energy sources. Every species tested can utilize butyrate, fumarate, DL-3-hydroxybutyrate, lactate, 2-oxoglutarate, propionate, adonitol, arabitol, xylitol, L-alanine, L-arginine, L-asparagine, L-aspartate, L-cysteine, L-glutamine, L-leucine, L-methionine, L-ornithine, L-proline, D-serine, L-serine, and L-threonine as sole carbon and energy sources, but not gluconate, D-glucosamine, lactose, salicin, benzoate, phenylacetate, L-lysine, L-tryptophan, or L-valine. The major fatty acid is $C_{18:1}$ *ω7c* or summed feature 8 ($C_{18:1}$ *ω7c* and/or $C_{18:1}$ *ω6c*). The major quinone is ubiquinone 10. Some species are globally distributed in marine environments. Species have been isolated from marine biofilms, the surface of marine algae, and seawater. Members of the class *Alphaproteobacteria*, family *Rhodobacteraceae*. The type species is *Epibacterium ulvae*.

Abridged description of the genus

Rod-shaped, Gram-negative staining, and possessing one or more polar flagella. Motility has been observed in every species, but some strains are non-motile. No photosynthetic growth occurs. All species are aerobes. *E. mobile* is the only species which has been observed to be facultatively anaerobic. The inability to reduce nitrate to nitrite has been observed in all species, but some strains can reduce nitrate. Catalase and oxidase-positive. Reproduces by normal cell division. Growth temperatures range from 4–40 ˚C, but optimal growth occurs between 24–37 ˚C. All species require NaCl for growth except *E. mobile*. Optimal NaCl concentrations are between 1 % and 3.5 % (*w/v*), but growth occurs between 0 % and 15 % (*w/v*) NaCl. All species have an optimal pH between 7 and 8, but growth occurs between pH 6.5 and pH 8.5.

Capable of degrading a variety of carbon sources including carbohydrates, alcohols, carboxylic acids, and amino acids. All species can utilize D-cellobiose, D-fructose, D-galactose, acetate, pyruvate, succinate, and L-tyrosine as sole carbon and energy sources. All species tested can utilize butyrate, fumarate, DL-3-hydroxybutyrate, lactate, 2-oxoglutarate, propionate, adonitol, arabitol, xylitol, L-alanine, L-arginine, L-asparagine, L-aspartate, L-cysteine, L-glutamine, L-leucine, L-methionine, L-ornithine, L-proline, D-serine, L-serine, and L-threonine as sole carbon and energy sources, but not gluconate, D-glucosamine, lactose, salicin, benzoate, phenylacetate, L-lysine, L-tryptophan, or L-valine. Most species can utilize D-glucose, D-mannose, D-xylose, malate, and mannitol as sole carbon energy sources, but not L-arabinose. The major quinone is ubiquinone 10. The polar lipids observed with ≥1.0 % of the total lipids in at least one species comprise phosphatidylcholine, phosphatidylethanolamine, phosphatidylglycerol, at least two unidentified aminolipids, at least four unidentified phospholipids, and at least nine unidentified lipids. The major fatty acid is $C_{18:1}\omega 7c$ or summed feature 8 ($C_{18:1}\omega 7c/\omega 6c$). The fatty acids observed with ≥ 1.0 % of the total fatty acids in at least

one species comprise $C_{12:0}$, $C_{16:0}$, $C_{18:0}$, $C_{17:1}$ *ω7c*, $C_{18:1}$ *ω6c*, $C_{18:1}$ *ω7c*, 11-methyl $C_{18:1}$ *ω7c*, $C_{10:0}$ 3-OH, $C_{12:0}$ 3-OH, $C_{16:0}$ 2-OH, $C_{18:1}$ 2-OH, and the unknown fatty acid ECL 11.799. The 12:0 3-OH fatty acid is amide linked.

Some species are globally distributed in marine environments. Species have been isolated from marine biofilms, the surface of marine algae, and seawater. Members of the class *Alphaproteobacteria*, family *Rhodobacteraceae*. The type species is *Epibacterium ulvae*. The DNA G+C content (mol %) is 52.6–61.4 as determined by HPLC. There are 4 species with validly published names.

Further descriptive information

Cell morphology. The cells of all four species in *Epibacterium* are Gram negative staining rods and were all isolated from marine environments (1-6). A collection of all characters in the *Epibacterium* can be found in Table 4-1, and the distinguishing characteristics of the *Epibacterium* species can be found in Table 4-2. Cell length varies from 0.8 μm to 3 μm, while cell diameter ranges between 0.4 μm and 1.2 μm. All *Epibacterium* species possess at least one polar flagellum and exhibit motility, but some strains of *E. mobile* are non-motile. One of the species, *E. mobile*, forms star-shaped aggregates. *E. scottomollicae* accumulates poly-β-hydroxybutyrate granules, but *E. mobile* and *E. multivorans* do not.

Colonial and cultural characteristics. On agar media, colonies can typically be observed after 1–4 days. Colonies range from 1 mm to 3 mm in diameter and are regularly shaped. Colonies of *E. mobile* are circular, smooth, butyrous or viscous, convex with entire margins, dark brown, and possess dark brown precipitates at the edges of colonies (2). Colonies of *E. multivorans* are beige, brilliant, and slightly umbonate with entire margins after 48 hours at 28 ˚C (5). Colonies of *E. scottomollicae* are 2 mm in diameter, beige, and round after 4 days at 20 ˚C (3). Colonies of *E. ulvae* are convex, brown or black, 1–3 mm in diameter, older colonies

possess an un-pigmented halo around a dark spot in the center of the colony, and no pigment is observed when grown as bacterial lawns (6).

Nutrition and growth conditions. Although pH optima vary between species, all species which have been tested grow optimally at pH 7. All species tested grow optimally at NaCl concentrations between 2 % (*w/v*) and 3 % (*w/v*). Optimal growth temperatures vary between species, and the data is incomplete. *E. ulvae* grows optimally between 24 ˚C and 26 ˚C, while *E. ulvae* grows optimally between 30 ˚C and 37 ˚C (Table 4-1).

Various carbon sources are utilized by *Epibacterium* as a sole source of carbon and energy (Table 4-1). All species can utilize D-cellobiose, D-fructose, D-galactose, acetate, pyruvate, succinate, and L-tyrosine as sole carbon and energy sources. All species tested can utilize lactate, propionate, 2-oxoglutarate, glycerol, L-alanine, L-arginine, L-asparagine, L-aspartate, L-leucine, L-ornithine, L-proline, D-serine, L-serine, and L-threonine as sole carbon and energy sources. Although there are conflicting reports for *E. scottomollicae*, all species can utilize glucose, mannose, and malate. Although there are missing data for one or two species, *Epibacterium* species do not utilize gluconate, lactose, salicin, benzoate, or L-lysine.

There are several characters that distinguish the *Epibacterium* species from one another (Table 4-2). *E. ulvae* is the only species tested that utilizes glycine as a sole carbon and energy source, but it cannot utilize D-xylose, sorbitol, or L-histidine. *E. mobile* is the only species tested capable of facultative anaerobic growth, growth in the absence of NaCl, and the utilization of L-arabinose as a sole source of carbon and energy. *E. multivorans* is the only species tested that possesses phosphatidylethanolamine and can use D-ribose as a sole carbon and energy source, but not glycine. *E. scottomollicae* is the only species tested that grows in the presence of > 10 % (*w/v*) NaCl, accumulates poly-β-hydroxybutyrate granules, is susceptible to gentamycin, and cannot utilize mannitol as a sole carbon and energy source.

Epibacterium species are susceptible to a variety of antibiotics, but not all species have been tested for the same antibiotics (Table 4-3). There are no data for antibiotic susceptibility in *E. multivorans*. All species tested are resistant to clindamycin, kanamycin, penicillin-G, spectinomycin, trimethoprim, and vancomycin. All species tested are susceptible to cefoxitin, chloramphenicol, erythromycin, rifampicin, and streptomycin. Susceptiblity to ampicillin, gentamycin, and tetracycline varies between the *Epibacterium* species, and susceptibility to tetracycline varies between strains of *E. mobile*.

Chemotaxonomic characteristics. The major fatty acid in *Epibacterium* is $C_{18:1}$ *ω7c*. Every species possesses $C_{18:1}$ *ω7c*, but its percentage ranges from 53 % to 79 %. The following fatty acids have been observed in all *Epibacterium* species: $C_{16:0}$, $C_{18:0}$, $C_{18:1}$ *ω7c* 11-CH3, $C_{10:0}$ 3-OH, $C_{12:0}$ 3-OH, and $C_{16:0}$ 2-OH. A complete list of the fatty acids in the *Epibacterium* species can be found in Table 4. The polar lipid content of the *Epibacterium* species is relatively incomplete as there are no data for *E. mobile* or *E. scottomollicae*. Neither *E. ulvae* nor *E. multivorans* possess diphosphatidylglycerol nor unidentified aminophospholipids. Both *E. ulvae* and *E. multivorans* possess phosphatidylcholine, phosphatidylglycerol, at least one unidentified aminolipid, and at least four unidentified lipids. *E. multivorans* possesses phosphatidylethanolamine and at least four unidentified phospholipids, but *E. ulvae* does not (Table 4-4).

Genome features and genetic methods available. Whole genome sequences are publicly available for the type strains of all the *Epibacterium* species, but none of these genomes are complete. There are, however, complete, whole-genome sequences available for *Epibacterium mobile* F1926 and *Epibacterium* sp. TM1040. *Epibacterium mobile* F1926 possesses 5 replicons in total: a chromosome of 3.26 Mbp, a megaplasmid of 1.26 Mbp, and three smaller plasmids of 0.15 Mbp, 0.11 Mbp, and 0.06 Mbp, respectively. *Epibacterium* sp.

TM1040 possess 3 replicons in total: a chromosome of 3.20 Mbp, a megaplasmid of 0.82 Mbp, and a second plasmid of 0.13 Mbp. Table 5 provides details of the whole-genome sequences of these 6 strains. Using the EDGAR server 2.3, the core genome of *Epibacterium* consists of 2,048 predicted coding sequences (7). The average amino acid identity of the core genes (cAAI) ranges from 0.81 to 0.95 with a mean of 0.86 and a median 0.84 (Fig. 4-1). There is currently no published genetics system for the *Epibacterium* species.

Ecology. *Epibacterium* species are found in aerobic, marine environments (1-3, 5, 6). Some species of *Epibacterium* have been isolated from the surface of marine algae and the phycosphere of dinoflagellates (6, 8). Other species have been isolated from marine biofilms and from marine invertebrates (1, 3). *E. mobile* is extremely abundant has been observed with a global distribution in marine environments in both bacterial isolates and metagenomic samples from the attached and pelagic fractions (9). The wide range of growth conditions and carbon sources that allow growth of *E. mobile* may help to explain its presence in such a wide variety of marine environments (Table 4-1).

Enrichment and isolation procedures

Several techniques have been published for isolating and enriching *Epibacterium* species. The type strain of *E. mobile* was isolated by floating a glass slide on the sea surface for 1 day to produce a slime on the glass. The slime was then diluted with sterilized seawater and cultured on a B2 agar plate (1). *E. mobile* HTCC2662 was isolated from seawater from the Sargasso Sea by using a dilution-to-extinction methodology and growing the cultures on marine agar 2216 for 4 days at 25 ˚C (2). *E. mobile* MBIC01099 was isolated by diluting a homogenized coelenterate (*Hexacorallia* sp.) with sterile seawater, enriching the culture in B6 medium supplemented with eosin Y, plating the enrichment onto B6 agar, and then incubating the plate at 25 ˚C for 1 day. *E.*

mobile LMG 24361 and *E. mobile* LMG 24372 were isolated along with *E. scottomollicae* (see below) (3).

E. multivorans was isolated by plating dilutions of surface seawater onto 1/100-strength marine agar and incubating at 26 ˚C (5). *E. scottomollicae* was isolated by exposing a stainless-steel cathode to seawater in the port of Genoa, Italy. The resulting electroactive biofilm was transferred to a 0.85 % NaCl solution via sonication, diluted, plated onto marine agar 2216, and incubated at 20 ˚C for several days (3). *E. ulvae* was isolated by rinsing algal specimens (*U. australis*) three times with sterile seawater, vortexing the rinsed alga in sterile seawater to suspend the epiphytic bacterial cells, diluting the cell suspension, plating the dilutions onto marine agar 2216, and incubating the plates at 25 ˚C for 48 hrs (6, 10).

Maintenance procedures

Strains of *Epibacterium* can be maintained on solid media or in liquid cultures. Because *Epibacterium* species are aerobes, shaking is recommended for liquid cultures in order to increase the oxygenation of the media.

Several types of rich media have been used to cultivate the *Epibacterium* species. The most common medium used is Bacto marine agar/broth (Difco 2216 / DSMZ medium 514). B6 medium, 1/5 LBM medium, and LB have been used to cultivate *E. mobile* (1, 2). B6 medium is composed of 0.025 % (*w/v*) Polypepton (Nihon Pharmaceuticals), 0.025 % (*w/v*) Polypepton S (Nihon Pharmaceuticals), 0.025 % (*w/v*) Polypepton Y (Nihon Pharmaceuticals), 0.05 % (*w/v*) brain heart infusion (Difco), 0.1 % (*w/v*) yeast extract, 0.025 % (*w/v*) malt extract, 0.025 (*w/v*) soluble starch, 0.05 % (*w/v*)potato glucose broth (Difco), 2.6 % (*w/v*) sea salt (Tropic Marin), 0.05% HEPES (pH 7.7), and 10 mM eosin Y (1). 1/5 LBM medium is composed of 0.2 % (*w/v*) tryptone and 0.1 % (*w/v*) yeast extract dissolved in Jamarin S synthetic seawater (Jamarin Laboratory) at pH 7.2 (11). Trypticase soy agar has been used to cultivate *E. scottomollicae*. *E.*

scottomollicae is also capable of growing on nutrient agar and R2A, but the growth was reported as weak (3).

There are two minimal media that have been used to cultivate *Epibacterium* species: basal medium (BM) and seawater medium (SWM) (3, 5). BM contains 200 mM NaCl, 50 mM $MgSO_4$, 10 mM KCl, 10 mM $CaCl_2$, 50–100 mM Tris HCl (pH 7.5), 19 mM NH_4Cl, 330 µM K_2HPO_4, and 100 µM $FeSO_4$. The sole carbon source is typically added to a final concentration of 0.1–0.2 % (*w/v* for solids and *v/v* for liquids). If amino acid supplementation is required, all twenty amino acids are provided at a concentration of 1 mg/L. The amino acid stock solution should be filter-sterilized and added to media that has been autoclaved and allowed to cool (12).

SWM is composed of 0.4 % (*w/v*) $NaSO_4$, 0.002 % (*w/v*) KH_2PO_4, 0.025 % (*w/v*) NH_4Cl, 2 % (*w/v*) NaCl, 0.3 % (*w/v*) $MgCl_2 \cdot 6\ H_2O$, 0.05 % (*w/v*) KCl, 0.015 % (*w/v*) $CaCl_2 \cdot 2H_2O$, 0.019 % (*w/v*) $NaHCO_3$, and 0.1 % (*v/v*) trace elements solution. The trace elements solution consists of 0.21 % (*w/v*) $FeSO_4 \cdot 7H_2O$, 1.3 % (*v/v*) 25 % HCl, 0.52 % (*w/v*) Titriplex-(III) (Na_2-EDTA), 0.003 % (*w/v*) H_3BO_3, 0.01 % (*w/v*) $MnCl_2 \cdot 4H_2O$, 0.019 % (*w/v*) $CoCl_2 \cdot 6H_2O$, 0.0024 % (*w/v*) $NiCl_2 \cdot 6H_2O$, 0.0002 % (*w/v*) $CuCl_2 \cdot 2H_2O$, 0.0144 % (*w/v*) $ZnSO_4 \cdot 7H_2O$, and 0.0036 % (*w/v*) $Na_2MoO_4 \cdot 2H_2O$, and it should be filter-sterilized before use. All components except for the $NaHCO_3$ and the trace elements solution should be dissolved in 90 % of the final desired volume, and the $NaHCO_3$ should be dissolved in 10 % of the final desired volume. Both solutions should be autoclaved separately and allowed to cool. Once cool, the trace elements and the $NaHCO_3$ solutions should be added to the remaining solution (13).

In order to store *Epibacterium* species, mid-log phase cultures in a rich medium are mixed with a sterile glycerol solution for a final concentration of 20 % (*v/v*) glycerol. The freezer stock can then be stored at -20 ˚C or -80 ˚C indefinitely (3, 5).

Differentiation of the genus *Epibacterium* from other genera

Over 40 phenotypic and chemotaxonomic characters were examined, but there are no characters that definitively distinguish *Epibacterium* from the closely related genera *Cribrihabitans*, *Leisingera*, *Phaeobacter*, *Pseudophaeobacter*, and *Ruegeria* (Table 4-6). Currently, the best way to distinguish *Epibacterium* species from other genera is through the use of whole-genome, sequence-based approaches.

Taxonomic comments

Ruegeria sp. TM1040 was isolated in 2004, but was never formally described (8). Between 2007 and 2008, the species *Ruegeria mobilis*, *Ruegeria pelagia*, and *Ruegeria scottomollicae* were isolated (1-3). Shortly after, *Ruegeria pelagia* was found to be a heterotypic synonym of *Ruegeria mobilis* (14). Then in 2012, the species *Tropicibacter multivorans* was isolated (5). The genus *Epibacterium* was first proposed by Penesyan *et al.* to accommodate two isolated strains of the type (and only) species, *Epibacterium ulvae* (6). After an extensive taxonomic evaluation based on whole-genome sequences, Wirth and Whitman reclassified *Ruegeria mobilis*, *Ruegeria scottomollicae*, *Ruegeria* sp. TM1040, and *Tropicibacter multivorans* as *Epibacterium mobile*, *Epibacterium scottomollicae*, *Epibacterium* sp. TM1040, and *Epibacterium multivorans*, respectively (15). This same study demonstrated that the genus of *Epibacterium* was monophyletic in a maximum likelihood tree based on the highly conserved core genes (15). Since then, the whole-genome sequences of many organisms within that clade have become publicly available on NCBI. Using the methodology of Wirth and Whitman, a maximum likelihood tree based on 51 of the most conserved core genes was constructed using IQTree v. 1.6.3 (Fig. 4-2).

List of species of the genus *Epibacterium*

Epibacterium mobile (Muramatsu, Uchino, Kasai, Suzuki, and Nakagawa 2007) Wirth and Whitman 2018, 2404^{VP} (*Ruegeria mobilis* Muramatsu, Uchino, Kasai, Suzuki, and Nakagawa 2007, 1307). *mo'bi.le*. L. neut. adj. *mobile*, mobile.

Description as for the genus and the following characteristics (1-4, 16). Cells are 0.6–1.2μm wide and 0.8–2.1μm long. Sometimes form star-shaped rosettes. Growth occurs between 5 ˚C and 45 ˚C (optimum, 30–37 ˚C). Growth occurs between pH 4 and pH 12 (optimum, pH 7). Growth occurs between 0 % (*w/v*) NaCl and 10 % (*w/v*) NaCl (optimum, 1–3.5 % (*w/v*) NaCl). Hydrolyzes esculin, alginic acid, and L-tyrosine, but not agar, carboxymethylcellulose, casein, cellulose, chitin, inulin, starch, or Tween 80. Utilizes L-arabinose, D-cellobiose, D-fructose, D-fucose, D-galactose, D-glucose, D-mannose, D-xylose, acetate, 4-aminobutyrate, lactate, malate, 2-oxoglutrate, propionate, pyruvate, succinate, adonitol, arabitol, glycerol, mannitol, sorbitol, xylitol, L-alanine, L-asparagine, L-aspartate, L-histidine, L-leucine, L-ornithine, L-phenylalanine, L-proline, D-serine, L-serine, L-threonine, L-tyrosine, and putrescine as sole carbon and energy sources, but not gluconate, lactose, salicin, or benzoate. Utilization of maltose, L-rhamnose, sucrose, trehalose, citrate, formate, and L-glutamate varies between strains. Produces acid from aesculin, D-arabinose, L-arabinose, D-cellobiose, esculin, D-fructose, gentiobiose, D-glucose, glycogen, and D-xylose, but not D-adonitol, amygdalin, D-arabitol, arbutin, dulcitol, erythritol, D-fucose, D-galactose, gluconate, 5-ketogluconate, *N*-acetylglucoasmine, methyl α-D-glucoside, glycerol, lactose, D-lyxose, methyl α-D-mannoside, melezitose, melibiose, raffinose, L-rhamnose, salicin, D-sorbitol, L-sorbose, D-tagatose, xylitol, or methyl β-D-xyloside. Acid production from *myo*-inositol varies between strains. There are conflicting reports for the production of acid from maltose, mannitol, D-mannose, D-ribose, sucrose, and trehalose. In assays with the API-ZYM system, reactions for alkaline phosphatase

and leucine arylamidase are positive; but reactions for α-chymotrypsin, cystine arylamidase, α-fucosidase, α-galactosidase, β-galactosidase, β-gluocsidase, β-glucuronidase, lipase (C14), α-mannosidase, and trypsin are negative. Reactions for esterase lipase (C8) vary between strains. There are conflicting reports for the activities of acid phosphatase, esterase lipase (C4), *N*-acetyl-β-glucosaminidase, α-glucosidase, napthol-AS-BI-phosphohydrolase, and valine arylamidase. Indole is not produced from tryptophan. The susceptibilities to antibiotics are summarized in Table 4-3. The fatty acid composition is summarized in Table 4-4. Ammonium sulfate and urea are used as sole nitrogen sources. Does not accumulate poly-β-hydroxybutyrate. Isolated from a slime attached to a glass slide that was floated on the surface for 1 day at Ishigaki Island, Japan in 1990. The DNA G+C content (mol %) is 58.4–59.5 as determined by HPLC. The type strain is MBIC01146^{T} (=NBRC 101030^{T} =CIP109181^{T}). The GenBank accession numbers are EU977137 (16S rRNA gene) and GCA_001681715 (genome).

Epibacterium multivorans (Lucena, Pujalte, Ruvira, Garay, Macián, and Arahal 2012) Wirth and Whitman 2018, 2404^{VP} (*Tropicibacter multivorans* Lucena, Pujalte, Ruvira, Garay, Macián, and Arahal 2012, 847^{VP}). *mul'ti.vor'ans*. L. adj. *multus* many, numerous; L. v. *vorare* to devour, swallow; N.L. part. adj. *multivorans* devouring many, referring to the utilization of numerous different substrates for growth.

Description as for the genus and the following characteristics (5). Cells are 0.5–1 µm wide and 2–2.5 µm long. Motile by means of polar flagella. Cells do not accumulate poly-β-hydroxybutyrate. Growth occurs between 15 ˚C and 37 ˚C. Growth occurs between 1.7 % (*w/v*) total salinity and 7 % (*w/v*) total salinity, but not at ≤ 0.35 % (*w/v*) total salinity or ≥ 8 % (*w/v*) total salinity. Requires Na^{+} and divalent cations (Mg^{2+} or Ca^{2+}) for growth. Does not reduce nitrate to nitrite. Hydrolyzes esculin, DNA, and urea, but not agar, alginate, casein, gelatin, starch, or Tween-80. Utilizes D-cellobiose, D-fructose, D-galactose, D-glucose, D-mannose, D-

ribose, D-xylose, acetate, butyrate, citrate, fumarate, DL-3-hydroxybutyrate, lactate, malate, 2-oxoglutarate, propionate, pyruvate, succinate, glycerol, *myo*-inositol, mannitol, sorbitol, L-alanine, L-arginine, L-aspartate, L-glutamate, L-histidine, L-leucine, L-ornithine, D-serine, L-serine, L-threonine, and L-tyrosine as sole carbon and energy sources, but not amygdalin, L-arabinose, galacturonate, gluconate, glucuronate, *N*-acetyl-D-glucosamine, glycerate, lactose, maltose, melibiose, L-rhamnose, saccharate, salicin, sucrose, trehalose, *trans*-aconitate, 4-aminobutyrate, D-glycerate, D-saccharate, L-citrulline, L-glycine, L-lysine, putrescine, or L-sarcosine. Does not produce acid from glucose. In assays with the API-ZYM system, reactions for acid phosphatase, alkaline phosphatase, α-glucosidase, and leucine arylamidase are positive, but reactions for α-chymotrypsin, cystine arylamidase, esterase (C4), esterase lipase (C8), α-fucosidase, α-galactosidase, β-galactosidase, *N*-acetyl-β-glucosaminidase, β-glucosidase, β-glucuronidase, lipase (C14), α-mannosidase, napthol-AS-BI-phosphohydrolase, trypsin, and valine arylamidase are negative. Does not produce indole from tryptophan. In assays with the Biolog GN2 microplates, oxidation of substrates after 48 hrs is negative for all substrates. The fatty acid composition is summarized in Table 4-4. The type strain was isolated from Mediterranean surface seawater at Malvarrosa beach, Valencia, Spain in July of 2008. The DNA G+C content (mol %) is 60.7 as determined by HPLC. The type strain is MD5^{T} (=CECT 7557^{T} =KCTC 23350^{T} =DSM 26470^{T}). The GenBank accession numbers are FR727679 (16S rRNA gene) and GCA_900112515 (genome).

Epibacterium scottomollicae (Vandecandelaere, Nercessian, Segaert, Achouak, Faimali, and Vandamme 2008) Wirth and Whitman 2018, 2404^{VP} (*Ruegeria scottomollicae* Vandecandelaere, Nercessian, Segaert, Achouak, Faimali, and Vandamme 2008, 2729^{VP}). *scot.to'mol.li.cae*. N.L. gen. n. *scottomollicae* in honor of Dr. Victoria Scotto-Mollica and Dr.

Alfonso Mollica, both of whom were pioneers in the field of microbe-induced corrosion of steels and the generation of electroactive seawater biofilms.

Description as for the genus and the following characteristics (3, 4, 16). Cells are 1 μm wide and 1.3 μm long. Long, slender, fibrillar extensions from the cell surface. Cells accumulate poly-β-hydroxybutyrate. Colonies are round, beige, and 2 mm in diameter after 4 days incubation on marine agar at 20 ˚C. Growth occurs between 4 ˚C and 40 ˚C, but growth at 45 ˚C varies between strains. Growth occurs between pH 5 and pH 9 (optimum pH 6.5–8.5). Growth occurs between 1 % and 15 % (*w/v*) NaCl, but not at 16% (*w/v*) NaCl. No growth occurs on peptone/yeast extract/glucose agar. Does not reduce nitrate to nitrite or gas. Hydrolyzes esculin, Tween 80, and L-tyrosine, but not casein, chitin, gelatin, starch, or xanthine. Utilizes D-cellobiose, D-fructose, D-galactose, D-xylose, acetate, pyruvate, succinate, and L-tyrosine as sole carbon and energy sources, but not L-arabinose, gluconate, maltose, salicin, sucrose, trehalose, adipate, benzoate, caprate, formate, phenylacetate, mannitol, or L-glutamate. There are conflicting reports for the utilization of D-glucose, D-mannose, citrate, and malate as sole carbon and energy sources. Produces acid from D-adonitol, arbutin, erythritol, esculin, D-fucose, D-galactose, gentiobiose, 5-ketogluconate, *N*-acetylglucosamine, methyl α-D-glucoside, glycogen, glycerol, mannitol, melibiose, salicin, D-sorbitol, xylitol, and methyl β-D-xyloside, but not from amygdalin, D-arabinose, D-arabitol, dulcitol, gluconate, D-lyxose, methyl α-D-mannoside, melezitose, raffinose, L-rhamnose, L-sorbose, or D-tagatose. There are conflicting reports for the production of acid from L-arabinose, D-cellobiose, D-fructose, D-glucose, *myo*-inositol, lactose, maltose, D-mannose, D-ribose, sucrose, trehalose, and D-xylose. In assays with the API-ZYM system, reactions for alkaline phosphatase, esterase (C4), and leucine arylamidase are positive, but reactions are negative for α-chymotrypsin, cystine arylamidase, α-fucosidase, β-galactosidase, β-glucosidase, β-glucuronidase, lipase (C14), α-mannosidase, trypsin, and valine

arylamidase. There are conflicting reports for the activities of acid phosphatase, esterase lipase (C8), α-galactosidase, *N*-acetyl-β-glucosaminidase, α-glucosidase, and naphthol-AS-BI-phosphohydrolase. Indole is not produced from tryptophan. The susceptibilities to antibiotics are summarized in Table 4-3. The fatty acid composition is summarized in Table 4-4. Isolated from a marine, electroactive biofilm in Genoa, Italy. The DNA G+C content (mol %) is 61.0±0.4 as determined by HPLC. The type strain is LMG 24367^{T} (=CCUG 55858^{T} =DSM 25328^{T}). The GenBank accession numbers are AM905330 (16S rRNA gene) and GCA_003003215 (genome).

Epibacterium ulvae Penesyan, Breider, Schumann, Tindall, Egan, and Brinkhoff 2013, 1594^{VP}. *ul'va.e*. N.L. gen. n. *ulvae* of/from *Ulva*, isolated from a marine alga *Ulva australis*.

Description as for the genus and the following characteristics (6). Cells are 0.4–0.6 μm wide and 2–3 μm long. Growth occurs between 12 ˚C and 34 ˚C (optimum 24–26 ˚C). Growth occurs between pH 6 and pH 9 (optimum pH 7–8). Growth occurs between 1 % and 6 % (*w/v*) NaCl (optimum 2–3 % (*w/v*) NaCl). Sodium ions are required for growth. Unable to hydrolyze gelatin, starch, or Tween-80. Utilizes D-cellobiose, D-fructose, D-galactose, D-glucose, maltose, D-mannose, sucrose, trehalose, acetate, citrate, lactate, malate, propionate, pyruvate, succinate, glycerol, mannitol, L-alanine, L-arginine, L-asparagine, L-aspartate, L-cysteine, L-glutamate, L-glutamine, glycine, L-leucine, L-methionine, L-proline, L-serine, L-threonine, and L-tyrosine as sole carbon and energy sources, but not L-arabinose, D-fucose, D-glucosamine, lactose, D-ribose, L-rhamnose, D-xylose, formate, sorbitol, L-histidine, L-lysine, L-phenylalanine, L-tryptophan, L-valine, or Tween-80. The susceptibilities to antibiotics are summarized in Table 4-3. The fatty acid composition is summarized in Table 4-4. Isolated from the surface of marine alga, *Ulva australis*, collected at Sharks Point, Clovelly, a rocky intertidal zone near Sydney, Australia. The DNA G+C content (mol %) is 52.6 as determined by HPLC. The type strain is

U95^T (=DSM 24752^T =LMG 26464^T). The GenBank accession numbers are JN935021 (16S rRNA gene) and GCA_900102795 (genome).

References:

1. Muramatsu Y, Uchino Y, Kasai H, Suzuki KI, Nakagawa Y. 2007. *Ruegeria mobilis* sp. nov., a member of the *Alphaproteobacteria* isolated in Japan and Palau. International Journal of Systematic and Evolutionary Microbiology 57:1304-1309.
2. Lee K, Choo YJ, Giovannoni SJ, Cho JC. 2007. *Ruegeria pelagia* sp. nov., isolated from the Sargasso Sea, Atlantic ocean. International Journal of Systematic and Evolutionary Microbiology 57:1815-1818.
3. Vandecandelaere I, Nercessian O, Segaert E, Achouak W, Faimali M, Vandamme P. 2008. *Ruegeria scottomollicae* sp. nov., isolated from a marine electroactive biofilm. International Journal of Systematic and Evolutionary Microbiology 58:2726-2733.
4. Oh KH, Jung YT, Oh TK, Yoon JH. 2011. *Ruegeria faecimaris* sp. nov., isolated from a tidal flat sediment. International Journal of Systematic and Evolutionary Microbiology 61:1182-1188.
5. Lucena T, Pujalte MJ, Ruvira MA, Garay E, Macian MC, Arahal DR. 2012. *Tropicibacter multivorans* sp. nov., an aerobic alphaproteobacterium isolated from surface seawater. International Journal of Systematic and Evolutionary Microbiology 62:844-8.
6. Penesyan A, Breider S, Schumann P, Tindall BJ, Egan S, Brinkhoff T. 2013. *Epibacterium ulvae* gen. nov., sp. nov., epibiotic bacteria isolated from the surface of a marine alga. International Journal of Systematic and Evolutionary Microbiology 63:1589-96.

7. Blom J, Kreis J, Spanig S, Juhre T, Bertelli C, Ernst C, Goesmann A. 2016. EDGAR 2.0: an enhanced software platform for comparative gene content analyses. Nucleic Acids Research 44:W22-8.

8. Miller TR, Belas R. 2004. Dimethylsulfoniopropionate metabolism by *Pfiesteria*-associated Roseobacter spp. Applied and Environmental Microbiology 70:3383-91.

9. Sonnenschein EC, Nielsen KF, D'Alvise P, Porsby CH, Melchiorsen J, Heilmann J, Kalatzis PG, Lopez-Perez M, Bunk B, Sproer C, Middelboe M, Gram L. 2017. Global occurrence and heterogeneity of the *Roseobacter*-clade species *Ruegeria mobilis*. ISME Journal 11:569-583.

10. Penesyan A, Marshall-Jones Z, Holmstrom C, Kjelleberg S, Egan S. 2009. Antimicrobial activity observed among cultured marine epiphytic bacteria reflects their potential as a source of new drugs. Fems Microbiology Ecology 69:113-24.

11. Suzuki M, Nakagawa Y, Harayama S, Yamamoto S. 2001. Phylogenetic analysis and taxonomic study of marine *Cytophaga*-like bacteria: proposal for *Tenacibaculum* gen. nov. with *Tenacibaculum maritimum* comb. nov. and *Tenacibaculum ovolyticum* comb. nov., and description of *Tenacibaculum mesophilum* sp. nov. and *Tenacibaculum amylolyticum* sp. nov. International Journal of Systematic and Evolutionary Microbiology 51:1639-52.

12. Baumann P, Baumann L. 1981. The marine Gram-negative eubacteria: genera *Photobacterium*, *Beneckea*, *Alteromonas*, *Pseudomonas*, and *Alcaligenes*. The Prokaryotes 2:1302-1331.

13. Zech H, Thole S, Schreiber K, Kalhofer D, Voget S, Brinkhoff T, Simon M, Schomburg D, Rabus R. 2009. Growth phase-dependent global protein and metabolite profiles of

Phaeobacter gallaeciensis strain DSM 17395, a member of the marine *Roseobacter*-clade. Proteomics 9:3677-97.

14. Lai QL, Yuan J, Li FY, Zheng TL, Shao ZZ. 2010. *Ruegeria pelagia* is a later heterotypic synonym of *Ruegeria mobilis*. International Journal of Systematic and Evolutionary Microbiology 60:1918-1920.

15. Wirth JS, Whitman WB. 2018. Phylogenomic analyses of a clade within the roseobacter group suggest taxonomic reassignments of species of the genera *Aestuariivita*, *Citreicella*, *Loktanella*, *Nautella*, *Pelagibaca*, *Ruegeria*, *Thalassobius*, *Thiobacimonas* and *Tropicibacter*, and the proposal of six novel genera. Internationl Journal of Systematic and Evolutionary Microbiology doi:10.1099/ijsem.0.002833.

16. Lee J, Whon TW, Shin NR, Roh SW, Kim J, Park SK, Kim MS, Shin KS, Lee JS, Lee KC, Kim YO, Bae JW. 2012. *Ruegeria conchae* sp. nov., isolated from the ark clam *Scapharca broughtonii*. International Journal of Systematic and Evolutionary Microbiology 62:2851-2857.

17. Nguyen LT, Schmidt HA, von Haeseler A, Minh BQ. 2015. IQ-TREE: a fast and effective stochastic algorithm for estimating maximum-likelihood phylogenies. Molecular Biology and Evolution 32:268-74.

18. Kalyaanamoorthy S, Minh BQ, Wong TKF, von Haeseler A, Jermiin LS. 2017. ModelFinder: fast model selection for accurate phylogenetic estimates. Nature Methods 14:587-589.

Table 4-1. Phenotypes of the *Epibacterium* species. Species: 1, *E. ulvae*; 2, *E. mobile*; 3, *E. multivorans*; 4, *E. scottomollicae*. All species are positive for the presence of polar flagella, oxidase and catalase activity, and the utilization of D-cellobiose, D-fructose, D-galactose, acetate, pyruvate, succinate, and L-tyrosine. All species tested are positive for the activities of alkaline phosphatase and leucine arylamidase; aerobic acid production from esculin, gentiobiose, and glycogen; utilization of lactate, propionate, 2-oxoglutarate, glycerol, L-alanine, L-arginine, L-asparagine, L-aspartate, L-leucine, L-ornithine, L-proline, D-serine, L-serine, and L-threonine; the hydrolysis of esculin; and the presence of phosphatidylcholine, phosphatidylglycerol, unidentified aminolipids, and unidentified lipids. All species tested are negative for the activities of α-chymotrypsin, cystine arylamidase, α-fucosidase, -galactosidase, -glucosidase, -glucuronidase, lipase (C14), α-mannosidase, and trypsin; aerobic acid production from amygdalin, D-arabitol, dulcitol, gluconate, D-lyxose, methyl-α-D-mannoside, melizitose, raffinose, L-rhamnose, L-sorbose, and D-tagatose; the utilization of gluconate, lactose, salicin, benzoate, and L-lysine; the hydrolysis of xanthine; and the presence of diphosphatidylglycerol. "ND" indicates no data available.

Characteristic	**1**	**2**	**3**	**4**
Morphology				
Diameter	0.4-0.6 µm	0.6-1.2 µm	0.5-1 µm	1 µm
Length	2-3 µm	0.8-2.1 µm	2-2.5 µm	1.3 µm
Motility	+	d	+	+
Facultatively anaerobic	ND	+	ND	-
Growth range (optimum)				
Temperature (˚C)	12-34 (24-26)	5-45 (30-37)	15-37	4-40
% NaCl (*w/v*)	1-6 (2-3)	0-10 (1-3.5)	1.7-7	1-15
pH	6-9 (7-8)	4-12 (5-7)	ND	5-9 (6.5-8.5)
Accumlation of poly-β-hydroxybutyrate	ND	-	-	+
Enzymatic Activity (API-ZYM)				
acid phosphatase	ND	v	+	v
esterase (C4)	ND	v	-	+
esterase lipase (C8)	ND	d	-	v
α-galactosidase	ND	-	-	v
N-acetyl-β-glucosaminidase	ND	v	-	v
α-glucosidase	ND	v	+	v
naphthol-AS-BI-phosphohydrolase	ND	v	-	v

valine arylamidase	ND	v	-	-
Reduction of nitrate to nitrite	ND	d	-	-
Aerobic acid production				
D-adonitol	ND	-	ND	+
D-arabinose	ND	+	ND	-
L-arabinose	ND	+	ND	v
arbutin	ND	-	ND	+
D-cellobiose	ND	+	ND	v
erythritol	ND	-	ND	+
D-fructose	ND	+	ND	v
D-fucose	ND	-	ND	+
D-galactose	ND	-	ND	+
5-ketogluconate	ND	-	ND	+
N-acetylglucosamine	ND	-	ND	+
D-glucose	ND	+	-	v
methyl α-D-glucoside	ND	-	ND	+
glycerol	ND	-	ND	+
myo-Inositol	ND	d	ND	v
lactose	ND	-	ND	v
maltose	ND	v	ND	v
mannitol	ND	v	ND	+
D-mannose	ND	v	ND	v
melibiose	ND	-	ND	+
D-ribose	ND	v	ND	v
salicin	ND	-	ND	+
D-sorbitol	ND	-	ND	+
sucrose	ND	v	ND	v
trehalose	ND	v	ND	v
xylitol	ND	-	ND	+

D-xylose	ND	+	ND	v
methyl β-D-xyloside	ND	-	ND	+
Carbohydrate utilization				
L-arabinose	-	+	-	-
D-fucose	-	+	ND	ND
D-glucose	+	+	+	v
maltose	+	d	-	-
D-mannose	+	+	+	v
D-ribose	-	ND	+	ND
L-rhamnose	-	d	-	ND
sucrose	+	d	-	-
trehalose	+	d	-	-
D-xylose	-	+	+	+
Carboxylic acid utilization				
4-aminobutyrate	ND	+	-	ND
citrate	+	d	+	v
formate	-	d	ND	-
malate	+	+	+	v
Alcohol utilization				
mannitol	+	+	+	-
sorbitol	-	+	+	ND
Amino acid utilization				
L-glutamate	+	d	+	-
glycine	+	ND	-	ND
L-histidine	-	+	+	ND
L-phenylalanine	-	+	ND	ND
putrescine	ND	+	-	ND
Hydrolysis of:				
Gelatin	-	d	-	-

Tween 80	-	v	-	+
Polar lipids				
phosphatidylethanolamine	-	ND	+	ND
unidentified phospholipids	-	ND	+	ND
DNA G+C (mol %)	52.6	58.4-59.5	60.7	59.6-61.4
isolation habitat	marine algae	marine biofilm	seawater	marine biofilm
Reference	(6)	(1-4, 16)	(5)	(3, 4, 16)

Table 4-2. Distinguishing characteristics of the *Epibacterium* species. Species: 1, *E. ulvae*; 2, *E. mobile*; 3, *E. multivorans*; 4, *E. scottomollicae*.

Characteristic	1	2	3	4
Facultatively anaerobic	ND	+	ND	-
Growth conditions				
≤ 5 ˚C	-	+	-	+
≥ 40 ˚C	-	+	-	+
< 1 % NaCl	-	+	-	-
> 10 % NaCl	-	-	-	+
Accumlation of poly-β-hydroxybutyrate	ND	-	-	+
Carbohydrate utilization				
L-arabinose	-	+	-	-
D-ribose	-	ND	+	ND
D-xylose	-	+	+	+
Alcohol utilization				
mannitol	+	+	+	-
sorbitol	-	+	+	ND
Amino acid utilization				
glycine	+	ND	-	ND
L-histidine	-	+	+	ND
Polar lipids				
phosphatidylethanolamine	-	ND	+	ND
unidentified phospholipids	-	ND	+	ND
Susceptibility to:				
gentamycin	-	-	ND	+
tetracycline	+	d	ND	-

Table 4-3. Antibiotic susceptibility in the *Epibacterium* species. Species: 1, *E. ulvae*; 2, *E. mobile*; 3, *E. scottomollicae*. No data available for *E. multivorans*. "+" indicates susceptibility to an antibiotic. "-" indicates resistance to an antibiotic.

Antibiotic	**1**	**2**	**3**
ampicillin	+	-	ND
cefoxitin	ND	+	+
chloramphenicol	+	+	ND
clindamycin	ND	-	-
erythromycin	ND	+	+
gentamycin	-	-	+
kanamycin	ND	-	ND
penicillin-G	ND	-	ND
rifampicin	ND	+	ND
spectinomycin	-	ND	ND
streptomycin	ND	+	+
tetracycline	+	d	-
trimethoprim	ND	-	-
vancomycin	ND	-	-
Reference	(6)	(2, 3)	(3)

Table 4-4. Fatty acids in the *Epibacterium* species. Species: 1, *E. ulvae*; 2, *E. mobile*; 3, *E. multivorans*; 4, *E. scottomollicae*. Values indicate the observed ranges for the percentages of total fatty acids in the cells. "—" indicates the fatty acid was not detected, "tr" indicates trace (<1.0 %), and "ND" indicates no data available.

Fatty acid	1	2	3	4
$C_{9:0}$	ND	ND	tr	ND
$C_{10:0}$	tr	—	ND	—
$C_{12:0}$	1.6 - 2.3	—	tr	tr
$C_{14:0}$	ND	ND	tr	ND
$C_{16:0}$	9.5 - 10.5	2.0 - 10.8	8.2	2.5
$C_{17:0}$	tr	tr	ND	ND
$C_{18:0}$	1.5 – 2.0	1.0 - 1.5	2.7	tr
$C_{17:1}$ *ω7c*	ND	tr	ND	1.0
$C_{18:0}$ iso	—	ND	—	ND
$C_{18:1}$ *ω6c*	ND	6.4 - 6.5	ND	ND
$C_{18:1}$ *ω7c*	71.0 - 76.0	52.5 - 74.9	70.9*	79.1
$C_{18:1}$ *ω9c*	ND	ND	—	ND
$C_{20:1}$ *ω7c*	ND	tr	ND	tr
$C_{18:1}$ 11-CH3	tr	—	ND	ND
$C_{18:1}$ *ω7c* 11-CH3	tr	1.2 - 12.2	5.3	2.5
$C_{19:0\ cy}$ *ω8c*	ND	—	ND	—
$C_{10:0}$ 3-OH	2.5 - 3.3	2.0 - 3.2	4.8	2.8
$C_{12:0}$ 3-OH	tr - 3.8	tr - 1.0	1.0	tr
$C_{12:1}$ 3-OH	—	ND	—	ND
$C_{16:0}$ 2-OH	tr - 1.5	tr - 13.5	3.8	4.3
$C_{18:0}$ 3-OH	ND	ND	—	ND
$C_{18:1}$ 2-OH	ND	1.1	ND	2.5
ECL 11.799	tr	3.0	ND	2.5
Summed feature 3†	ND	tr	ND	ND
Reference	(6)	(1, 2, 4)	(5)	(3, 4)

*: Measurements were performed on summed feature 8 (comprises $C_{18:1}$ *ω6c* and/or $C_{18:1}$ *ω7c*)

†: Summed feature 3 comprises iso-$C_{15:0}$ 2-OH and/or $C_{16:1}$ *ω7c*

Table 4-5. Genome sequences for the *Epibacterium* species. All genomes were downloaded from NCBI (https://www.ncbi.nlm.nih.gov). Unless noted, all genomes represent the type strain of the respective species.

Strain	Assembly level	Genome size (Mbp)	Number of PEG*	Number of REG†	Assembly gap length (bp)
E. mobile MBIC01146^T	Contig	4.72	4358	50	0
E. mobile F1926	Complete	4.83	4465	71	0
E. multivorans MD5^T	Scaffold	4.15	3870	61	10
E. scottomollicae LMG 24367^T	Scaffold	4.68	4410	54	174
E. ulvae U95^T	Contig	3.99	3850	54	0
E. sp. TM1040\	Complete	4.15	3839	79	0

Table 5 (continued)

Strain	Number of replicons	Number of scaffolds	Number of contigs	GenBank assembly
E. mobile MBIC01146^T	—	—	59	GCA_001681715
E. mobile F1926	5	—	—	GCA_000376545
E. multivorans MD5^T	—	41	42	GCA_900112515
E. scottomollicae LMG 24367^T	—	72	73	GCA_003003215
E. ulvae U95^T	—	—	30	GCA_900102795
E. sp. TM1040	3	—	—	GCA_000014065

*: Predicted protein-encoding genes (PEG)
†: Predicted RNA-encoding genes (REG)

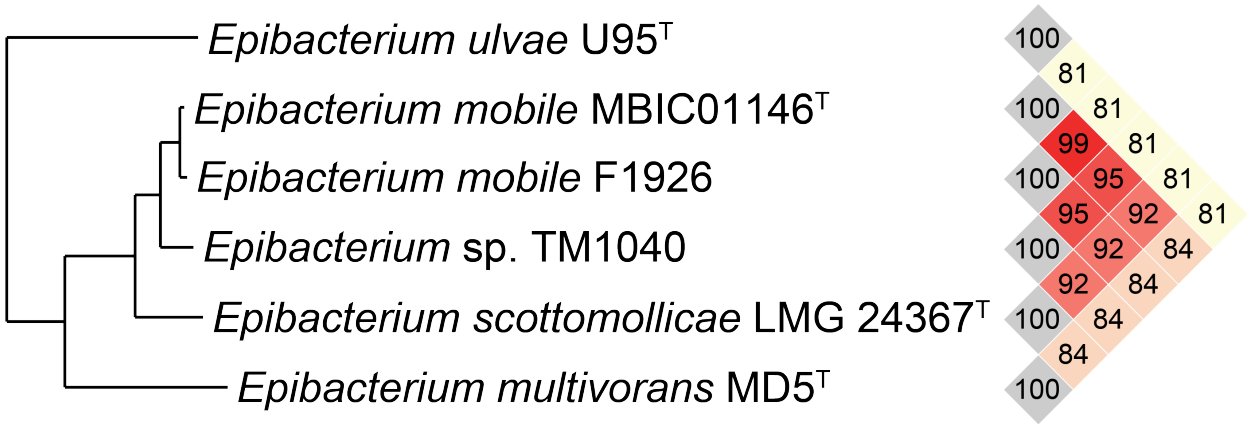

Figure 4-1. Heatmap of the average amino acid identity of the core genes (cAAI) for the *Epibacterium* species. cAAI values are shown in the grid on the right-hand side. A sub-tree from the maximum likelihood tree (**Fig. 2**) is shown on the left-hand side.

Table 4-6. Distinguishing characteristics of *Epibacterium* from other, closely related genera. Genera: 1, *Epibacterium*; 2, *Cribrihabitans*; 3, *Leisingera*; 4, *Phaeobacter*; 5, *Pseudophaeobacter*; 6, *Ruegeria*.

Characteristic	**1**	**2**	**3**	**4**	**5**	**6**
Polar flagellum(a)*	+	+	D	+	ND	-
Oxidase	+	-	+	+	+	+
API-ZYM†						
α-glucosidase	D	-	-	+	-	D
naphthol-AS-BI-phosphohydrolase	D	+	D	D	-	D
diphosphatidylglycerol‡	-	+	-	D	D	D

*: No data available for polar flagellation of *Leisingera methylohalidivorans*, *Pseudophaeobacter arcticus*, *Pseudophaeobacter leonis*, *Ruegeria denitrificans*, or *Ruegeria intermedia*.

†: No data available for API-ZYM tests of *Epibacterium ulvae*, *Phaeobacter porticola*, or *Ruegeria intermedia*.

‡: No data available for the presence of diphosphatidylglycerol in *Epibacterium mobile*, *Epibacterium scottomollicae*, *Leisingera aquimarina*, *Leisingera caerulea*, *Phaeobacter italicus*, *Ruegeria denitrificans*, or *Ruegeria litorea*.

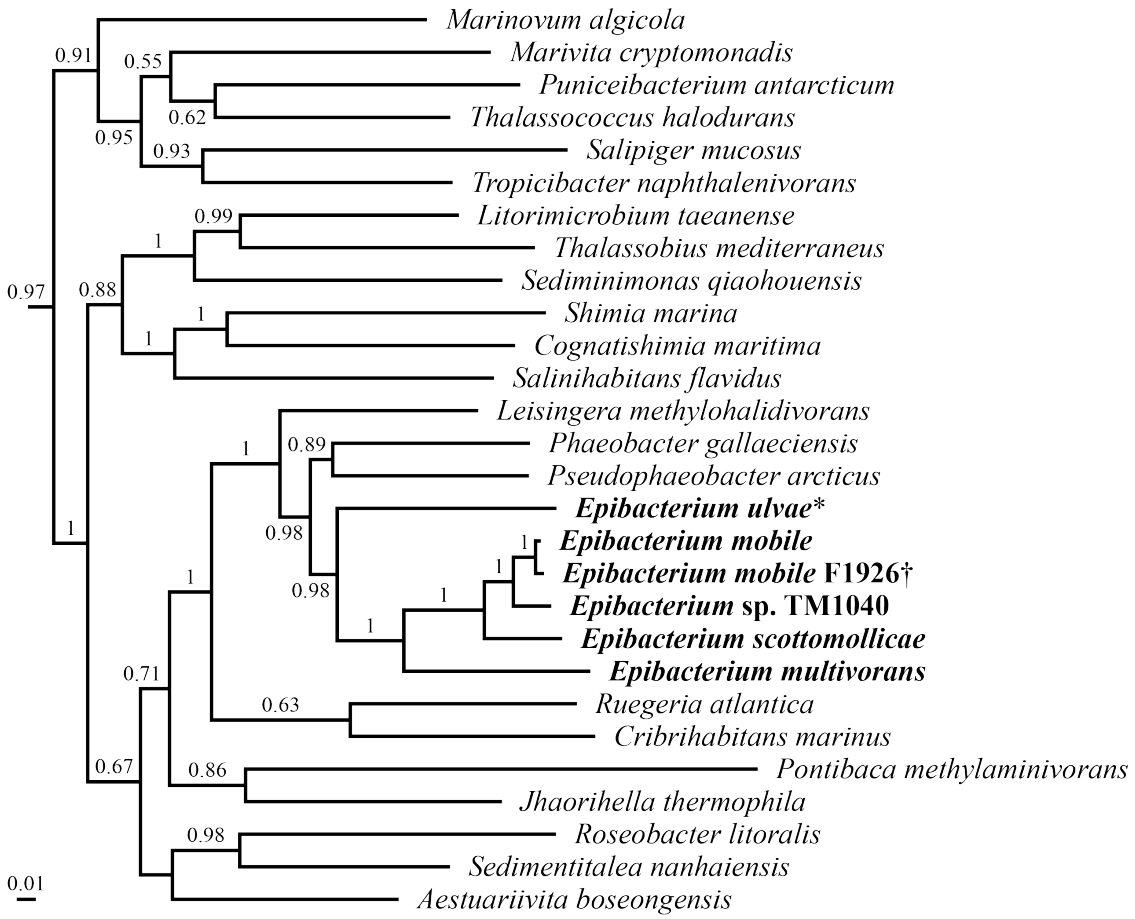

Figure 4-2. Maximum likelihood phylogeny of the *Epibacterium* species and its relatives. The tree was based on the concatenated, multiple alignment of 52 of the most conserved genes present in the whole-genome sequences examined by Wirth and Whitman (2018) with the addition of *Epibacterium mobile* F1926 (GCA_000376545) and the recently published genomes for *Cribrihabitans marinus* CZ-AM5^T (GCA_900109035), *Phaeobacter piscinae* 27-4^T (GCA_002407245), *Phaeobacter porticola* P97^T (GCA_001888185), *Primorskyibacter insulae* SSK3-2^T (GCA_900302505), *Puniceibacterium antarcticum* SM1211^T (GCA_002760615), *Ruegeria denitrificans* CECT 5091^T (GCA_001458295), *Ruegeria marisrubri* ZGT118^T (GCA_001507595), *Ruegeria mediterranea* M15Ø_3 (GCA_900302455), and *Ruegeria profundi* ZGT108^T (GCA_001507545). The tree was constructed using IQTree version 1.6.3 with the best model (LG+F+I+G4) identified by Bayesian information criterion and 100 bootstrap replicates (17, 18). The tree was rooted on the genus "*Ketogulonicigenium*", and the following genera were pruned from the tree: *Cognatiyoonia*, *Flavimaricola*, *Limimaricola*, *Loktanella*, "*Ketogulonicigenium*", *Pseudaestuariivita*, *Pseudoctadecabacter*, and *Wenxinia*. For the remaining genera, all species except for the type species were pruned from the tree with the exception of the members of *Epibacterium*. Bolded taxa indicate the current members of the genus *Epibacterium*. Unless indicated, all genomic sequences were taken from the type strain of their respective species. The numbers on the branches indicate the fraction of bootstrap support after 100 replicates. The scale bar indicates the number of substitutions per site.

*: *E. ulvae* is the type species of *Epibacterium*
†: *E. mobile* F1926 is not the type strain

CHAPTER 5

AN EFFICIENT METHOD FOR SYNTHESIZING DIMETHYLSULFONIO-^{34}*S*-PROPIONATE HYDROCHLORIDE FROM $^{34}S_8$[4]

[4] Wirth, J.S. and W.B. Whitman. 2019. *Journal of Labeled Compounds and Radiopharmaceuticals*. 62:52-58.
Reprinted here with permission of the publisher.

Abstract

Dimethylsulfoniopropionate (DMSP, (2-carboxyethyl)dimethylsulfonium) is a highly abundant compound in marine environments. As a precursor to the climatically active gas, dimethylsulfide (DMS), DMSP connects the marine and terrestrial sulfur cycles. However, the fate of DMSP in microbial biomass is not well understood as only a few studies have performed isotopic labeling experiments. A previously published method synthesized ^{34}S-labeled DMSP from $^{34}S_8$, but the efficiency was only 26 % and required five separate reactions, expensive reagents, and purification of the products of each reaction. In this study, a method of synthesizing ^{34}S-labeled DMSP from $^{34}S_8$ is described. Improvements include elemental steps, inexpensive reagents, purification of only one intermediate, and less time to complete. The efficiency of this method is 65 % and results in pure DMSP with >98 % isotope enrichment as determined by ^{1}H-NMR and GC-MS.

Introduction

Dimethylsulfoniopropionate (**4**, DMSP, (2-carboxyethyl)dimethylsulfonium) is a highly abundant compound in marine surface waters. In the North Sea, the concentration of DMSP cycles seasonally from micromolar levels in the summer to picomolar levels in the spring and fall (1, 2). The majority of marine DMSP comes from halophytic plants and algae, where it is believed to regulate osmotic pressure in addition to antioxidant, predator deterrent, and/or cryoprotectant functions (2). There is also evidence that at least 0.5 % of marine bacteria are capable of producing DMSP, but this contribution to global sulfur cycle is not yet fully understood (3). Concurrent with its role as an osmoregulatory molecule, plants that produce the most DMSP are generally halotolerant and of marine origin, with sugarcane being the only non-marine exception. During ^{35}S-labeling studies with bacterial cells, approximately 15 % of added DMSP accumulated intracellularly, but was not metabolized (2). Molar levels of intracellular DMSP have been observed in some organisms, and it is estimated that up to 10 % of the total fixed carbon in the oceans is in the form of DMSP (4). Furthermore, DMSP released from phytoplankton blooms can satisfy up to 15 % of the microbial carbon demand and 100 % of the microbial sulfur demand (4). DMSP is the precursor for the majority of atmospheric dimethylsulfide (**3**, DMS), which is a climatically-active gas and connects the marine and terrestrial sulfur cycles (5). It was previously believed that H_2S was responsible for the transfer of sulfur between marine and terrestrial environments, but the necessary atmospheric concentrations were never detected and the surface layers of the ocean are too oxidizing to sustain equilibrium with the atmosphere (5). However, the concentration of DMS in marine surface layers is sufficiently high, and DMS is resistant to oxidation in the lower atmosphere (5). Its photooxidation in the upper atmosphere produces sulfur species that can be transferred to

terrestrial environments via rain and promote the formation of "cloud-condensation nuclei", resulting in an increased albedo effect and global cooling (2, 4, 6, 7).

Bacterial catabolism of DMSP proceeds through one of two known pathways. It can either undergo cleavage to form DMS and either acrylic acid or 3-hydroxypropionate, or it can undergo demethylation to form methylmercaptopropionic acid, which can further be broken down into methanethiol, carbon dioxide, and acetaldehyde (2). In both cases, the DMS and methanethiol can be metabolized further and assimilated into biomass. Because very few studies have performed isotope-labeling experiments with DMSP, the fate of DMSP in microbial biomass is not well understood (8-11). DMSP hydrochloride can be easily synthesized via a Michael addition of DMS to acrylic acid under acidic conditions in methylene chloride (12). Unfortunately, DMS enriched with a sulfur isotope is not commercially available, and the only commercially available form of isotopically-labeled sulfur suitable for conversion to DMS is elemental sulfur (**1**, S_8). Thus, incorporation of a specific sulfur isotope requires a synthetic pathway to convert S_8 to DMSP.

Experimental

General. Unless stated otherwise, all chemicals were purchased from commercial sources with ACS-grade purity or higher and were used without further purification. Metallic sodium was provided by Dr. Robert Phillips (Department of Chemistry, University of Georgia). $^{34}S_8$ and $I^{13}CH_3$ were purchased from Sigma-Aldrich (St. Louis, MO) with 99 % atom enrichment. NH_3 (*l*) was generated by dripping 30 % NH_4OH (*aq*) onto NaOH pellets, drying the NH_3 (*g*) by passing it over KOH pellets, and condensing the NH_3 (*g*) on a cold-finger filled with dry-ice and ethanol. Dry HCl (*g*) was generated by dripping concentrated HCl (*aq*) into concentrated H_2SO_4 and bubbling the resulting HCl (*g*) through concentrated H_2SO_4. All glassware used in the experiments was acid washed in 3 % HCl (*aq*) for 24 hours to remove trace

contaminants and then baked at 180 ˚C for 24 hours to degrade any remaining organic compounds.

Because of the price of $^{34}S_8$, S_8 was used to determine the efficiency of reaction (I), Na_2S was used to determine the combined efficiency of reactions (II) and (III), and DMS was used to determine the efficiency of reaction (III) (Scheme 5-1). Because of the presence of excess Na and the potential for oxidation of Na_2S, a modified version of the methylene blue assay was used to calculate the amount of S^{2-} synthesized from reaction (I) and the amount of Na_2S used in reaction (II) (Scheme 5-1). The methylene blue assays were performed twice on a 10^{-5} dilution of each solution of Na_2S (13-16). All reported efficiencies are relative to the amount of sulfur used.

DMSP was analyzed via ^{1}H-NMR by Dr. Dongtao Cui (Chemical Sciences Magnetic Resonance Facility, University of Georgia). DMSP (5 mg) was dissolved in 600 µL of D_2O and NMR spectra were obtained on a Bruker AVANCE III HD NMR spectrometer at a frequency of 400 MHz. NMR spectra were aligned by shifting the D_2O peak to the reference point of 4.790 ppm (17).

DMS formed from DMSP by alkaline hydrolysis was analyzed via GC-MS at the Proteomics and Mass Spectrometry Facility (University of Georgia) with a modified version of the protocol described by Niki *et al*. (2004) (18). A 5 mL serum vial was charged with **4**, **4A**, or **4B** (6 mg) dissolved in 100 µL water and crimp-sealed with a teflon-coated butyl rubber stopper, and the headspace was flushed with N_2 for 10 minutes. A syringe was used to add 100 µL of 4 M NaOH (*aq*), and the vial was incubated at 30 ˚C for 1 hour to convert **4**, **4A**, or **4B** to equimolar amounts of **3**, **3A**, or **3B**, respectively (19). 500 µL of the headspace was applied to the injection port (heated at 150 ˚C) of the GC (HP-5890, Agilent) with a splitless duration of 2.75 minutes and an EC-5 (0.25 mm i.d. × 30 m × 0.25 µm film thickness, Alltech) column. The carrier gas was He with a head pressure capped at 12 psi. The GC oven was programmed to rise

from 50 ˚C to 150 ˚C at a rate of 15 ˚C min^{-1}. **3**, **3A**, and **3B** were detected by a mass spectrometer (HP-5971A, Agilent) with an EI ion source running in scan mode (monitored *m/z* range was 45–67) with 12 scans per second and a detector temperature of 150 ˚C.

(2-Carboxyethyl)dimethylsulfonium-^{34}*S* chloride. $Na_2{}^{34}S$ (**2A**) was synthesized as previously described (20, 21). A 10 mL serum vial containing a teflon-coated stir-bar was charged with $^{34}S_8$ (**1A**) (0.1071 g, 394 µmol) and freshly-shaved, hexane-washed Na (0.1742 g, 7.577 mmol), flushed with N_2 for 1 hour, and then incubated at -78 ˚C under a slow stream of nitrogen for the duration of the reaction. The vial was charged with approximately 8 mL of NH_3 (*l*), incubated with stirring until no yellow color could be seen, and then stirred for an additional 30 minutes. The vial was then flushed with a steady stream of N_2 until all NH_3 had evaporated, leaving behind a white and silvery powder composed of excess Na and **2A**. Dimethylsulfide-^{34}*S* (**3A**) was synthesized from the resulting **2A** as previously described (22). The vial containing **2A** was crimp-sealed with a teflon-coated butyl rubber stopper, and its headspace was replaced with N_2 and pressurized to 10 psi. The contents of the vial were dissolved in 3 mL of an anaerobic stock solution of 1.5 M NaOH (*aq*), and incubated on ice for 5 minutes. A glass syringe was used to add ICH_3 (470 µL, 1.0716 g, 7.550 mmol) to the vial, and the vial was incubated at 4 ˚C with vigorous stirring for 4 hours. To stop the reaction, a syringe was used to add 2 mL of 3 M $Na_2S_2O_3$ (*aq*), and the vial was incubated at 4 ˚C with vigorous stirring for 30 minutes. The vial was chilled to -196 ˚C in N_2 (*l*) and connected to a receiving flask. **3A** was distilled from the solution by cooling the receiving flask in N_2 (*l*) while warming the vial to 40 ˚C for 2.5 hours. (2-carboxyethyl)dimethylsulfonium-^{34}*S* (**4A**) was synthesized as described previously (12). The receiving flask containing distilled **3A** was immediately charged with -80 ˚C CH_2Cl_2 (12 mL). The receiving flask was removed from the N_2 (*l*) and was immediately charged with acrylic acid (260 µL, 0.2733 g, 3.792 mmol). Immediately afterwards, the solution was stirred vigorously at

room temperature for 30 minutes while bubbling in dry HCl (*g*). The solution was dried at 50 ˚C under a vacuum for 2.5 hrs. The resulting white solids were washed with CH_2Cl_2 to yield white crystals composed of pure **4A** (0.3551 g, 2.0578 mmol, 65.3 %).

(2-Carboxyethyl)di(methyl-^{13}*C*)sulfonium-^{34}*S* chloride. $Na_2{}^{34}S$ (**2A**) was synthesized from $^{34}S_8$ (**1A**) (0.1005 g, 370 µmol) and freshly-shaved, hexane-washed Na (0.1564 g, 6.803 mmol) using the methods described above. Di(methyl-^{13}*C*)sulfide-^{34}*S* (**3B**) was synthesized from the resulting **2A** and $I^{13}CH_3$ (450 µL, 1.0305 g, 7.210 mmol) using the method described above. (2-carboxyethyl)di(methyl-^{13}*C*)sulfonium-^{34}*S* (**4B**) was synthesized from the resulting **3B** and acrylic acid (250 µL, 0.2628 g, 3.646 mmol) using the method described above. This yielded white crystals composed of pure **4B** (0.3307 g, 1.895 mmol, 64.0 %).

Results and Discussion

A previous study employed a strategy for the synthesis of **4A** that avoided the production of volatile intermediates, but this approach required five separate reactions with purification of each intermediate and only produced an overall yield of 26 % (Scheme 5-2) (23). In the approach utilized here, the loss of volatile intermediates, namely H_2S (from aqueous **2**, **2A**, **2B**) and DMS (**3**, **3A**, **3B**), were minimized by using a combination gas-tight reaction vessels and careful control of the temperature and pH. Loss of H_2S was reduced by using concentrated sodium hydroxide solutions (24). Loss of DMS was reduced with low temperatures as it is a liquid below 38 ˚C and a solid below -98 ˚C. By taking advantage of these facts, a new method of producing **4A** was developed (Schemes 5-1 and 5-3). However, because $^{34}S_8$ (**1A**) is quite expensive, the protocol was first optimized using S_8 (**1**), and the reactions were repeated multiple times to ensure repeatability. **1** was first reduced to **2** via a Birch reduction with Na in NH_3 (*l*) (20, 21). Subsequent evaporation of the NH_3 yielded a white powder primarily composed of anhydrous **2** with an efficiency of 78.0 ± 7.1 %. The conversion of **2** to **3** was accomplished by the

nucleophilic attack of S^{2-} on the methyl group of ICH_3 under anaerobic and basic conditions, and the resulting **3** was subsequently purified via distillation (22). Finally, **3** was converted to **4** via Michael addition to acrylic acid in CH_2Cl_2 with an efficiency of 106.2 ± 13.7 % (12). The efficiency of the conversion and purification of **2** to **3** was not determined because measurements of the amount of **3** required large dilutions of the headspace, which proved to be inaccurate (data not shown). However, the efficiency of the conversion of **2** to **4** was 75.5 ± 7.4 %.

Because the boiling point of ICH_3 (43 ˚C) is very close to that of DMS (38 ˚C), there was a potential for unreacted ICH_3 to co-distill, which would lower the purity of the final product. However, $S_2O_3^{2-}$ is capable of converting ICH_3 to non-volatile compounds (25). Thus, $Na_2S_2O_3$ was added in excess to ensure that all unreacted ICH_3 was consumed prior to distillation.

To verify the purity of compounds **4A** and **4B**, ^{1}H-NMR was performed. The spectrum of **4A** was nearly identical to that of a **4** standard (Fig. 5-1). However, the spectrum for **4B** was very different. The triplet at approximately 3.5 ppm was split into a triplet of triplets due to the isotopic coupling with the methyl-^{13}C atoms. The isotopic coupling also split the singlet indicative of the methyl protons into a doublet of doublets (Fig. 5-1C). This complex splitting pattern has been observed in [^{13}C]DMSO [((methyl-^{13}C)sulfinyl)methane-^{13}C] and is due to the $AX_3A'X'_3$ spin system (22). Based on the isotopic coupling observed in the ^{1}H-NMR, there was ≥99 % enrichment of the methyl-^{13}C atoms in **4B**. Furthermore, ^{1}H-NMR showed that the resulting compounds were contaminated with <1 % 3-hydroxypropionate.

In order to determine the enrichment of the ^{34}S atoms, GC-MS analyses were performed on DMS formed from DMSP. Alkaline hydrolysis converted **4**, **4A**, and **4B** into equimolar amounts of **3**, **3A**, and **3B**, respectively (19), which was then analyzed via GC-MS. The relative abundance of the peaks at *m/z* 62, 64, and 66 were examined for **4**, **4A**, and **4B**, respectively (Fig. 5-2, 5-3, 5-4). For **4A**, the ratio of the *m/z* values at 62 and 64 indicated that there was a ≥99 %

enrichment of the ^{34}S atom (Fig. 5-3). For **4B**, the peak at *m/z* = 66 could not be directly compared to the peak at *m/z* = 62 because the three minor peaks corresponding to *m/z* = 57-59 (Fig. 5-2) were shifted to 61-63, respectively (Fig. 5-4). However, the peak at *m/z* = 66 showed a 98.9 % relative enrichment as compared to the peak at *m/z* = 64. This value agreed with the value determined by integrating the peaks in the ^{1}H-NMR spectrum, which qualitatively suggested that $^{13}CH_3$ was enriched by ≥99 % in **4B** as compared to $^{12}CH_3$ (Fig. 5-1C). Taken together with the high atom enrichment of **4A**, these data indicated that it was very likely that there was a >98 % enrichment of the ^{13}C- and ^{34}S-atoms in **4B** (Fig. 5-4).

Because this method uses ICH_3 and acrylic acid, it allows for isotopic labeling at one or more of the atoms in **4**. Acrylic-1-^{13}C acid, acrylic-$^{13}C_3$ acid, $I^{13}CH_3$, and ICD_3 are commercially available and can be used in place of unlabeled acrylic acid or ICH_3, respectively. Supporting this claim, **4B** was synthesized from **1A** and $I^{13}CH_3$ with an overall yield of 64.0 %. This indicated that the use of ^{13}C-labeled reactants has little effect on the overall efficiency and supports the claim that this synthetic method facilitates complex labeling experiments in DMSP-utilizing organisms. Furthermore, the products of reactions (I) and/or (II) (Scheme 5-3) could be applied in other syntheses to generate a variety of ^{34}S-labeled compounds.

Conclusions

A straight-forward method for the synthesis of a variety of dimethylsulfoniopropionate hydrochloride [(2-carboxyethyl)dimethylsulfonium hydochloride] isotopomers was developed and possessed a 250 % increase in efficiency as compared to the previously published method (23). This method is simpler, uses fewer purification steps, uses fewer and less expensive reagents, and can be completed within two days. The resulting DMSP is ≥99 % pure and possesses >98 % atom enrichment. Furthermore, the simplicity of this method allows for its adaptation to produce other ^{34}S-labeled compounds.

Funding, acknowledgements, and conflicts of interest

Funding. This research was supported in part by a NSF Dimensions of Biodiversity grant OCE-1342694.

Acknowledgements. Dr. Robert Phillips (Department of Chemistry, University of Georgia) generously provided the metallic sodium used in the experiment and demonstrated how to produce liquid ammonia from ammonium hydroxide. The specialty glassware needed for performing the Birch reduction was produced by Kyle Meyer (Chemistry Glass Shop, University of Georgia). ^{1}H-NMR spectra were obtained by Dr. Dongtao Cui (Chemical Sciences Magnetic Resonance Facility, University of Georgia), who also helped in the interpretation. Dr. Dennis R. Phillips (Proteomics and Mass Spectrometry Facility, University of Georgia) provided access to a GC-MS and helped optimize the GC-MS method.

Conflicts of Interest. There are no conflicts of interest to declare.

References:

1. van Duyl FC, Gieskes WWC, Kop AJ, Lewis WE. 1998. Biological control of short-term variations in the concentration of DMSP and DMS during a *Phaeocystis* spring bloom. Journal of Sea Research 40:221-231.
2. Reisch CR, Moran MA, Whitman WB. 2011. Bacterial catabolism of dimethylsulfoniopropionate (DMSP). Frontiers in Microbiology 2:172.
3. Curson ARJ, Liu J, Martinez AB, Green RT, Chan YH, Carrion O, Williams BT, Zhang SH, Yang GP, Page PCB, Zhang XH, Todd JD. 2017. Dimethylsulfoniopropionate biosynthesis in marine bacteria and identification of the key gene in this process. Nature Microbiology 2:9.

4. Yoch DC. 2002. Dimethylsulfoniopropionate: its sources, role in the marine food web, and biological degradation to dimethylsulfide. Applied and Environmental Microbiology 68:5804-5815.
5. Lovelock JE, Maggs RJ, Rasmussen RA. 1972. Atmospheric dimethyl sulphide and the natural sulphur cycle. Nature 237:452.
6. Hatakeyama S, Okuda M, Akimoto H. 1982. Formation of sulfur dioxide and methanesulfonic acid in the photooxidation of dimethyl sulfide in the air. Geophysical Research Letters 9:583-586.
7. Charlson RJ, Lovelock JE, Andreae MO, Warren SG. 1987. Oceanic phytoplankton, atmospheric sulphur, cloud albedo and climate. Nature 326:655.
8. Reisch CR, Crabb WM, Gifford SM, Teng Q, Stoudemayer MJ, Moran MA, Whitman WB. 2013. Metabolism of dimethylsulphoniopropionate by *Ruegeria pomeroyi* DSS-3. Molecular Microbiology 89:774-91.
9. Todd JD, Curson ARJ, Nikolaidou-Katsaraidou N, Brearley CA, Watmough NJ, Chan YH, Page PCB, Sun L, Johnston AWB. 2010. Molecular dissection of bacterial acrylate catabolism - unexpected links with dimethylsulfoniopropionate catabolism and dimethyl sulfide production. Environmental Microbiology 12:327-343.
10. Saló V, Simó R, Vila-Costa M, Calbet A. 2009. Sulfur assimilation by *Oxyrrhis marina* feeding on a ^{35}S-DMSP-labelled prey. Environmental Microbiology 11:3063-3072.
11. Ruiz-González C, Galí M, Sintes E, Herndl GJ, Gasol JM, Simó R. 2012. Sunlight effects on the osmotrophic uptake of DMSP-sulfur and leucine by polar phytoplankton. Plos One 7:14.

12. Chambers ST, Kunin CM, Miller D, Hamada A. 1987. Dimethylthetin can substitute for glycine betaine as an osmoprotectant molecule for *Escherichia coli*. Journal of Bacteriology 169:4845-7.

13. Long F. 2017. Aspects of sulfur metabolism of methane-producing archaeon *Methanococcus maripaludis*. PhD. University of Georgia, Athens, Georgia.

14. Huber R, Langworthy TA, König H, Thomm M, Woese CR, Sleytr W, Stetter KO. 1986. *Thermotoga maritima* sp. nov. represents a new genus of unique extremely thermophilic eubacteria growing up to 90°C. Archives of Microbiology 144:324-333.

15. Windberger E, Huber R, Trincone A, Fricke H, Stetter KO. 1989. *Thermotoga thermarum* sp. nov. and *Thermotoga neapolitana* occurring in African continental solfataric springs. Archives of Microbiology 151:506-512.

16. Finster K, Liesack W, Tindall BJ. 1997. *Sulfurospirillum arcachonense* sp. nov., a new microaerophilic sulfur-reducing bacterium. International Journal of Systematic Bacteriology 47:1212-7.

17. Gottlieb HE, Kotlyar V, Nudelman A. 1997. NMR chemical shifts of common laboratory solvents as trace impurities. Journal of Organic Chemistry 62:7512-7515.

18. Niki T, Fujinaga T, Watanabe MF, Kinoshita J. 2004. Simple determination of dimethylsulfide (DMS) and dimethylsulfoniopropionate (DMSP) using solid-phase microextraction and gas chromatography-mass spectrometry. Journal of Oceanography 60:913-917.

19. Reisch CR, Moran MA, Whitman WB. 2008. Dimethylsulfoniopropionate-dependent demethylase (DmdA) from *Pelagibacter ubique* and *Silicibacter pomeroyi*. Journal of Bacteriology 190:8018-8024.

20. Fehér F. 1963. Sulfur, selenium, tellurium, p 358-360. *In* Brauer G, Riley RF (ed), Handbook of Preparative Inorganic Chemistry, 2 ed, vol 1. Academic Press, New York.

21. Bonneau PR, Wiley JB, Kaner RB. 2007. Metathetical precursor route to molybdenum disulfide, p 33-37, Inorganic Syntheses, vol 30.

22. Beerli R, Borschberg H-J. 1991. Preparation of [$^{13}C_2$]DMSO. Journal of Labelled Compounds and Radiopharmaceuticals 29:957-961.

23. Brock NL, Menke M, Klapschinski TA, Dickschat JS. 2014. Marine bacteria from the *Roseobacter* clade produce sulfur volatiles via amino acid and dimethylsulfoniopropionate catabolism. Organic & Biomolecular Chemistry 12:4318-23.

24. Xia J, Pérez-Salado Kamps Á, Rumpf B, Maurer G. 2000. Solubility of hydrogen sulfide in aqueous solutions of single strong electrolytes sodium nitrate, ammonium nitrate, and sodium hydroxide at temperatures from 313 to 393 K and total pressures up to 10 MPa. Fluid Phase Equilibria 167:263-284.

25. Wang Q, Gan J, Papiernik SK, Yates SR. 2000. Transformation and detoxification of halogenated fumigants by ammonium thiosulfate. Environmental Science & Technology 34:3717-3721.

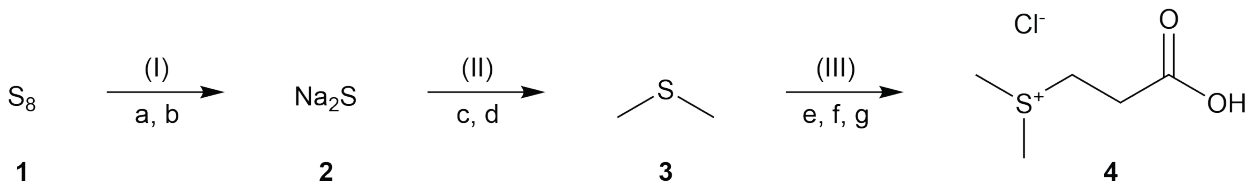

Scheme 5-1. Synthesis of **4**. Reagents: a, Na; b, NH_3 (*l*); c, ICH_3; d, NaOH (*aq*); e, acrylic acid; f, CH_2Cl_2; g, HCl (*g*).

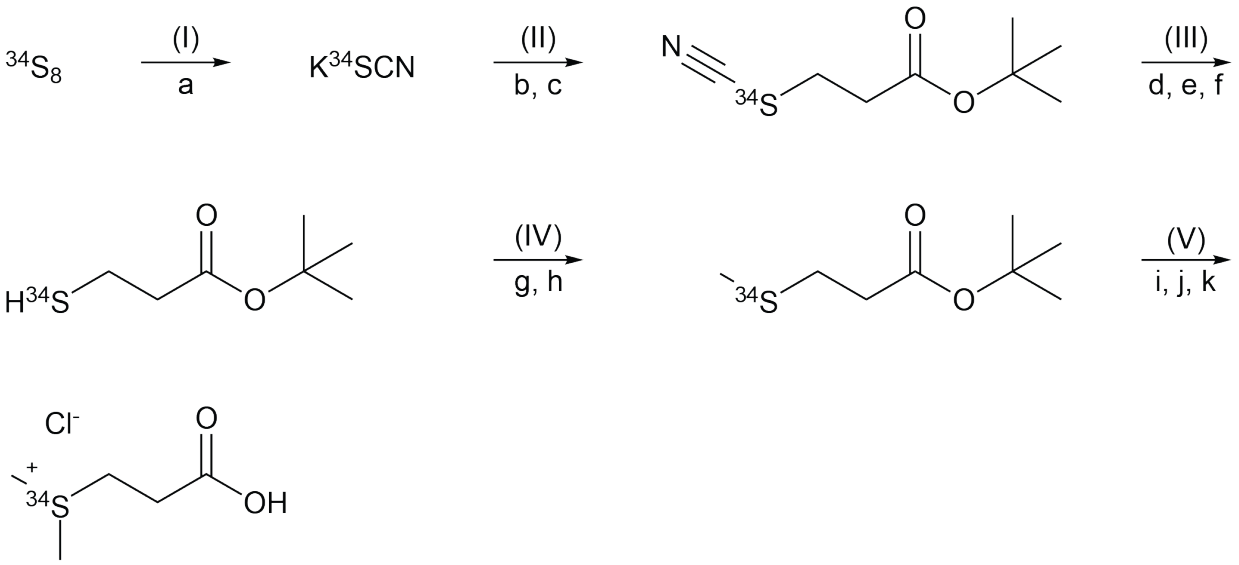

Scheme 5-2. Published method for the synthesis of **4A** (23). Reported efficiencies: reaction (I), 99 %; reaction (II), 92 %; reaction (III), 87 %; reaction (IV), 63 %; reaction (V), 51 %. Reagents: a, KCN (*aq*); b, acetonitrile; c, *tert*-butyl 3-bromopropionate; d, H_2O; e, THF; f, SmI_2; g, KOH in methanol; h, ICH_3; i, nitromethane; j, trimethyloxonium tetrafluoroborate; k, trifluoroacetic acid. The products of reactions (II), (III) and (IV) were purified by TLC. The product of reaction (V) was purified with ion-exchange chromatography.

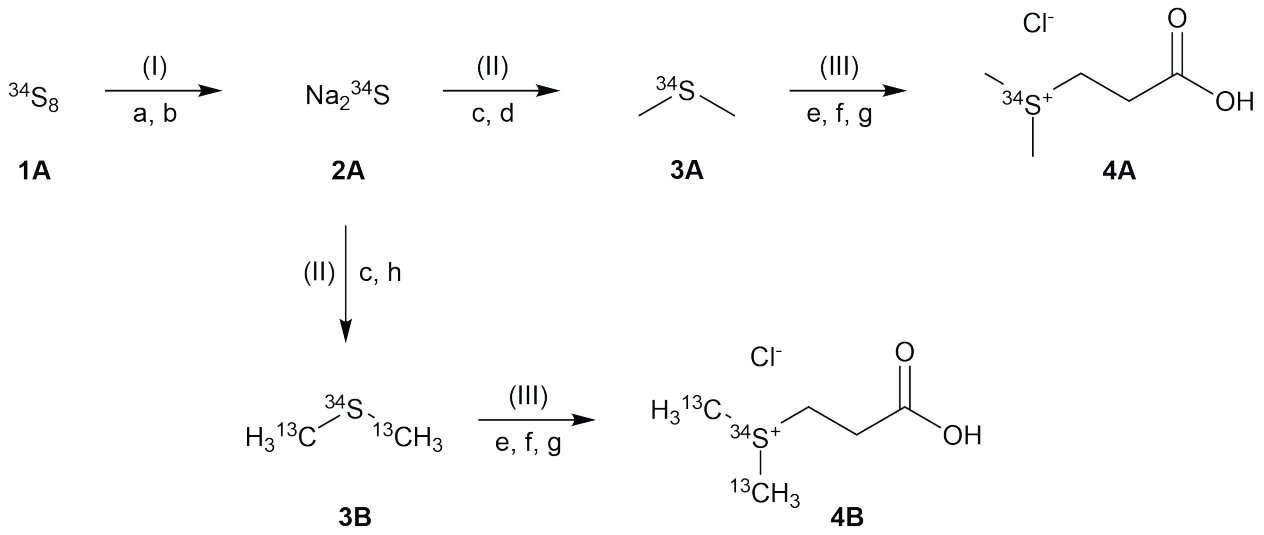

Scheme 5-3. Synthesis of **4A** and **4B**. Reagents: a, Na; b, NH_3 (*l*); c, ICH_3; d, NaOH (*aq*); e, acrylic acid; f, CH_2Cl_2; g, HCl (*g*), h, $I^{13}CH_3$.

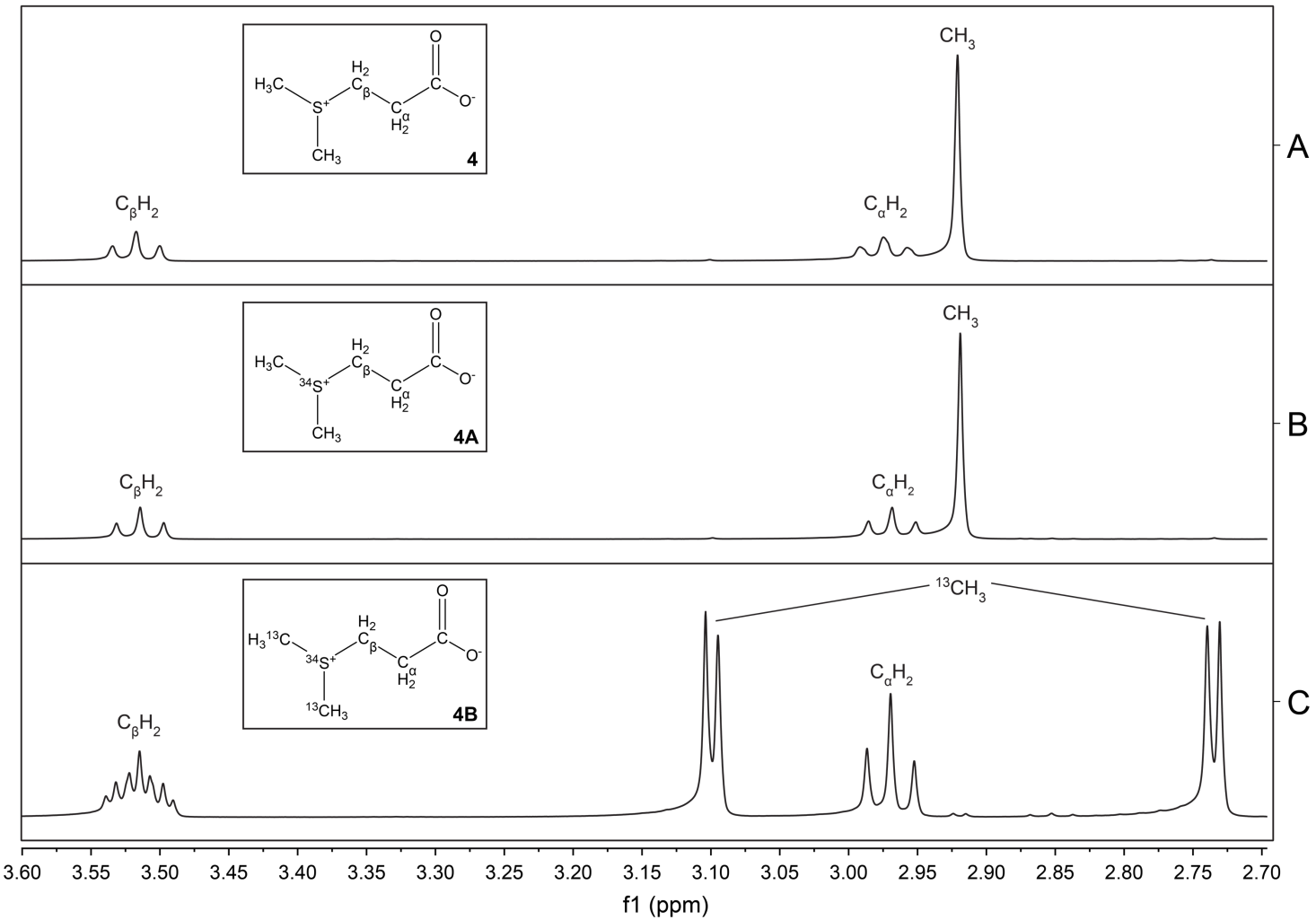

Figure 5-1. ^{1}H-NMR spectra. All spectra have been aligned by shifting the D_2O peak to 4.790 ppm (17). Peak heights have been adjusted for clarity. The molecule corresponding to each spectrum is shown inside the box. Peaks have been labeled with their corresponding atoms. (A) ^{1}H-NMR spectrum of **4** (400 MHz, D_2O). ^{1}H-NMR δ 3.52 (t, 2H, $C_\beta H_2$, J = 6.9 Hz), δ 2.98 (t, 2H, $C_\alpha H_2$, J = 6.9 Hz), δ 2.92 (s, 6H, CH_3). (B) ^{1}H-NMR spectrum of **4A** (400 MHz, D_2O). ^{1}H-NMR δ 3.51 (t, 2H, $C_\beta H_2$, J = 6.9 Hz), δ 2.97 (t, 2H, $C_\alpha H_2$, J = 6.9 Hz), δ 2.92 (s, 3H). (C) ^{1}H-NMR spectrum of **4B**. ^{1}H-NMR δ 3.51 (tt, 2H, $C_\beta H_2$, J = 6.8 Hz, 2.9 Hz), δ 2.97 (t, 2H, $C_\alpha H_2$, J = 6.9 Hz), δ 2.92 (dd, 6H, $^{13}CH_3$, J = 145.7 Hz, 3.6 Hz).

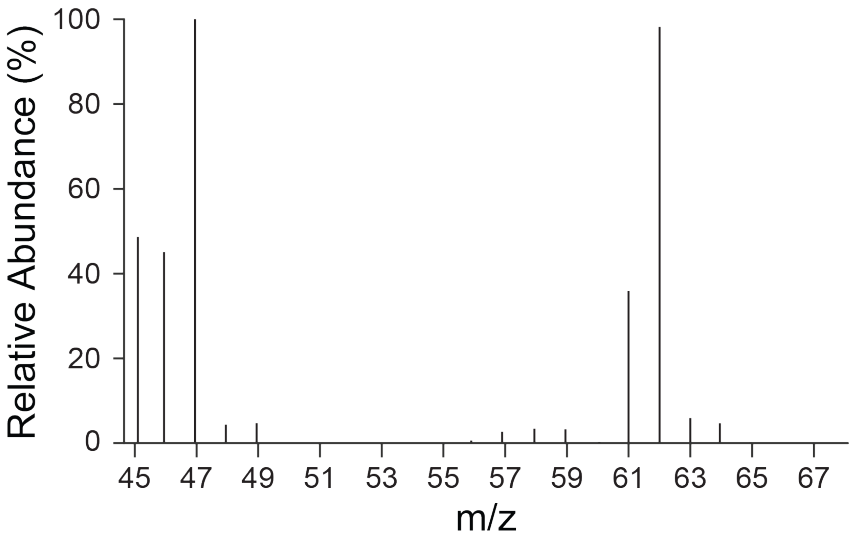

m/z	Intensity	Relative
45.10	2729515	48.64
45.95	2527357	45.03
46.95	5612041	100.00
47.95	244298	4.35
48.95	262760	4.68
55.90	34217	0.61
56.90	151226	2.69
57.95	191645	3.41
58.95	181407	3.23
60.05	15372	0.27
61.00	2013908	35.89
62.00	5510967	98.20
63.00	330274	5.89
63.95	260473	4.64
64.95	9010	0.16

Figure 5-2. GC-MS spectrum of dimethylsulfide produced by the alkaline hydrolysis of **4**. Peaks with less than 0.1 % relative abundance were omitted from the table.

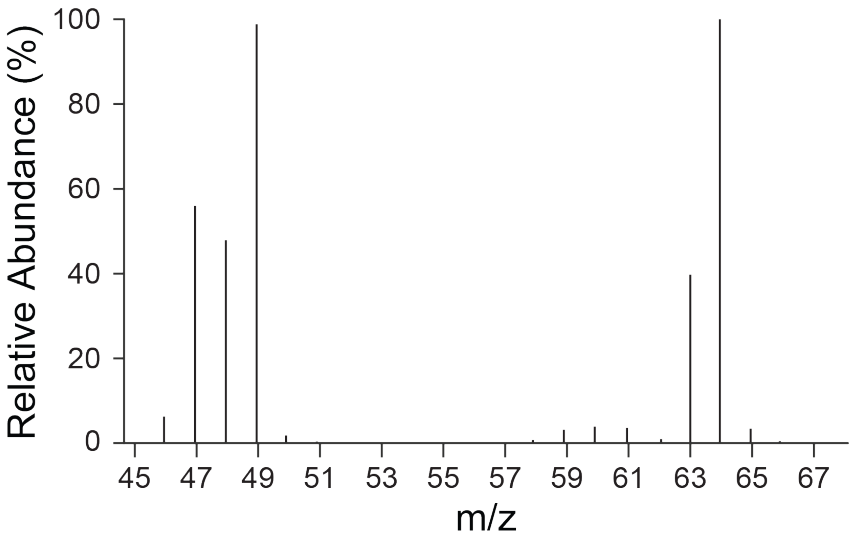

m/z	Intensity	Relative
45.95	325631	6.23
46.95	2924768	55.98
47.95	2501316	47.88
48.95	5162289	98.81
49.90	93377	1.79
50.90	19647	0.38
57.90	37487	0.72
58.90	164444	3.15
59.90	204001	3.90
60.95	187106	3.58
62.05	49390	0.95
63.00	2078325	39.78
63.95	5224674	100.00
64.95	179914	3.44
65.90	21834	0.42

Figure 5-3. GC-MS spectrum of dimethylsulfide produced by the alkaline hydrolysis of **4A**. Peaks with less than 0.1 % relative abundance were omitted from the table.

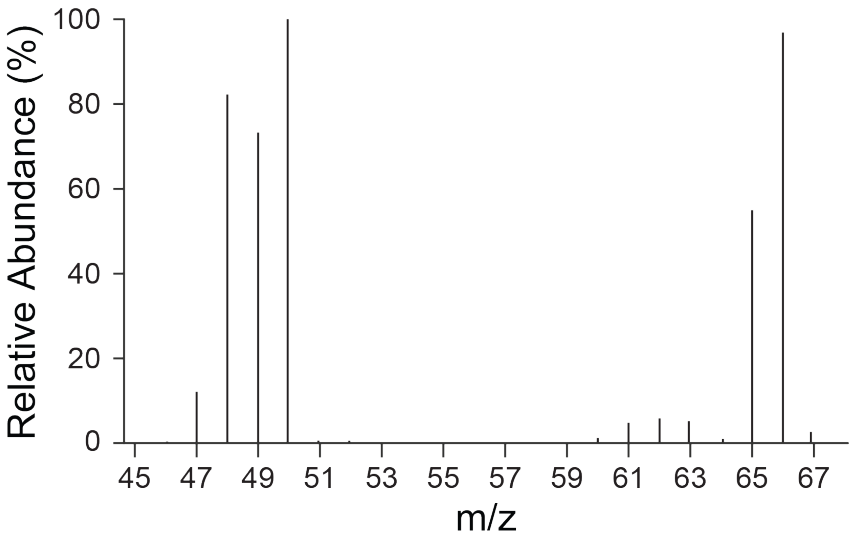

m/z	Intensity	Relative
46.05	17956	0.34
47.00	638249	12.10
48.00	4338070	82.25
49.00	3864464	73.27
49.95	5274039	100.00
50.95	30698	0.58
51.95	28416	0.54
60.00	62569	1.19
61.00	252671	4.79
62.00	307792	5.84
62.95	273197	5.18
64.05	52790	1.00
65.00	2896262	54.92
66.00	5109027	96.87
66.90	137835	2.61

Figure 5-4. GC-MS spectrum of dimethylsulfide produced by the alkaline hydrolysis of **4B**. Peaks with less than 0.1 % relative abundance were omitted from the table.

CHAPTER 6

BIOSYNTHESIS OF CYSTEINE AND METHIONINE FROM DIMETHYLSULFONIOPROPIONATE IN *RUEGERIA POMEROYI* DSS-3[5]

[5] Wirth, J.S., Wang, T., and W.B. Whitman. 2018. To be submitted to *Molecular Microbiology*.

Abstract

Dimethylsulfoniopropionate (DMSP) is abundant in marine environments and acts as an important source of reduced carbon and sulfur for marine bacteria. Previous research has shown that the production of methanethiol is required to synthesize methionine from DMSP. These findings led to the hypothesis that the majority of methionine synthesized from DMSP is accomplished via the direct capture of methanethiol and a lesser fraction is synthesized from the random reassembly of sulfide and methyl-tetrahydrofolate. In this study, we demonstrate that only one-third of methionine is synthesized via the direct capture of methanethiol and the rest is synthesized via the random reassembly of sulfide and methyl-tetrahydrofolate. Furthermore, we demonstrate that for both *Ruegeria pomeroyi* and *Ruegeria lacuscaerulensis*, 100 μM DMSP is the major source of reduced sulfur but not the major source of reduced carbon when grown on 2 mM glucose.

Introduction

Dimethylsulfoniopropionate (DMSP) is abundant in marine surface waters. In the North Sea, the concentration of DMSP cycles seasonally from micromolar levels in the summer to picomolar levels in the spring and fall (1, 2). The majority of marine DMSP comes from halophytic plants and algae, where it is believed to regulate osmotic pressure but may also provide antioxidant, predator deterrent, and/or cryoprotectant functions (2). There is also evidence that at least 0.5 % of marine bacteria are capable of producing DMSP (3). Consistent with its role in osmoregulation, plants that produce the most DMSP are generally halotolerant and of marine origin, with sugarcane being the only non-marine exception. During ^{35}S-labeling studies with the protist, *Oxyrrhis marina*, approximately 15 % of added DMSP accumulated intracellularly but was not metabolized (4). Molar levels of intracellular DMSP have been observed in some organisms, and it is estimated that up to 10 % of the total fixed carbon in the ocean is in the form of DMSP (5). Furthermore, DMSP released from phytoplankton blooms can satisfy up to 15 % of the microbial carbon demand and 100 % of the microbial sulfur demand (5).

DMSP is the precursor for the majority of atmospheric dimethylsulfide (DMS), which is a climatically-active gas and connects the marine and terrestrial sulfur cycles (6). It was previously believed that H_2S was responsible for the transfer of sulfur between marine and terrestrial environments, but the necessary atmospheric concentrations were never detected and the surface layers of the ocean are too oxidizing to sustain an equilibrium with the atmosphere (6). However, the concentration of DMS in marine surface layers is sufficiently high, and DMS is resistant to oxidation in the lower atmosphere (6). Its photooxidation in the upper atmosphere produces sulfur species that can be transferred to terrestrial environments via rain and promote

the formation of cloud-condensation nuclei, resulting in an increased albedo effect and global cooling (2, 5, 7, 8).

Bacterial catabolism of DMSP proceeds through one of two pathways (Fig. 6-1). In the demethylation pathway, DMSP is demethylated to form methylmercaptopropionate, which can further be broken down into methanethiol, carbon dioxide, and acetaldehyde. Methanethiol can then be assimilated into biomass or broken down to formaldehyde and H2S. Alternatively, DMSP can undergo cleavage to form DMS and acrylate (2, 9). Because very few studies have performed isotope-labeling experiments with DMSP, the fate of DMSP in microbial biomass is not well understood (4, 10-13).

A previous study examined the fate of isotopically labeled atoms from either di(^{13}C-methyl)sulfoniopropionate ([methyl-^{13}C]DMSP) (Fig. 6-2A) or dimethylsulfoniopropionate-1-^{13}C ([1-^{13}C]DMSP) (Fig. 6-2B) in *R. pomeroyi* (10). This study found that the methyl carbon of L-methionine and the C-3 position of L-serine were enriched by 99 % and 30 %, respectively, when grown on [methyl-^{13}C]DMSP (10). However, when *R. pomeroyi* was grown on [1-^{13}C]DMSP, L-methionine was not enriched (10). Taken together, this demonstrated that the methyl carbon of L-methionine was coming directly from the methyl carbons of DMSP but ruled out the possibility that methylmercaptopropionate (Fig. 6-1) was being directly converted to L-methionine via reductive carboxylation and transamination. The labeling observed at the C-3 position of L-serine when grown on [methyl-^{13}C]DMSP was due to its synthesis via L-glycine, water, and 5,10-methylenetetrahydrofolate (Fig. 6-3).

These results indicated that L-methionine was being synthesized from either one or both of the following pathways (Fig. 6-3): methanethiol was converted to L-methionine directly via a γ-substitution with *O*-acyl-L-homoserine ("methanethiol" pathway) (Fig. 6-3: blue lines), or methanethiol was first broken down to formaldehyde and sulfide, which was converted to L-

homocysteine via a γ-substitution with *O*-acyl-L-homoserine, and subsequently converted to L-methionine through methylation via the THF pool ("reassembly" pathway) (Fig. 6-3: green lines).

In order to investigate which pathways are being used to synthesize L-methionine, *R. pomeroyi* DSS-3 was grown in the presence of di(methyl-^{13}C)sulfonio-^{34}S-propionate ([^{13}C][^{34}S]DMSP). By feeding the cells a 1:1 mixture of DMSP and [^{13}C][^{34}S]DMSP, the resulting L-methionine isotopomers could be analyzed to determine which pathways were utilized. For example, if all of the L-methionine is synthesized via the "methanethiol" pathway (Fig. 6-3: blue lines), then the resulting L-methionine will be either unlabeled (mass shift = 0) or doubly labeled with both ^{13}C and ^{34}S (mass shift = 3). However, if all the L-methionine is synthesized via the "reassembly" pathway then there should be a mixture of unlabeled L-methionine (mass shift = 0) and L-methionine labeled with ^{13}C only (mass shift = 1), labeled with ^{34}S only (mass shift = 2), and labeled with both ^{13}C and ^{34}S (mass shift = 3). It is also possible that both pathways are used by *R. pomeroyi*, and examination of the relative enrichment of each isotopomer of L-methionine allows the determination of the fraction of L-methionine synthesized from each pathway. Furthermore, it is possible to examine the ^{34}S-labeling of L-cysteine, which provides important information about the source of reduced sulfur for biosynthesis.

Results

Chemostat growth. After maintaining steady-state growth for 6 days, 100 μM DMSP (1:1::DMSP:[^{13}C][^{34}S]DMSP) was added to the culture at a rate of 10 nmol min^{-1} (Fig. 6-4A). The specific labeling of [^{13}C][^{34}S]DMSP in the medium was 50.8 ± 0.3 %. The concentration of DMSP in the chemostat culture was 0.8 ± 0.1 μM, and the rates of DMS and methanethiol production were 0.36 ± 0.03 and 0.13 ± 0.04 nmol min^{-1}, respectively, indicating that only 5.0 ±

0.3 % of the total DMSP provided was lost as gas (Fig. 6-4B). Furthermore, the rate of unmetabolized DMSP detected in the outflow was 0.08 ± 0.01 nmol min^{-1} (Fig. 6-4C). Taken together, this suggested that 94.2 ± 0.4 % of the DMSP was consumed by the cells. Using this information, the amount of sulfur and reduced C-1 carbon provided to the cells from DMSP was estimated (Table 6-1). The estimated cellular demand for sulfur and reduced carbon is shown in Table 6-2.

Specific labeling of cysteine. Cysteine was expected to be synthesized exclusively by random reassembly of the sulfur and serine pools. The serine pool could be either unlabeled if derived from glucose or ^{13}C-labeled at the C-3 position if derived from methylene-THF and glycine (Fig. 6-3). The enrichments of ^{34}S-containing cysteine isotopomers indicated that DMSP was the major source of sulfur for cysteine biosynthesis. After 4 days, the ^{34}S-labeling of cysteine was 47.4 ± 1.4 %, or very close the enrichment of the medium [^{13}C][^{34}S]DMSP (Fig. 6-5C). In contrast, the ^{13}C-enrichment of cysteine was 11.1 ± 1.7 %, or much less than the enrichment of [^{13}C][^{34}S]DMSP (Fig. 6-5C). Presumably, this was a consequence of the dilution of the serine pool by 3-phosphoglycerate from glucose.

Specific labeling of methionine. As was seen with cysteine, the ^{34}S-enrichment of methionine indicated that DMSP was the major sulfur source for methionine biosynthesis (Fig. 6-5D). However, the enrichment of ^{13}C-containing methionine was much higher than that observed in cysteine (Fig. 6-5D). In principle, the high ^{13}C enrichment could be due to either direct biosynthesis via methanethiol or reassembly if the C-1 pool of methyl-THF was highly labeled. In fact, results were consistent with formation of 64.9 ± 1.1 % of methionine via the reassembly pathway during steady state growth. Moreover, the portion of methionine made via reassembly did not differ greatly over the five days of the experiment, varying between 61.6 ±

3.6 and 66.9 ± 0.6 %. This implied that the metabolism of DMSP did not change materially during the time of the experiment.

Specific labeling of metabolic pools. The labeling of the sulfide and methyl-THF pools provide insight into DMSP metabolism in *R. pomeroyi*. The enrichment of the methyl-THF, serine, sulfide, and methanethiol pools were calculated from the average labeling on days 4 and 5, when only about 5 % of the initial unlabeled biomass remained. At that time, ^{13}C enrichment in the methyl-THF pool was 10.5 ± 1.0 %, ^{13}C enrichment in the serine pool was 10.1 ± 1.5 %, ^{34}S enrichment in the sulfide pool was 46.6 ± 1.6 %, and the enrichment of both ^{13}C and ^{34}S in the methanethiol pool was 49.8 ± 2.4 % (Fig. 6-6).

Because the [^{13}C][^{34}S]DMSP was 50.8 ± 0.3 % of the total DMSP provided to the culture, we can conclude that sulfur from DMSP accounted for 91.7 ± 3.1 % of the total sulfide pool during steady state growth. Even after only 24 hours of introducing DMSP to the culture, 57.3 ± 6.8 % of the sulfide can be attributed to DMSP (Fig. 6-6). This suggests that sulfate reduction is almost entirely shut down during DMSP metabolism. This conclusion is also supported by the fact that the DMSP-derived sulfur consumed by the cell (Table 6-1) was nearly three times the estimated sulfur demand (Table 6-2).

The results for the C-1 pools were much different. Although the amount of C-1 equivalents consumed by the cell is potentially more than twice the amount of sulfur (Table 6-1), the ^{13}C-labeled methyl-THF and ^{13}C-labeled serine both constituted approximately 10 % of the total methyl-THF and serine pools during steady state growth (Fig. 6-6). Because the [^{13}C][^{34}S]DMSP was 50.8 ± 0.3 % of the total DMSP provided to the culture, we can conclude that the methyl carbons from DMSP accounted for 17.7 ± 2.8 % of the total methyl-THF pool and 19.8 ± 2.9 % of the total serine pool. The remaining methyl-THF is presumably coming from glucose via the conversion of 3-phosphoglycerate to serine. The demand for C-1 equivalents is

about 12.9 ± 0.6 nmol min^{-1} (Table 6-2), and between 74.2 ± 3.6 % and 147.4 ± 7.2 % of this demand could be provided by the methyl carbons of DMSP (Table 6-1). However, the dilution of the C-1 pool by unlabeled carbon indicates that there was a significant rate of oxidation of the C-1 pool to carbon dioxide.

DMSP metabolism by *R. lacuscaerulensis*. In a similar experiment, *R. pomeroyi* and *R. lacuscaerulensis* were grown in chemostat to compare their DMSP metabolisms. Previous studies have demonstrated that *R. lacuscaerulensis* produces much less methanethiol as compared to *R. pomeroyi* (unpublished), so it was hypothesized that the metabolism would also very greatly between these two organisms. On the contrary, the specific labeling of the metabolic pools for the methionine precursors did not very greatly (Fig. 6-7). The [^{13}C]methyl-THF pools were not statistically different, and although the ^{34}S-labeled sulfide and doubly-labeled methanethiol pools were statistically different, their values were roughly similar. *R. pomeroyi* and *R. lacuscaerulensis* had 45.4 ± 3.2 % and 55.1 ± 2.3 % ^{34}S-labeled sulfide, respectively, and 55.1 ± 2.3 % and 44.7 ± 8.5 % doubly-labeled methanethiol, respectively (Fig. 6-7). However, the utilization of the two methionine biosynthetic pathways differed significantly. The percentages of methionine synthesized via the direct capture of methionine by *R. pomeroyi* and *R. lacuscaerulensis* were 33.7 ± 1.8 % and 48.9 ± 3.3 %, respectively (Fig. 6-7). These results suggest that although the catabolism of DMSP does not differ greatly between *R. pomeroyi* and *R. lacuscaerulensis*, anabolism from the resulting metabolites is significantly different.

Discussion

Previously, it was demonstrated that only roseobacter strains which could metabolize DMSP to methanethiol were able to incorporate a significant amount ^{35}S from [^{35}S]DMSP into TCA-insoluble material (13). This finding led to the hypothesis that the majority of methionine biosynthesis in the roseobacter group is accomplished by the direct capture of methanethiol via

either cystathionine γ-synthase (MetB) or *O*-acylhomoserine thiolase (MetY) (13-15). This hypothesis was supported in a second study which found that a mutant of *Corynebacterium glutamicum* lacking the 5,10-methylene-tetrahydrofolate reductase gene (*metF*) could not grow on sulfate as the sole sulfur source, but the *C. glutamicum* Δ*metF* strain could grow on sulfate plus methanethiol (16). Furthermore, when *C. glutamicum* Δ*metF* was grown on 99 % [$^{13}C_6$]glucose and naturally labeled methanethiol, 95 % of the resulting methionine was unlabeled at the methyl carbon, indicating that nearly all of the methionine in this mutant was synthesized via the direct capture of methanethiol (16). Although the majority of methionine sulfur in *R. pomeroyi* DSS-3 was derived from DMSP (Fig. 6-5), only about one-third was synthesized via the methanethiol pathway. This result does not disagree with previous experiments but refutes the interpretation that the direct capture of methanethiol is the major source of methionine. Moreover, it demonstrates that even at the low concentrations of <1 μM used in these chemostats, DMSP becomes the major sulfur source for *R. pomeroyi*.

In order for *R. pomeroyi* to synthesize cysteine from DMSP, it must first convert methanethiol to sulfide (Fig. 6-3), and this may explain why *R. pomeroyi* synthesizes more methionine via the reassembly pathway. Although the direct capture of methanethiol is more energy efficient for the biosynthesis of methionine, if too much of the methanethiol is captured directly then there will be an increase in the cost of cysteine biosynthesis. This is because *R. pomeroyi* possesses a methionine γ-lyase (MegL), which is responsible for the majority of the methanethiol produced during growth on methionine (data not shown), and is capable of converting methionine to methanethiol. However, if too large of a fraction methanethiol was converted to methionine to the point where the cell would need to break down methionine in order to produce cysteine, then the cell would lose energy activating homoserine to *O*-acylhomoserine only to have it converted back to homoserine by MegL.

Experimental Procedures

General. All glassware used in the amino acid extractions and subsequent derivatizations (see below) was acid washed in 3 % (*v/v*) HCl for 24 hours to remove trace contaminants and then baked at 180 ˚C for 24 hours to degrade any remaining organic compounds. Dry HCl was generated as previously described (17). Methanolic HCl was generated by bubbling dry HCl into methanol while stirring. The solution was titrated to determine the concentration of HCl and stored in a stoppered glass bottle under an atmosphere of nitrogen at -20 ˚C for no more than one month.

Synthesis of substrates. Di(methyl-^{13}C)sulfonio-^{34}S-propionate ([^{13}C][^{34}S]DMSP) hydrochloride was synthesized as previously described (17). Briefly, $^{34}S_8$ was reduced to $Na_2{}^{34}S$ via a Birch reduction in liquid ammonia (18, 19). The resulting $Na_2{}^{34}S$ was converted to di(methyl-^{13}C)sulfide-^{34}S ([^{13}C][^{34}S]DMS) via methylation with $I^{13}CH_3$ under basic conditions and purified via distillation (20). The purified [^{13}C][^{34}S]DMS was then converted to [^{13}C][^{34}S]DMSP hydrochloride via a Michael addition to acrylic acid and washed with CH_2Cl_2 to remove any excess reactants (21). The isotopic purity of the resulting compound was greater than 98 % (17).

Chemostat cultures. *R. pomeroyi* DSS-3 was grown at 30 ˚C on a carbon-limited chemostat as previously described (22). Briefly, the chemostat was inoculated with 1 mL of a culture of *R. pomeroyi* grown in ½ YTSS medium at 30 ˚C for 24 hours. At this point, a pump connected to a reservoir containing marine basal medium (MBM) supplemented with 2 mM glucose was then turned on, and the chemostat was allowed to fill to the maximum volume of 150 mL at a rate of 0.1 mL min^{-1}. After 21 days, the culture had reached steady-state, and 50 µM DMSP and 50 µM [^{13}C][^{34}S]DMSP (100 µM total DMSP) was added to the reservoir. Upon the addition of DMSP, the outflow was collected in a sterile bottle on ice. After each 24 h interval,

the cells were harvested via centrifugation at 6,000 × g for 30 minutes at 4 ˚C. Pellets were washed once with 10 mL of distilled, deionized water and then stored at -80 ˚C until processing. The chemostat was allowed to run for five days, at which point the contents of the chemostat were harvested. The fraction of labeled to unlabeled DMSP in the sterile media was determined as previously described (17). Briefly, 2 mL of sterile medium was transferred to a 10 mL serum vial. The vial was crimp-sealed with a teflon-coated, butyl rubber stopper and the headspace was replaced with nitrogen. A syringe was used to add 2 mL of 4 M NaOH to the vials, which were then vortexed followed by incubation at 37 ˚C for 2.5 hours. The resulting DMS was analyzed via GC-MS, and the relative abundances at m/z = 62 (corresponding to the unlabeled DMS) and m/z = 66 (corresponding to the [^{13}C][^{34}S]DMS) were compared.

Chemostat cultures of either *R. pomeroyi* DSS-3 or *R. lacuscaerulensis* ITI-1157 were grown as described above with one exception: 50 µM total DMSP (25 µM DMSP and 25 µM [^{13}C][^{34}S]DMSP) was added to the chemostat instead of 100 µM total DMSP. All other conditions were identical to those described above.

Amino acid extraction. Amino acids were extracted and prepared for derivatization as previously described (23, 24). Cell pellets were thawed on ice and resuspended in 2 mL of a solution of 6 M urea dissolved in 0.5 M Tris, pH 8.6 (lysis buffer) and then incubated at -80 ˚C for 20 minutes. The suspension was thawed and then lysed via four passages through a cell disruptor (One Shot, Constant Systems Ltd.) at 14.5 kPsi (approximately 100,000 kPa) (9). The cell disruptor was then washed with 1 mL of lysis buffer and again with 2 mL of lysis buffer. The lysate and both washes were combined and transferred to a glass serum vial, which was then crimp-sealed with a teflon-coated butyl rubber stopper. The headspace of the vial was replaced with nitrogen gas, and a syringe was used to add 500 µL of a freshly prepared, filter-sterilized, aqueous solution of 0.2 M dithiothreitol. The vial was then incubated at 100 ˚C for 10 minutes to

reduce all cysteinyl residues to free thiols. The vial was cooled, and a syringe was used to add 100 µL of ICH_3. In order to methylate the free thiols, the vial was incubated at 60 ˚C with shaking at 300 rpm (Thermo Scientific MaxQ 4450 model 4324) for 30 minutes. The contents of the vial were transferred to Spectra/Por® 7 pre-treated regenerated cellulose dialysis tubing with a 2,000 molecular weight cut-off (Spectrum Laboratories, Inc.; PN: 132107) and dialyzed twice in 1 L distilled, deionized water for 12 hours at 4 ˚C for a total of 24 hours. The dialyzed cell lysate was transferred to a Balch tube, and the liquid was evaporated with a stream of nitrogen at 50 ˚C. The vial was crimp-sealed with a butyl rubber stopper, and the headspace was replaced with nitrogen gas. A syringe was used to add 2 mL of an anaerobic 6 M HCl solution, and proteins were converted to free amino acids by incubating the tube at ≥110 ˚C for 24 hours. The tube was cooled to room temperature, and the liquid was evaporated with a stream of nitrogen at 50 ˚C. The solids were dissolved in 1 mL of distilled, deionized water, and the liquid was transferred to a 1.5 mL microcentrifuge tube. The tube was centrifuged at 17,000 × g for 10 minutes to pellet the black precipitate, and the supernatant was transferred to a clean glass serum vial. The liquid was evaporated with a stream of nitrogen at 50 ˚C, leaving behind solids composed primarily of amino acid hydrochloride salts and other water-soluble cellular debris.

Derivatization of amino acids. Amino acids were converted to their *N*-trifluoroacetyl amino acid methyl esters as previously described (23-25). The vial containing the amino acid hydrochloride salts was crimp-sealed with a butyl rubber stopper, and the headspace was replaced with nitrogen gas. A syringe was used to add 1 mL of freshly prepared 4 M methanolic HCl. The vial was incubated in a boiling water bath for 30 minutes, and allowed to cool for 5-10 minutes. This was repeated three times for a total of 2 hours in the boiling water bath. The vial was cooled to room temperature, and the liquid was evaporated with a stream of nitrogen at 50 ˚C. 1.5 mL of methylene chloride was applied to the solids to help exclude water and was

subsequently removed with a stream of nitrogen gas at room temperature. The vial was crimp-sealed with a teflon-coated butyl rubber stopper and was incubated at 50 ˚C for 2 hours while flushing the headspace with nitrogen gas to remove any remaining water from the vials. The vial was cooled to room temperature while flushing and then pressurized with nitrogen gas to 12 psi (approximately 83 kPa). A gas-tight, glass syringe was used to add 250 µL of methylene chloride and 250 µL of trifluoroacetic anhydride (TFAA). The vial was vortexed briefly and incubated at room temperature. After 4 hours, the vial was chilled on ice, and the majority of the liquid was evaporated by flushing the headspace with a slow stream of nitrogen gas resulting in a dark brown oil. Because the *N*-trifluoroacetyl amino acid methyl esters are volatile, care was taken not to take the liquid to dryness.

Preparation of TLC standards. 50 mg mL^{-1} solutions of L-methionine (SigmaAldrich: M9625) and *S*-methyl-L-cysteine (Sigma: M6626) were prepared in 1M HCl and filtered with a 0.2 µm filter. 500 µL of each solution (25 mg of each compound) was added to its own serum vial, and the liquid was evaporated with a stream of nitrogen gas at 50 ˚C. The amino acids were then derivatized as described above. A glass syringe was used to add 25-50 µL of methyl acetate to dilute the resulting oils.

TLC-purification of methionine and *S*-methylcysteine derivatives. Methionine and *S*-methylcysteine derivatives were purified as previously described (24). A glass syringe was used to add 150µL of methyl acetate to dilute the dark brown oil to decrease viscosity and ensure complete transfer. A syringe was used to spot all of the liquid from the derivatized cell material as a thin band onto a glass-backed silica gel (500 µm layer) preparative TLC plate (Analtech: P02012). 5-10 µL of each standard was spotted on either side of the band, and all spots were incubated at room temperature for several minutes to dry. A developing chamber was equilibrated with 2.5 % methyl acetate in methylene chloride for ≥ 4 hours prior to running so

that the atmosphere was saturated. The TLC plate was developed for approximately 40 minutes, or until the solvent front had nearly reached the top of the plate. The plate was allowed to dry completely and then stained with iodine vapor for several seconds. The positions of the L-methionine and *S*-methyl-L-cysteine standards were marked, and the plate was incubated at room temperature for several minutes until the yellow color from the iodine could no longer be seen. The silica gel from the bands of cellular material corresponding to the positions of the standards were transferred to glass serum vials. The vials were crimp-sealed with a teflon-coated butyl rubber stopper, and a glass syringe was used to add 5 mL of methyl acetate to the vial. After overnight incubation with gentle shaking, a gas-tight, glass syringe was used to transfer the liquid to new serum vials. The samples were concentrated by evaporating the majority of the liquid with a stream of nitrogen gas leaving behind 25-50 µL of a pale, yellow liquid.

Analysis of methionine and S-methylcysteine derivatives via GC-MS. TLC-purified methionine and cysteine derivatives were analyzed via GC-MS at the Proteomics and Mass Spectrometry Facility (University of Georgia) using a modified version of the method described by White (2003) (24). 1 µL of the purified derivatives were applied to the injection port (heated at 280 ˚C) of the GC (HP-5890, Agilent) with a splitless duration of 2.75 minutes and an EC-5 (0.25 mm i.d. × 30 m × 0.25 µm film thickness, Alltech) column. The carrier gas was He with a head pressure capped at 12 psi (approximately 83 kPa). The GC oven was programmed to remain at 60 ˚C for 6 minutes and then rise from 60 ˚C to 280 ˚C at a rate of 25 ˚C min^{-1}. The derivatives were detected by a mass spectrometer (HP-5971A, Agilent) with an EI ion source running in scan mode (monitored *m/z* range was 50–350) with 12 scans per second and a detector temperature of 280 ˚C. Under these conditions, the methionine derivative (M^+ = 259) had a retention time of 11.4-11.6 minutes and the *S*-methylcysteine derivative (M^+ = 245) had a

retention time of 10.6-10.9 minutes. All derivatives were measured 3 times to obtain the error in the GC-MS measurements.

Calculation of isotopomer enrichments. The relative abundances of each mass shift were corrected using the "skewed method" to convert the raw data into the enrichment values for each isotopomer as previously described (26). Briefly, the natural abundance of each mass shift was calculated using a custom R script, and this process was repeated for each of the four possible isotopomers (unlabeled, ^{13}C-labeled, ^{34}S-labeled, or ^{13}C+^{34}S-labeled) for the derivatives of both methionine and cysteine. The resulting values were then applied to the raw data as previously described (26).

Calculation of the specific labeling of the sulfide pool and the serine pool. Because cysteine is synthesized exclusively through the random reassembly of sulfide and carbon (Fig. 6-3), the sulfide pool can be approximated with the following equations:

$$\frac{S_U}{S_L} = \frac{c_0 + c_1}{c_2 + c_3} \qquad \textbf{Eq. 6-1}$$

$$S_U + S_L = 1 \qquad \textbf{Eq. 6-2}$$

Where S_U is the fraction of unlabeled sulfide, S_L is the fraction of labeled sulfide, c_0 is the fraction of unlabeled cysteine, c_1 is the fraction of ^{13}C-labeled cysteine, c_2 is the fraction of ^{34}S-labeled cysteine, and c_3 the fraction of doubly-labeled cysteine. After solving **equations 6-1 and 6-2** for S_U and S_L, the following equations were obtained:

$$S_L = \left(\frac{c_0 + c_1}{c_2 + c_3} + 1\right)^{-1} \qquad \textbf{Eq. 6-3}$$

$$S_U = 1 - S_L \qquad \textbf{Eq. 6-4}$$

These equations were applied to each replicate for each day, and the average fraction of labeled sulfide for each day was calculated.

Similarly, the ^{13}C-labeling of the serine pool can be approximated with the following equations:

$$\frac{Ser_U}{Ser_L} = \frac{c_0 + c_2}{c_1 + c_3} \qquad \textbf{Eq. 6-5}$$

$$Ser_U + Ser_L = 1 \qquad \textbf{Eq. 6-6}$$

Where Ser_U is the fraction of unlabeled serine, and Ser_L is the fraction of labeled serine. After solving equations 6-5 and 6-6 for Ser_U and Ser_L, the following equations were obtained:

$$Ser_L = \left(\frac{c_0 + c_2}{c_1 + c_3} + 1\right)^{-1} \qquad \textbf{Eq. 6-7}$$

$$Ser_U = 1 - S_L \qquad \textbf{Eq. 6-8}$$

These equations were applied to each replicate for each day, and the average fraction of labeled serine for each day was calculated.

Calculation of the specific labeling of the methyl-THF pool and the fraction methionine synthesized via the reassembly pathway. It was assumed that the sulfide pool used for cysteine biosynthesis was equivalent to the sulfide pool used for methionine biosynthesis. However, cysteine is synthesized via serine so the methyl-THF pool could not be approximated using the observed enrichments for cysteine (Fig. 6-3). Because ^{13}C-labeled methionine and ^{34}S-labeled methionine can only be synthesized via the reassembly pathway (Fig. 6-3), the following equations were assumed to be true:

$$m_1 = C_L S_U F_R \qquad \textbf{Eq. 6-9}$$

$$m_2 = C_U S_L F_R \qquad \textbf{Eq. 6-10}$$

$$C_U + C_L = 1 \qquad \textbf{Eq. 6-11}$$

Where S_U and S_L are the average fractions of unlabeled and labeled sulfide for each day, respectively, as calculated from cysteine in equations 6-3 and 6-4, C_U is the fraction of unlabeled methyl-THF, C_L is the fraction of labeled methyl-THF, F_R is the fraction of methionine

synthesized via the reassembly pathway, m_1 is the enrichment of ^{13}C-labeled methionine, and m_2 is the enrichment of ^{34}S-labeled methionine. In order to solve for C_U and C_L, equations 6-9 and 6-10 were combined to produce the following equation:

$$\frac{m_1}{m_2} = \frac{C_L S_U}{C_U S_L} \qquad \textbf{Eq. 6-12}$$

After solving for C_U and C_L in equations 6-11 and 6-12, the following equations were obtained:

$$C_U = \frac{m_2 S_U}{m_1 S_L + m_2 S_U} \qquad \textbf{Eq. 6-13}$$

$$C_L = 1 - C_U \qquad \textbf{Eq. 6-14}$$

Next, C_U in equation 6-10 was replaced with the term defined in equation 6-13, and the resulting equation was solved for F_R which produced the following equation:

$$F_R = \frac{m_1 S_L + m_2 S_U}{S_U S_L} \qquad \textbf{Eq. 6-15}$$

Equations 6-13 and 6-14 were used to calculate the specific labeling of the methyl-THF pool, and Equation 6-15 was used to calculate the fraction of methionine synthesized via the reassembly pathway for each of the triplicates for each day.

Calculation of the specific labeling of the methanethiol pool and the fraction of methionine synthesized via the methanethiol pathway. Because unlabeled methionine and doubly-labeled methionine can be synthesized by both the reassembly pathway and the methanethiol pathway (Fig. 6-3), the following equations were assumed to be true:

$$m_0 = C_U S_U F_R + M_U F_M \qquad \textbf{Eq. 6-16}$$

$$m_3 = C_L S_L F_R + M_L F_M \qquad \textbf{Eq. 6-17}$$

$$F_R + F_M = 1 \qquad \textbf{Eq. 6-18}$$

Where M_U is the fraction of unlabeled methanethiol, M_L is the fraction of doubly-labeled methanethiol, F_M is the fraction of methionine synthesized via the methanethiol pathway, m_0 is the fraction of unlabeled methionine, and m_3 is the fraction of doubly-labeled methionine.

Solving equations 6-16 and 6-17 M_U and M_L, and equation 6-18 for F_R produces the following equations:

$$M_U = \frac{m_0 - C_U S_U F_R}{1 - F_R} \qquad \textbf{Eq. 6-19}$$

$$M_L = \frac{m_3 - C_L S_L F_R}{1 - F_R} \qquad \textbf{Eq. 6-20}$$

$$F_M = 1 - F_R \qquad \textbf{Eq. 6-21}$$

Equations 6-19 and 6-20 were used to calculate the specific labeling of the methanethiol pool for each replicate, and equation 6-21 was used to calculate the fraction of methionine synthesized via the methanethiol pathway for each of the triplicates for each day.

References:

1. van Duyl FC, Gieskes WWC, Kop AJ, Lewis WE. 1998. Biological control of short-term variations in the concentration of DMSP and DMS during a *Phaeocystis* spring bloom. Journal of Sea Research 40:221-231.
2. Reisch CR, Moran MA, Whitman WB. 2011. Bacterial catabolism of dimethylsulfoniopropionate (DMSP). Frontiers in Microbiology 2:172.
3. Curson ARJ, Liu J, Martinez AB, Green RT, Chan YH, Carrion O, Williams BT, Zhang SH, Yang GP, Page PCB, Zhang XH, Todd JD. 2017. Dimethylsulfoniopropionate biosynthesis in marine bacteria and identification of the key gene in this process. Nature Microbiology 2:9.
4. Saló V, Simó R, Vila-Costa M, Calbet A. 2009. Sulfur assimilation by *Oxyrrhis marina* feeding on a ^{35}S-DMSP-labelled prey. Environmental Microbiology 11:3063-3072.
5. Yoch DC. 2002. Dimethylsulfoniopropionate: its sources, role in the marine food web, and biological degradation to dimethylsulfide. Applied and Environmental Microbiology 68:5804-5815.

6. Lovelock JE, Maggs RJ, Rasmussen RA. 1972. Atmospheric dimethyl sulphide and the natural sulphur cycle. Nature 237:452.

7. Hatakeyama S, Okuda M, Akimoto H. 1982. Formation of sulfur dioxide and methanesulfonic acid in the photooxidation of dimethyl sulfide in the air. Geophysical Research Letters 9:583-586.

8. Charlson RJ, Lovelock JE, Andreae MO, Warren SG. 1987. Oceanic phytoplankton, atmospheric sulphur, cloud albedo and climate. Nature 326:655.

9. Reisch CR, Stoudemayer MJ, Varaljay VA, Amster IJ, Moran MA, Whitman WB. 2011. Novel pathway for assimilation of dimethylsulphoniopropionate widespread in marine bacteria. Nature 473:208-11.

10. Reisch CR, Crabb WM, Gifford SM, Teng Q, Stoudemayer MJ, Moran MA, Whitman WB. 2013. Metabolism of dimethylsulphoniopropionate by *Ruegeria pomeroyi* DSS-3. Molecular Microbiology 89:774-91.

11. Todd JD, Curson ARJ, Nikolaidou-Katsaraidou N, Brearley CA, Watmough NJ, Chan YH, Page PCB, Sun L, Johnston AWB. 2010. Molecular dissection of bacterial acrylate catabolism - unexpected links with dimethylsulfoniopropionate catabolism and dimethyl sulfide production. Environmental Microbiology 12:327-343.

12. Ruiz-González C, Galí M, Sintes E, Herndl GJ, Gasol JM, Simó R. 2012. Sunlight effects on the osmotrophic uptake of DMSP-sulfur and leucine by polar phytoplankton. Plos One 7:14.

13. Kiene RP, Linn LJ, Gonzalez J, Moran MA, Bruton JA. 1999. Dimethylsulfoniopropionate and methanethiol are important precursors of methionine and protein-sulfur in marine bacterioplankton. Applied and Environmental Microbiology 65:4549-4558.

14. González JM, Kiene RP, Moran MA. 1999. Transformation of sulfur compounds by an abundant lineage of marine bacteria in the α-subclass of the class *Proteobacteria*. Applied and Environmental Microbiology 65:3810.

15. Kiene RP, Linn LJ, Bruton JA. 2000. New and important roles for DMSP in marine microbial communities. Journal of Sea Research 43:209-224.

16. Bolten CJ, Schroder H, Dickschat J, Wittmann C. 2010. Towards methionine overproduction in *Corynebacterium glutamicum* — methanethiol and dimethyldisulfide as reduced sulfur sources. Journal of Microbiology Biotechnology 20:1196-1203.

17. Wirth JS, Whitman WB. 2019. An efficient method for synthesizing dimethylsulfonio-^{34}*S*-propionate hydrochloride from $^{34}S_8$. Journal of Labelled Compounds and Radiopharmaceuticals 62:52-58.

18. Fehér F. 1963. Sulfur, selenium, tellurium, p 358-360. *In* Brauer G, Riley RF (ed), Handbook of Preparative Inorganic Chemistry, 2 ed, vol 1. Academic Press, New York.

19. Bonneau PR, Wiley JB, Kaner RB. 2007. Metathetical precursor route to molybdenum disulfide, p 33-37, Inorganic Syntheses, vol 30.

20. Beerli R, Borschberg H-J. 1991. Preparation of [$^{13}C_2$]DMSO. Journal of Labelled Compounds and Radiopharmaceuticals 29:957-961.

21. Chambers ST, Kunin CM, Miller D, Hamada A. 1987. Dimethylthetin can substitute for glycine betaine as an osmoprotectant molecule for Escherichia coli. Journal of Bacteriology 169:4845-7.

22. Reisch CR, Moran MA, Whitman WB. 2008. Dimethylsulfoniopropionate-dependent demethylase (DmdA) from *Pelagibacter ubique* and *Silicibacter pomeroyi*. Journal of Bacteriology 190:8018-8024.

23. White RH. 1981. A method for the measurement of sulfur-34 abundance in bound cysteine and methionine. Analytical Biochemistry 114:349-354.

24. White RH. 2003. The biosynthesis of cysteine and homocysteine in *Methanococcus jannaschii*. Biochimica Et Biophysica Acta-General Subjects 1624:46-53.

25. Thomas SJ. 1982. Identification of amino acids by the retention indices of their *N*-trifluoroacetyl methyl and *n*-butyl ester derivatives. Bachelor of Science. University of Illinois at Urbana-Champaign, Urbana, Illinois.

26. Midani FS, Wynn ML, Schnell S. 2017. The importance of accurately correcting for the natural abundance of stable isotopes. Analytical Biochemistry 520:27-43.

27. Koch AL. 2007. Growth Measurement, p 179-199. *In* Reddy CA, Beveridge TJ, Breznak JA, Marzluf GA, Schmidt TM, Snyder LR (ed), Methods for General and Molecular Microbiology, 3rd ed. American Society for Microbiology, Washington, D.C.

28. Hashsham SA, Baushke SW. 2007. Energetics, Stoichiometry, and Kinetics of Microbial Growth, p 286-308. *In* Reddy CA, Beveridge TJ, Breznak JA, Marzluf GA, Schmidt TM, Snyder LR (ed), Methods for General and Molecular Microbiology, 3rd ed. American Society for Microbiology, Washington, D.C.

29. White D, Drummond J, Fuqua C. 2012. The Physiology and Biochemistry of Prokaryotes, 4 ed. Oxford University Press, Inc., New York.

30. Neidhardt FC, Ingraham JL, Schaechter M. 1990. Physiology of the bacterial cell: a molecular approach. Sinauer Associates, Inc., Sunderland, Mass.

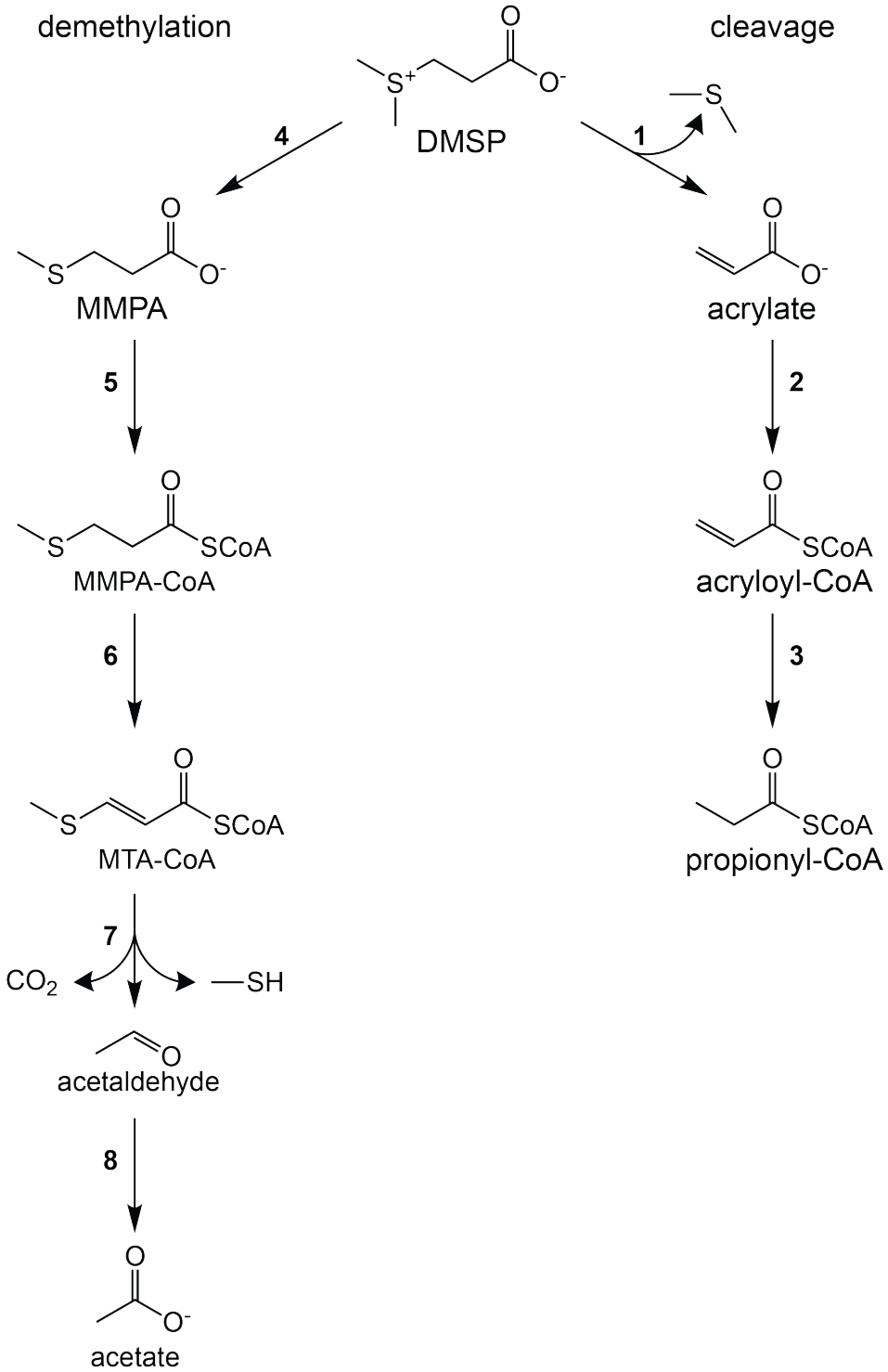

Figure 6-1. Metabolism of DMSP in *Ruegeria pomeroyi* DSS-3. The two possible pathways for DMSP degradation are shown with the cleavage pathway on the right and the demethylation/demethiolation pathway on the left. Abbreviations: MMPA, methylmercaptopropionic acid; MTA-CoA, methylthioacryloyl-CoA. Genes: 1, *dddD* (SPO1703), *dddP* (SPO2299), *dddQ* (SPO1596), and/or *dddW* (SPO0453); 2, *prpE* (SPO2934); 3, *acuI* (SPO1914); 4, *dmdA* (SPO1913); 5, *dmdB* (SPO2045/SPO0677); 6, *dmdC* (SPO3804/SPO0298/SPO2915); 7, *dmdD* (SPO3805); 8, aldehyde dehydrogenase (SPO0097).

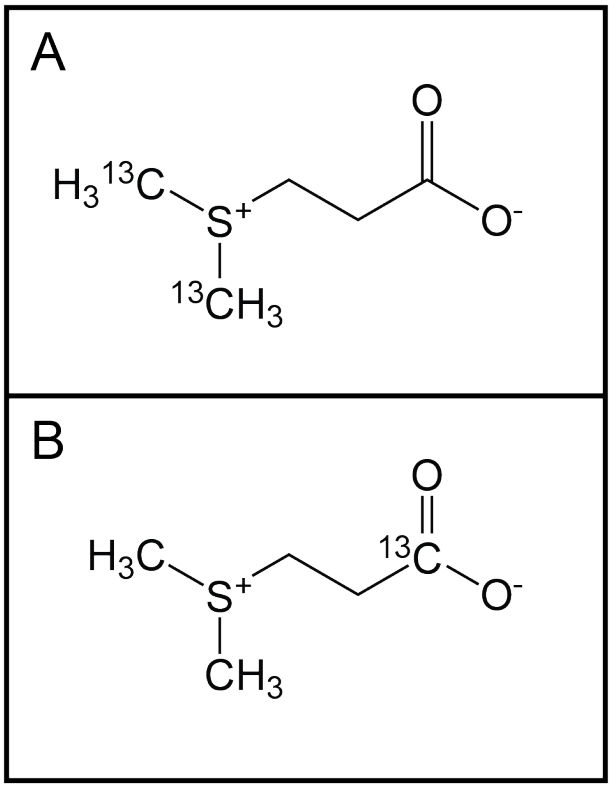

Figure 6-2. DMSP isotopomers employed in previous studies. (A) di(methyl-^{13}C)sulfoniopropionate. (B) dimethylsulfoniopropionate-1-^{13}C.

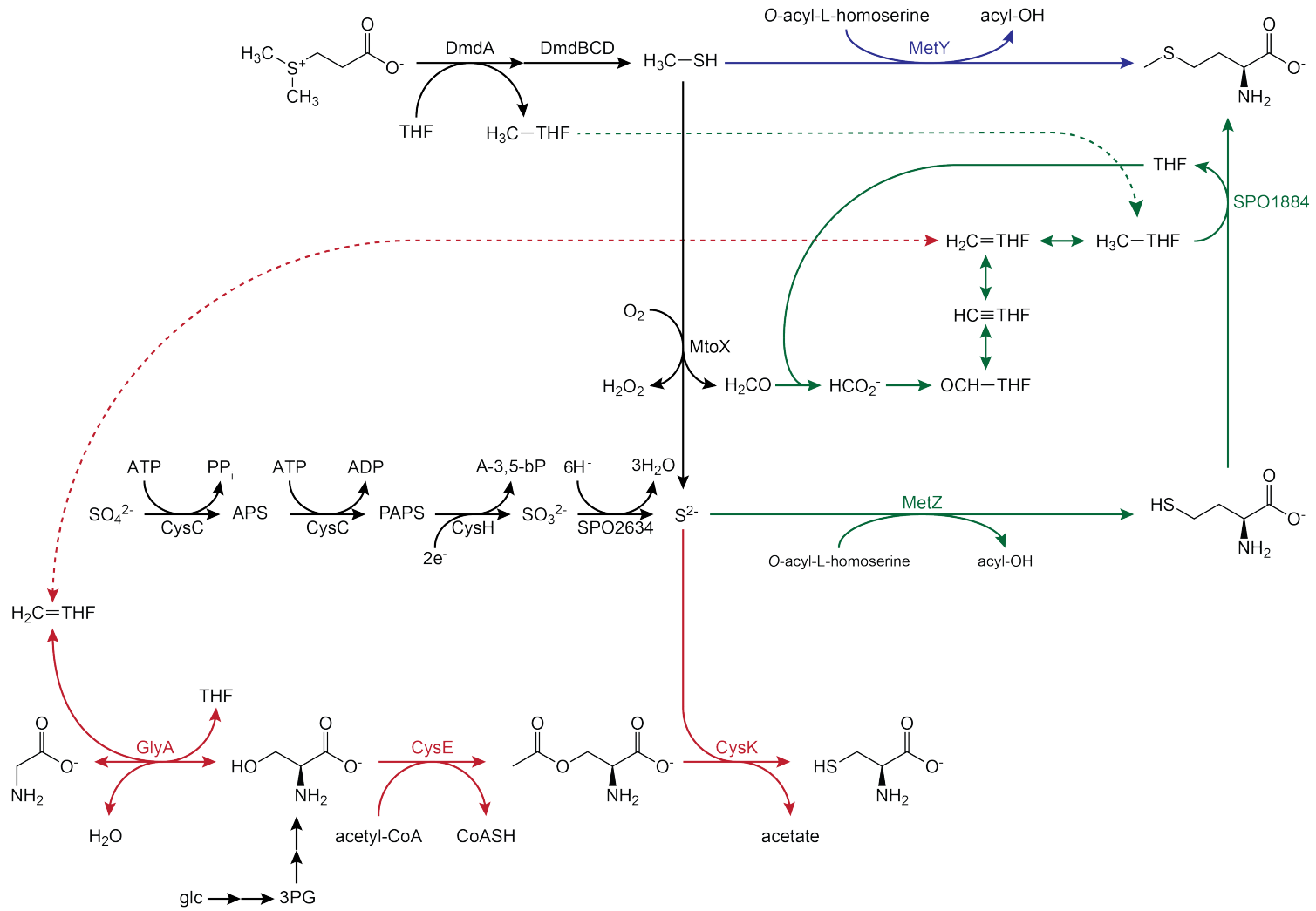

Figure 6-3. Putative pathways for the biosynthesis of L-methionine and L-cysteine from DMSP. Both possible routes for synthesizing L-methionine are shown with the "methanethiol" pathway highlighted in blue and the "reassembly" pathway highlighted in green. The pathway for L-cysteine biosynthesis is highlighted in red. Black arrows indicate reactions that are used in multiple pathways. Dashed lines connect common intermediates found in the THF pool. "glc" indicates glucose, "3PG" indicates 3-phosphoglycerate, "APS" indicates adenosine-5'-phosphosulfate, "PAPS" indicates 3'-phosphoadenosine-5'-phosphosulfate, and "A-3,5-bP" indicates adenosine-3',5'-bisphosphate.

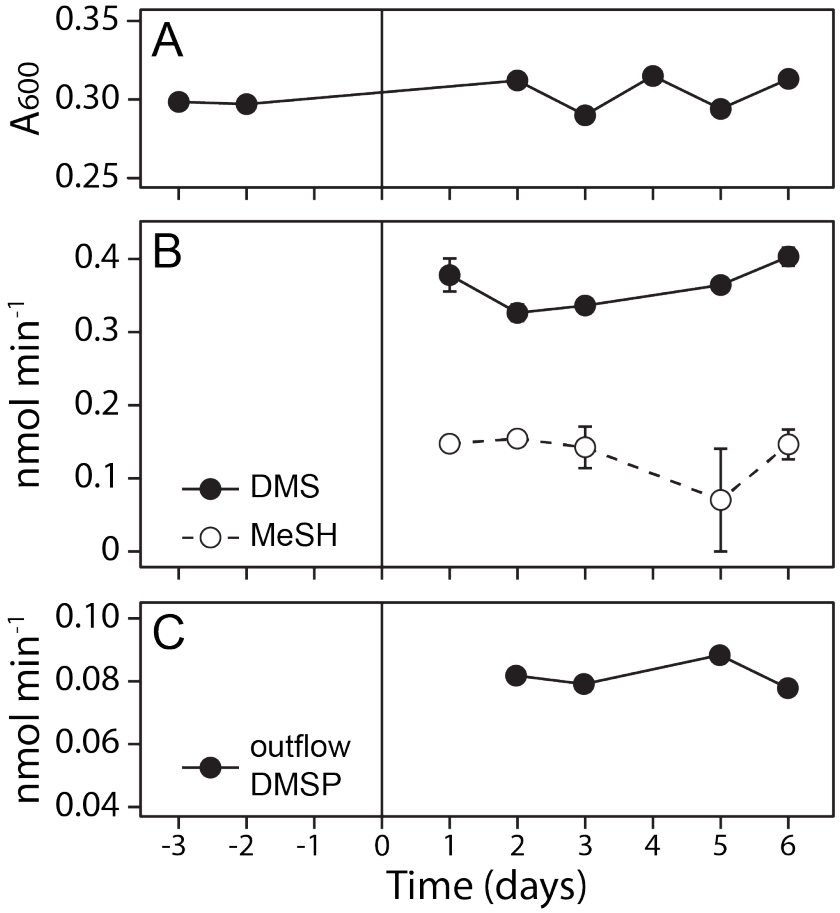

Figure 6-4. Growth of *R. pomeroyi* in chemostat. Cultures were grown on MBM supplemented with 2 mM glucose. The vertical indicates the addition of 100 µM DMSP (1:1::DMSP:[^{13}C][^{34}S]DMSP) to the chemostat at a rate of 10 nmol min^{-1}. Error bars indicate the standard errors of the mean. (A) The vertical axis indicates the growth of the culture as measured by the absorbance at 600 nm. (B) The vertical axis indicates the rate of dimethylsulfide (DMS) and methanethiol (MeSH) gas production by *R. pomeroyi*. Filled circles with solid lines indicate DMS, and hollow circles with dashed lines indicate MeSH. (C) The vertical axis indicates the rate of excess DMSP detected in the chemostat outflow, including both soluble and particulate (cellular) DMSP.

Table 6-1. Sulfur and reduced carbon provided to chemostat cultures by DMSP. Values were calculated by subtracting the rate of DMSP addition from the amount of gas produced and the amount of DMSP detected in the outflow. The amount of reduced C-1 carbon was calculated by assuming that both methyl carbons were utilized and assuming that only one methyl carbon was utilized. All values are reported in units of nmol min^{-1}. The error indicates the 95 % confidence interval.

Day	Sulfur consumed	1 CH_3 consumed	2 CH_3 consumed
1	9.48 ± 0.10	9.62 ± 0.07	19.10 ± 0.17
2	9.44 ± 0.06	9.59 ± 0.04	19.03 ± 0.10
3	9.44 ± 0.39	9.59 ± 0.03	19.03 ± 0.42
4	ND	ND	ND
5	9.48 ± 0.88	9.55 ± 0.02	19.02 ± 0.86
6	9.37 ± 0.10	9.52 ± 0.16	18.90 ± 0.06
Average	9.45 ± 0.03	9.58 ± 0.03	19.03 ± 0.05

Table 6-2. Cellular demand for sulfur and reduced carbon. The amount of dry weight was calculated from the A_{660} as previously described (27). The doubling time of the culture (1040 min) was calculated by dividing the natural log of 2 by the dilution rate of the chemostat (28). The reduced carbon and sulfur demand was calculated by determining the amount of each compound to required to sustain the calculated dry weight, and then dividing that value by the calculated doubling time. The sulfur demand was calculated as the sum of the rates of cysteine and methionine biosynthesis. The reduced C-1 carbon demand was calculated by adding the rates of serine (C-1), methionine, dATP, dGTP, dTTP, ATP, and GTP biosynthesis together. Because purines require 2 equivalents of reduced C-1 carbon, the values for dATP, dGTP, ATP, and GTP were multiplied by 2 (29). The values for each metabolite (μmol mg^{-1} dry weight) were assumed to be equal to those for *E. coli* (30). All values are reported with units of nmol min^{-1}. The error indicates the 95 % confidence interval.

Day	Sulfur demand	Reduced carbon demand
2	3.39	13.2
3	3.15	12.3
4	3.42	13.3
5	3.19	12.4
6	3.40	13.3
Average	3.31 ± 0.16	12.9 ± 0.6

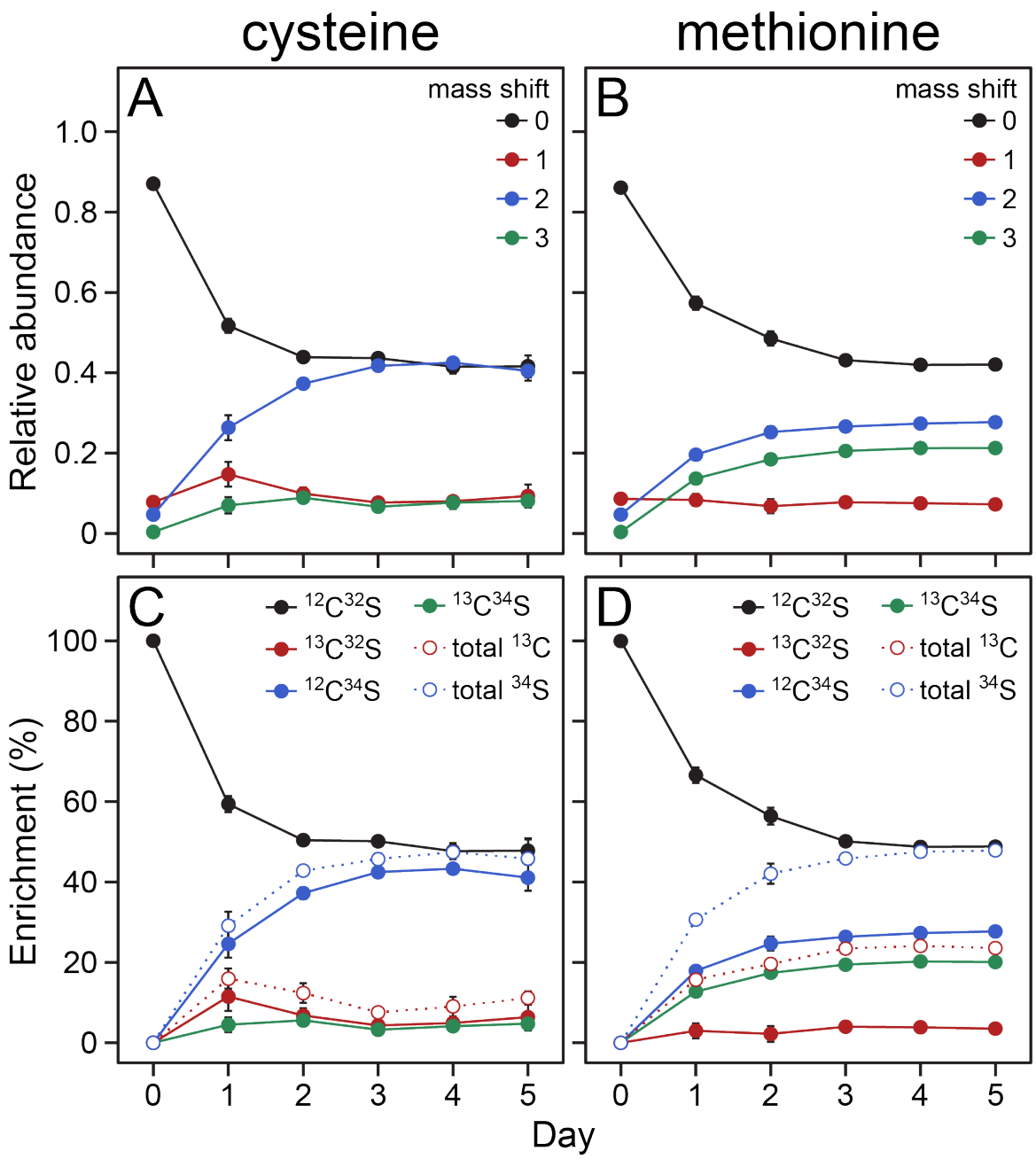

Figure 6-5. Labeling profile of methionine and cysteine. All plots depict the labeling of the cellular methionine and cysteine for the five days following the addition of 100 µM DMSP (50.8 % enriched with [^{13}C][^{34}S]DMSP). For all plots, the data at time = 0 are the calculated natural abundances (A and B) or isotopomer enrichments (C and D), and error bars indicate the 95 % confidence intervals. The relative abundance of the isotopologues with mass shifts between 0 and 3 are shown for cysteine (A) and methionine (B). (A and B) Black indicates mass shift = 0, red indicates mass shift = 1, blue indicates mass shift = 2, and green indicates mass shift = 3. The relative percent enrichments of each isotopomer are shown for cysteine (C) and methionine (D). (C and D) Black indicates unenriched amino acids, red indicates ^{13}C-labeled amino acids, blue indicates ^{34}S-labeled amino acids, green indicates amino acids labeled with both ^{13}C and ^{34}S. Hollow red circles with dotted red lines indicate the total ^{13}C enrichment, and hollow blue circles with dotted blue lines indicate the total ^{34}S enrichment.

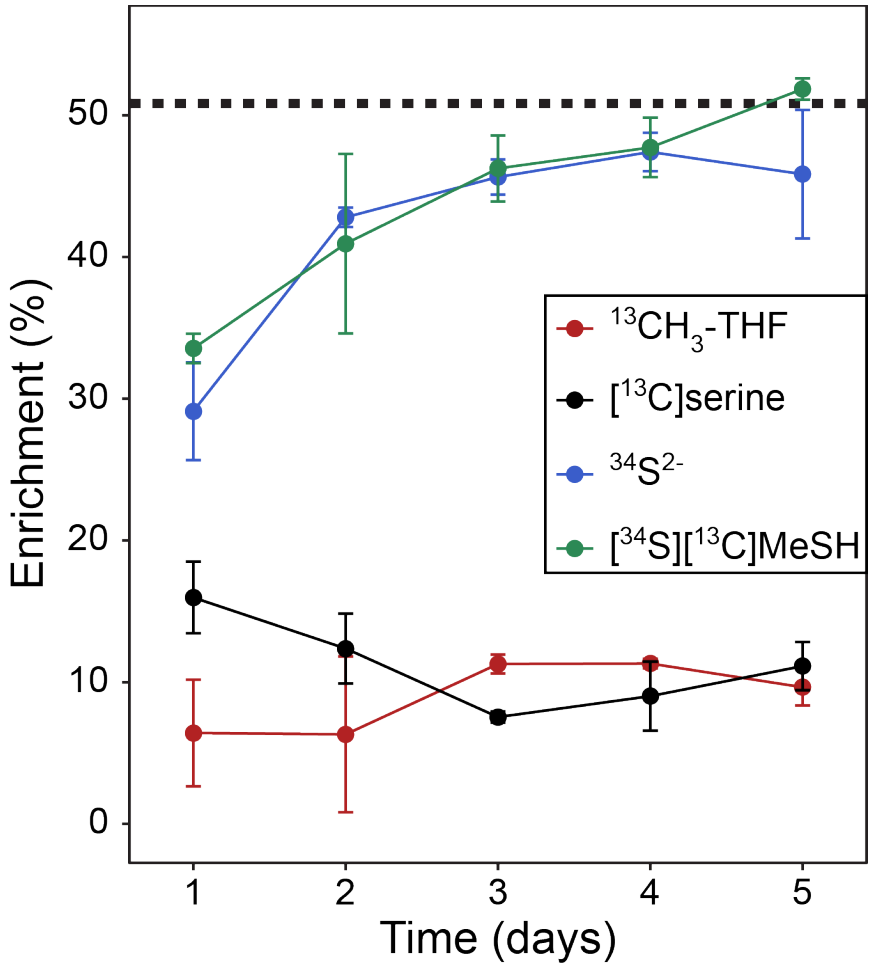

Figure 6-6. Specific labeling of the molecules derived from methyl-THF, serine, sulfide, and methanethiol. The percentages of each pool that was labeled following the addition of DMSP (50.8 % enriched with [^{13}C][^{34}S]DMSP) are shown. The dashed line indicates the percentage of [^{13}C][^{34}S]DMSP and the width of line indicates its 95 % confidence interval. Red indicates the percentage of ^{13}C-labeled methyl-THF, black indicates the percentage of ^{13}C-labled serine, blue indicates the percentage of ^{34}S-labeled sulfide, and green indicates the percentage of doubly-labeled methanethiol. Error bars indicate the 95 % confidence intervals.

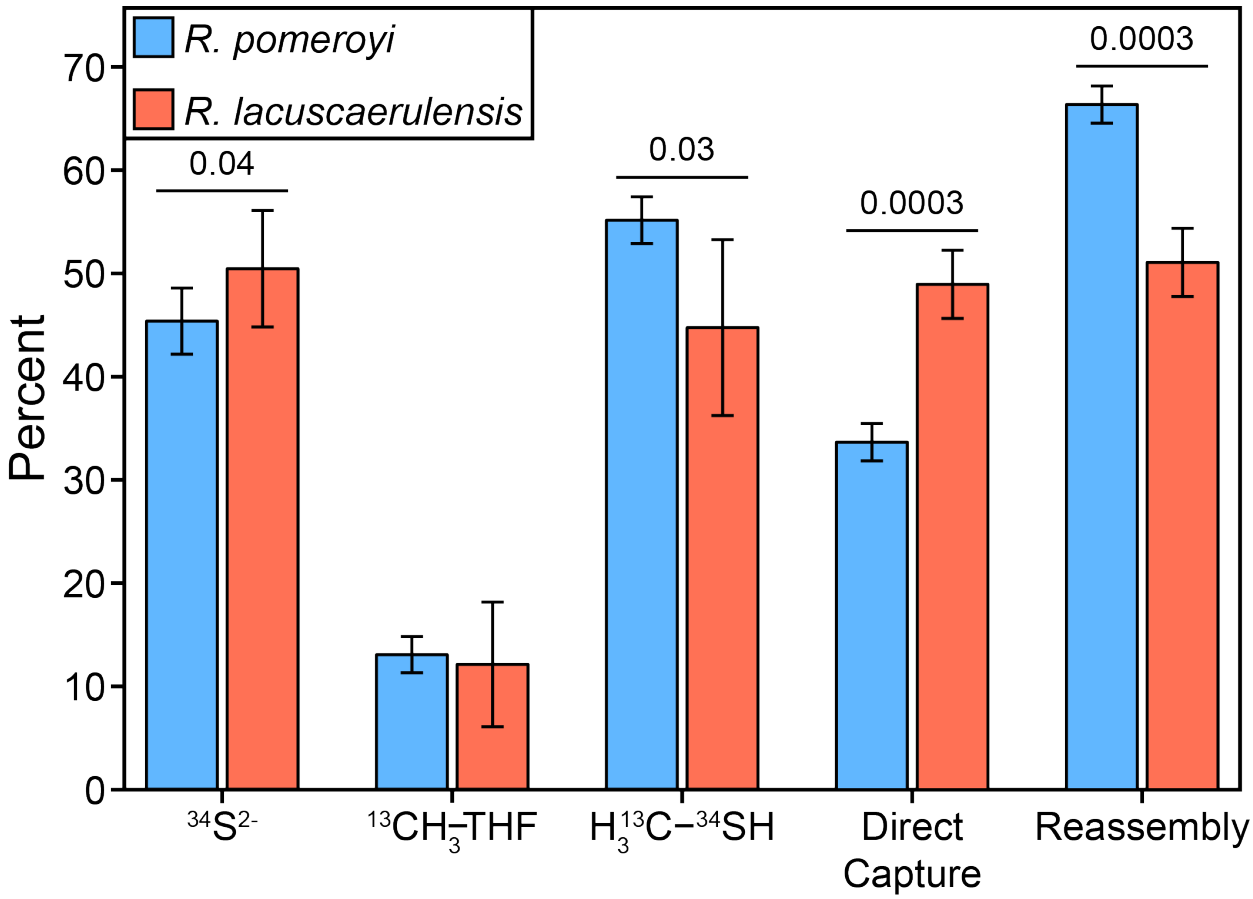

Figure 6-7. Comparison of DMSP metabolism for *R. pomeroyi* and *R. lacuscaerulensis*. Bars indicate either the percentages of each pool that was labeled after five days following the addition of DMSP (50.18 ± 2.24 % enriched with [^{13}C][^{34}S]DMSP), or the percentages of methionine synthesized via the respective pathways. Orange bars indicate *R. lacuscaerulensis* and blue bars indicate *R. pomeroyi*. Errorbars indicate the 95 % confidence intervals. *p*-values < 0.05 are shown above each comparison.

CHAPTER 7

DEGRADATION OF METHIONINE AND *S*-METHYLMETHIONINE IN *RUEGERIA POMEROYI* DSS-3

Introduction

S-methylmethionine (SMM) is an abundant organosulfur compound that is synthesized exclusively by plants via a methyl transfer from *S*-adenosylmethionine to methionine (1). In cells, SMM is converted back to methionine by transferring a methyl group to homocysteine using a different enzyme (1). SMM has been called "vitamin U" due to its ability to heal and prevent peptic ulcers, and it has also been shown to possess anti-inflammatory, analgesic, hypolipidemic, and radioprotective properties and to have a therapeutic effect on gastritis, diaphragmatic hernias, gastric duodenal, liver injuries, gastric ulcers, and renal damage (2-4). In plants, it is present in the free state, and its role is still not clear (1, 5). Because plants lack two negative feedback loops present in other eukaryotes that serve to regulate the synthesis of *S*-adenosylmethionine, it has been hypothesized that SMM is used as a source of free methionine in the event that the too much *S*-adenosylmethionine has been synthesized (1).

The catabolism of SMM has been studied in plants, animals, and bacteria (3, 5-7). In plants and animals, it is converted to dimethylsulfide (DMS) and homoserine or demethylated back to methionine as described above (1, 8). SMM is converted to methionine in *Escherichia coli* by the *S*-methylmethionine:homocysteine methyltransferase, MmuM (7). A soil bacterium has also been isolated that can grow on SMM as the sole carbon source, and it possesses an enzyme capable of producing DMS from SMM (6). However, this enzyme has never been characterized, and its composition and sequence are not known.

DMS is a climatically-active gas and connects the marine and terrestrial sulfur cycles (9). Its oxidation in the upper atmosphere produces sulfur species that promote the formation of "cloud-condensation nuclei", resulting in an increased albedo effect and global cooling (10-13). Because of this, it is imperative to understand all forms of metabolism that produce DMS, including the bacterial production of DMS from SMM.

Methods

Growth experiments. For all growth experiments, a colony was picked into 3 mL of marine basal medium (MBM) supplemented with 2 mM glucose and incubated at 30 ˚C with shaking overnight. The cultures were diluted with sterile 2 % (*w/v*) sea salts solution to an A_{600} of 0.1. Wild-type *R. pomeroyi* DSS-3 was grown as previously described (14). Briefly, 16 µL of the diluted culture (approximately 2×10^6 cells) was used to inoculate 6 mL of MBM supplemented with either 2 mM glucose, 2 mM glucose and 100 µM *S*-methyl-L-methionine iodide, or 2 mM glucose and 100 µM *S*-methyl-DL-methionine chloride. When the headspace was measured, the culture tubes (27.1 mL) were crimp-sealed with a teflon-coated butyl rubber stopper, laid on their sides to maximize the surface area for oxygenation, and incubated at 30 ˚C with shaking. The A_{600}, DMS, and methanethiol were measured over time. For growth experiments without headspace measurement, growth was performed in a 96-well plate (PN: 353072). 2 µL of the diluted culture (approximately 2.5×10^5 cells) was used to inoculate 198 µL of MBM supplemented with one of the following carbon sources: no carbon, 2 mM glucose, 2 mM glucose and 100 µM *S*-methyl-L-methionine iodide, 1 mM *S*-methyl-L-methionine iodide, or 3 mM *S*-methyl-L-methionine iodide. The plate was incubated at 30 ˚C with shaking, and the A_{600} was measured with a SPECTRAmax 384 PLUS (Molecular Devices) plate reader supported by SoftMax Pro 7.0 software.

Measurement of DMS and methanethiol. DMS and methanethiol were measured as previously described (15). Briefly, a gas-tight syringe was used to inject 1 mL of the headspace onto an SRI 8610-C gas chromatograph with a Chromosil 330 column, nitrogen carrier gas with a flow rate of 60 mL min^{-1}, an oven temperature of 60 ˚C, and a flame photometric detector. Under these conditions, DMS and methanethiol had retention times of approximately 1.60 minutes and 1.03 minutes, respectively. A standard curve generated from known amounts of DMS and methanethiol was used to convert peak area to amounts of DMS and methanethiol in the gas phase. The DMS and methanethiol concentrations in the aqueous phase were then calculated by using the distribution coefficient for 10 ppm DMS or methanethiol at 30 ˚C in artificial seawater (16).

Osmolyte analyses. 300 mL of MBM supplemented with 2 mM glucose and 100 µM *S*-methyl-DL-methionine chloride was inoculated with 3 mL of an overnight culture of *R. pomeroyi* DSS-3 grown on MBM supplemented with 2 mM glucose. The culture was incubated at 30 ˚C with shaking to mid-log phase (36 hours). A tube containing sterile medium was also incubated to control for loss of SMM due to abiotic degradation. After incubation, the A_{660} was measured, and the culture was incubated on ice for 30 minutes. A portion of the culture, 4 mL, was saved, and the remainder was centrifuged at 6,000 × g for 40 minutes. A 4 mL portion of the spent medium was saved, and the remainder was discarded. The pellet was resuspended in 20 mL of a sterile 2 % (*w/v*) sea salts solution, and 4 mL of this cell suspension was saved. The remainder was incubated on ice for 10 minutes and then centrifuged at 6,000 × g for 20 minutes. A 4 mL portion of the resulting supernatant was saved, and the remainder was discarded. The pellet was resuspended in 16 mL of a sterile 2 % (*w/v*) sea salts solution. This resulted in seven samples: sterile medium, mid-log culture, spent medium (first supernatant), the pellet (first cell

suspension), sterile wash buffer, wash supernatant (second supernatant), and the washed pellet (second cell suspension).

In order to determine the amount of *S*-methyl-DL-methionine present in each of these samples, 1 mL of each sample was transferred to a 12 mL vial, the vial was crimp-sealed with a teflon-coated butyl rubber stopper, and 1 mL of 4 M NaOH was added with a syringe. The vials were incubated at 104 ˚C for 1 hour to convert the *S*-methyl-DL-methionine to equimolar amounts of DMS and then allowed to cool to room temperature (17). A 1 mL portion of headspace from each of these vials was analyzed as described above. All alkaline hydrolyses and subsequent headspace analyses were repeated in triplicate for each sample. The A_{660} was used to calculate the total dry weight with the following equation:

$$W = 364.74 \times A + 6.7 \times A^2$$

where W is the concentration of dry weight ($\mu g\ mL^{-1}$) and A is the absorbance at 660 nm (18). It was assumed that the dry weight constituted 30 % of the total weight, and that the volume of water was equal to the volume of the cell (19, 20). Intracellular concentrations of *S*-methyl-DL-methionine were then calculated based on this value.

Strain construction. A Δ*megL*::*tetAR* mutant was constructed as previously described (14, 21). Briefly, 1,000-1,500 base pairs of the regions upstream and downstream of *megL* (SPOA0318) and the *tetAR* genes from pRK415 were PCR amplified and cloned into the pCR2.1 vector, which contains a kanamycin marker and is unable to replicate in *R. pomeroyi*. The resulting plasmid was methylated by CpG methyltransferase as recommended by New England Biolabs and electroporated into wild-type *R. pomeroyi* DSS-3. Mutants were selected for tetracycline resistance and screened for kanamycin sensitivity. A disruption of SPOA0317 by a Tn5 transposon was isolated by screening a transposon library (provided by Mary Ann Moran) for colonies capable of growing on 2 mM glucose as the sole carbon source but incapable of

growing on 2.4 mM L-methionine. Transposon insertion sites were identified by isolating genomic DNA from the isolated colonies, and sequencing the DNA with Tn5-specific primers.

Methionine γ-lyase assays. Assays were performed as previously described (22). Briefly, wild-type and mutant strains of *R. pomeroyi* DSS-3 were grown in 5 mL of ½ YTSS medium to mid-log phase, and the A_{660} was measured in order to determine the dry weight as described above. Cells were harvested via centrifugation at 7,000 × g for 20 min at 4 ˚C and resuspended in 3 mL of ice-cold 100 mM potassium phosphate (pH 7.5). Assays were performed in crimp-sealed 12 mL vials that contained 500 µL of 100 mM potassium phosphate (pH 7.5) supplemented with one of the following: nothing, 25 mM L-methionine, 25 mM *S*-methyl-L-methionine iodide, 100 µL 50 % (*w/v*) trichloroacetic acid (TCA), 25 mM L-methionine and 100 µL of 50 % (*w/v*) TCA, or 25 mM *S*-methyl-L-methionine iodide and 100 µL of 50 % (*w/v*) TCA. Assays were started by the addition of 200 µL of cell suspension or sterile 100 mM potassium phosphate (pH 7.5) and incubated at 30 ˚C for 60 minutes. Assays that did not already contain TCA were stopped by the addition of 100 µL of 50 % (*w/v*) TCA. The headspace of the vials was analyzed for the presence of DMS and methanethiol as described above.

***in vitro* assays for DMS production from SMM.** For whole-cell assays, wild-type *R. pomeroyi* DSS-3 was grown in 50 mL of MBM supplemented with either 2 mM glucose or 3 mM dimethylsulfoniopropionate (DMSP) and incubated at 30 ˚C with shaking for 48 hours. The glucose culture was used to inoculate 500 mL of MBM supplemented with either 2 mM glucose or 2 mM glucose and 100 µM *S*-methyl-L-methionine iodide, and 5 mL of the DMSP culture was used to inoculate 500 mL of MBM supplemented with 3 mM DMSP. The cultures were incubated at 30 ˚C with shaking until mid-log phase, and the A_{660} was recorded in order to calculate the total dry weight as described above. Cell pellets were harvested via centrifugation, washed with 2 % (*w/v*) sea salts in 80 mM HEPES (pH 6.8), and stored at -80 ˚C. Pellets were

resuspended in 2 % (*w/v*) sea salts in 80 mM HEPES (pH 6.8) for a final concentration of 8 mg dry weight per mL. 500 µL assays were performed in 12 mL vials containing 2 % (*w/v*) sea salts in 80 mM HEPES (pH 6.8) supplemented with one of the following: nothing, 1 mM *S*-methyl-DL-methionine chloride, 10 mM *S*-methyl-DL-methionine chloride, 100 µL 50 % (*w/v*) TCA, 1 mM *S*-methyl-DL-methionine chloride and 100 µL 50 % (*w/v*) TCA, or 10 mM *S*-methyl-DL-methionine chloride and 100 µL 50 % (*w/v*) TCA. Assays were started by the addition of 100 µL of either a cell suspension or 2 % (*w/v*) sea salts in 80 mM HEPES (pH 6.8) and incubated at 30 ˚C for 60 minutes. Assays that did not already contain TCA were stopped by the addition of 100 µL of 50 % (*w/v*) TCA. The headspace was analyzed for the presence of DMS as described above. The remaining cell suspensions were pelleted and stored at -80 ˚C.

For cell-free assays, the pelleted cells from the whole-cell assays were resuspended in buffer composed of 2 % (*w/v*) sea salts, 20 % (*v/v*) glycerol, 500 µM polymethylsulfonyl fluoride, and 80 mM HEPES (pH 6.8). Cells were lysed three times via French press at 14.5 kPsi (100,000 kPa) (14). The cell lysate was centrifuged at 35,000 × g for 45 minutes, and the supernatant was passed through a 0.2 µm filter to remove any remaining cellular debris. Assays were performed on the whole cells, the cell lysate, and the cell-free lysate with identical conditions as those described above with the exception that activity on 10 mM *S*-methyl-L-methionine chloride was not examined.

TLC analysis of *S*-methyl-DL-methionine. L-methionine and *S*-methyl-DL-methionone were separated on TLC as described previously (23, 24). Briefly, 2 µL of 0.1 % (*w/v*) L-methionine (2 µg) and 2 µL of 1 % (*w/v*) *S*-methyl-DL-methionine (20 µg) were spotted onto an aluminum-backed silica gel (250 µm layer) TLC plate (Whatman; PN: 4420 222) and allowed to dry. The plate was developed for approximately 4 hours in a chamber that had been equilibrated overnight with a mobile phase composed of 50 % (*v/v*) of 30 % ammonium

hydroxide and 95 % ethanol. Once dry, 0.2 % (*w/v*) ninhydrin in 100 % ethanol was sprayed onto the plate, which was then incubated at 100 ˚C until a red color appeared.

Results

Growth in the presence of SMM. Previous experiments demonstrated that *R. pomeroyi* produced methanethiol when grown in the presence of L-methionine (25). However, it was not known if *R. pomeroyi* could grow on *S*-methylmethionine (SMM). An experiment with the bacterioplankton in seawater indicated the DMSP might be formed from SMM (Kiene, personal communication). To investigate this further, *R. pomeroyi* was grown in minimal medium containing 2 mM glucose and supplemented with 100 µM *S*-methyl-L-methionine. Although *R. pomeroyi* converted approximately 65 % of the *S*-methyl-L-methionine to DMS, no methanethiol was produced (Fig. 7-1). Furthermore, methanethiol production during growth on L-methionine did not vary between the wild-type strain and a mutant with a deletion of *dmdD*, the enzyme responsible for producing methanethiol from DMSP (data not shown). Combined with the fact that limited alkaline hydrolysis of the cultures did not yield an increase in DMS (data not shown), these data indicated that *R. pomeroyi* did not convert *S*-methyl-L-methionine to DMSP.

S-methyl-L-methionine is quite expensive, but a racemic mixture of *S*-methyl-DL-methionine is relatively inexpensive. Because of this, the growth of *R. pomeroyi* on the racemic mixture was also investigated. Surprisingly, nearly 15 % of the racemic mixture provided was converted to methanethiol, but the amount of DMS produced was still approximately 65 % (Fig. 7-1). In order to rule out the possibility that the racemic mixture was contaminated with methionine, its purity was examined with thin-layer chromatography (Fig. 7-2). Methionine contamination was not observed even under conditions where 10 % contamination would have been readily detected.

SMM as an osmolyte. Previous studies have shown that marine bacteria use DMSP as an intracellular osmolyte (11). Intracellular DMSP concentrations between 38 mM and 1 M have been observed in marine phytoplankton and 850 μM in microbial mats (12). Because SMM is structurally similar to DMSP and because up to 35 % of the SMM was not converted to either DMS or methanethiol, it was hypothesized that *R. pomeroyi* could be using SMM as an osmoregulatory compound. To test this, the SMM content of cells grown in the presence of *S*-methyl-DL-methionine was measured. The cells contained intracellular SMM concentrations of roughly 960 μM, and this dropped to roughly 630 μM after washing the pellet with buffer (Table 7-1). This suggested that although SMM was actively transported into the cell, it was probably not functioning as a major osmolyte in *R. pomeroyi*.

Assaying the conversion of SMM to DMS *in vitro*. After the initial observation that *S*-methyl-L-methionine was converted DMS, it was hypothesized that the protein responsible was MegL (SPOA0318) (Scheme 7-1). To test this hypothesis, a Δ*megL* mutant was constructed. At the same time, a mutant was isolated containing a Tn5 transposon inserted in the upstream gene (SPOA0317). This gene was annotated as a transcriptional regulator, and it was hypothesized to regulate the expression of *megL*. Whole-cells were incubated with either L-methionine or *S*-methyl-L-methionine, and the headspace was analyzed for the presence of either methanethiol or DMS, respectively (Fig. 7-3). In the mutants, the methanethiol from methionine but not DMS from SMM was greatly reduced. This demonstrated that MegL was responsible for the majority of methanethiol produced during growth on L-methionine (Fig. 7-3A). However, it also indicated that MegL was not responsible for DMS production during growth in the presence of SMM (Fig. 7-3B). The specific activity with 25 mM *S*-methyl-L-methionine was quite low, so other concentrations were tested. Higher activity was found with 1 mM *S*-methyl-L-methionine than 25 mM (Fig. 7-4). DMS production following growth on other carbon sources was also tested to

determine if the activity was constitutive. Figure 7-4 shows activity was high following growth on glucose, suggesting that the activity was constitutive. When cells were grown in the presence of either 100μM DMSP or 100μM SMM, large quantities of these organosulfur compounds were carried over, which made it impossible to determine how much DMS was produced from the SMM provided in the assays as opposed to DMS produced from the retained organosulfur compounds (Fig. 7-4).

With this knowledge, attempts were made at obtaining activity from cell-free lysates. If possible, this would allow for the fractionation of proteins and lead to the subsequent identification of the protein(s) responsible for facilitating the reaction(s). Unfortunately, neither sonication (data not shown), bead-beating (data not shown), freeze-thaw (data not shown), nor French-pressing resulted in cell-free extracts that possessed high levels of the desired activity (Fig. 7-5).

Growth on SMM as a sole carbon source. Another possible method to identify the gene(s) responsible for the conversion of *S*-methyl-L-methionine to DMS was transposon mutagenesis. However, in order to be able to rapidly screen plates for colonies that could not grow on SMM, it was necessary to determine if the WT strain could grow on SMM as a sole carbon source. Unfortunately, no growth was observed on media containing either 1 mM or 3 mM *S*-methyl-L-methionine as the sole carbon source (Fig. 7-6) even after 200 hours of incubation (data not shown). Furthermore, growth on minimal medium supplemented with 2 mM glucose and 3 mM *S*-methyl-L-methionine was not different from growth on minimal medium supplemented with 2 mM glucose. The same was true for medium supplemented with the racemic mixture of SMM (data not shown). Taken together, this indicated that although *R. pomeroyi* can convert SMM to DMS, it cannot utilize it as a sole carbon and energy source. Thus, it is not possible to screen a transposon-mutant pool for the inability to grow on SMM.

Conclusions

Although SMM was not converted to DMSP, the production of methanethiol was observed during growth on the racemic mixture of SMM. The current hypothesis is that the D-isomer can interact with DmdA to produce D-methionine, which is then converted to methanethiol via MegL. In contrast, the L-isomer is sterically hindered and cannot undergo the same reaction. Unfortunately, the Δ*megL* strain does not grow well in minimal medium and cannot be used to test the hypothesis. To test this, *in vitro* assays with purified DmdA have been planned to determine if THF becomes methylated in the presence of *S*-methyl-D-methionine.

Although *R. pomeroyi* cannot use SMM as a sole carbon source, it may be possible to develop a strain that can. If this reaction is facilitated by one or more of the DMSP-lyases in *R. pomeroyi* (DddP, DddQ, or DddW), then vinylglycine would be formed from SMM (Scheme 7-2). Vinylglycine is known to act as a suicide inactivator for several pyridoxal-dependent enzymes by irreversibly binding to the target protein (26). However, cystathionine γ-synthetase (MetB) from *Salmonella enterica* is capable forming both α-ketobutyrate and cystathionine from vinylglycine (26). Because *R. pomeroyi* does not possess a homologue for this gene, it may be possible to introduce *metB* on a plasmid and confer the ability to utilize SMM as a sole carbon source. Should this prove successful, then a transposon mutant pool could be transformed with the plasmid and screened for colonies that can no longer utilize SMM as a sole carbon source.

Another possibility would be to introduce an *R. pomeroyi* genome library into a *S. enterica* indicator strain, and then select for colonies that are capable of growing in the presence of *S*-methyl-L-methionine. Previous research has shown that a *S. enterica* Δ*metA* strain is auxotrophic for methionine, but L-vinylglycine can restore growth (26). A second study demonstrated that *E. coli* is capable of converting *S*-methyl-L-methionine to L-methionine with the use of a permease, encoded by *mmuP*, and a demethylase, encoded by *mmuM* (7). Initial

experiments have demonstrated that *S. enterica metA*-53 requires either L-methionine or vinylglycine for growth and cannot grow in the presence of *S*-methyl-L-methionine, even when *mmuP* from *E. coli* is provided on a plasmid (data not shown). Because of this, this strain is suitable for screening an *R. pomeroyi* genomic library for gene(s) capable of converting *S*-methyl-L-methionine to L-vinylglycine and DMS. One last alternative would be to screen individual *R. pomeroyi* colonies from a transposon mutant pool for their inability to produce DMS from SMM, although this experiment would likely require the screening of thousands of colonies and would be very labor intensive.

References

1. Ranocha P, McNeil SD, Ziemak MJ, Li C, Tarczynski MC, Hanson AD. 2001. The *S*-methylmethionine cycle in angiosperms: ubiquity, antiquity and activity. The Plant Journal 25:575-584.
2. Meinders A. 1955. Vitamin-U. Journal of the American Medical Association 157:1458-1458.
3. Gessler NN, Bezzubov AA, Podlepa EM, Bykhovskii VY. 1991. Metabolism of *S*-methylmethionine (vitamin U) in animals. Applied Biochemistry and Microbiology 27:275-280.
4. Oktay S, Bayrak G, Alev B, Ipekci H, Ustundag UV, Turkyilmaz IB, Pisiriciler R, Emekli-Alturfan E, Tunali-Akbay T, Yanardag R, Yarat A. 2018. The effect of vitamin U on the lung tissue of pentyleneterazole-induced seizures in rats. Naunyn-Schmiedebergs Archives of Pharmacology 391:177-184.
5. Gessler NN, Bezzubov AA, Podlepa EM, Bykhovskii VY. 1991. *S*-methylmethionine (vitamin U) metabolism in plants. Applied Biochemistry and Microbiology:192-199.

6. Mazelis M, Levin B, Mallinson N. 1965. Decomposition of methyl methionine sulfonium salts by a bacterial enzyme. Biochimica et Biophysica Acta 105:106-14.

7. Thanbichler M, Neuhierl B, Bock A. 1999. *S*-methylmethionine metabolism in *Escherichia coli*. Journal of Bacteriology 181:662-5.

8. Gessler NN, Bezzubov AA. 1988. *S*-methylmethionine sulfonium hydrolase activity in plant and animal tissues. Applied Biochemistry and Microbiology 24:200-205.

9. Lovelock JE, Maggs RJ, Rasmussen RA. 1972. Atmospheric dimethyl sulphide and the natural sulphur cycle. Nature 237:452.

10. Hatakeyama S, Okuda M, Akimoto H. 1982. Formation of sulfur dioxide and methanesulfonic acid in the photooxidation of dimethyl sulfide in the air. Geophysical Research Letters 9:583-586.

11. Reisch CR, Moran MA, Whitman WB. 2011. Bacterial catabolism of dimethylsulfoniopropionate (DMSP). Frontiers in Microbiology 2:172.

12. Yoch DC. 2002. Dimethylsulfoniopropionate: its sources, role in the marine food web, and biological degradation to dimethylsulfide. Applied and Environmental Microbiology 68:5804-5815.

13. Charlson RJ, Lovelock JE, Andreae MO, Warren SG. 1987. Oceanic phytoplankton, atmospheric sulphur, cloud albedo and climate. Nature 326:655.

14. Reisch CR, Stoudemayer MJ, Varaljay VA, Amster IJ, Moran MA, Whitman WB. 2011. Novel pathway for assimilation of dimethylsulphoniopropionate widespread in marine bacteria. Nature 473:208-11.

15. Reisch CR, Crabb WM, Gifford SM, Teng Q, Stoudemayer MJ, Moran MA, Whitman WB. 2013. Metabolism of dimethylsulphoniopropionate by *Ruegeria pomeroyi* DSS-3. Molecular Microbiology 89:774-91.

16. Przyjazny A, Janicki W, Chrzanowski W, Staszewski R. 1983. Headspace gas chromatographic determination of distribution coefficients of selected organosulfur compounds and their dependence on some parameters. Journal of Chromatography 280:249-260.

17. Segurel MA, Razungles AJ, Riou C, Trigueiro MG, Baumes RL. 2005. Ability of possible DMS precursors to release DMS during wine aging and in the conditions of heat-alkaline treatment. Journal of Agricultural and Food Chemistry 53:2637-45.

18. Koch AL. 2007. Growth Measurement, p 179-199. *In* Reddy CA, Beveridge TJ, Breznak JA, Marzluf GA, Schmidt TM, Snyder LR (ed), Methods for General and Molecular Microbiology, 3rd ed. American Society for Microbiology, Washington, D.C.

19. Neidhardt FC, Ingraham JL, Schaechter M. 1990. Physiology of the bacterial cell: a molecular approach. Sinauer Associates, Inc., Sunderland, Mass.

20. Reisch CR, Moran MA, Whitman WB. 2008. Dimethylsulfoniopropionate-dependent demethylase (DmdA) from *Pelagibacter ubique* and *Silicibacter pomeroyi*. Journal of Bacteriology 190:8018-8024.

21. Henriksen JR. 2008. Physiology of dimethylsulfoniopropionate metabolism in a model marine roseobacer, *Silicibacter pomeroyi*. Doctor of Philosophy. University of Georgia, Athens, GA.

22. Takakura T, Mitsushima K, Yagi S, Inagaki K, Tanaka H, Esaki N, Soda K, Takimoto A. 2004. Assay method for antitumor L-methionine gamma-lyase: comprehensive kinetic analysis of the complex reaction with L-methionine. Analytical Biochemistry 327:233-40.

23. Brenner M, Niederwieser A, Pataki G. 1969. Amino Acids and Derivatives, p 730-786. *In* Stahl E (ed), Thin-layer chromatography: a laboratory handbook, 2nd ed. Springer.

24. Keenan TW, Lindsay RC. 1968. Evidence for a dimethyl sulfide precursor in milk. Journal of Dairy Science 51:112-&.

25. Crabb W. 2010. Metabolism of organosulfur compounds in *Ruegeria pomeroyi* DSS-3. Master of Science. University of Georgia, Athens, Georgia.

26. Johnston M, Marcotte P, Donovan J, Walsh C. 1979. Mechanistic studies with vinylglycine and *β*-haloaminobutyrates as substrates for cystathionine *γ*-synthetase from *Salmonella typhimurium*. Biochemistry 18:1729-38.

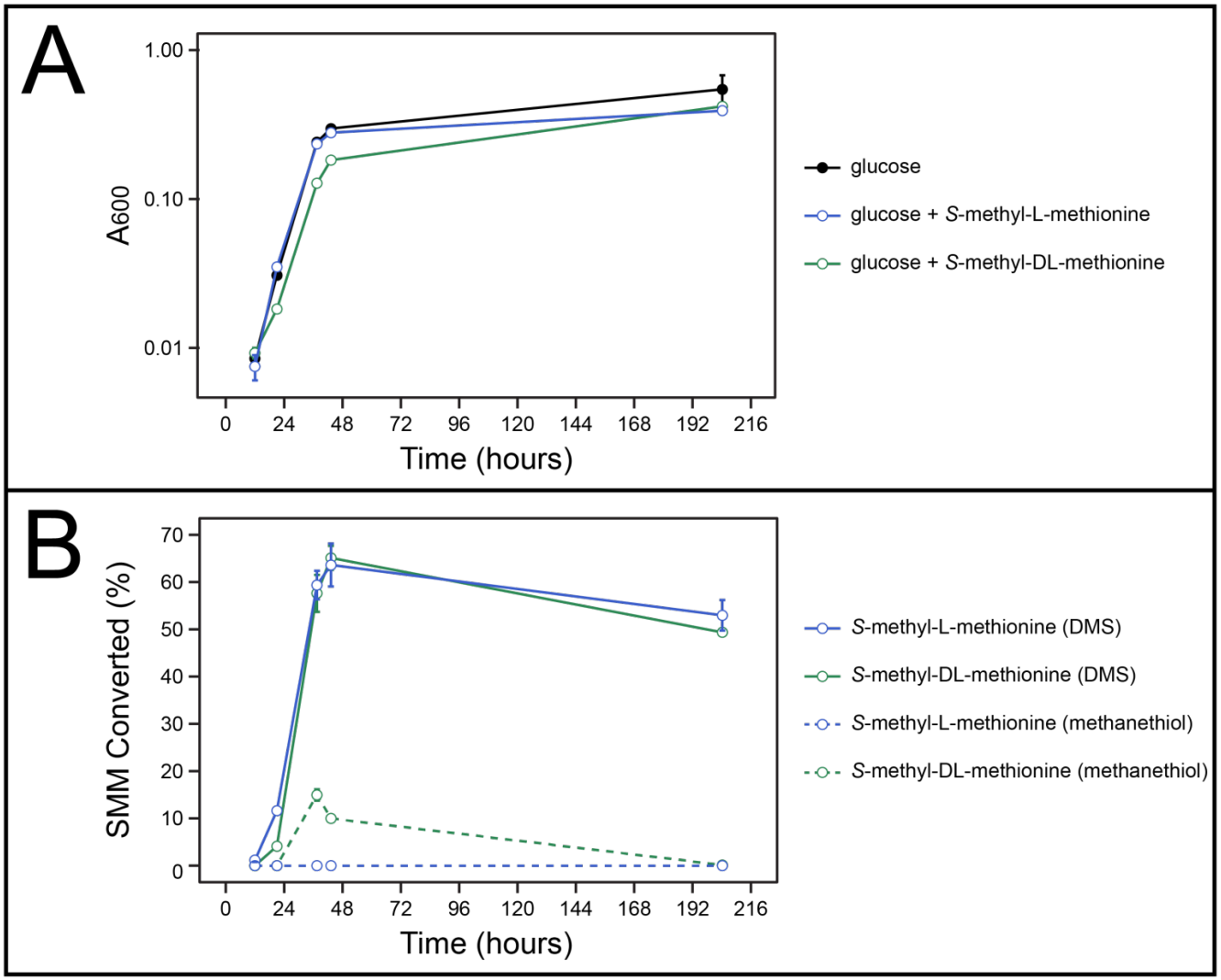

Figure 7-1. Growth and gas production from SMM stereoisomers by *Ruegeria pomeroyi* DSS-3. The horizontal axis indicates time. (A) Growth on: black, MBM supplemented with 2mM glucose only; blue, MBM supplemented 2 mM glucose and 100 µM *S*-methyl-L-methionine; and green, MBM supplemented with 2 mM glucose and 100 µM *S*-methyl-DL-methionine. (B) Gas production. Solid lines indicate the percent of SMM converted to DMS. Dashed lines indicate the percent of SMM converted to methanethiol.

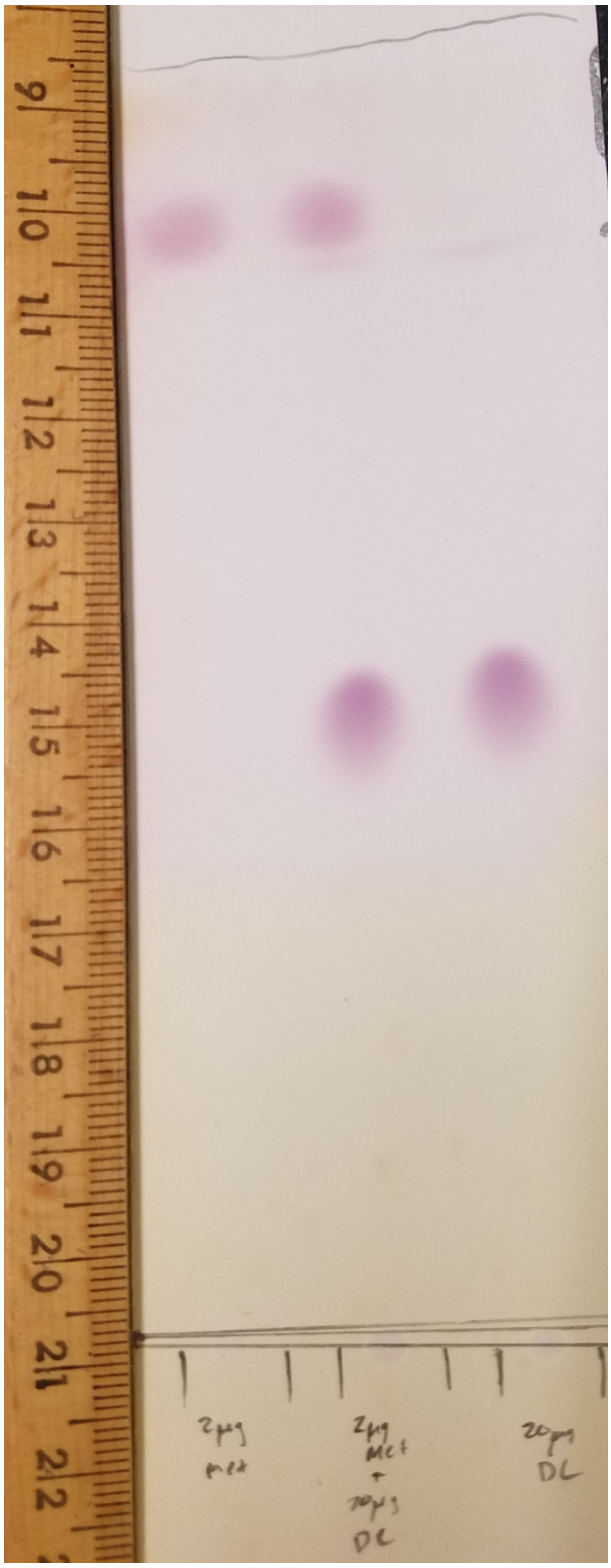

Figure 7-2. Thin-layer chromatography of L-methionine and *S*-methyl-DL-methionine. The left lane contains 2 µg of L-methionine ($R_f = 0.87$). The middle lane contains 2 µg of L-methionine ($R_f = 0.87$) and 20 µg of *S*-methyl-DL-methionine ($R_f = 0.46$). The right lane contains 20 µg of *S*-methyl-DL-methionine ($R_f = 0.48$). A ruler has been provided for scale.

Table 7-1. Intracellular and extracellular *S*-methyl-DL-methionine concentrations. Values are reported as the mean of three independent replicates following growth with 2 mM glucose and 100 µM *S*-methyl-DL-methionine chloride . The error indicates the standard error of the mean.

Sample	Total (µmol)	Fraction (%)	Concentration (µM)
Sterile medium	34.1 ± 1.2	100.0	114 ± 4
Culture	10.2 ± 0.6	30.0 ± 2.1	34 ± 2
Pellet	10.1 ± 0.5	30.0 ± 1.8	961 ± 50*
Spent medium	15.2 ± 0.5	45.0 ± 2.1	51 ± 1
Wash buffer	0	0	0
Washed pellet	6.6 ± 0.2	19.4 ± 0.1	628 ± 18*
Wash supernatant	0	0	0

*: Reported values are the calculated intracellular concentrations based on the amount of dry weight as determined by A_{660}.

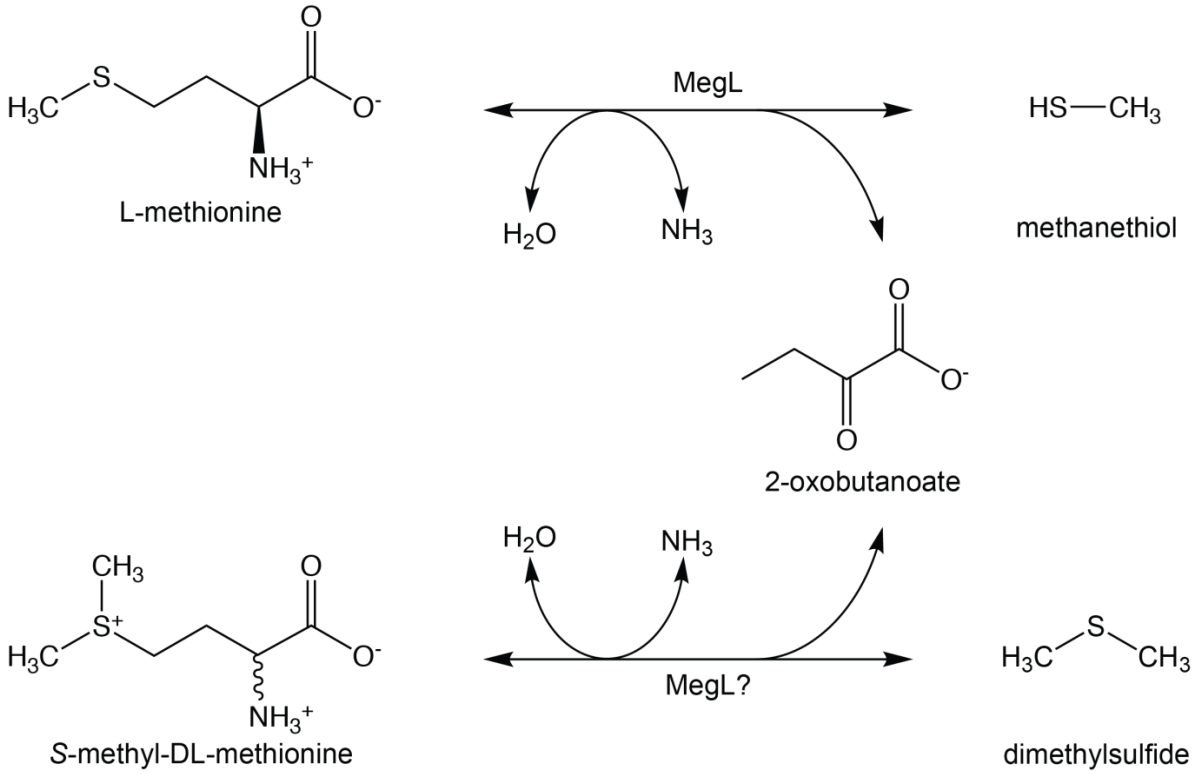

Scheme 7-1. Methionine γ-lyase reactions. Methionine γ-lyase (MegL) is known to facilitate the conversion of L-methionine to methanethiol (top reaction). It was hypothesized that MegL in *R. pomeroyi* (SPOA0318) could also facilitate the conversion of *S*-methyl-DL-methionine to DMS (bottom reaction).

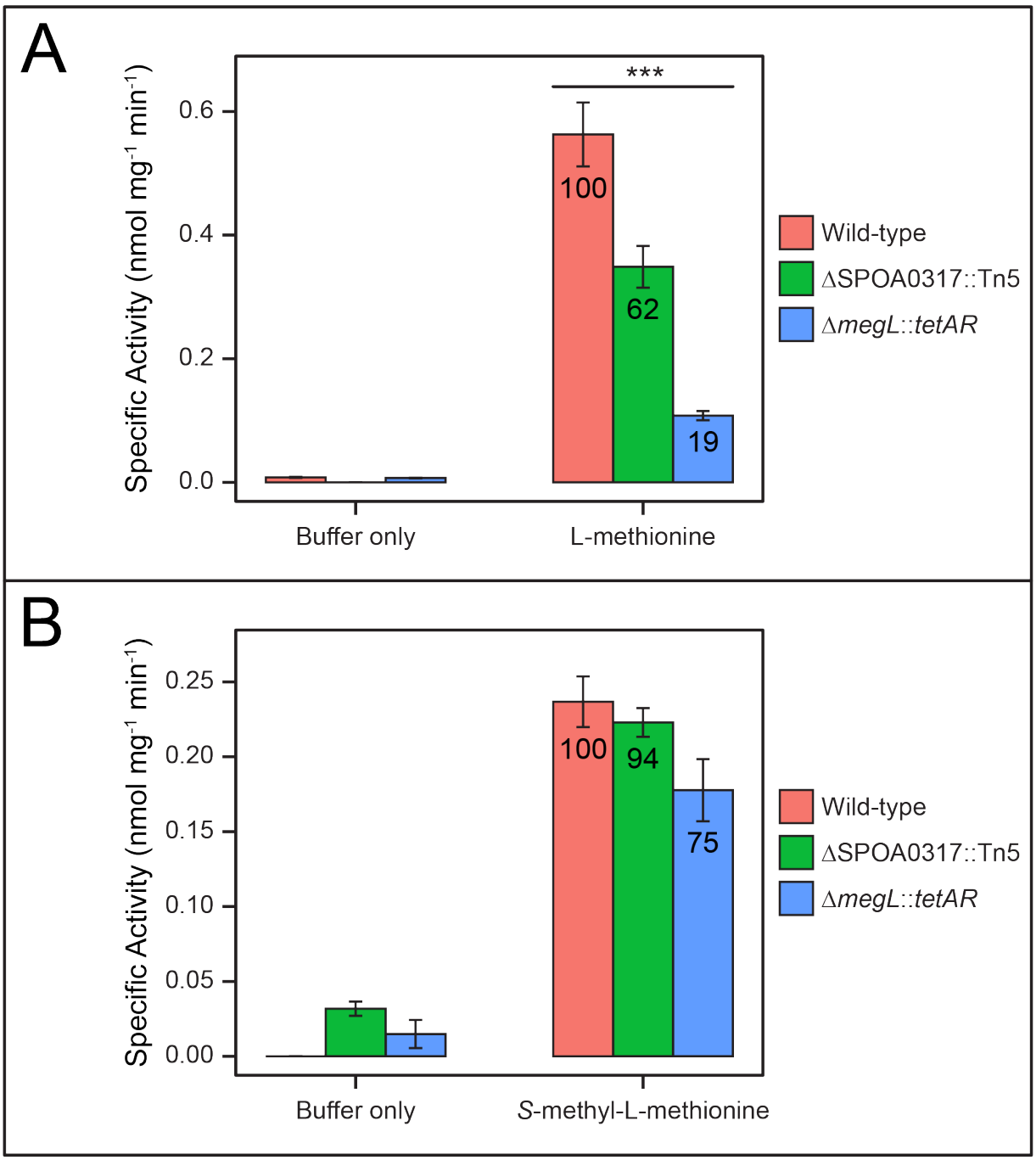

Figure 7-3. Whole-cell assays of methionine γ-lyase activity in *R. pomeroyi* strains. The vertical axis shows the mean specific activity (nmol mg of dry weight^{-1} minute^{-1}) for three independent replicates. Error bars indicate the standard error of the mean. Red bars indicate the activity of the wild-type strain. Green bars indicate the activity of the ΔSPOA0317::Tn5 strain. Blue bars indicate the activity of the Δ*megL*::*tetAR* (SPOA0318) strain. Percentages indicate the relative mean activity as compared to the wild-type strain. (A) Methanethiol production from either buffer only or 25 mM L-methionine. Values for 25 mM L-methionine are statistically different between strains (p = 0.00037). (B) DMS production from either buffer only or 25 mM *S*-methyl-L-methionine. Values for 25 mM *S*-methyl-L-methionine are not statistically different between strains (p = 0.0967).

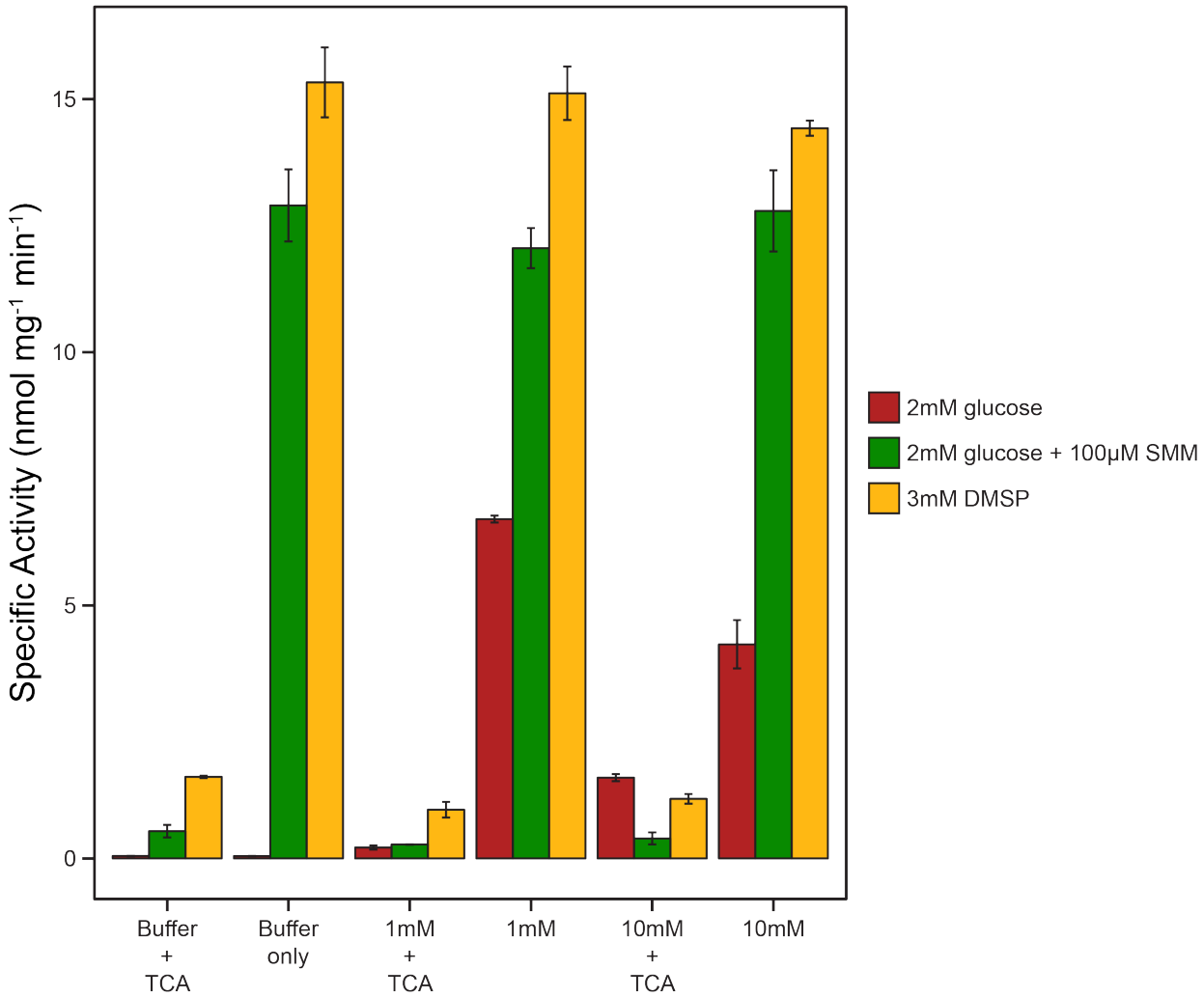

Figure 7-4. Whole-cell assays for the conversion of *S*-methyl-DL-methionine to DMS in *R. pomeroyi*. The vertical axis shows the mean specific activity [nmol DMS formed (mg of dry weight)$^{-1}$ (min)$^{-1}$] for four independent replicates. The horizontal axis indicates the contents of the assay (and concentration of *S*-methyl-L-methionine) prior to the addition of whole cells. Error bars indicate the standard error of the mean. Red bars indicate the activity of wild-type cells grown on MBM supplemented with 2 mM glucose. Green bars indicate the activity of wild-type cells grown on MBM supplemented with 2 mM glucose and 100 µM *S*-methyl-DL-methionine. Yellow bars indicate the activity of wild-type cells grown on MBM supplemented with 3 mM DMSP.

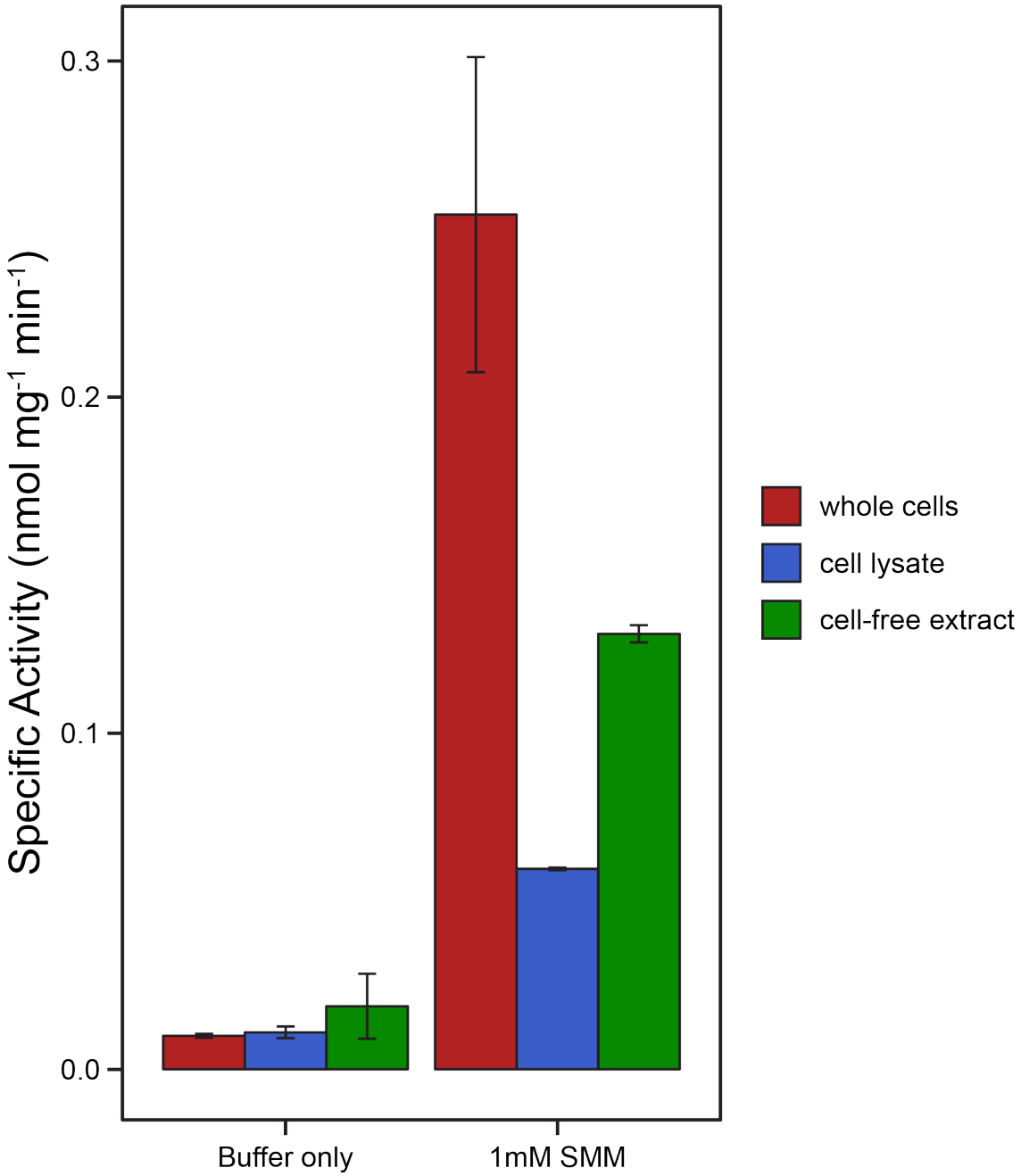

Figure 7-5. Cell-free assays for the conversion of *S*-methyl-DL-methionine to DMS in *R. pomeroyi*. The vertical axis shows the mean specific [nmol DMS (mg of dry weight)$^{-1}$ (min)$^{-1}$] for three independent replicates. The horizontal axis indicates the contents of the assay prior to the addition of cell material. Error bars indicate the standard error of the mean. Red bars indicate the activity of whole cells. Blue bars indicate the activity of the cell lysate. Green bars indicate the activity of the cell-free extract.

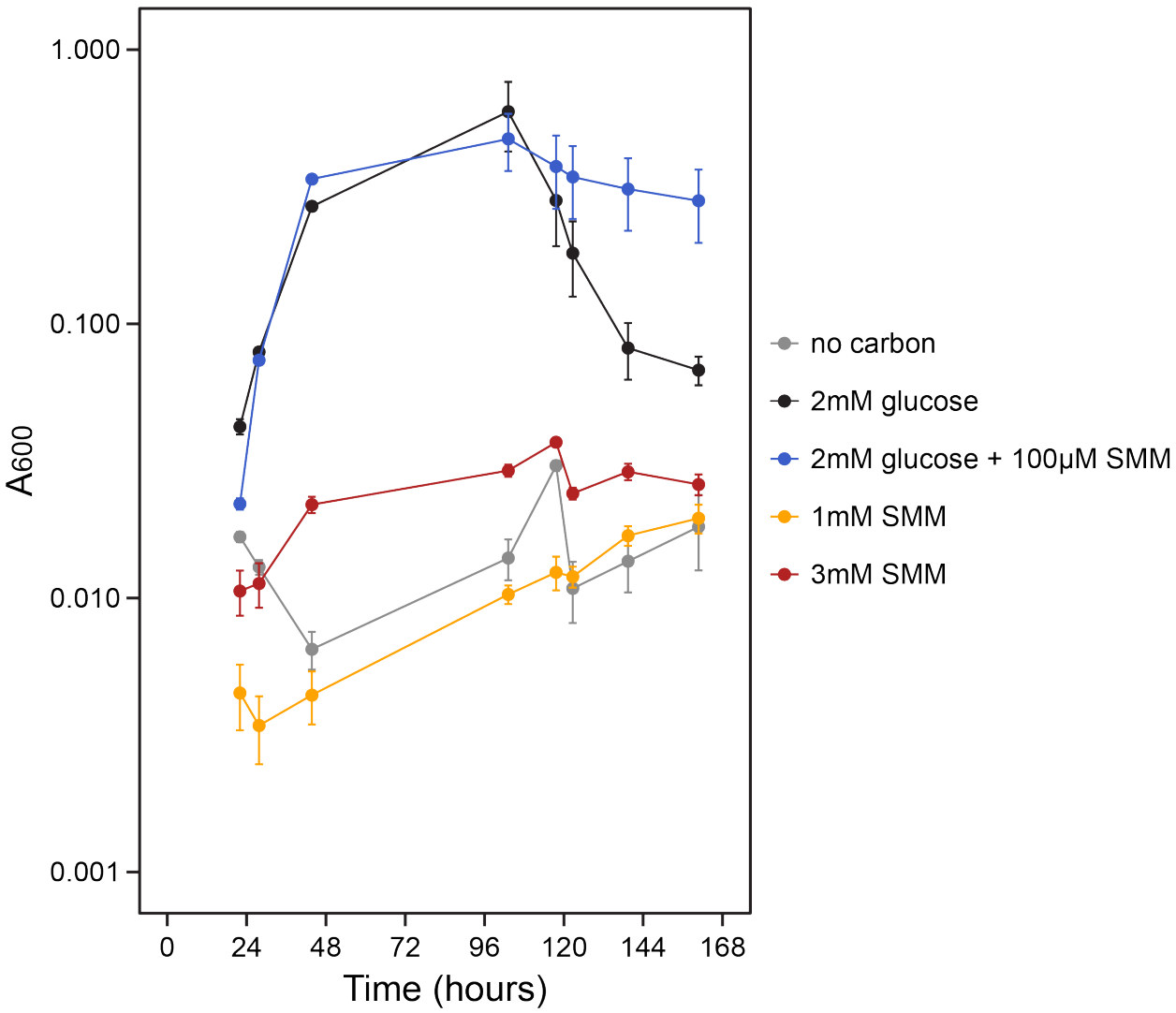

Figure 7-6. Growth of *R. pomeroyi* DSS-3 with *S*-methyl-L-methionine as the sole carbon source. The vertical axis indicates growth of *R. pomeroyi* as measured by the change in absorbance at 600 nm. Points indicate the mean of four independent replicates. Error bars indicate the standard error of the mean. Grey indicates growth on MBM with no added carbon source. Black indicates growth on MBM supplemented with 2 mM glucose. Blue indicates growth on MBM supplemented with 2 mM glucose and 100 µM *S*-methyl-L-methionine. Yellow indicates growth on MBM supplemented with 1 mM *S*-methyl-L-methionine. Red indicates growth on MBM supplemented with 3 mM *S*-methyl-L-methionine.

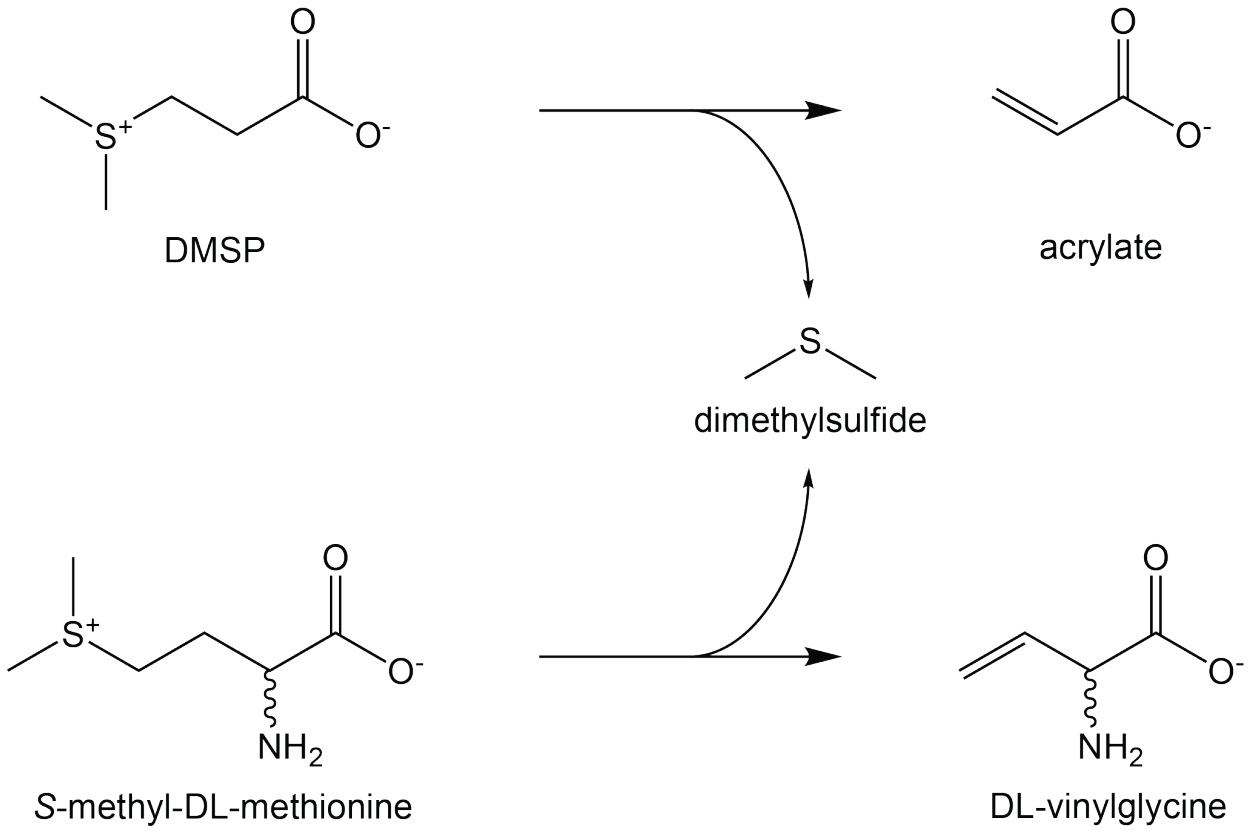

Scheme 7-2. Proposed pathway for the production of DMS from *S*-methyl-DL-methionine. The top reaction is catalyzed by DMSP-lyases (DddP, DddQ, DddW) in *R. pomeroyi* DSS-3. The bottom reaction is proposed to occur by the interaction of SMM with the DMSP-lyases.

CHAPTER 8

CONCLUSIONS

Phylogeny of the roseobacter group. Prior to the analyses outlined in Chapter 2, 16S rRNA gene sequence identity was the primary basis for the taxonomic assignment of the members of the roseobacter group to their respective genera. The net result was a taxonomy that did not represent the evolution of the group. This claim was supported by the low cophenetic correlation coefficient that was observed in the 16S rRNA gene sequence identity (0.72) and by the fact that it was not correlated with the cophenetic distances of a maximum likelihood phylogenetic tree based on the most conserved core genes ($r = 0.40$). Recently, whole-genome sequences have become available for many of the type strains within the roseobacter group, enabling the construction a taxonomy that more accurately reflected the evolution of the group.

Initially, a clade from the ARB-Silva 16S rRNA gene tree containing 29 genera was used to select the organisms for analysis, but this methodology was inherently flawed as there was a strong possibility that closely related genera were absent from this clade. To address this problem, a better phylogenetic marker was identified, RpoC, that possessed both a high cophenetic correlation coefficient (0.94) and was highly correlated with the cophenetic distances of the core gene tree (0.94). Using the RpoC protein sequences as a phylogenetic marker, 5 additional closely related genera were identified and added to the analysis, resulting in a total of 108 species representing 36 genera.

For the 82 species with whole-genome sequences available, multiple analyses were performed in an attempt to delimit the genera within this group of organisms. These included phylogenetic reconstruction of a maximum likelihood tree and the calculation of the average

amino acid identity of the core genes (cAAI), percentage of conserved proteins (POCP), and the average nucleotide identity (ANI). Evaluation of these methods indicated that cAAI was the most informative method as it possessed both a high cophenetic correlation coefficient (0.98) and was highly correlated with the cophenetic distances of the core gene tree ($r = 0.95$). Furthermore, previous research had indicated that average amino acid identity was suitable for delimiting higher taxonomic ranks. By applying a gradient of cAAI values as the threshold for genus delineation and comparing these delineations to the topology of the maximum likelihood tree, several taxonomic reassignments were proposed. Species were removed from the genera *Aestuariivita*, *Loktanella*, *Ruegeria*, *Thalassobius*, and *Tropicibacter*. These proposals also removed all validly published species from the genera *Citreicella*, *Nautella*, *Pelagibaca*, and *Thiobacimonas*. Some of these species were moved into the genera *Epibacterium*, *Phaeobacter*, *Ruegeria*, *Salipiger*, or *Shimia*, while others were moved into the novel genera *Cognatishimia*, *Cognatiyoonia*, *Flavimaricola*, *Limimaricola*, *Pseudaestuariivita*, or *Yoonia*. Furthermore, the proposed taxonomy resulted in genera that formed monophyletic clades in a maximum likelihood tree based on the most conserved core genes.

Importantly, the methods used to delimit genera in the roseobacter group were relatively simple, mostly automated, and easy to reproduce without extensive experience in bioinformatics. Because of this, these methods may be applicable to many other prokaryotic genera, although the thresholds for delineation will likely differ between different taxonomic groups. A previous study proposed the use of a universal cut-off of 50 % POCP for bacterial genera, but this was demonstrated to be inappropriate as a universal cut-off (see Chapter 2 for more details).

Following this extensive taxonomic rearrangement, two of the genera that were modified, *Epibacterium* (Chapter 4) and *Ruegeria* (Chapter 3), were described in greater detail. Because of the high amount of phenotypic diversity present in these genera, most species cannot be

distinguished from one another by phenotypic data alone. This trend holds true for distinguishing these genera from one another and from the other closely related genera *Cribrihabitans*, *Leisingera*, *Phaeobacter*, and *Pseudophaeobacter*. While investigating these genera, the whole-genomes of several species became available including *Cribrihabitans marinus*. This species disrupted the monophyletic clade of *Ruegeria,* and its taxonomic placement warrants further investigation. However, there are two *Cribrihabitans* species whose whole-genome sequences are not currently available. Because of this, the taxonomic placement of these organisms should be re-evaluated once these sequences become available.

The taxonomic placement of the most recent addition to the genus, *Ruegeria kandeliae*, is not supported by the cAAI or the phylogenetic tree. This is likely due to the fact that the taxonomic placement of this species was done primarily on the basis of 16S rRNA gene sequences, a metric that has been shown to be poorly correlated with the evolution of the roseobacter group (see Chapters 2 and 3 for more details). Because of this, an in-depth analysis of the phylogenetic placement of *R. kandeliae* is required to accurately assign *R. kandeliae* within the roseobacter group.

Synthesis of dimethylsulfonio-^{34}*S*-propionate and di(methyl-^{13}*C*)sulfonio-^{34}*S*-propionate. A previously published method for the synthesis of dimethylsulfonio-^{34}*S*-propionate employed a strategy that avoided the production of volatile intermediates, namely hydrogen sulfide and dimethylsulfide (DMS). However, this method had many drawbacks including several purification steps, expensive reagents, and an overall yield of only 26 %. Most importantly, this method did not enable the labeling of both methyl carbons, which was necessary for the labeling experiment proposed in Chapter 6. In order to address these issues, a new synthetic method was developed. By reducing $^{34}S_8$ to sulfide with metallic sodium, methylating the sulfide to DMS, and reacting the purified DMS with acrylic acid, the percent

yield was increased by 250 %. This method also used inexpensive reagents and fewer purification steps. Furthermore, this method resulted in ≥99 % pure DMSP with >98 % atom enrichment.

Biosynthesis of methionine and cysteine from dimethylsulfoniopropoionate. Previously, it was demonstrated that only roseobacter strains which could metabolize DMSP to methanethiol were able to incorporate a significant amount ^{35}S from [^{35}S]DMSP into TCA-insoluble material. This finding led to the hypothesis that the majority of methionine biosynthesis in the roseobacter group is accomplished by the direct capture of methanethiol via either cystathionine γ-synthase (MetB) or *O*-acylhomoserine thiolase (MetY). In Chapter 6, it was demonstrated that although the majority of methionine sulfur in *R. pomeroyi* DSS-3 was derived from DMSP, only one-third was synthesized via the methanethiol pathway. This result does not disagree with previous experiments but refutes the interpretation that the direct capture of methanethiol is the major source of methionine. Moreover, it demonstrates that even at the low concentrations of <1 μM used in these chemostats, DMSP becomes the major sulfur source for *R. pomeroyi*.

In order for *R. pomeroyi* to synthesize cysteine from DMSP, it must first convert methanethiol to sulfide, and this may explain why *R. pomeroyi* synthesizes more methionine via the reassembly pathway. Although the direct capture of methanethiol is more energy efficient for the biosynthesis of methionine, if too much of the methanethiol is captured directly then there will be an increase in the cost of cysteine biosynthesis. *R. pomeroyi* possesses a methionine γ-lyase (MegL), which is responsible for the majority of the methanethiol produced during growth on methionine (data not shown), and is capable of converting methionine to methanethiol. However, if too large of a fraction of methanethiol was converted to methionine, the cell would

need to break down methionine in order to produce cysteine, and it would lose energy activating homoserine to *O*-acylhomoserine only to have it converted back to homoserine by MegL.

Degradation of methionine and *S*-methylmethionine. Based on whole-cell assays with the wild-type and Δ*megL R. pomeroyi* strains, it was clear that although MegL (SPOA0318) facilitates the production of methanethiol from methionine, it does not perform an analogous reaction with *S*-methylmethionine (SMM) to produce DMS. Although SMM was not converted to DMSP by *R. pomeroyi*, the production of methanethiol observed during growth on the racemic mixture of SMM suggested that the D-isomer can interact with DmdA to produce D-methionine, but the L-isomer is sterically hindered and cannot undergo the same interaction. If this hypothesis is accurate, then it is likely that the resulting D-methionine can then undergo γ-lysis to produce methanethiol via MegL. This can be tested by performing *in vitro* assays with purified DmdA to determine if THF becomes methylated in the presence of *S*-methyl-D-methionine.

If the production of DMS from SMM is facilitated by one or more the DMSP lyases in *R. pomeroyi*, then vinylglycine would be produced. Vinylglycine is known to be toxic to other bacteria, and it is likely that *R. pomeroyi* cannot utilize it as a sole carbon source. If this is the case, it could explain why *R. pomeroyi* is incapable of growth on SMM as a sole carbon source. There are several experiments that may be used to determine the gene(s) responsible for the conversion of SMM to DMS, including the construction of an *R. pomeroyi* transposon library that contains the *metB* gene from *Salmonella enterica*, the introduction of an *R. pomeroyi* genomic library into an *E. coli* Δ*mmuM* strain, or screening an *R. pomeroyi* transposon library for colonies that cannot produce DMS from SMM.

The importance of studying microbial physiology and phylogeny. Microbial physiology and functional genomics are fundamentally linked fields that work to improve our understanding of the microbial world. Because of the advancements in sequencing technologies,

the number of species with whole-genome sequences is ever increasing. By applying functional genomics, we can predict the functions of thousands of gene products and derive a hypothetical metabolic network of the reactions occurring within a given cell. However, it is important to not only know which reactions are possible, but also understand which reactions are employed under specific conditions. Understanding the regulation and application of metabolic pathways provides a much clearer picture of how microbial cells function in nature, which can provide insight into the evolution and diversification of the microbial world. This enables powerful predictions and leads to the generation of hypotheses that advance the field of microbiology as a whole.

Similarly, understanding the phylogenetic relationships between organisms plays an important role in assessing the metabolic potential of many species. The phylogenetic relationships between a set of organisms can further improve our understanding of the evolution of various metabolic networks. All microbes must employ strategies to balance chemical equations in an energetically favorable manner. If a metabolic network is well understood, then predictions can be made for other organisms with similar gene content, even if those organisms cannot be cultured. In this way, combining microbial physiology and phylogenetics results in a clearer understanding of the natural world than either field could achieve in isolation.

APPENDIX A

CHAPTER 2 SUPPLEMENTARY INFORMATION[1]

[1] Wirth, J.S. and W.B. Whitman. 2018. *International Journal of Systematic and Evolutionary Microbiology*. 68:2393-2411.

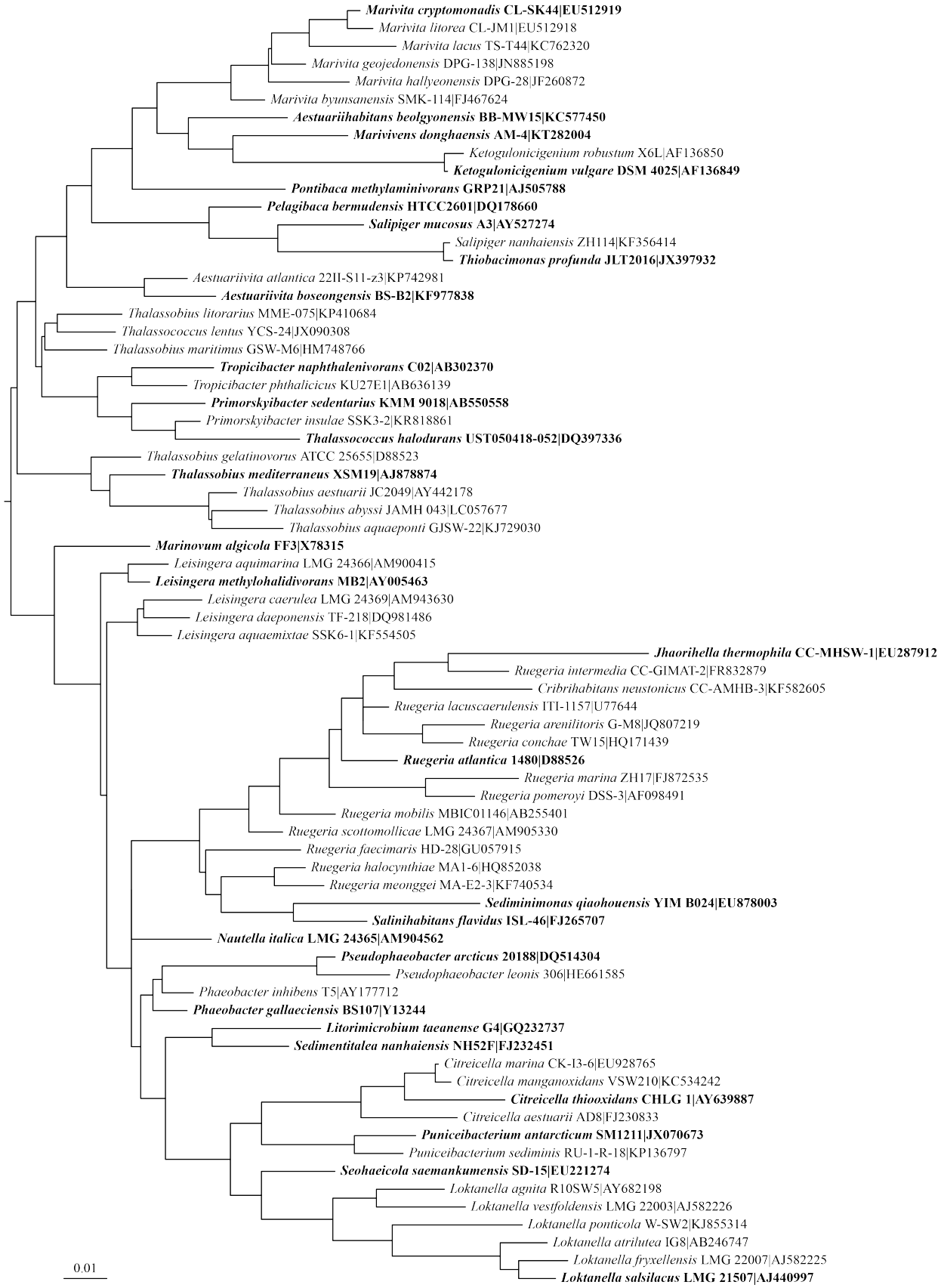
Marivita cryptomonadis CL-SK44|EU512919
Marivita litorea CL-JM1|EU512918
Marivita lacus TS-T44|KC762320
Marivita geojedonensis DPG-138|JN885198
Marivita hallyeonensis DPG-28|JF260872
Marivita byunsanensis SMK-114|FJ467624
Aestuariihabitans beolgyonensis BB-MW15|KC577450
Marivivens donghaensis AM-4|KT282004
Ketogulonicigenium robustum X6L|AF136850
Ketogulonicigenium vulgare DSM 4025|AF136849
Pontibaca methylaminivorans GRP21|AJ505788
Pelagibaca bermudensis HTCC2601|DQ178660
Salipiger mucosus A3|AY527274
Salipiger nanhaiensis ZH114|KF356414
Thiobacimonas profunda JLT2016|JX397932
Aestuariivita atlantica 22II-S11-z3|KP742981
Aestuariivita boseongensis BS-B2|KF977838
Thalassobius litorarius MME-075|KP410684
Thalassococcus lentus YCS-24|JX090308
Thalassobius maritimus GSW-M6|HM748766
Tropicibacter naphthalenivorans C02|AB302370
Tropicibacter phthalicicus KU27E1|AB636139
Primorskyibacter sedentarius KMM 9018|AB550558
Primorskyibacter insulae SSK3-2|KR818861
Thalassococcus halodurans UST050418-052|DQ397336
Thalassobius gelatinovorus ATCC 25655|D88523
Thalassobius mediterraneus XSM19|AJ878874
Thalassobius aestuarii JC2049|AY442178
Thalassobius abyssi JAMH 043|LC057677
Thalassobius aquaeponti GJSW-22|KJ729030
Marinovum algicola FF3|X78315
Leisingera aquimarina LMG 24366|AM900415
Leisingera methylohalidivorans MB2|AY005463
Leisingera caerulea LMG 24369|AM943630
Leisingera daeponensis TF-218|DQ981486
Leisingera aquaemixtae SSK6-1|KF554505
Jhaorihella thermophila CC-MHSW-1|EU287912
Ruegeria intermedia CC-GIMAT-2|FR832879
Cribrihabitans neustonicus CC-AMHB-3|KF582605
Ruegeria lacuscaerulensis ITI-1157|U77644
Ruegeria arenilitoris G-M8|JQ807219
Ruegeria conchae TW15|HQ171439
Ruegeria atlantica 1480|D88526
Ruegeria marina ZH17|FJ872535
Ruegeria pomeroyi DSS-3|AF098491
Ruegeria mobilis MBIC01146|AB255401
Ruegeria scottomollicae LMG 24367|AM905330
Ruegeria faecimaris HD-28|GU057915
Ruegeria halocynthiae MA1-6|HQ852038
Ruegeria meonggei MA-E2-3|KF740534
Sediminimonas qiaohouensis YIM B024|EU878003
Salinihabitans flavidus ISL-46|FJ265707
Nautella italica LMG 24365|AM904562
Pseudophaeobacter arcticus 20188|DQ514304
Pseudophaeobacter leonis 306|HE661585
Phaeobacter inhibens T5|AY177712
Phaeobacter gallaeciensis BS107|Y13244
Litorimicrobium taeanense G4|GQ232737
Sedimentitalea nanhaiensis NH52F|FJ232451
Citreicella marina CK-I3-6|EU928765
Citreicella manganoxidans VSW210|KC534242
Citreicella thiooxidans CHLG 1|AY639887
Citreicella aestuarii AD8|FJ230833
Puniceibacterium antarcticum SM1211|JX070673
Puniceibacterium sediminis RU-1-R-18|KP136797
Seohaeicola saemankumensis SD-15|EU221274
Loktanella agnita R10SW5|AY682198
Loktanella vestfoldensis LMG 22003|AJ582226
Loktanella ponticola W-SW2|KJ855314
Loktanella atrilutea IG8|AB246747
Loktanella fryxellensis LMG 22007|AJ582225
Loktanella salsilacus LMG 21507|AJ440997
0.01

Figure S2-1. 16S rRNA gene sequence tree. The tree is the "original" roseobacter clade pruned from the ARB-Silva tree of life (1). Bolded taxa indicate the type species of each genus based on current taxonomic assignments. For the genera represented in this tree, all species were selected for analysis. The scale bar indicates the number of substitutions per site.

Table S2-1. Sequences used in this study. Unless noted, all genomes represent the type strain of the respective species and were downloaded from NCBI (https://www.ncbi.nlm.nih.gov). All 16S rRNA gene sequences represent the type strain of the respective species and were downloaded from NCBI.

Organism	Strain	Group*	Genome Representation	Assembly Level
Aestuariihabitans beolgyonensis‡	BB-MW15	Original	Unavailable	—
Aestuariivita atlantica	22II-S11-z3	Original	Full	Contig
Aestuariivita boseongensis‡	BS-B2	Original	Full	Contig
Citreicella aestuarii§	AD8	Original	Full	Scaffold
Citreicella manganoxidans	VSW210	Original	Unavailable	—
Citreicella marina	CK-I3-6	Original	Full	Scaffold
Citreicella thiooxidans‡	CHLG 1	Original	Full	Scaffold
Cribrihabitans marinus‡	CZ-AM5	Original	Unavailable	—
Cribrihabitans neustonicus	CC-AMHB-3	Original	Unavailable	—
Cribrihabitans pelagius	KMU-32	Original	Unavailable	—
Epibacterium ulvae‡	U95	Expanded	Full	Contig
Jhaorihella thermophila‡	CC-MHSW-1	Original	Full	Contig
"*Ketogulonicigenium robustum*"‖	X6L	Original	Full	Complete
"*Ketogulonicigenium vulgare*"‡‖	DSM 4025	Original	Full	Complete
Leisingera aquaemixtae	SSK6-1	Original	Full	Contig
Leisingera aquimarina	LMG 24366	Original	Full	Scaffold
Leisingera caerulea	LMG 24369	Original	Full	Scaffold
Leisingera daeponensis	TF-218	Original	Full	Scaffold
Leisingera methylohalidivorans‡	MB2	Original	Full	Complete
Litorimicrobium taeanense‡	G4	Original	Full	Scaffold

Loktanella aestuariicola	J-TF4	Original	Unavailable	—
Loktanella agnita	R10SW5	Original	Unavailable	—
Loktanella atrilutea	IG8	Original	Full	Contig
Loktanella cinnabarina	LL-001	Original	Full	Contig
Loktanella fryxellensis	LMG 22007	Original	Full	Scaffold
Loktanella hongkongensis	UST950701-009P	Original	Full	Scaffold
Loktanella koreensis	GA2-M3	Original	Full	Contig
Loktanella litorea	DPG-5	Original	Full	Contig
Loktanella maricola	DSW-18	Original	Full	Scaffold
Loktanella marina	MDM-7	Original	Full	Contig
Loktanella maritima	KMM 9530	Original	Full	Scaffold
Loktanella ponticola	W-SW2	Original	Unavailable	—
Loktanella pyoseonensis	JJM85	Original	Full	Scaffold
Loktanella rosea	Fg36	Original	Full	Contig
Loktanella salsilacus‡	LMG 21507	Original	Full	Contig
Loktanella sediminilitoris	D1-W3	Original	Full	Scaffold
Loktanella sediminum	S3B03	Original	Full	Contig
Loktanella soesokkakensis	DSSK1-5	Original	Full	Contig
Loktanella tamlensis	SSW-35	Original	Full	Scaffold
Loktanella variabilis	J-MR2-Y	Original	Unavailable	—
Loktanella vestfoldensis	LMG 22003	Original	Full	Scaffold
Marinovum algicola‡	FF3	Original	Full	Scaffold
Marivita byunsanensis	SMK-114	Original	Unavailable	—
Marivita cryptomonadis‡	CL-SK44	Original	Full	Contig
Marivita geojedonensis	DPG-138	Original	Full	Contig

Marivita hallyeonensis	DPG-28	Original	Full	Contig
Marivita lacus	TS-T44	Original	Unavailable	—
Marivita litorea	CL-JM1	Original	Unavailable	—
Marivivens donghaensis‡	AM-4	Original	Unavailable	—
Nautella italica‡	LMG 24365	Original	Full	Contig
Pelagibaca bermudensis‡	HTCC2601	Original	Full	Scaffold
Phaeobacter gallaeciensis‡	BS107	Original	Full	Complete
Phaeobacter inhibens	T5	Original	Full	Scaffold
Pontibaca methylaminivorans‡	GRP21	Original	Full	Contig
Primorskyibacter aestuariivivens	OITF-36	Original	Unavailable	—
Primorskyibacter insulae	SSK3-2	Original	Unavailable	—
Primorskyibacter sedentarius‡	KMM 9018	Original	Unavailable	—
Pseudooctadecabacter jejudonensis‡	SSK2-1	Expanded	Full	Contig
Pseudophaeobacter arcticus‡	20188	Original	Full	Scaffold
Pseudophaeobacter leonis	306	Original	Full	Contig
Puniceibacterium antarcticum	SM1211	Original	Unavailable	—
Puniceibacterium sediminis‡	RU-1-R-18	Original	Full	Scaffold
Roseobacter denitrificans	Och 114	Expanded	Full	Complete
Roseobacter litoralis‡	Och 149	Expanded	Full	Complete
Roseobacter sp. CCS2#	CCS2	Expanded	Full	Contig
Ruegeria arenilitoris	G-M8	Original	Full	Contig
Ruegeria atlantica‡	1480	Original	Full	Contig
Ruegeria conchae	TW15	Original	Full	Contig
Ruegeria faecimaris	HD-28	Original	Full	Scaffold
Ruegeria halocynthiae	MA1-6	Original	Full	Contig

Ruegeria intermedia	CC-GIMAT-2	Original	Full	Scaffold
Ruegeria lacuscaerulensis	ITI-1157	Original	Full	Scaffold
Ruegeria marina	ZH17	Original	Full	Scaffold
Ruegeria meonggei	MA-E2-3	Original	Full	Contig
Ruegeria mobilis	MBIC01146	Original	Full	Contig
Ruegeria pomeroyi	DSS-3	Original	Full	Complete
Ruegeria scottomollicae	LMG 24367	Original	Full	Scaffold
Ruegeria sp. TM1040#	TM1040	Original	Full	Complete
Salinihabitans flavidus‡	ISL-46	Original	Full	Scaffold
Salipiger mucosus‡	A3	Original	Full	Scaffold
Sedimentitalea nanhaiensis‡	NH52F	Original	Full	Scaffold
Sedimentitalea todarodis	KHS03	Original	Unavailable	—
Sediminimonas qiaohouensis‡	YIM B024	Original	Full	Scaffold
Seohaeicola nanhaiensis	SS011A0-7#2-2	Original	Unavailable	—
Seohaeicola saemankumensis‡	SD-15	Original	Unavailable	—
Seohaeicola zhoushanensis	NF48	Original	Unavailable	—
Shimia biformata	CC-AMW-C	Expanded	Unavailable	—
Shimia haliotis	WM35	Expanded	Full	Contig
Shimia isoporae	SW6	Expanded	Full	Scaffold
Shimia marina‡	CL-TA03	Expanded	Full	Scaffold
Shimia sagamensis	JAMH 011	Expanded	Full	Scaffold
Thalassobius abyssi	JAMH 043	Original	Full	Scaffold
Thalassobius aestuarii	JC2049	Original	Full	Contig
Thalassobius aquaeponti	GJSW-22	Original	Unavailable	—
Thalassobius gelatinovorus	ATCC 25655	Original	Full	Contig

Thalassobius litorarius	MME-075	Original	Unavailable	—
Thalassobius maritimus	GSW-M6	Original	Full	Scaffold
Thalassobius mediterraneus‡	XSM19	Original	Full	Contig
Thalassococcus halodurans‡	UST050418-052	Original	Full	Scaffold
Thalassococcus lentus	YCS-24	Original	Unavailable	—
Thiobacimonas profunda‡	JLT2016	Original	Full	Complete
Tropicibacter litoreus	R37	Original	Full	Contig
Tropicibacter mediterraneus	M17	Original	Unavailable	—
Tropicibacter multivorans	MD5	Original	Full	Scaffold
Tropicibacter naphthalenivorans‡	C02	Original	Full	Scaffold
Tropicibacter phthalicicus	KU27E1	Original	Full	Scaffold
Wenxinia marina‡	HY34	Expanded	Full	Scaffold
Wenxinia saemankumensis	S-22	Expanded	Full	Contig

Table S2-1 (continued).

Organism	IMG Taxon ID†	Genbank assembly	WGS project	16S rRNA Accession Number
Aestuariihabitans beolgyonensis‡	—	—	—	KC577450
Aestuariivita atlantica	—	GCA_001205715	AQQZ01	KP742981
Aestuariivita boseongensis‡	—	GCA_001262635	JXYH01	KF977838
Citreicella aestuarii§	2615840712	—	—	FJ230833
Citreicella manganoxidans	—	—	—	KC534242
Citreicella marina	—	GCA_900100085	FNEJ01	EU928765
Citreicella thiooxidans‡	—	GCA_900102075	FNAV01	AY639887
Cribrihabitans marinus‡	—	—	—	JX306766
Cribrihabitans neustonicus	—	—	—	KF582605

Cribrihabitans pelagius	—	—	—	LC101916
Epibacterium ulvae‡	—	GCA_900102795	FMWG01	JN935021
Jhaorihella thermophila‡	—	—	FNVD01	EU287912
"*Ketogulonicigenium robustum*"‖	—	GCA_002117445	—	AF136850
"*Ketogulonicigenium vulgare*"‡‖	—	GCA_000223375	—	AF136849
Leisingera aquaemixtae	—	GCA_001458395	CYSR01	KF554505
Leisingera aquimarina	—	GCA_000473165	AXBE01	AM900415
Leisingera caerulea	—	GCA_000473325	AXBI01	AM943630
Leisingera daeponensis	—	GCA_000473145	AXBD01	DQ981486
Leisingera methylohalidivorans‡	—	GCA_000511355	—	AY005463
Litorimicrobium taeanense‡	—	GCA_900110775	FOEP01	GQ232737
Loktanella aestuariicola	—	—	—	KJ855316
Loktanella agnita	—	—	—	AY682198
Loktanella atrilutea	—	GCA_900128995	FQUE01	AB246747
Loktanella cinnabarina	—	GCA_000466965	BATB01	AB688112
Loktanella fryxellensis	—	GCA_900110065	FOCI01	AJ582225
Loktanella hongkongensis	—	GCA_000365005	AQOX01	AY600300
Loktanella koreensis	—	GCA_900109295	FOIZ01	DQ344498
Loktanella litorea	—	GCA_900114675	FOZM01	JN885197
Loktanella maricola	2695420968	—	—	EF202613
Loktanella marina	—	GCA_900184895	FXZK01	KU522242
Loktanella maritima	2731639257	—	—	AB894236
Loktanella ponticola	—	—	—	KJ855314
Loktanella pyoseonensis	—	GCA_900102015	FNAT01	AM983542
Loktanella rosea	—	GCA_900156505	FTPR01	AY682199

Loktanella salsilacus‡	—	GCA_900114485	FOTF01	AJ440997
Loktanella sediminilitoris	2734482292	—	—	KC311338
Loktanella sediminum	—	GCA_900129845	FQXB01	KJ620985
Loktanella soesokkakensis	—	GCA_900172345	FWFY01	KC987356
Loktanella tamlensis	—	GCA_900115105	FOYP01	DQ533556
Loktanella variabilis	—	—	—	KJ569528
Loktanella vestfoldensis	—	GCA_000382265	ARNL01	AJ582226
Marinovum algicola‡	—	GCA_900109145	FNYY01	X78315
Marivita byunsanensis	—	—	—	FJ467624
Marivita cryptomonadis‡	—	GCA_002115725	JFKD01	EU512919
Marivita geojedonensis	—	GCA_002115805	JFKC01	JN885198
Marivita hallyeonensis	—	GCA_900129875	FQXC01	JF260872
Marivita lacus	—	—	—	KC762320
Marivita litorea	—	—	—	EU512918
Marivivens donghaensis‡	—	—	—	KT282004
Nautella italica‡	—	GCA_001258055	CVRM01	AM904562
Pelagibaca bermudensis‡	—	GCA_000153725	AATQ01	DQ178660
Phaeobacter gallaeciensis‡	—	GCA_000511385	—	Y13244
Phaeobacter inhibens	—	GCA_000473105	AXBB01	AY177712
Pontibaca methylaminivorans‡	—	GCA_900156525	FTPS01	AJ505788
Primorskyibacter aestuariivivens	—	—	—	KX578605
Primorskyibacter insulae	—	—	—	KR818861
Primorskyibacter sedentarius‡	—	—	—	AB550558
Pseudooctadecabacter jejudonensis‡	—	GCA_900172275	FWFT01	KF515220
Pseudophaeobacter arcticus‡	—	GCA_000473205	AXBF01	DQ514304

Pseudophaeobacter leonis	—	GCA_002087335	MWVJ01	HE661585
Puniceibacterium antarcticum	—	—	—	JX070673
Puniceibacterium sediminis‡	2724679734	—	—	KP136797
Roseobacter denitrificans	—	GCA_000014045	—	DQ915623
Roseobacter litoralis‡	—	GCA_000154785	—	DQ915624
Roseobacter sp. CCS2#	—	GCA_000169435	AAYB01	AAYB01000001.1:c857108-855652
Ruegeria arenilitoris	—	GCA_900185035	FXYG01	JQ807219
Ruegeria atlantica‡	—	GCA_001458195	CYPU01	D88526
Ruegeria conchae	—	GCA_000192475	AEYW01	HQ171439
Ruegeria faecimaris	2724679780	—	—	GU057915
Ruegeria halocynthiae	—	GCA_900106805	FNNP01	HQ852038
Ruegeria intermedia	2695420938	—	—	FR832879
Ruegeria lacuscaerulensis	—	GCA_000161775	ACNX01	U77644
Ruegeria marina	—	GCA_900101475	FMZV01	FJ872535
Ruegeria meonggei	—	GCA_900172215	FWFP01	KF740534
Ruegeria mobilis	—	GCA_001681715	LNWY01	AB255401
Ruegeria pomeroyi	—	GCA_000011965	—	AF098491
Ruegeria scottomollicae	2728369517	—	—	AM905330
Ruegeria sp. TM1040#	—	GCA_000014065	—	NC_008044.1:144962-146416
Salinihabitans flavidus‡	—	GCA_900110425	FODS01	FJ265707
Salipiger mucosus‡	—	GCA_000442255	APVH01	AY527274
Sedimentitalea nanhaiensis‡	—	GCA_000473225	AXBG01	FJ232451
Sedimentitalea todarodis	—	—	—	KP172215
Sediminimonas qiaohouensis‡	—	GCA_000423645	AUIJ01	EU878003
Seohaeicola nanhaiensis	—	—	—	KF312716

Seohaeicola saemankumensis‡	—	—	—	EU221274
Seohaeicola zhoushanensis	—	—	—	KP063901
Shimia biformata	—	—	—	KC169813
Shimia haliotis	—	GCA_900114415	FOSZ01	KC196071
Shimia isoporae	2728369275	—	—	FJ976449
Shimia marina‡	—	GCA_001458175	CYPW01	AY962292
Shimia sagamensis	2724679805	—	—	LC008540
Thalassobius abyssi	2728369514	—	—	LC057677
Thalassobius aestuarii	—	GCA_900114635	FOTQ01	AY442178
Thalassobius aquaeponti	—	—	—	KJ729030
Thalassobius gelatinovorus	—	GCA_001458355	CYSA01	D88523
Thalassobius litorarius	—	—	—	KP410684
Thalassobius maritimus	—	GCA_900129685	FQWM01	HM748766
Thalassobius mediterraneus‡	—	GCA_001458435	CYSF01	AJ878874
Thalassococcus halodurans‡	2617270859	—	—	DQ397336
Thalassococcus lentus	—	—	—	JX090308
Thiobacimonas profunda‡	—	GCA_001969385	—	JX397932
Tropicibacter litoreus	—	GCA_900172225	FWFO01	HE860713
Tropicibacter mediterraneus	—	—	—	HE860710
Tropicibacter multivorans	—	GCA_900112515	FOMC01	FR727679
Tropicibacter naphthalenivorans‡	—	GCA_001458375	CYSE01	AB302370
Tropicibacter phthalicicus	2734482174	—	—	AB636139
Wenxinia marina‡	—	GCA_000836695	AONG01	DQ640643
Wenxinia saemankumensis	—	GCA_900141735	FQYO01	KF748921

* Group indicates the data set used during analysis. All analyses were initially performed with the 96 "original" species. All analyses were repeated with both the 108 "original" and "expanded" species.
† Genomes not available from NCBI were downloaded from IMG (https://img.jgi.doe.gov).
‡ Type species of the respective genus.
§ *Citreicella aestuarii* was excluded from whole genome analyses due to file compatibility issues with the EDGAR 2.0 server.
|| "*Ketogulonicigenium*" is not a validly published genus.
Ruegeria sp. TM1040 and *Roseobacter* sp. CCS2 are not validly published species.

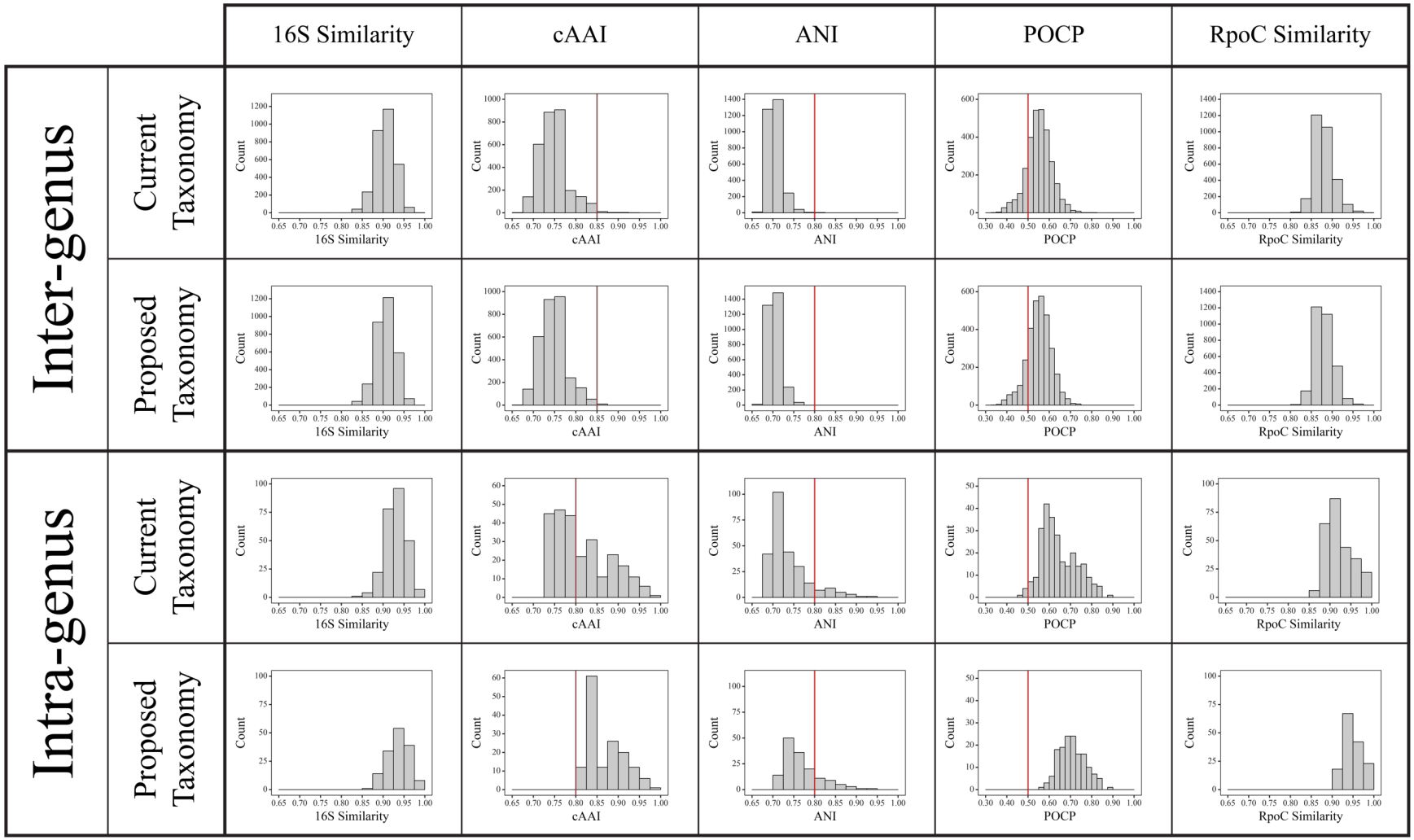

Figure S2-2. Distribution of 16S rRNA gene sequence percent identity, cAAI, ANI, POCP, and RpoC protein sequence percent identity. Histograms represent the values for all pairwise comparisons. Red vertical lines have been added to histograms and indicate specific cutoffs. For inter-genus cAAI comparisons, the line marks 0.85, the maximum allowed AAI value for inter-genus comparisons. For intra-genus cAAI, the line marks 0.80, the minimum allowed AAI value for intra-genus comparisons. For ANI, the

line marks 0.80, the minimum value for ANI to be considered reliable. For POCP, the line marks 0.50, the genus boundary proposed by Qin *et al.* (2)

Table S2-2. Correlations with the cophenetic distances of the maximum likelihood curated core-gene tree. The values indicate the correlation of a similarity matrix for each metric with a cophenetic distance matrix produced from the maximum likelihood curated core-gene tree. Only the 81 taxa with whole genome sequences were used.

Metric	Correlation with curated core-gene tree
16S	0.40
ANI	0.71
cAAI	0.95
POCP	0.81
RpoC	0.94

Table S2-3. Pairwise correlations of all metrics used in this study. The values indicate the correlation of the similarity matrix for a given metric with the similarity matrix of a different metric. Only the 81 taxa with whole genome sequences were used.

	16S	ANI	cAAI	POCP
ANI	0.30			
cAAI	0.42	0.82		
POCP	0.42	0.65	0.82	
RpoC	0.47	0.73	0.93	0.79

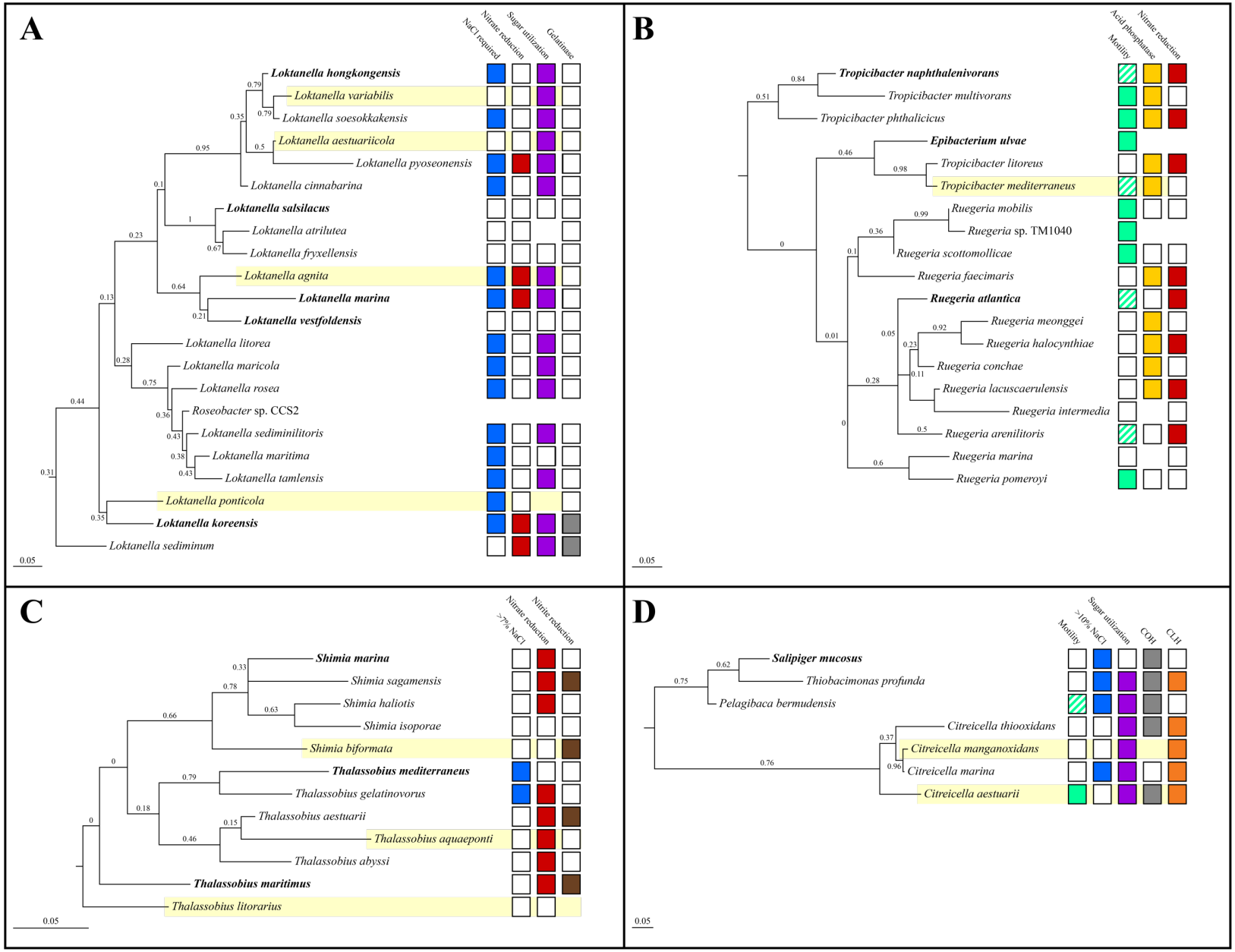
A
NaCl required
Nitrate reduction
Sugar utilization
Gelatinase
Loktanella hongkongensis
Loktanella variabilis
Loktanella soesokkakensis
Loktanella aestuariicola
Loktanella pyoseonensis
Loktanella cinnabarina
Loktanella salsilacus
Loktanella atrilutea
Loktanella fryxellensis
Loktanella agnita
Loktanella marina
Loktanella vestfoldensis
Loktanella litorea
Loktanella maricola
Loktanella rosea
Roseobacter sp. CCS2
Loktanella sediminilitoris
Loktanella maritima
Loktanella tamlensis
Loktanella ponticola
Loktanella koreensis
Loktanella sediminum
0.05
B
Motility
Acid phosphatase
Nitrate reduction
Tropicibacter naphthalenivorans
Tropicibacter multivorans
Tropicibacter phthalicicus
Epibacterium ulvae
Tropicibacter litoreus
Tropicibacter mediterraneus
Ruegeria mobilis
Ruegeria sp. TM1040
Ruegeria scottomollicae
Ruegeria faecimaris
Ruegeria atlantica
Ruegeria meonggei
Ruegeria halocynthiae
Ruegeria conchae
Ruegeria lacuscaerulensis
Ruegeria intermedia
Ruegeria arenilitoris
Ruegeria marina
Ruegeria pomeroyi
0.05
C
>7% NaCl
Nitrate reduction
Nitrite reduction
Shimia marina
Shimia sagamensis
Shimia haliotis
Shimia isoporae
Shimia biformata
Thalassobius mediterraneus
Thalassobius gelatinovorus
Thalassobius aestuarii
Thalassobius aquaeponti
Thalassobius abyssi
Thalassobius maritimus
Thalassobius litorarius
0.05
D
Motility
>10% NaCl
Sugar utilization
COH
CLH
Salipiger mucosus
Thiobacimonas profunda
Pelagibaca bermudensis
Citreicella thiooxidans
Citreicella manganoxidans
Citreicella marina
Citreicella aestuarii
0.05

Figure S2-3. Phenotypic characteristics of ambiguous taxa without whole genome sequences. Trees were constructed by pruning the 16S rRNA gene sequence maximum likelihood tree (Fig. S2-1). Bolded taxa indicate the type species of each genus based on the proposed taxonomic assignments. Highlighted taxa indicate species without whole genome sequences. Phenotypes are shown in boxes adjacent to the tree. White boxes indicate the absence of the respective phenotype, red boxes indicate the ability to reduce nitrate to nitrite, purple boxes indicate the ability to utilize sugars as a sole carbon source, and spaces without boxes indicate missing data. (**a**) Delimiting genera within the *Loktanella* genus. Blue boxes indicate a requirement for NaCl for growth, and grey boxes indicate the ability to hydrolyze gelatin (3-20). (**b**) Delimiting genera within the *Epibacterium*, *Ruegeria*, and *Tropicibacter* genera (21-40). Solid green boxes indicate motility via polar flagella, striped green boxes indicate motility via peritrichous flagella, and yellow boxes indicate the presence of acid phosphatase activity. (**c**) Delimiting genera within the *Shimia* and *Thalassobius* genera. Blue boxes indicate the ability to grow in the presence of >7% NaCl (w/v) and brown boxes indicate the ability to reduce nitrate to gas (21, 41-51). (**d**) Delimiting the genus boundary within the *Citreicella, Pelagibaca, Salipiger*, and *Thiobacimonas* clade. Solid green boxes indicate motility via lateral flagella, striped green boxes indicate motility via gliding, blue boxes indicate the ability to grow in the presence of >10% NaCl (w/v), grey boxes indicate chemoorganoheterotrophic (COH) growth, and orange boxes indicate chemolithoheterotrophic (CLH) growth (52-59).

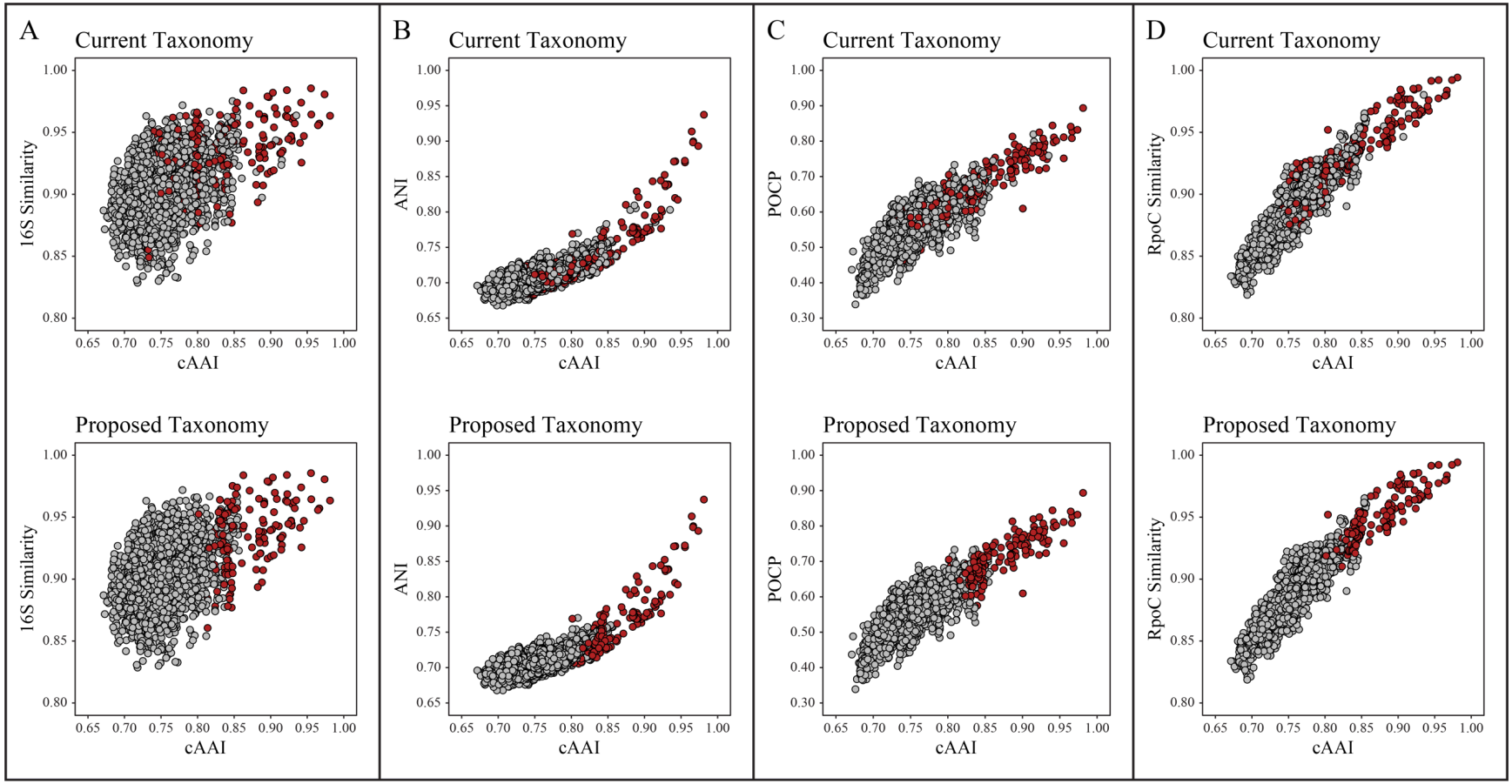

Figure S2-4. Distribution of metrics used in this study within and between genera. Plots depict the relationship between cAAI and the four other metrics used in this study. Grey dots indicate comparisons between genera, and red dots indicate comparisons within genera. (**a**) All pairwise comparisons of cAAI versus 16S rRNA gene sequence similarity; $r = 0.42$. (**b**) All pairwise comparisons of cAAI versus ANI; $r = 0.82$. (**c**) All pairwise comparisons of cAAI versus POCP; $r = 0.82$. (**d**) All pairwise comparisons of cAAI versus RpoC protein sequence similarity; $r = 0.93$.

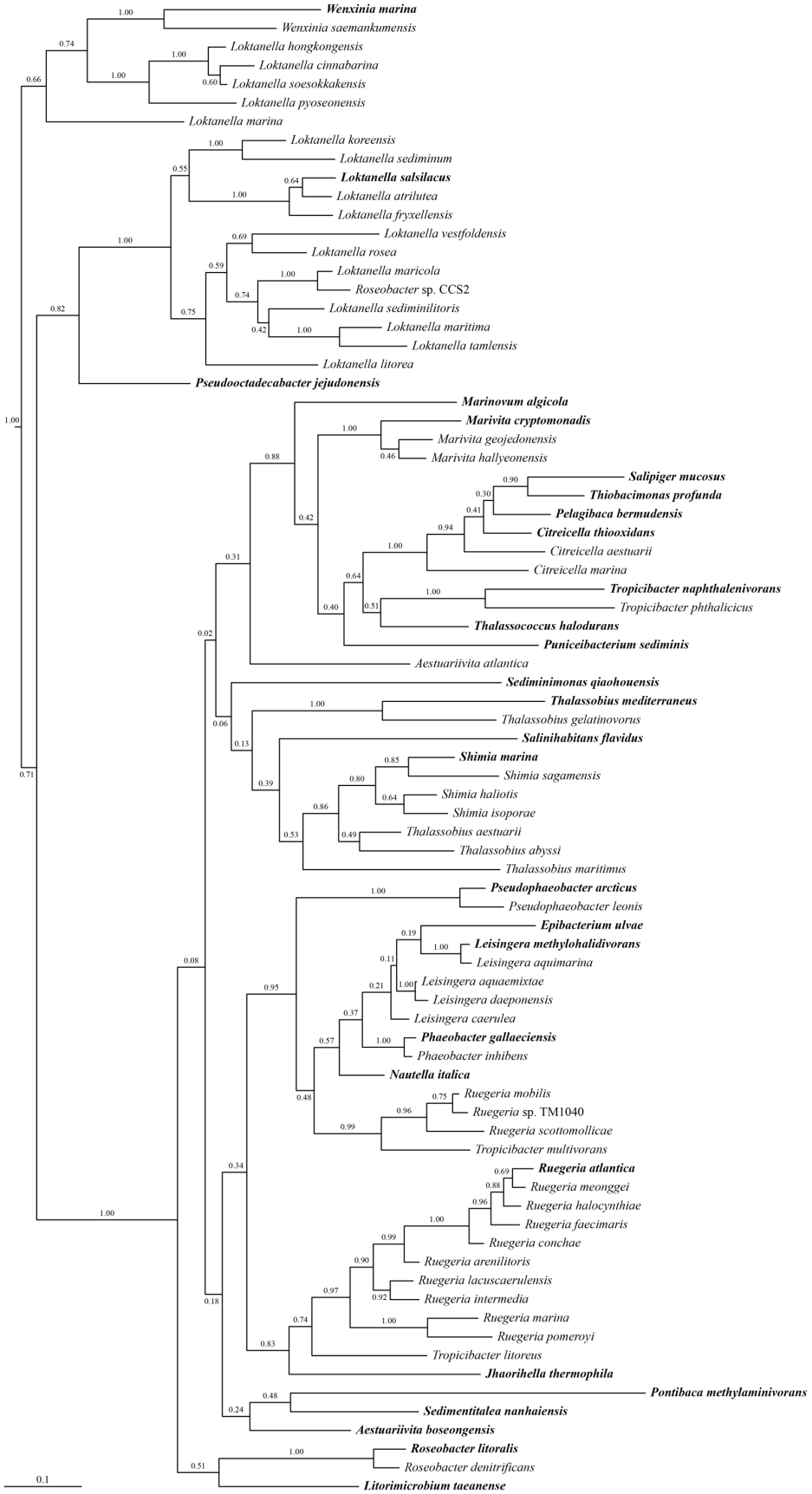
Wenxinia marina
Wenxinia saemankumensis
Loktanella hongkongensis
Loktanella cinnabarina
Loktanella soesokkakensis
Loktanella pyoseonensis
Loktanella marina
Loktanella koreensis
Loktanella sediminum
Loktanella salsilacus
Loktanella atrilutea
Loktanella fryxellensis
Loktanella vestfoldensis
Loktanella rosea
Loktanella maricola
Roseobacter sp. CCS2
Loktanella sediminilitoris
Loktanella maritima
Loktanella tamlensis
Loktanella litorea
Pseudooctadecabacter jejudonensis
Marinovum algicola
Marivita cryptomonadis
Marivita geojedonensis
Marivita hallyeonensis
Salipiger mucosus
Thiobacimonas profunda
Pelagibaca bermudensis
Citreicella thiooxidans
Citreicella aestuarii
Citreicella marina
Tropicibacter naphthalenivorans
Tropicibacter phthalicicus
Thalassococcus halodurans
Puniceibacterium sediminis
Aestuariivita atlantica
Sediminimonas qiaohouensis
Thalassobius mediterraneus
Thalassobius gelatinovorus
Salinihabitans flavidus
Shimia marina
Shimia sagamensis
Shimia haliotis
Shimia isoporae
Thalassobius aestuarii
Thalassobius abyssi
Thalassobius maritimus
Pseudophaeobacter arcticus
Pseudophaeobacter leonis
Epibacterium ulvae
Leisingera methylohalidivorans
Leisingera aquimarina
Leisingera aquaemixtae
Leisingera daeponensis
Leisingera caerulea
Phaeobacter gallaeciensis
Phaeobacter inhibens
Nautella italica
Ruegeria mobilis
Ruegeria sp. TM1040
Ruegeria scottomollicae
Tropicibacter multivorans
Ruegeria atlantica
Ruegeria meonggei
Ruegeria halocynthiae
Ruegeria faecimaris
Ruegeria conchae
Ruegeria arenilitoris
Ruegeria lacuscaerulensis
Ruegeria intermedia
Ruegeria marina
Ruegeria pomeroyi
Tropicibacter litoreus
Jhaorihella thermophila
Pontibaca methylaminivorans
Sedimentitalea nanhaiensis
Aestuariivita boseongensis
Roseobacter litoralis
Roseobacter denitrificans
Litorimicrobium taeanense
0.1

Figure S2-5. RpoC maximum likelihood tree. Tree was generated using PhyML server 3.0 (http://www.atgc-montpellier.fr/phyml/) with smart model selection (60, 61). Bolded taxa indicate the type species of each genus based on current taxonomic assignments. Numbers on branches indicate the fraction of bootstrap support after 1000 replicates. The scale bar indicates the number of substitutions per site. The tree is rooted on the genus "*Ketogulonicigenium*" (omitted from tree).

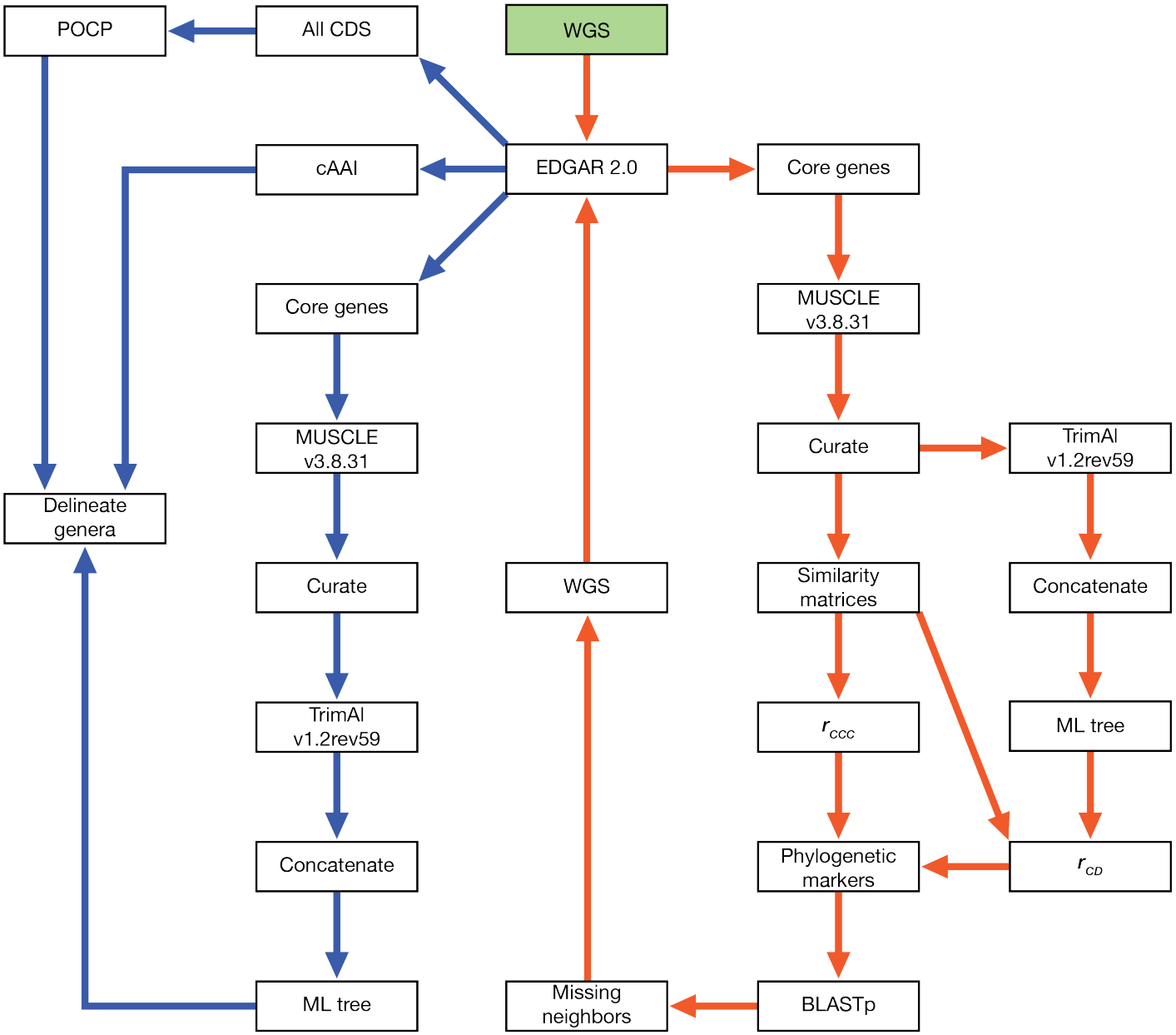
POCP
All CDS
WGS
cAAI
EDGAR 2.0
Core genes
Core genes
MUSCLE v3.8.31
MUSCLE v3.8.31
Curate
TrimAl v1.2rev59
Delineate genera
Curate
WGS
Similarity matrices
Concatenate
TrimAl v1.2rev59
r_{ccc}
ML tree
Concatenate
Phylogenetic markers
r_{cD}
ML tree
Missing neighbors
BLASTp

Figure S2-6. Diagram of workflow. Workflow starts at the green box, follows orange lines first, and follows blue lines second. See methods for more detailed descriptions of each step. Starting at the green box and following the orange lines, whole genome sequences in genbank format were uploaded to the EDGAR 2.0 server (https://edgar.computational.bio.uni-giessen.de), and the core genes identified were downloaded as a fasta (62). This fasta was parsed into one fasta per core gene containing one entry per taxon. These fasta were aligned individually with MUSCLE v3.8.31 using the default settings (63). The aligned core genes were then curated by removing genes where one or more taxa contained >5 % gaps in their respective alignment (64). The curated, core gene alignments were trimmed with TrimAl v1.2rev59 using the 'automated1' option, the trimmed alignments were concatenated, and this concatenated alignment used to construct a maximum likelihood tree (65). The curated, core gene alignments were also used to calculate a similarity matrix for each curated, core gene. These similarity matrices were used to calculate the cophenetic correlation coefficients and were used to calculate their correlation with the cophenetic distances of the maximum likelihood tree. Any genes with a cophenetic correlation coefficient > 0.90 and a correlation with the cophenetic distances of the maximum likelihood tree > 0.90 were considered suitable phylogenetic markers. One of the phylogenetic markers (RpoC) was then used as input in BLASTp to search for any closely related organisms absent from the original analysis. The whole genome sequences for these missing neighbors were then added to the EDGAR 2.0 server. After adding the missing neighbors to the analysis, the following outputs were downloaded (blue lines): all CDS from each taxa, the cAAI, and the core genes. As before, the core genes were aligned, curated, trimmed, concatenated, and used to construct a maximum likelihood tree. The POCP was calculated from all CDS. Using the maximum likelihood tree, POCP, and cAAI, the genera were then delineated.

References:

1. Yarza P, Richter M, Peplies J, Euzeby J, Amann R, Schleifer KH, Ludwig W, Glockner FO, Rossello-Mora R. 2008. The All-Species Living Tree project: a 16S rRNA-based phylogenetic tree of all sequenced type strains. Systematic and Applied Microbiology 31:241-50.
2. Qin QL, Xie BB, Zhang XY, Chen XL, Zhou BC, Zhou J, Oren A, Zhang YZ. 2014. A proposed genus boundary for the prokaryotes based on genomic insights. Journal of Bacteriology 196:2210-5.
3. Van Trappen S, Mergaert J, Swings J. 2004. *Loktanella salsilacus* gen. nov., sp. nov., *Loktanella fryxellensis* sp. nov. and *Loktanella vestfoldensis* sp. nov., new members of the *Rhodobacter* group, isolated from microbial mats in Antarctic lakes. International Journal of Systematic and Evolutionary Microbiology 54:1263-9.
4. Hosoya S, Yokota A. 2007. *Loktanella atrilutea* sp. nov., isolated from seawater in Japan. International Journal of Systematic and Evolutionary Microbiology 57:1966-9.
5. Lau SC, Tsoi MM, Li X, Plakhotnikova I, Wu M, Wong PK, Qian PY. 2004. *Loktanella hongkongensis* sp. nov., a novel member of the *α-Proteobacteria* originating from marine biofilms in Hong Kong waters. International Journal of Systematic and Evolutionary Microbiology 54:2281-4.
6. Tsubouchi T, Shimane Y, Mori K, Miyazaki M, Tame A, Uematsu K, Maruyama T, Hatada Y. 2013. *Loktanella cinnabarina* sp. nov., isolated from a deep subseafloor sediment, and emended description of the genus *Loktanella*. International Journal of Systematic and Evolutionary Microbiology 63:1390-5.

7. Park JM, Park S, Jung YT, Cho JY, Yoon JH. 2014. *Loktanella variabilis* sp. nov., isolated from a tidal flat. International Journal of Systematic and Evolutionary Microbiology 64:2579-85.
8. Moon YG, Seo SH, Lee SD, Heo MS. 2010. *Loktanella pyoseonensis* sp. nov., isolated from beach sand, and emended description of the genus *Loktanella*. International Journal of Systematic and Evolutionary Microbiology 60:785-9.
9. Park S, Lee JS, Lee KC, Yoon JH. 2013. *Loktanella soesokkakensis* sp. nov., isolated from the junction between the North Pacific Ocean and a freshwater spring. Antonie Van Leeuwenhoek 104:397-404.
10. Weon HY, Kim BY, Yoo SH, Kim JS, Kwon SW, Go SJ, Stackebrandt E. 2006. *Loktanella koreensis* sp. nov., isolated from sea sand in Korea. International Journal of Systematic and Evolutionary Microbiology 56:2199-202.
11. Yoon JH, Jung YT, Lee JS. 2013. *Loktanella litorea* sp. nov., isolated from seawater. International Journal of Systematic and Evolutionary Microbiology 63:175-80.
12. Liang J, Zhang Z, Liu Y, Wang M, Zhang XH. 2015. *Loktanella sediminum* sp. nov., isolated from marine surface sediment. International Journal of Systematic and Evolutionary Microbiology 65:686-91.
13. Yoon JH, Kang SJ, Lee SY, Oh TK. 2007. *Loktanella maricola* sp. nov., isolated from seawater of the East Sea in Korea. International Journal of Systematic and Evolutionary Microbiology 57:1799-802.
14. Tanaka N, Romanenko LA, Kurilenko VV, Svetashev VI, Kalinovskaya NI, Mikhailov VV. 2014. *Loktanella maritima* sp. nov. isolated from shallow marine sediments. International Journal of Systematic and Evolutionary Microbiology 64:2370-5.

15. Ivanova EP, Zhukova NV, Lysenko AM, Gorshkova NM, Sergeev AF, Mikhailov VV, Bowman JP. 2005. *Loktanella agnita* sp. nov. and *Loktanella rosea* sp. nov., from the north-west Pacific Ocean. International Journal of Systematic and Evolutionary Microbiology 55:2203-7.

16. Park S, Jung YT, Yoon JH. 2013. *Loktanella sediminilitoris* sp. nov., isolated from tidal flat sediment. International Journal of Systematic and Evolutionary Microbiology 63:4118-23.

17. Lee SD. 2012. *Loktanella tamlensis* sp. nov., isolated from seawater. International Journal of Systematic and Evolutionary Microbiology 62:586-90.

18. Jung YT, Park S, Lee JS, Yoon JH. 2016. *Loktanella marina* sp. nov., isolated from seawater of Yellow Sea in South Korea. International Journal of Systematic and Evolutionary Microbiology 66:2528-2533.

19. Jung YT, Park S, Park JM, Yoon JH. 2014. *Loktanella ponticola* sp. nov., isolated from seawater. International Journal of Systematic and Evolutionary Microbiology 64:3717-23.

20. Park S, Jung YT, Won SM, Park JM, Yoon JH. 2014. *Loktanella aestuariicola* sp. nov., an alphaproteobacterium isolated from a tidal flat. Antonie Van Leeuwenhoek 106:707-14.

21. Rüger HJ, Höfle MG. 1992. rarine star-shaped-aggregate-forming bacteria: *Agrobacterium antlanticum* sp. nov.; *Agrobacterium meteori* sp. nov.; *Agrobacterium ferrugineum* sp. nov., nom. rev.; *Agrobacterium gelatinovorum* sp. nov., nom. rev.; and *Agrobacterium stellulatum* sp. nov., nom. rev. International Journal of Systematic Bacteriology 42:133-143.

22. Yi H, Lim YW, Chun J. 2007. Taxonomic evaluation of the genera *Ruegeria* and *Silicibacter*: a proposal to transfer the genus *Silicibacter* Petursdottir and Kristjansson 1999 to the genus *Ruegeria* Uchino et al. 1999. International Journal of Systematic and Evolutionary Microbiology 57:815-819.

23. Muramatsu Y, Uchino Y, Kasai H, Suzuki KI, Nakagawa Y. 2007. *Ruegeria mobilis* sp. nov., a member of the *Alphaproteobacteria* isolated in Japan and Palau. International Journal of Systematic and Evolutionary Microbiology 57:1304-1309.

24. Park S, Yoon JH. 2012. *Ruegeria arenilitoris* sp. nov., isolated from the seashore sand around a seaweed farm. Antonie Van Leeuwenhoek International Journal of General and Molecular Microbiology 102:581-589.

25. Lee J, Whon TW, Shin NR, Roh SW, Kim J, Park SK, Kim MS, Shin KS, Lee JS, Lee KC, Kim YO, Bae JW. 2012. *Ruegeria conchae* sp. nov., isolated from the ark clam *Scapharca broughtonii*. International Journal of Systematic and Evolutionary Microbiology 62:2851-2857.

26. Oh KH, Jung YT, Oh TK, Yoon JH. 2011. *Ruegeria faecimaris* sp. nov., isolated from a tidal flat sediment. International Journal of Systematic and Evolutionary Microbiology 61:1182-1188.

27. Kim YO, Park S, Nam BH, Kang SJ, Hur YB, Lee SJ, Oh TK, Yoon JH. 2012. *Ruegeria halocynthiae* sp. nov., isolated from the sea squirt *Halocynthia roretzi*. International Journal of Systematic and Evolutionary Microbiology 62:925-930.

28. Kämpfer P, Arun AB, Rekha PD, Busse HJ, Young CC, Glaeser SP. 2013. *Ruegeria intermedia* sp. nov., a moderately thermophilic bacterium isolated from a coastal hot spring. International Journal of Systematic and Evolutionary Microbiology 63:2538-2544.

29. Petursdottir SK, Kristjansson JK. 1997. *Silicibacter lacuscaerulensis* gen. nov., sp. nov., a mesophilic moderately halophilic bacterium characteristic of the Blue Lagoon geothermal lake in Iceland. Extremophiles 1:94-99.

30. Huo YY, Xu XW, Li X, Liu C, Cui HL, Wang CS, Wu M. 2011. *Ruegeria marina* sp. nov., isolated from marine sediment. International Journal of Systematic and Evolutionary Microbiology 61:347-350.

31. Kim YO, Park S, Nam BH, Jung YT, Kim DG, Yoon JH. 2014. *Ruegeria meonggei* sp. nov., an alphaproteobacterium isolated from ascidian *Halocynthia roretzi*. Antonie Van Leeuwenhoek International Journal of General and Molecular Microbiology 105:551-558.

32. González JM, Covert JS, Whitman WB, Henriksen JR, Mayer F, Scharf B, Schmitt R, Buchan A, Fuhrman JA, Kiene RP, Moran MA. 2003. *Silicibacter pomeroyi* sp. nov. and *Roseovarius nubinhibens* sp. nov., dimethylsulfoniopropionate-demethylating bacteria from marine environments. International Journal of Systematic and Evolutionary Microbiology 53:1261-1269.

33. Lucena T, Ruvira MA, Macian MC, Pujalte MJ, Arahal DR. 2013. Description of *Tropicibacter mediterraneus* sp. nov. and *Tropicibacter litoreus* sp. nov. Systematic and Applied Microbiolology 36:325-9.

34. Penesyan A, Breider S, Schumann P, Tindall BJ, Egan S, Brinkhoff T. 2013. *Epibacterium ulvae* gen. nov., sp. nov., epibiotic bacteria isolated from the surface of a marine alga. International Journal of Systematic and Evolutionary Microbiology 63:1589-96.

35. Vandecandelaere I, Nercessian O, Segaert E, Achouak W, Faimali M, Vandamme P. 2008. *Ruegeria scottomollicae* sp. nov., isolated from a marine electroactive biofilm. International Journal of Systematic and Evolutionary Microbiology 58:2726-2733.

36. Alavi M, Miller T, Erlandson K, Schneider R, Belas R. 2001. Bacterial community associated with *Pfiesteria*-like dinoflagellate cultures. Environmental Microbiology 3:380-96.

37. Miller TR, Hnilicka K, Dziedzic A, Desplats P, Belas R. 2004. Chemotaxis of *Silicibacter* sp. strain TM1040 toward dinoflagellate products. Applied and Environmental Microbiology 70:4692-701.

38. Lucena T, Pujalte MJ, Ruvira MA, Garay E, Macian MC, Arahal DR. 2012. *Tropicibacter multivorans* sp. nov., an aerobic alphaproteobacterium isolated from surface seawater. International Journal of Systematic and Evolutionary Microbiology 62:844-8.

39. Harwati TU, Kasai Y, Kodama Y, Susilaningsih D, Watanabe K. 2009. *Tropicibacter naphthalenivorans* gen. nov., sp. nov., a polycyclic aromatic hydrocarbon-degrading bacterium isolated from Semarang Port in Indonesia. International Journal of Systematic and Evolutionary Microbiology 59:392-6.

40. Iwaki H, Nishimura A, Hasegawa Y. 2012. *Tropicibacter phthalicus* sp. nov., a phthalate-degrading bacterium from seawater. Current Microbiology 64:392-6.

41. Arahal DR, Macian MC, Garay E, Pujalte MJ. 2005. *Thalassobius mediterraneus* gen. nov., sp. nov., and reclassification of *Ruegeria gelatinovorans* as *Thalassobius gelatinovorus* comb. nov. International Journal of Systematic and Evolutionary Microbiology 55:2371-2376.

42. Choi DH, Cho BC. 2006. *Shimia marina* gen. nov., sp. nov., a novel bacterium of the *Roseobacter* clade isolated from biofilm in a coastal fish farm. International Journal of Systematic and Evolutionary Microbiology 56:1869-73.

43. Hameed A, Shahina M, Lin SY, Lai WA, Hsu YH, Liu YC, Huang YM, Young CC. 2013. *Shimia biformata* sp. nov., isolated from surface seawater, and emended description of the genus *Shimia* Choi and Cho 2006. International Journal of Systematic and Evolutionary Microbiology 63:4533-9.

44. Hyun DW, Kim MS, Shin NR, Kim JY, Kim PS, Whon TW, Yun JH, Bae JW. 2013. *Shimia haliotis* sp. nov., a bacterium isolated from the gut of an abalone, *Haliotis discus hannai*. International Journal of Systematic and Evolutionary Microbiology 63:4248-53.

45. Nogi Y, Mori K, Uchida H, Hatada Y. 2015. *Shimia sagamensis* sp. nov., a marine bacterium isolated from cold-seep sediment. International Journal of Systematic and Evolutionary Microbiology 65:2786-90.

46. Chen MH, Sheu SY, Chen CA, Wang JT, Chen WM. 2011. *Shimia isoporae* sp. nov., isolated from the reef-building coral *Isopora palifera*. International Journal of Systematic and Evolutionary Microbiology 61:823-7.

47. Nogi Y, Mori K, Makita H, Hatada Y. 2015. *Thalassobius abyssi* sp. nov., a marine bacterium isolated from the cold-seep sediment. International Journal of Systematic and Evolutionary Microbiology doi:10.1099/ijsem.0.000758.

48. Yi H, Chun J. 2006. *Thalassobius aestuarii* sp. nov., isolated from tidal flat sediment. Journal of Microbiology 44:171-6.

49. Park S, Lee MH, Lee JS, Oh TK, Yoon JH. 2012. *Thalassobius maritimus* sp. nov., isolated from seawater. International Journal of Systematic and Evolutionary Microbiology 62:8-12.

50. Park I, Cha IT, Seo MJ. 2016. *Thalassobius litorarius* sp. nov., isolated from a tidal flat. International Journal of Systematic and Evolutionary Microbiology 66:1666-1672.

51. Park S, Jung YT, Won SM, Park JM, Yoon JH. 2014. *Thalassobius aquaeponti* sp. nov., an alphaproteobacterium isolated from seawater. Antonie Van Leeuwenhoek 106:535-42.

52. Martinez-Canovas MJ, Quesada E, Martinez-Checa F, del Moral A, Bejar V. 2004. *Salipiger mucescens* gen. nov., sp. nov., a moderately halophilic, exopolysaccharide-producing bacterium isolated from hypersaline soil, belonging to the *α-Proteobacteria*. International Journal of Systematic and Evolutionary Microbiology 54:1735-40.

53. Lai Q, Fu Y, Wang J, Chen S, Zhong H, Sun F, Shao Z. 2011. *Citreicella marina* sp. nov., isolated from deep-sea sediment. International Journal of Systematic and Evolutionary Microbiology 61:728-31.

54. Pujalte MJ, Lucena T, Ruvira MA, Arahal DR, Macián MC. 2014. The family *Rhodobacteraceae*, p 439-512. *In* Rosenberg E, DeLong EF, Lory S, Stackebrandt E, Thompson F (ed), The Prokaryotes: *Alphaproteobacteria* and *Betaproteobacteria* doi:10.1007/978-3-642-30197-1_377. Springer Berlin Heidelberg, Berlin, Heidelberg.

55. Sorokin DY, Tourova TP, Muyzer G. 2005. *Citreicella thiooxidans* gen. nov., sp. nov., a novel lithoheterotrophic sulfur-oxidizing bacterium from the Black Sea. Systematic and Applied Microbiology 28:679-87.

56. Cho JC, Giovannoni SJ. 2006. *Pelagibaca bermudensis* gen. nov., sp. nov., a novel marine bacterium within the *Roseobacter* clade in the order *Rhodobacterales*. International Journal of Systematic and Evolutionary Microbiology 56:855-9.

57. Li S, Tang K, Liu K, Jiao N. 2015. *Thiobacimonas profunda* gen. nov., sp. nov., a member of the family *Rhodobacteraceae* isolated from deep-sea water. International Journal of Systematic and Evolutionary Microbiology 65:359-64.

58. Park MS, Chung BS, Lee HJ, Jin HM, Lee SS, Oh YK, Jeon CO. 2011. *Citreicella aestuarii* sp. nov., isolated from a tidal flat. International Journal of Systematic and Evolutionary Microbiology 61:2595-9.

59. Rajasabapathy R, Mohandass C, Dastager SG, Liu Q, Li WJ, Colaco A. 2015. *Citreicella manganoxidans* sp. nov., a novel manganese oxidizing bacterium isolated from a shallow water hydrothermal vent in Espalamaca (Azores). Antonie Van Leeuwenhoek 108:1433-9.

60. Guindon S, Dufayard JF, Lefort V, Anisimova M, Hordijk W, Gascuel O. 2010. New algorithms and methods to estimate maximum-likelihood phylogenies: assessing the performance of PhyML 3.0. Systematic Biology 59:307-21.

61. Lefort V, Longueville JE, Gascuel O. 2017. SMS: Smart Model Selection in PhyML. Molecular Biology and Evolution doi:10.1093/molbev/msx149.

62. Blom J, Kreis J, Spanig S, Juhre T, Bertelli C, Ernst C, Goesmann A. 2016. EDGAR 2.0: an enhanced software platform for comparative gene content analyses. Nucleic Acids Research 44:W22-8.

63. Edgar RC. 2004. MUSCLE: multiple sequence alignment with high accuracy and high throughput. Nucleic Acids Research 32:1792-7.

64. Beukes CW, Palmer M, Manyaka P, Chan WY, Avontuur JR, van Zyl E, Huntemann M, Clum A, Pillay M, Palaniappan K, Varghese N, Mikhailova N, Stamatis D, Reddy TBK, Daum C, Shapiro N, Markowitz V, Ivanova N, Kyrpides N, Woyke T, Blom J, Whitman WB, Venter SN, Steenkamp ET. 2017. Genome data provides high support for generic boundaries in *Burkholderia* sensu lato. Frontiers in Microbiology 8:1154.

65. Capella-Gutierrez S, Silla-Martinez JM, Gabaldon T. 2009. trimAl: a tool for automated alignment trimming in large-scale phylogenetic analyses. Bioinformatics 25:1972-3.